AN INTEGRATED BIOPROCESS FOR ACID ROCK DRAINAGE (ARD) REMEDIATION AND RENEWABLE ENERGY GENERATION

Rob van Hille, Tynan Marais, Rob Huddy, Madelyn Johnson-Robertson, Mariette Smart, Jennifer Couperthwaite, Emma Horn, Robert Pott, Nikhil Naidoo, Matthew Burke, June Jian and Susan T.L. Harrison

WATER RESEARCH COMMISSION

TT 789/19

AN INTEGRATED BIOPROCESS FOR ACID ROCK DRAINAGE (ARD) REMEDIATION AND RENEWABLE ENERGY GENERATION

Report to the
Water Research Commission

by

Rob van Hille[1,2], Tynan Marais[2], Rob Huddy[2], Madelyn Johnson-Robertson[2], Mariette Smart[2], Jennifer Couperthwaite[2], Emma Horn[3], Robert Pott[2], Nikhil Naidoo[4], Matthew Burke[2], June Jian[2] and Susan T.L. Harrison[2]

[1]The Moss Group
[2]Centre for Bioprocess Engineering Research, University of Cape Town
[3]Department of Chemical Engineering, Cape Peninsula University of Technology
[4]School of Chemical and Mechanical Engineering, University of the Witwatersrand

WRC Report No. TT 789/19
ISBN 978-0-6392-0104-7

May 2019

Obtainable from

Water Research Commission

Private Bag X03

GEZINA 0031

orders@wrc.org.za or download from www.wrc.org.za

EXECUTIVE SUMMARY

BACKGROUND

South Africa is a water scarce country that is facing multiple challenges associated with the management of freshwater resources. These include increasingly unpredictable climatic conditions, a growing population and a significant increase in the number of people who have been provided with basic services. These challenges have highlighted the need to conserve existing water resources.

Although considered an industry in decline by many, mining has historically been a cornerstone of the South African economy and remains a significant contributor to GDP and employment. Active mining operations and legacy sites have resulted in widespread environmental degradation and remain a substantial risk to surface and groundwater resources through the discharge of untreated or partially treated mining-impacted water. Gold and coal resources are often associated with sulphidic gangue minerals and the oxidation of these minerals gives rise to acid rock drainage, which is characterised by low pH, elevated metal concentrations and a high sulphate load. Coal mining may also give rise to circum-neutral impacted water, which is characterised by elevated sulphate concentrations. The discharge of high sulphate effluent into receiving water bodies has resulted in salinisation of water resources in Gauteng, Mpumalanga and Limpopo. Increased salinity can have a negative impact on the environment and increase the cost of treating water to potable quality.

Mining-impacted water can be divided into two broad categories. These are mine drainage, which is primarily due to groundwater rebound and is pumped out of active mines or can decant from abandoned workings and rock drainage, which is primarily associated with runoff and leachate from surface impoundments. Mine drainage is typically high volume and can be characterised by particularly low pH and high metal and sulphate loading. It has traditionally been treated by active chemical and physical processes. There has been substantial investment in treatment facilities to deal with these discharges and South Africa boasts a number of treatment operations that represent global best practice. Rock drainage is typically characterised by smaller volumes and the number and location of many of the affected sites make them unattractive for tradition active remediation technologies, both from an economic and logistical perspective.

South African researchers have played a leading role in the development of passive and semi-passive technologies that may be more suitable for treating low-volume rock drainage discharges. Several of these are based around biological sulphate reduction (BSR), a technology that has been extensively researched, but less widely implemented. The major challenges associated with BSR technologies are the provision of a suitable electron donor, reaction kinetics and the management of the sulphide product. Passive and semi-passive processes have tended to rely on a mixture of complex organic carbon sources, often lignocellulose based, in column or packed bed reactors to provide the organic carbon necessary to support the BSR. While these systems are able to provide sufficient organic carbon in the short term, the rate of carbon liberation becomes limiting relatively quickly, resulting in a significant drop-off in performance or necessitating supplementation with a liquid carbon source. Packed bed systems often experience structural challenges as a result of compaction or channelling that significantly reduce performance.

The broad objective of the research described in this report was to develop and test an integrated process for treating high sulphate mine water that could be sustained by the anaerobic decomposition of a complex organic carbon source and combines the sulphate reduction and partial sulphide oxidation reactions in a single, passive reactor unit. This type of system would likely be implemented in rural areas and as it would not require skilled operators on site and could depend on local community involvement. To provide some benefit to these communities, the potential to couple water treatment with renewable energy generation was investigated. The intention was to derive biogas from the pre-treatment reactors used to generate the organic carbon source, but also to investigate the potential for the incorporation of microbial fuel cell technology into a sulphate reduction bioprocess.

AIMS

The aims of the project were as follows:

1. To test the digestibility of a number of biomass types to assess their rate of digestion, biogas yield, residual COD and volatile fatty acid profile of the residual COD
2. To assess the effect of temperature on the kinetics and performance of the AD unit, across a range consistent with typical seasonal variations
3. To construct a channel reactor for the simultaneous reduction of sulphate and oxidation of sulphide to elemental sulphur. The channel will contain carbon microfibers for SRB attachment and sulphide oxidation will be achieved in a floating sulphur biofilm at the air-water interface
4. To assess the performance of the system, first using a defined growth medium to support the sulphate reducing community and then using effluent from the AD blended with synthetic ARD and if successful, real ARD
5. To assess the effect of temperature on the sulphate reduction and sulphide oxidation reactions, across a range typical of seasonal variations
6. To optimise the mechanism for harvesting sulphur from the biofilm and characterise the sulphur product
7. To assess the potential of using the sulphate reduction component of the reactor as a microbial fuel cell, quantifying the power and current densities

METHODOLOGY

The first component of the research focussed on evaluating a number of potential organic carbon sources as substrates for anaerobic digestion to generate biogas and a carbon-rich digestate to use as a feed for the downstream reactor units. This was premised on previous research on the anaerobic digestion of *Spirulina* biomass.

Batch anaerobic digestion was performed on grass, manure and a range of unicellular and filamentous algal species, with microcrystalline cellulose as a control substrate. The performance of the reactors was judged on biogas formation, methane content and the rate of generation and accumulation of volatile fatty acids (VFAs) within the reactor.

The anaerobic digestion experiments did not yield particularly encouraging results, but did point to the fact that the rate of hydrolysis of complex substrates and accumulation of VFAs was enhanced by operating at a pH below pH 6, where methanogenesis is supressed and hydrolytic and acidogenic reactions promoted. A series of batch, fed-batch and continuous flow reactors using grass cuttings were investigated to assess the potential for accelerated hydrolysis.

The most significant part of the research was directed towards the design and evaluation of a modified, hybrid linear flow channel reactor (LFCR) that could be capable of simultaneous sulphate reduction in the bulk volume and partial oxidation of the sulphide product to elemental sulphur in a floating sulphur biofilm, with a simple and safe method for recovering the biosulphur product. The LFCR had previously been optimised as a dedicated sulphide oxidation unit, but tests using a sealed unit had also shown good sulphate reduction performance. Based on the understanding of the hydrodynamics within the reactor it was hypothesised that the reactor could support discrete anaerobic and aerobic communities.

The reactor was designed to include carbon microfibres to provide a large surface area for the attachment and retention of the sulphate reducing community and a heat exchanger to facilitate temperature control. An initial proof of concept study yielded positive results, prompting more comprehensive studies on the effect of hydraulic residence time (4 days to 12 hours) and temperature (30˚C to 10˚C) on performance. In addition, experiments were performed to assess the impact of changes in reactor geometry (2 ℓ and 8 ℓ units) and feed composition (lactate and acetate based). Finally, a series of 2000 ℓ pilot-scale reactors were designed and constructed for evaluation on an actual mine site.

The final component of the research was to investigate the potential to generate electricity by incorporating microbial fuel cell (MFC) technology into the mine water treatment process. This involved initial proof of concept testing, using a bacterial species that has been used in previous MFC research, to evaluate the proposed reactor configuration. The second phase involved a shift from using *Shewanella* to testing the sulphate reducing consortium and finally to assessing the potential of the LFCR as an MFC.

The final aim was to assess the full integrated system on synthetic and actual mine water, but due to the challenges associated with generating sufficient organic carbon from the complex substrates, mine water was only tested using batch reactor units.

RESULTS AND DISCUSSION

The anaerobic digestion of grass and manure did not yield particularly encouraging results. The majority of the biogas was generated within the first seven days, with the grass fed digesters producing around 1 ℓ of gas and the manure fed digesters closer to 3 ℓ of biogas. Each reactor was loaded with an effective 30 g of total COD, so the conversion rates were low. Analysis of the volatile fatty acid (VFA) data showed some accumulation in the first days after initiation, but rapid depletion as it became clear that hydrolysis and acidogenesis were the rate limiting reactions. The pH across all the AD reactors, with the exception of one of those loaded with microcrystalline cellulose (Avicel), remained close to neutral. The pH initially decreased to below pH in the one Avicel fed reactor and this was associated with suppression of biogas formation and the accumulation of VFAs, particularly acetate. This result suggested that it might be possible to operate pre-treatment reactors under mildly acidic conditions to generate the required VFAs. The *Spirulina* fed digester could not replicate the encouraging data produced earlier, but this was attributed to the way the biomass had been processed, with the carryover of a substantial salt load into the digester.

A number of micro- and filamentous algal species were cultivated in the laboratory and outdoor conditions, harvested and tested as substrates for AD. Biogas generation improved after the microbial community had been given time to adapt to the particular substrates and partial hydrolysis of the algae by microwave treatment led to further improvement. The most encouraging data were generated using pre-treated *Parachlorella hussii* biomass, achieving solubilisation of approximately 25% of total COD and methane generation close to 70% of the theoretical maximum. However, there was no accumulation of VFAs in the reactor and the rate of VFA generation was still too low to be viable as a source of electron donor for sulphate reduction. Optimistic calculations of the volume of algal suspension that would need to be processed to produce enough soluble COD to remove 1500 mg/ℓ of sulphate from 10 000 ℓ of mine water per day (see discussion below) showed this was not a viable option.

Experiments performed to assess the potential of the accelerated hydrolysis of grass under acidic conditions yielded mixed results. A fermentative environment was established within the first week, even in reactors not deliberately inoculated and an increase in soluble COD and VFA concentrations were measured. The acidic conditions at the start of the experiments suppressed methanogenic activity and there was little evidence of biogas formation. Once again, the rates of hydrolysis and acidogenesis were slow. Mixing acidic water with the grass cuttings did result in the consumption of a significant amount of acidity and a rapid increase in pH in almost all reactors, with the exception of those started at pH 2 and pH 2.5. This phenomenon was repeated when synthetic and real mine water were tested, suggesting that pre-treatment through a grass bed could be used as a neutralisation step to create an environment more conducive for biological sulphate reduction. Complete removal of sulphate (2500 mg/ℓ) from real mine water was demonstrated in a reactor loaded with grass cuttings, but this took approximately 60 days with a maximum volumetric sulphate reduction rate of only 3.18 mg/ℓ.h.

The development of the hybrid linear flow channel reactor (LFCR) was more successful. The initial proof of concept study showed that simultaneous sulphate reduction and partial sulphide oxidation could be achieved in a single, passive reactor. Partial sulphide oxidation occurred within the floating sulphur biofilm (FSB), with deposition of elemental sulphur within the organic matrix. The combination of the slightly alkaline pH, absence of turbulent mixing and the presence of the FSB effectively controlled the evolution of hydrogen sulphide gas. The reactors were operated, uncovered, on a laboratory bench with no significant odour problems, despite aqueous sulphide concentrations as high as 250 mg/ℓ. The development of a harvesting screen, supported

just below the air-liquid interface, facilitated easy and effective harvesting of the FSB. A key component to the success of the hybrid reactor was maintaining a sufficiently high aqueous sulphide concentration in the bulk volume to consume all oxygen diffusing into the reactor in the time between biofilm disruption and re-forming (typically around 24 hours), thereby maintaining anoxic conditions and preventing inhibition of the sulphate reducing community.

The efficient retention of the sulphate reducing community, by attachment to the carbon micrfibres, meant that hybrid reactor could be successfully operated at hydraulic residence times as low as 12 hours, maintaining a sulphate reduction efficiency of around 70% (1 g/ℓ feed concentration) under conditions where washout was observed in conventional stirred tank reactors. A volumetric sulphate reduction rate of over 60 mg/ℓ.h was achieved in the hybrid LFCR at the 12 hour HRT.

The potential for the scale up of the hybrid LFCR was demonstrated, with the successful inoculation of a 2000 ℓ unit on a mine site. Complete biofilm formation was observed within 24 hours, with substantial sulphur deposition in the biofilm observed in the days that followed.

The performance of the hybrid LFCR, on lactate and acetate based media, was evaluated across a temperature range from 30˚C to 10˚C. A reduction in temperature had a negative effect on the rate of sulphate reduction and sulphide oxidation. Temperature had a more significant effect on the acetate fed system, with an almost 90% reduction in the sulphate reduction rate and conversion efficiency as a consequence of decreasing the temperature from 30˚C to 10˚C. The acetate fed reactor was generally less stable and predictable than the lactate fed reactors, indicating that acetate utilising species are more susceptible to a range of environmental factors.

The lactate fed reactors showed greater resilience, with the decrease in sulphate reduction rate closer to 50% over the temperature range tested. At 15˚C and below incomplete utilisation of lactate was observed, indicating that the lactate fermenting species are also significantly inhibited at low temperature.

Despite the presence of residual acetate and sulphate in the lactate fed systems there was no evidence to suggest supplementary sulphate reduction by acetate utilising species, suggesting they are effectively excluded from lactate fed systems.

An increase in aqueous sulphide in the effluent at low temperature suggests that the sulphide oxidisers are more significantly affected by low temperature, or that the disparity between volume (sulphate reduction occurs in the bulk volume) and surface area (partial sulphide oxidation occurs in the floating biofilm) assumes greater relevance at lower temperature.

The final component of the research involved a fundamental, academic study on whether there was any potential to incorporate microbial fuel cell (MFC) technology as part of a semi-passive mine water treatment system. The work showed the electricity generation was possible, using the sulphate reducing community and the LFCR configuration, albeit at very low efficiency. A maximum power density of 2.56 mW/m^2 of cathode area (9.10 mW/m^3) was achieved using a 1 kΩ resistor.

KEY CHALLENGE

The development and evaluation of the hybrid LFCR was very successful. This unit has potential for integration into passive or semi-passive systems to treat mining impacted water. However, the key challenge remains the consistent provision of sufficient electron donor and organic carbon to sustain sulphate reduction and sulphide oxidation. Research aimed at addressing this has been less successful.

The magnitude of the challenge can best be understood by way of an example. In order to reduce the sulphate concentration of a relatively low volume discharge (10 000 ℓ/day) from 2000 mg/ℓ to an acceptable 500 mg/ℓ requires the reduction of 15 kg of sulphate per day. Assuming an optimal COD to sulphate ratio of 0.7, this equates to a requirement of 10.5 kg of suitable COD per day.

Based on the data generated in this study on the digestion of algae, the most encouraging values were achieved using partially treated *P. Hussii*, with the liberation of 8.3 g/ℓ of soluble COD from a loading of 30 g/ℓ after two days, or 4.15 g/ℓ.day. This computes to 0.138 g soluble COD per g of algae per day. Assuming all

the liberated COD can be used optimally for sulphate reduction, the system would require a loading of 76.1 kg of algae per day. Using the maximum volumetric growth rate of 0.0111 g/ℓ.d for *P. Hussii* and a 100% harvesting efficiency it would take the processing of 6.85 Mℓ of algal suspension per day to produce sufficient COD. This is clearly not viable.

Similarly, data generated on the use of pasture grass to support biological sulphate reduction (WRC K5/2762 – in progress) suggest 3.7 g of partially dried (2 day old) grass was required to reduce 1 g of sulphate. Using the example above, this would equate to 55.5 kg of grass per day. *Erogrostis curvula* is the most popular pasture grass in the summer rainfall areas of South Africa and yields between 8 and 20 t/ha annually. Therefore, at least one hectare of pasture would be required to produce enough substrate to treat the 10 kℓ/d discharge. However, this ignores degradation kinetics, which are slow for grass. Data from this study show that just over 55 mg of soluble COD/g grass is released in the first 24 hours, after which the rate slows considerably. Using this COD liberation rate and the optimum COD:sulphate ratio, the requirement for grass becomes 191 kg/d or almost 70 t/year.

An additional challenge associated with complex substrates is that only a fraction of the available COD is readily available, so to prevent the system becoming severely constrained by the rate of hydrolysis (as is common in packed bed reactors) the turnover of fresh biomass needs to be high. This creates a problem of how to dispose of the partially degraded substrate. In a mine water treatment scenario the biomass is likely to be associated with potentially toxic metals, which have been adsorbed or precipitated onto the biomass, so could be considered a hazardous waste.

CONCLUSIONS AND RECOMMENDATIONS

The primary success of this research has been the development of the hybrid LFCR. The reactor was able to sustain high rates of sulphate reduction and partial sulphide oxidation, with relatively simple recovery of the biosulphur product, under passive conditions. The carbon fibres facilitated effective biomass retention, which allowed operation at dilution rates greater than the growth rate of sulphate reducers, without significant loss of efficiency due to washout. Under optimal conditions the volumetric sulphate reduction rate achieved was equivalent or higher to more complex, active reactor systems.

The research into the provision of a sustainable organic carbon source was less successful, with the result that the fully integrated system could not be evaluated, even at laboratory scale. Hydrolysis and acidogenesis cannot be sustained at the necessary rates, even under conditions that promote hydrolysis and suppress methanogenesis. Therefore, coupling the anaerobic digestion of complex organic substrates for the generation of renewable energy, to the treatment of mining impacted water using the digestate to provide the electron donor does not seem viable for the substrates evaluated, unless the anaerobic digesters are sufficiently large. This is primarily a consequence of the slow rate of hydrolysis.

The key to unlocking the potential of the hybrid LFCR as part of an integrated semi-passive system to treat mining impacted water remains overcoming the challenge of providing a sustainable electron donor and carbon source at the rate required. The substrates evaluated in this research are unlikely to meet the requirements. However, coal fines may provide a solution as they are readily available on coal mine sites, are far less bulky than alternatives and have an attractive COD to mass ratio. Further research into the biosolubilisation of coal fines is strongly recommended.

ACKNOWLEDGEMENTS

The project team wishes to thank the following people for their contributions to the project.

Reference Group	**Affiliation**
Dr Henry Roman	*Department of Science and Technology*
Dr Sashnee Raja	*University of the Witwatersrand*
Dr Rob Huddy	*University of Cape Town*
Ms Delia Raman	*Eskom*
Mr Phil Hobbs	*CSIR*
Ms R Mühlbauer	*Anglo American*
Ms Gail Nussey	*Sasol*
Mr Terry Harck	*Solution [H^+]*

CONTENTS

LIST OF FIGURES

LIST OF TABLES

ACRONYMS & ABBREVIATIONS

AD	Anaerobic digestion
ALD	Anoxic limestone drain
AMD	Acid mine drainage
ARD	Acid rock drainage
BSR	Bacterial sulphate reduction
COD	Chemical oxygen demand
CSTR	Continuously stirred tank reactor
HLPC	High performance liquid chromatography
HRT	Hydraulic retention time
LFCR	Linear flow channel reactor
MFC	Microbial fuel cell
PEM	Proton exchange membrane
SEM	Scanning electron microscopy
SRB	Sulphate reducing bacteria
VFA	Volatile fatty acid
VSLR	Volumetric sulphate loading rate
VSRR	Volumetric sulphate reduction rate

This page was intentionally left blank

CHAPTER 1: LITERATURE REVIEW

1.1 INTRODUCTION

The project aims to develop an integrated semi-passive system for the treatment of acid rock drainage (ARD) originating from diffuse sources, such as waste rock dumps, coal discards, tailings impoundments and low-volume discharges. The technology is not aimed at treating high-volume discharges that are actively pumped from underground basins.

Specifically, the project will draw on recent research that aims two address three of the primary constraints that have prevented the more widespread implementation of technologies based on biological sulphate reduction. These are the high cost of the organic electron donor, the retention of biomass within the sulphate reducing unit and the management of the sulphide product.

Recent research, support by the Water Research Commission (Projects K5/2109 and K5/2110), demonstrated that the digestate from the anaerobic digestion (AD) of microalgae contained sufficient soluble COD and a suitable volatile fatty acid (VFA) profile to sustain biological sulphate reduction at rates equivalent to those achieved using more traditional electron donors. This project will assess a variety of potential complex organic substrates for their potential as feedstocks for AD, with particular interest in the composition of the digestate.

The primary focus of the project is the development and optimisation of a modified linear flow channel reactor (LFCR) which is capable of good biomass retention and the simultaneous reduction of sulphate and partial oxidation of the sulphide product to elemental sulphur. The sulphide oxidation occurs in a floating sulphur biofilm, which can be harvested and the sulphur recovered as a value-adding product. Extensive research into the reactor configuration and sulphide oxidation has been conducted over the past five years, so the potential for sulphur recovery has been demonstrated. The nature of the fluid flow within the reactor results in very little turbulent mixing, allowing for the development of discrete anaerobic and microaerobic zones, which suggest that the sulphate reducing and sulphide oxidising reactions can be spatially separated. The attachment of sulphate reducing species to carbon microfibres will help to maintain a high biomass concentration and retain them within the anaerobic part of the reactor. Evidence of partial sulphide oxidation and the formation of a sulphur biofilm in purpose built sulphate reducing channel reactors have been shown, suggesting the combined reactor is viable.

The final component of the project is to evaluate the potential for renewable energy generation as an additional benefit. Energy security is a critical issue in South Africa and the system has the potential to provide some energy to surrounding communities, in the form of biogas from the anaerobic digestion and potentially electricity from microbial fuel cells (MFC). Anaerobic digestion is a mature technology, so the focus of the current project will be to quantify the biogas potential of the suggested feedstocks, bearing in mind that the primary objective of the AD unit is to generate suitable electron donors for the sulphate reduction. The MFC component represents the most “blue sky” aspect of the project and is based on published literature describing the use of sulphate reducing species in MFCs and the potential for the carbon fibres, to which the sulphate reducers attach, to act as electrodes in an MFC.

1.2 GENERATION OF ACID ROCK DRAINAGE

Acidic minewater is derived from the exposure of sulphidic minerals to both oxygen and water as a consequence of mining and the processing of metal ores and coal (Johnson and Hallberg, 2005). These waters are generally classified according to their origin, with minewater originating from the rebound of groundwater through mined underground workings referred to as acid mine drainage (AMD), while flows

originating from sulphide minerals exposed at the surface, through natural weathering, or in the form of tailings, waste rock, ore stockpiles and coal discards are referred to as acid rock drainage (ARD).

Acid minewaters may be generated abiotically, through chemical weathering, but the presence of iron and sulphur oxidising microorganisms can increase the kinetics of the process up to a thousand-fold. The reactions involved are detailed below (Equations 1-4) (Akcil and Koldas, 2006).

$$FeS_2 + \frac{7}{2}O_2 + H_2O \rightarrow Fe^{2+} + 2SO_4^{2-} + 2H^+ \quad \text{Equation 1}$$

$$Fe^{2+} + \frac{1}{4}O_2 + H^+ \rightarrow Fe^{3+} + \frac{1}{2}H_2O \quad \text{Equation 2}$$

$$Fe^{3+} + 3H_2O \rightarrow Fe(OH)_3 + 3H^+ \quad \text{Equation 3}$$

$$FeS_2 + 14Fe^{3+} + 8H_2O \rightarrow 15Fe^{3+} + 2SO_4^{2-} + 16H^+ \quad \text{Equation 4}$$

Pyrite (FeS_2) is the most abundant sulphide mineral and is the primary mineral responsible for the generation of acidic drainage water. The process is initiated by weathering and oxidation (Equation 1) at a neutral pH. The first reaction is abiotic. The reaction described by Equation 2 may be abiotic, but occurs slowly under acidic conditions in the absence of catalytic microorganisms. The rate of reaction is significantly enhanced when the second reaction is catalysed by aerobic iron-oxidising bacteria such as *Acidithiobacillus ferrooxidans, Leptospirillum ferroxidans* and *Leptospirillum ferriphilum* (Zagury *et al*., 2007; Johnson and Hallberg, 2003).

These particular bacteria are characterised as acidophilic, aerobic, chemoautotrophic species which are most active between pH 1.0 and pH 3.5. The iron-oxidisers are capable of increasing the rate of Fe^{2+} oxidation (Equation 2) by several orders of magnitude (Gazea *et al*., 1996). Ferric iron has limited solubility and if the pH is higher than pH 2.3-3.5, it precipitates as oxyhydroxide, releasing H^+ and therefore lowers the pH as per Equation 3 (Zagury *et al*., 2007). The oxyhydroxide precipitate gives water a red-orange colour, which is a common characteristic of ARD discharge.

In addition to the oxidative reactions, the ferric ions may react with more pyrite (Equation 4), or other sulphide minerals, producing more ferrous iron to drive Equation 2. In the presence of sufficient dissolved oxygen, a continuous cycle is maintained (Johnson and Hallberg, 2003). The process becomes self-sustaining as the pH continues to decrease, as more ferric iron will remain in solution to chemically attack the pyrite.

A second group of microorganisms, capable of oxidising reduced sulphur species, are typically found in these environments and contribute to AMD formation. This group, which includes *Acidithiobacillus thiooxidans* and *Acidithiobacillus caldus*, utilises reduced sulphur species as the electron donor to produce sulphate and protons. The proton acidity contributes to the low pH which typically characterises acid minewater. A consequence of the low pH is the dissolution of acid-labile minerals, leading to the further release of heavy metals and ions contributing to salinity.

South Africa faces a significant threat from both AMD and ARD, although the former has received the bulk of the attention from Government, the media, most mining companies and companies involved in the development and implementation of treatment options. In South Africa, AMD is associated with groundwater rebound through abandoned underground mine workings, primarily from the gold mining impacted basins of the Witwatersrand. This process results in high volumes (several 100 Mℓ/day) of heavily impacted water. The most appropriate management strategy is to pump and treat using conventional, active processes such as the high density sludge process, followed by reverse osmosis.

The second type, ARD, originates from diffuse sources, primarily associated with the coal industry in South Africa. These sources include waste rock dumps, spoil heaps and open pits. The volume of these discharges is significantly lower than those from the underground basins, but may vary substantially depending on the site. However, given the number of potential sites, AMD from diffuse sources will

affect a far greater area and may persist for a longer period. The nature of these discharges makes it feasible for remediation by passive and semi-passive options.

1.3 TREATMENT TECHNOLOGIES

A variety of technologies have been developed for the treatment of AMD and ARD. The established methods are based on oxidation, neutralisation, precipitation and sedimentation. The oxidation converts iron and aluminium to their less soluble oxidised form, which makes subsequent precipitation more efficient.

The most appropriate treatment is dependent upon the volume of the effluent, concentration type of contaminants and the pH of the water (Gazea *et al*., 1996). Acid drainage treatment technologies can be divided into two broad categories, active and passive treatment systems.

1.3.1 Active treatment technologies

Active treatment typically involves the installation of agitated reactors or similar units, which require constant energy input. Furthermore, the addition of alkaline chemicals and reagents to treat the acidic effluent can become costly, given that the drainage may persist for several decades, or longer, at decommissioned mine sites (Gazea *et al*., 1996). Many of the active treatment technologies depend on the addition of lime or limestone, which are non-renewable resources. Lime addition to sulphate rich effluents typically results in substantial gypsum precipitation, which needs to be managed. The long-term sustainability of many active treatment technologies is therefore questionable, both from an economic and environmental perspective. There is a diverse range of active treatment technologies, such as chemical precipitation, ion-exchange, membrane technology and biological sulphate reduction.

1.3.1.1 Chemical treatment

The most commonly used chemical treatment method is the addition of an alkaline material to raise the pH, in conjunction with aeration, to accelerate the rate of chemical oxidation of ferrous iron. The most common reagents are lime ($Ca(OH)_2$), slaked lime, calcium carbonate ($CaCO_3$), sodium carbonate (Na_2CO_3) or sodium hydroxide (NaOH). However, each compound varies in cost and effectiveness and therefore the preferred agents are generally lime or calcium oxide, due to economic concerns (Johnson and Hallberg, 2005). Liming as a treatment process is effective in the removal of sulphate to the saturation level of gypsum ($CaSO_4.2H_2O$) and neutralisation of acidity (Equations 5 and 6) as well as the precipitation of dissolved metals as metal hydroxides. However, the resulting sludge (gypsum and metal hydroxides) is voluminous and unstable at a low pH, leading to resolubilisation of the metal hydroxides (reverse of Equation 7) (Lorax International, 2003). The major disadvantage of these treatment processes are the production and disposal of the sludge and the high cost of chemicals (Lorax International, 2003; Johnson and Hallberg, 2005).

$$Ca(OH)_2 + H_2SO_4 \rightarrow CaSO_4.2H_2O(s) \quad \text{Equation 5}$$

$$CaCO_3 + H_2O + H_2SO_4 \rightarrow CaSO_4.2H_2O + CO_2 \quad \text{Equation 6}$$

$$Ca(OH)_2 + H_2SO_4 + Me \rightarrow 2H^+ + CaSO_4 + Me(OH)_2 \quad \text{Equation 7}$$

The high density sludge (HDS) process represents a technological advancement over conventional chemical technologies. It makes use of iron oxide seeds, which are added to the neutralisation reactor. The seeds promote secondary nucleation which results in the deposition of new precipitate on the existing particles. This enhances the precipitation process and leads to the formation of a denser, more granular sludge which significantly enhances the solid-liquid separation efficiency (Loewenthal *et al*.,

2001; Hove *et al.*, 2009). The HDS process has been selected as the initial step for the management of AMD from the dewatering of the Witwatersrand basins.

1.3.1.2 Adsorption and ion-exchange

Adsorption refers to the binding of charged species in solution to reactive groups, with opposite charge, on a solid support. The technology was widely investigated for the polishing of residual heavy metals from partially treated waste streams, with much of the focus on using biologically derived adsorbents. Despite the body of research this technology has found very limited application.

Ion-exchange refers to the replacement of a particular ion or group of ions in solution with more benign or desirable counter-ions that balance the surface charge of the solid exchanger. The resins are derived from both natural (zeolite) and synthetic (synthetic polymers) sources. They may be manufactured to contain single or multiple functional groups, depending on the application (Chiarle *et al.*, 2000).

The GYP-CIX process is an example of an ion exchange technology developed specifically to treat AMD, whereby the cations (Ca^{2+}) are removed from the water via several fluidised contacting stages with a strong acid cation resin. Thereafter the anions (SO_4^{2-}) are removed via a weak base anion resin, resulting in a treated water product with a neutral pH with very little dissolved sulphates, metals and other substances. Thereafter the resin is regenerated and recycled with the only by-product being the gypsum sludge (Lorax International, 2003; Feng *et al.*, 2000). The process was evaluated in a 2001 study by Schoeman and Steyn as one of three potential options for the treatment of AMD at the Grootvlei mine. In addition, it was one of the 13 processes evaluated during stage 1 selection for the Emalahleni Water Reclamation plant, but was not considered for further evaluation (Günther and Mey, 2008). More recently Earth Metallurgical Solutions has proposed an ion exchange based process for the treatment of AMD in Gauteng. Richard Doyle, the CEO, was quoted in Mining Weekly (19 November 2010) saying that the company had recently completed trials which indicated that AMD and associated reverse osmosis (RO) brines could be treated to produce potable water and high value products such as explosive components and thermal salts. The article implied that value recovery from AMD made process commercially viable.

1.3.1.3 Membrane technology

The two commercial technologies which utilise membranes in mine water treatment, are reverse osmosis and electrodialysis. Electrodialysis involves an electric potential being utilised to move dissolved ions through a selectively permeable membrane. Similarly, reverse osmosis involves the forceful movement of water through a semi-permeable membrane (which excludes all but pure water) via high-pressure pumps. Reverse osmosis is a very flexible technology in that it can treat numerous types of wastewater. However, the membrane may be severely affected by fouling, depending on the quality of the feed water (Lorax International, 2003). Reverse osmosis has emerged as the technology of choice for second stage treatment of AMD in South Africa, following an initial neutralisation and precipitation step, and has been employed at the Emalahleni Water Reclamation Plant for several years, achieving very high water recoveries (Günther and Naidu, 2008). Despite the high water recoveries, a substantial amount of hypersaline brine is produced which needs to be managed. This, together with the lime and energy requirements means the process remains costly. Eutectic freeze crystallisation is being considered as an option to assist with brine management (Nathoo *et al.*, 2009).

1.3.1.4 Biological sulphate reduction (BSR)

Biological sulphate reduction (BSR) has the potential to be a more economical alternative to the costly physical and chemical processes described above. This technology is essentially dependent on the

ability of anaerobic sulphate reducing bacteria (SRB) to utilise sulphate as their terminal electron acceptor. Most SRB are heterotrophic and require an organic carbon source (volatile fatty acid or short chain alcohol) as the electron donor. A small number of autotrophic species exist that are able to utilise hydrogen as the electron donor and fix carbon dioxide. Sulphate reduction may be assimilatory, where the sulphide is incorporated in sulphur-containing amino acids, or dissimilatory, where the sulphide is released to the external medium. The latter process forms the basis of AMD remediation processes as it is not directly linked to biomass growth. A generalised reaction for dissimilatory sulphate reduction is shown below (Zagury *et al*., 2007; Oyekola, 2008).

$$2CH_2O + SO_4^{2-} \rightarrow 2HCO_3^- + H_2S \qquad \text{Equation 8}$$

Whilst the sulphate is reduced to sulphide there is the simultaneous generation of alkalinity, predominantly as bicarbonate (HCO_3^-). From an ARD treatment perspective the alkalinity acts to neutralise the acidity while the sulphide is available for the precipitation of metals as metal sulphides (Johnson and Hallberg, 2005). Metal sulphides are particularly insoluble, even at relatively low pH values and produce more compact precipitates than hydroxide equivalents. Theoretically, sulphide precipitation is a highly effective method to reduce heavy metal concentrations to insignificant levels and thermodynamic data suggest that individual metal sulphides can be sequentially precipitated by adjusting the pH (Hammack *et al*., 1993). However, the extremely high supersaturation induced by the low solubility promotes primary nucleation, resulting in the precipitation of a large number of very small (< 0.2 µm) particles, complicating downstream separation (Mokone *et al.,* 2010).

Sulphide is a toxic, corrosive and malodorous compound which needs to be removed from the treated effluent prior to ultimate discharge. While metal sulphide precipitation can potentially remove a portion of the sulphide, the fact that most ARD is derived from pyrite (FeS_2) means that if the sulphate reduction process is more than 50% efficient there will always be residual sulphide. In reality the residual sulphide is normally significantly higher as the majority of the iron is removed prior to the sulphate reduction step. One attractive option for the management of residual sulphide is the partial oxidation to elemental sulphur, which can be recovered as a value adding product. This has been achieved in an active process (Janssen *et al*., 1995) and more recently in a passive system (van Hille and Mooruth, 2011; Molwantwa and Rose, 2013).

1.3.2 Passive/semi-passive treatment technologies

Natural processes typically ameliorate ARD pollution. As the contaminated water flows through the receiving systems the toxicity is remediated naturally as a result of chemical and biological reactions and dilution with uncontaminated waters. These phenomena formed the basis for the development of passive treatment technologies, which depend on naturally occurring chemical and biological reactions. Ideally these systems require no further addition of chemicals and little or no operational and maintenance inputs. Passive systems depend on processes that are kinetically slower than those involved in active systems and thus require longer hydraulic retention times (HRTs) and larger areas to achieve similar results (Hedin *et al*., 1994). As a consequence the application of passive systems tends to be limited to low volume, relatively benign wastewaters, typical of the juvenile acidity phase of AMD and to ARD from diffuse sources or at end-of-pipe from certain processes.

The interest in passive systems was sparked by research in the late 1980s which indicated that natural *Sphagnum* wetlands improved the quality of mine drainage without incurring any obvious ecological damage (Wieder and Lang, 1992). A number of experimental wetlands were constructed to mimic the *Sphagnum* moss wetlands. However, *Sphagnum* moss was not readily available, proved difficult to transplant and had the tendency to accumulate heavy metals to toxic levels within a few months (Spratt and Wieder, 1988). Despite the initial setbacks research continued and a design evolved that proved tolerant to years of exposure to contaminated mine drainage and was effective at lowering the

concentration of dissolved metals. The systems typically consisted of a series of small wetlands (< 1 ha), vegetated with cattails (*Typha latifolia*) (Wieder, 1989).

During later development the importance of anaerobic processes in metal removal was recognised. It was found that in such situations a complex ecosystem was not required and treatment cells could operate effectively without plants. Recent evidence (White *et al*., 2011) suggests that plant derived organics actually reduce the efficiency of wetlands, primarily due to the complexation of metals by phenolic compounds.

Pre-treatment systems were also developed, where the acidic waters were contacted with limestone in an anoxic environment prior to entering the settling pond or wetland system (Gazea *et al*., 1996).

1.3.2.1 Anoxic limestone drains (ALDs)

Anoxic limestone drains are an alternative method of adding alkalinity to ARD and developed as a popular "pre-treatment" stage in passive systems (Younger, 1995). An ALD is essentially buried under several metres of clay and a plastic liner is placed as an additional gas barrier between the limestone and the clay soil. Hence the ALD is almost entirely sealed from atmospheric oxygen and the accumulation of CO_2 promoted. The ARD water is then directed downwards via a well to the limestone whilst minimising the amount of exposure to the atmosphere (Gazea *et al*., 1996).

It is imperative that the ferrous iron remain in its reduced form. If oxidised to ferric the iron precipitates as ferric hydroxide forming a layer on the surface of the limestone. This is known as "armouring" and significantly reduces the effectiveness of the limestone and its ability to dissolve. Furthermore the accumulation of carbon dioxide is encouraged as it accelerates the rate of dissolution of limestone and hence the rate of increase in concentration of alkalinity.

Therefore, in order for an ALD to be an effective treatment method the acidic water should have a low ferric iron (Fe^{3+} < 2 mg/ℓ) and aluminium concentration (Al^{3+} < 2 mg/ℓ) and a low dissolved oxygen concentration (DO < 1 mg/ℓ) in order to prevent armouring (Gazea *et al*., 1996; Johnson and Hallberg, 2005).

1.3.2.2 Wetlands

The use of wetlands as passive treatment method for ARD is a relatively low-cost alternative. However, it does require a large area of land and is a slow biological process. Wetland systems can be broadly divided into two categories, aerobic and anaerobic wetlands.

Aerobic wetlands have been used effectively to treat n*et al*kaline waters. These typically contain sufficient alkalinity to buffer the acidity produced by metal hydrolysis. The aerobic systems rely primarily on oxidation reactions and the metals precipitates as hydroxides, oxyhydroxides and oxides. Aerobic wetland cells are designed to retard the flow of water sufficiently for metal oxidation, hydrolysis, precipitation and settling of the precipitate to occur. The hydrolysis reactions release protons, which retard the oxidation rate if sufficient buffering is not available. In such cases crushed limestone may be added to maintain the pH between 5.5 and 6.5, which enhances the precipitation of oxidised iron, aluminium and manganese, the primary constituents of n*et al*kaline mine waters (Younger, 1995; Gazea *et al*., 1996).

The design of aerobic constructed wetlands is similar to natural wetlands. They consist of basins and channels with a relatively impermeable base to reduce seepage. The efficiency of aerobic wetlands is dependent on dissolved oxygen concentration, so the systems are designed to include features that enhance aeration, such as steps or waterfalls. Each aeration step provides sufficient oxygen to reduce the iron concentration by approximately 50 mg/ℓ (Hedin *et al.,* 1994). Aerobic wetlands are designed to

be shallow (10-50 cm) to further enhance aeration, but may include deeper (1-2 m) regions for sludge accumulation. The length to width ratio is typically 10 or greater to provide sufficient HRT.

Anaerobic or compost wetlands are mainly used in the treatment of acidic waters, whereby alkalinity is generated through bacterial activity and limestone dissolution. To encourage sulphate reduction a rich organic substrate (electron donor), such as peat, wood chips or cow manure is provided, typically in layers 30-45 cm thick (Gazea *et al*., 1996). A compost loading in the region of 250-300 kg/m^2 is normally used.

1.3.2.3 Semi-passive treatment options

The disadvantages of active treatment systems and enhanced sustainability of more passive systems has been highlighted in the preceding sections. In South Africa, the research into passive treatment options has focussed heavily on the development of passive anaerobic sulphate reduction technologies (Pulles *et al*., 2003). The research has been led by Pulles Howard and de Lange (PHD) and Golder Associates Africa (GAA), with contributions from a number of academic institutions, particularly Rhodes University, the University of Cape Town and the University of Pretoria and has addressed the problem at both a fundamental science and more applied pilot plant level (Pulles and Heath, 2009).

The programme addressed two primary challenges, the low sulphate reduction efficiencies reported for systems developed abroad and significant inhibition of existing systems at pH levels below pH 4.5.

The development of the IMPI process began in 1995, with the aim of developing a system that could achieve high rates of sulphate reduction over a sustained period, utilising lignocellulosic material as the source of electron donor. The hydrolysis of lignocellulose was identified as the rate limiting step. The long-term reactor studies that were undertaken as part of the programme allowed the characterisation of five distinct phases of sulphate reduction in passive systems (Coetser *et al*., 2005; Molwantwa *et al*., 2010). These were a lag phase (90-150 days), where the microbial community became established and adapted to the environment, a high performance phase (< 8 months), during which high rates of sulphate reduction were maintained, followed by a crash phase and finally a sustained phase, where relatively low rates of sulphate reduction were observed. Eventually, sulphate reduction ceased once all the hydrolysable lignocellulose had been consumed. Pulles and Heath (2009) suggested that many published studies were not conducted for long enough to reach the crash phase, resulting in optimistic projections of longer-term performance.

The initial target of the research was to develop a system capable of sustained sulphate reduction of over 600 mM/m^3.d, considered the threshold for economic viability. Based on the understanding that hydrolysis of lignocellulose was rate limiting, research was conducted to investigate the potential of pre-treatment, using white rot fungi to break down the lignin matrix. The technical feasibility of the system was demonstrated, but unfavourable economics led to the termination of the research.

The second approach, pursued in collaboration with Rhodes University, focussed on understanding the mechanisms of lignocellulose hydrolysis. The research suggested that the degradation of lignocellulose was enhanced under sulphidogenic conditions (Roman, 2006) and that the provision of some readily usable organic carbon (molasses) could significantly reduce the effect of the crash phase and enhance the level of sulphate reduction in phase 4 (sustained phase). These insights led to the development of the patented degrading packed bed reactor (DPBR), which formed the basis of the IMPI process (Figure 1). The DPBR has an optimised packing configuration, with layers of different carbon sources designed to ensure efficient performance. The upper part of the reactor is responsible for removing dissolved oxygen and generating sulphide and alkalinity, which the lower part of the reactor is the site of accelerated lignocelluose degradation and volatile fatty acid production. To ensure efficient operation the influent is typically supplemented with molasses (0.05-0.1%) as a readily utilisable carbon source (Coetser *et al*., 2005).

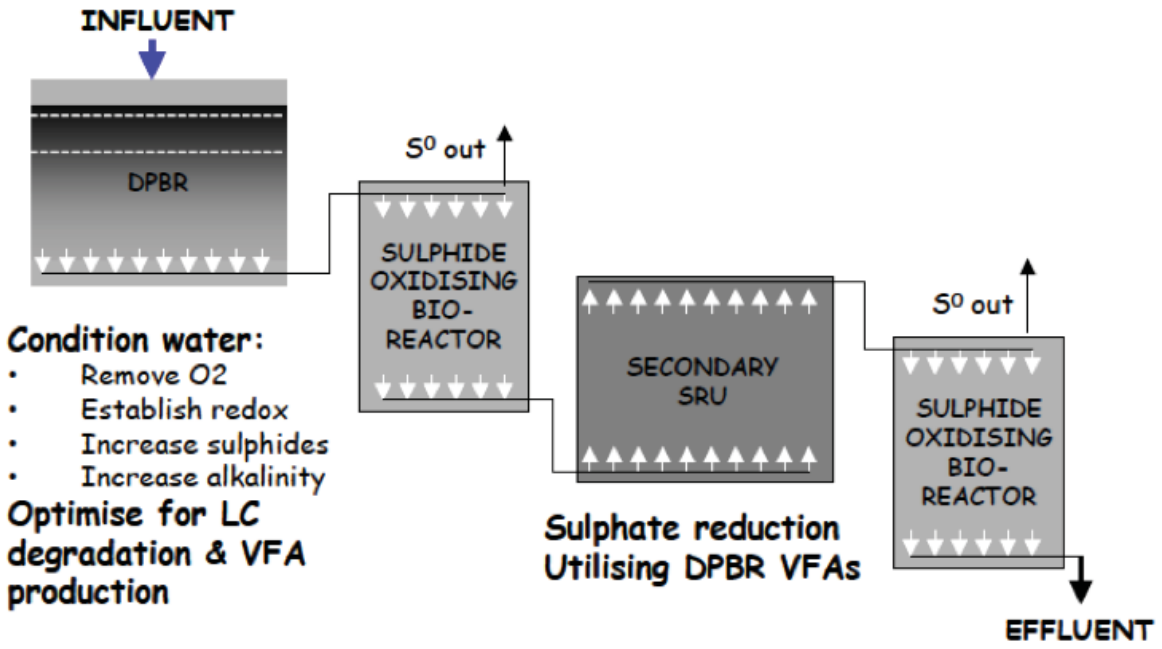

Figure 1: Schematic representation of the IMPI process (Pulles and Heath, 2009)

The overall configuration typically consisted of two sulphate reducing units, the DPBR and a secondary sulphate reduction unit, and two biological sulphide oxidising units which are operated under conditions that promote the partial oxidation of sulphide to elemental sulphur, rather than the complete oxidation back to sulphate. The sulphide oxidation units were not supplied with organic carbon.

A long term (4 years) study conducted at Vryheid Coronation Colliery (VCC) showed stable performance, with sulphate reduction rates significantly higher than the 600 mM/m^3.d target. Performance improved over the summer months, confirming the impact of temperature on sulphate reduction rate.

A full scale system, designed to treat 200 m^3 of minewater, was constructed at the Middelburg mine in Mpumalanga. The system contained a novel sulphide oxidation reactor, the linear flow channel reactor (LFCR) which made use of a floating sulphur biofilm to achieve partial oxidation of sulphide. The system was plagued by a number of construction and operational issues, as well as challenges with the LFCR and performance did not meet expectations. A detailed study into the LFCR was conducted at the University of Cape Town, leading to further optimisation in design and operating parameters (van Hille and Mooruth, 2013).

The passive bio-neutralisation programme was launched in 2003, with the aim of treating acid minewaters (pH <3). The patented DPBR formed the basis for the treatment system. A detailed microbial ecology study identified three distinct microbial communities and it was speculated that the success of the system depended on the interaction and tight special orientation of these communities. The first community was responsible for removing residual oxygen from the system and establishing the necessary redox environment (-250 to -350 mV). The second community, characterised by *Clostridium* species enabled the efficient degradation of lignocellulose and the generation of substrate, small charge-neutral carbon compounds, for the sulphate reducing bacteria than made up the third community. Alkalinity, in the form of bicarbonate, is generated following the oxidation of the organic electron donor, coupled to the sulphate reduction reaction. Laboratory scale tests, treating simulated minewater with an average pH of 3, have shown consistent performance over a six year period, with effluent pH values ranging between pH 5.5 and pH 7.

The evaluation of the medium to long term performance of the DPBR-based systems suggested that the liberation of organic carbon from the complex lignocellulosic material becomes the rate limiting step, ultimately governing sulphate reduction efficiency. As the system approaches the longer term steady state the concentration of organic carbon in the effluent stream becomes negligible, resulting in downstream processes becoming carbon deficient, unless additional carbon supplementation is included. This was identified as a challenge constraining the further development on the integrated process, so an alternative method of generating electron donor for the sulphate reduction and sulphide oxidation reactions was sought. The digestate from the anaerobic digestion of algae and other carbon sources offers potential.

1.4 ANAEROBIC DIGESTION

Anaerobic digestion is the term used to describe the biological process that leads to the ultimate gasification of organic carbon to carbon dioxide and methane, under anaerobic conditions. It has traditionally been used in the wastewater treatment industry to reduce both the volume and COD of waste sludge (Levin *et al.*, 2007). While these processes have been carried out for decades and in some cases the biogas has been converted to energy, interest in the economical recovery of fuel methane from industrial and agricultural wastes has only recently became a focus area (Nishio *et al.*, 2007).

Anaerobic digestion of complex organic substrates, such as agricultural residues, is a complex process, involving a number of different groups of microorganisms. A schematic representation of the process, typically consisting of four metabolic stages, is shown in Figure 2. Initially, particulate organic matter such as cellulose, hemicellulose, pectin and lignin are solubilised in a hydrolysis step, catalysed by extracellular enzymes. The soluble products of this stage are converted into organic acids, alcohol, hydrogen and carbon dioxide by acidogenic organisms. The simple organic substrates are further metabolised by acetogenic organisms to produce acetate, the primary organic substrate for methanogenesis, hydrogen and carbon dioxide. Aside from acetate, CO_2 and hydrogen methanogenic organisms may also directly ferment other substrates, of which formic acid and methanol are the most important (Bouallagui *et al.*, 2005).

As a technology anaerobic digestion offers a number of significant advantages over competing technologies for the treatment of carbonaceous industrial and agricultural effluents. These include low energy requirements, reduced sludge production and the possible economic recovery of energy. Despite these advantages the widespread commercialisation of this technology, particularly for energy recovery, is constrained by poor operational stability, typically associated with the inhibition of one or several the groups of microorganisms involved.

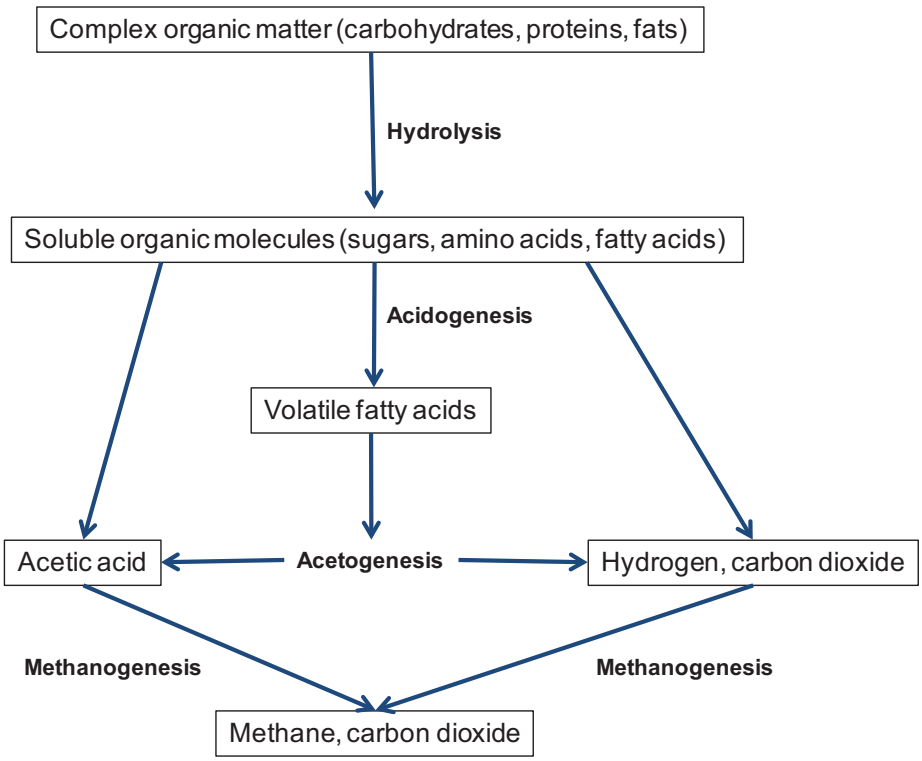

Figure 2: Sub-process associated with anaerobic digestion (adapted from Amaya *et al*., 2013)

1.4.1 Inhibition

The most common reason for poor performance is the inability to maintain the correct balance between acid forming and methane forming microbial communities. These two groups differ widely in their physiology, nutritional requirements, growth kinetics and susceptibility to environmental perturbations (Chen *et al.,* 2007). Inhibitory substances may be present at high concentrations in wastewaters and sludges, or may be formed during the initial phases of anaerobic digestion. Inhibition is typically identified by a decrease in steady state methane production and an accumulation of organic acids. The most significant inhibitors are discussed briefly below.

1.4.1.1 Ammonia

Ammonia is produced by the biological degradation of nitrogen-containing compounds, most commonly urea and proteins (Kayhanian, 1999). Its aqueous speciation is pH dependent, with the ammonium ion (NH_4^+) dominating at low pH and free ammonia (NH_3) under alkaline conditions. The free form is freely membrane permeable and has been suggested to be the primary source of inhibition, resulting in a proton imbalance or potassium deficiency (Gallert *et al.*, 1998). Of the organisms involved in anaerobic digestion, the methanogens are most susceptible to inhibition by ammonia (Kayhanian, 1994). The extent of inhibition is mediated by a number of factors, such as pH, temperature, the presence of antagonistic cations (Na^+, Ca^{2+}, Mg^{2+}) and acclimation, to the extent that literature values for 50% reduction in methane production vary from 1.7-14.0 g/ℓ total ammonia nitrogen (Chen *et al*., 2007).

1.4.1.2 Sulphide

Sulphate is a common constituent of many industrial and agricultural wastewaters. Under anaerobic conditions it is reduced to sulphide by sulphate reducing bacteria (SRB) (Hilton and Oleszkiewicz, 1988). Inhibition occurs at two levels, initially through competition for substrate and secondarily as a result of sulphide toxicity. SRB are not able to utilise complex organic carbon sources, so do not compete with hydrolytic or acidogenic microbes. Competition between SRB and acetogenic and

methanogenic bacteria has been observed, but results are often contradictory. The extent of competition appears related to the initial microbial concentrations and the COD/SO_4^{2-} ratio, with SRB dominating at COD/SO_4^{2-} ratios below 1.7, MPB above 2.7 and active competition occurring between the two (Choi and Rim, 1991). Temperature has also been shown to have an effect with SRB more likely to dominate at 37°C and MPB at 55°C (Colleran and Pender, 2002).

With respect to sulphide toxicity, there are considerable discrepancies in the published literature with respect to the nature of sulphide toxicity and the relative toxicity of dissociated and undissociated sulphide. Mechanistically, sulphide inhibits cellular activity by denaturing native proteins, interfering with coenzyme sulphide linkages and affecting assimilatory sulphide metabolism (Speece, 1983; Vogels *et al*., 1988). Unionised sulphide appears to play the dominant roles between pH 6.4 and 7.2, with total sulphide concentrations becoming more important above pH 7.8. Fermentative microbes are less susceptible to sulphide toxicity than acetogenic or SRB, with the MPB being the most susceptible (McCartney and Oleszkiewicz, 1991). For MPB the published IC_{50} values range between 50 and 250 mg/ℓ, depending on pH (Parkin *et al.*, 1983; Oleszkiewicz *et al*., 1989; McCartney and Oleszkiewicz, 1993). Sulphide removal and acclimation of MPB have been shown to improve AD performance.

1.4.1.3 Light metal ions

The effect of aluminium, calcium, magnesium, potassium and sodium on methanogenesis has been extensively studied (Chen *et al*., 2007). These ions may be present in the wastewater, be released by digestion of organic matter or be added for pH control. In all cases moderate amounts of the ions are required for growth, but excessive amounts are inhibitory. Excessive amounts of Ca and Mg affect the system primarily through the precipitation of carbonate and phosphate, resulting in the loss of essential nutrients and buffering capacity, as well as scaling of the microbes (Keenan *et al*., 1993; van Langerak *et al*., 1998). Potassium and sodium are more acutely toxic, given their role in maintaining membrane potential among other functions (Jarrell *et al*., 1984; Soto *et al*., 1991). The IC_{50} values reported in literature differ significantly due to matrix composition and degree of acclimation, but range between 0.15-0.74 M for potassium (Mouneimne *et al*., 2003) and 5.6-53 g/ℓ for sodium (Soto *et al*., 1993; Kim *et al*., 2000; Vallero *et al*., 2003a, b).

1.4.1.4 Heavy metal ions

Heavy metals may be present in significant concentrations in municipal sewage and sludge, as well as a number of industrial effluents. While these elements form essential components of enzyme that drive many anaerobic reactions they become acutely toxic at elevated concentrations (Sterrit and Lester, 1980). Significantly, they are not biodegradable and although present below toxic concentrations may be accumulated to inhibitory levels within the cells over time. The toxicity of heavy metals is affected by a number of factors such as form of the metal, pH and redox potential, but once again the methanogenic microbes are more susceptible than acetogens (Zayed and Winter, 2000). Published IC_{50} values vary considerably and appear particularly affected by solids content, which has a mitigating effect. However, the relative sensitivity of acidogenesis and methanogensis to heavy metals is Cu>Zn>Cr>Cd>Ni>Pb and Cd>Cu>Cr>Zn>Pb>Ni respectively (Lin, 1992; 1993).

1.4.1.5 Organics

A wide range of organic compounds have been found to be inhibitory to anaerobic processes. These are predominantly non-polar compounds which accumulate in bacterial membranes, resulting in swelling of the membranes, leakage of cellular components, disruption of ionic gradients and eventually cell lysis (Sikkema *et al*., 1994; Chen *et al*., 2007). The inhibition concentrations vary for specific compounds and are affected by the concentration of the compound, biomass concentration, exposure time, cell age, acclimation and temperature. Some of the major classes of inhibitory organic compounds are chlorophenols, halogenated aliphatics, N-substituted aromiatics, long chain fatty acids and lignin

and lignin related compounds (Chen *et al*., 2007). A number of these groups form important fractions of wastewaters and can have a significant impact on efficiency of biogas formation.

1.5 BIOLOGICAL SULPHATE REDUCTION UTILISING DIGESTER OVERFLOW

1.5.1 Anaerobic digestate

Anaerobic digestion incorporates a series of processes in which microorganisms break down biodegradable material in the absence of oxygen (McKendry, 2002). Anaerobic digestion technology is widely used to harness energy from renewable sources. This process produces methane (65-70%) and carbon dioxide (30-35%) rich biogas suitable for energy production, as an alternative to fossil fuels (Gunaseelan, 1997; McKendry, 2002). The biogas produced from anaerobic digestion can be utilised directly or indirectly to derive energy in a number of processes. Examples of these processes are: use in a combined heat and power unit (CHP) where the gas is combusted to produce heat and electricity; directly compressed or liquefied to produce a transport fuel (De Schamphelaire and Verstraete, 2009) or purified and used in the production of more traditional transport fuels such as petroleum or diesel (De Schamphelaire and Verstraete, 2009). The anaerobic digestion literature focuses primarily on biogas composition and yield per unit of substrate, with little consideration given to the composition of the digestate. Some studies report a residual COD value, but not a more detailed analysis.

The organic loading rate (OLR) determines the amount of volatile solids loaded into the digester. If the OLR is too high, the acidogenic bacteria proliferate, causing a decrease in pH and a low biogas production rate. Various OLRs have been reported in literature based on the amount of volatile solids (VS) per litre of material fed. The OLR is selected according to the type of substrate (e.g. low for high nitrogen organics) and reactor configuration (Speece, 1983). Typical ranges reported are 1.4-3.5 g VS/ℓ.day (Golueke *et al.,* 1957; Chen, 1987; Chandra *et al.*, 2006; Antonopoulou and Lyberatos, 2009). From the perspective of generating a substrate for biological sulphate reduction it may be beneficial to operate a digester at an OLR higher than the optimum for biogas production in order to produce a digestate with a high VFA load.

1.5.2 Anaerobic digestion of microalgae

There has been significant interest in the exploitation of microalgae for a number of potential applications in South Africa, given the favourable climatic conditions and wealth of indigenous species. There has been a particular focus on the potential of microalgae as a renewable energy source, both as a source of lipids for biodiesel production and as a substrate for anaerobic digestion.

Microalgae have a number of advantages over conventional sources of biomass for energy, as they have a greater productivity per unit area, can be cultivated on non-arable land, so don't impact on food security, and can potentially be grown on effluent water to improve the overall water quality. In addition to the generation of biomass, large scale cultivation of algae has the potential to assimilate significant amounts of carbon dioxide. As a result, a number of companies that are characterised by significant carbon emissions have expressed an interest in microalgal cultivation to offset their emissions.

A research programme was conducted at the University of Cape Town to assess the potential for biogas generation from the anaerobic digestion of microalgae (Inglesby, 2011). Part of the study involved tracking the rate and profile of volatile fatty acid liberation during batch anaerobic digestion and assessing the impact of mechanical pretreatment on this.

The research was focussed on *Spirulina sp.*, a filamentous cyanobacterium, and *Scenedesmus sp.,* a unicellular alga. Both species were isolated from natural environments in the Western Cape province of South Africa. The VFA liberation data for the whole cell biomass is summarised in Figure 3 and

shows rapid and extensive liberation of VFAs, particularly acetate, from the *Spirulina*, but significantly less from the *Scenedesmus.*

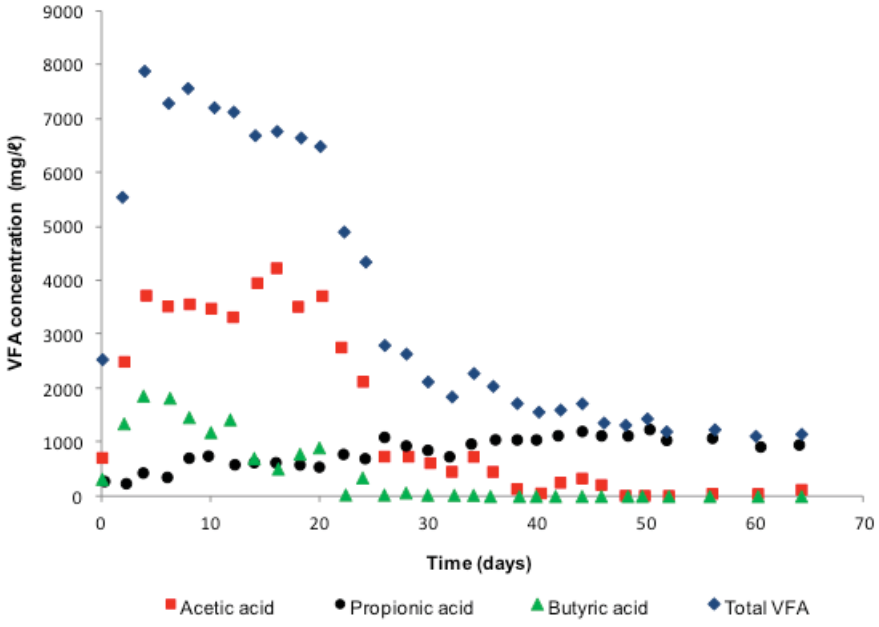

(a) *Spirulina* substrate loaded digesters

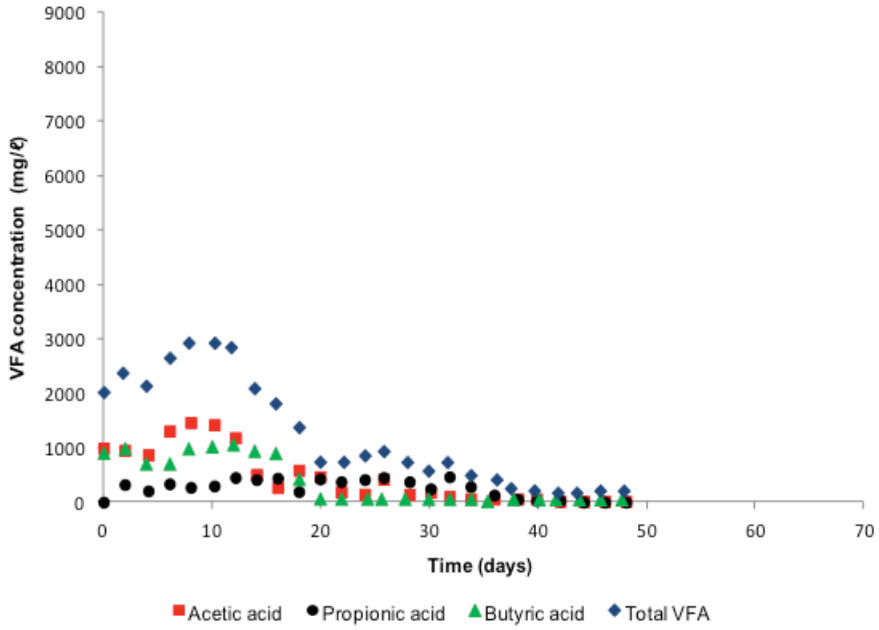

(b) *Scenedesmus* substrate loaded digesters

Figure 3: Volatile fatty acid liberation during batch anaerobic digestion of whole cell *Spirulina* and *Scenedesmus* biomass (Harrison *et al*., 2015)

This was attributed to the fact that *Spirulina* lacks a cellulosic cell wall, instead having a cell wall composed of protein and polysaccharide, which are easier to digest. In addition, *Spirulina* grows naturally in saline water and appeared to experience osmotic shock when transferred to the digester.

The digestibility of *Scenedesmus* was significantly enhanced by mechanical pretreatment using high pressure homogenisation (Figure 4).

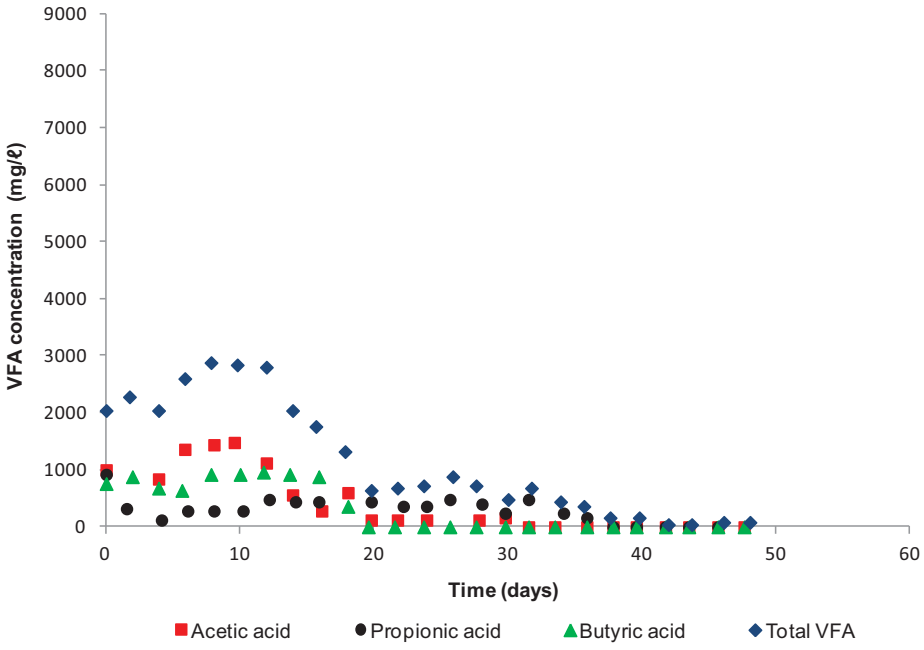

(a) *Scenedesmus* whole cell loaded digesters

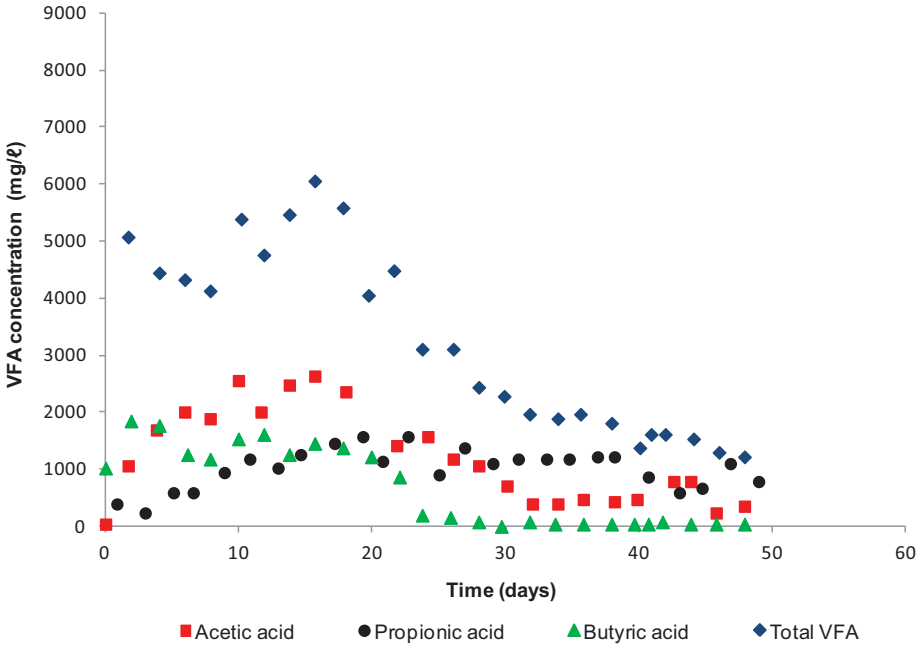

(b) *Scenedesmus* ruptured cell loaded digesters

Figure 4: Effect of mechanical pretreatment on the liberation of VFAs during the anaerobic digestion of *Scenedesmus* biomass (Harrison *et al*., 2015)

The anaerobic digestion study concluded with the operation of a 4 ℓ fed-batch digester fed every second day with *Spirulina* biomass. Although the organic loading rate was initially optimised to maximise biogas yield, the digestate recovered after fresh slurry was added still had a residual COD of 3-4 g/ℓ, comprised primarily of acetate and propionate. These VFAs can be utilised as electron donors for biological sulphate reduction and were subsequently tested in the 1 ℓ CSTRs.

The VSRR is the most relevant measure of reactor efficiency and the data for the digestate reactors are summarised in Figure 5. During steady state at the five day HRT the VSRR achieved in the 5 g/ℓ reactor (40.4 mg/ℓ.h) was double that achieved in the 2.5 g/ℓ reactor, reflecting the similar percentage

conversions. By contrast, the VSRRs achieved in the corresponding lactate-fed reactors were 11.3 mg/ℓ.h and 24.3 mg/ℓ.h for the 2.5 g/ℓ and 5 g/ℓ reactors respectively. Following the reduction of the HRT to four days, the VSRR for the 2.5 g/ℓ reactor increased to 25.5 mg/ℓ.h which is consistent with the linear increase observed in the 1 g/ℓ lactate-fed reactor. The VSRR for the 5 g/ℓ reactor also increased by a similar proportion, to 49.2 mg/ℓ.h. The data for the 2.5 g/ℓ reactor at the three day HRT were inconsistent, so a steady state value could not be derived. The performance of the 5 g/ℓ reactor was more consistent, with a mean VSRR of 62.4 mg/ℓ.h, which was substantially higher than the 27.7 mg/ℓ.h obtained in the corresponding lactate-fed reactor.

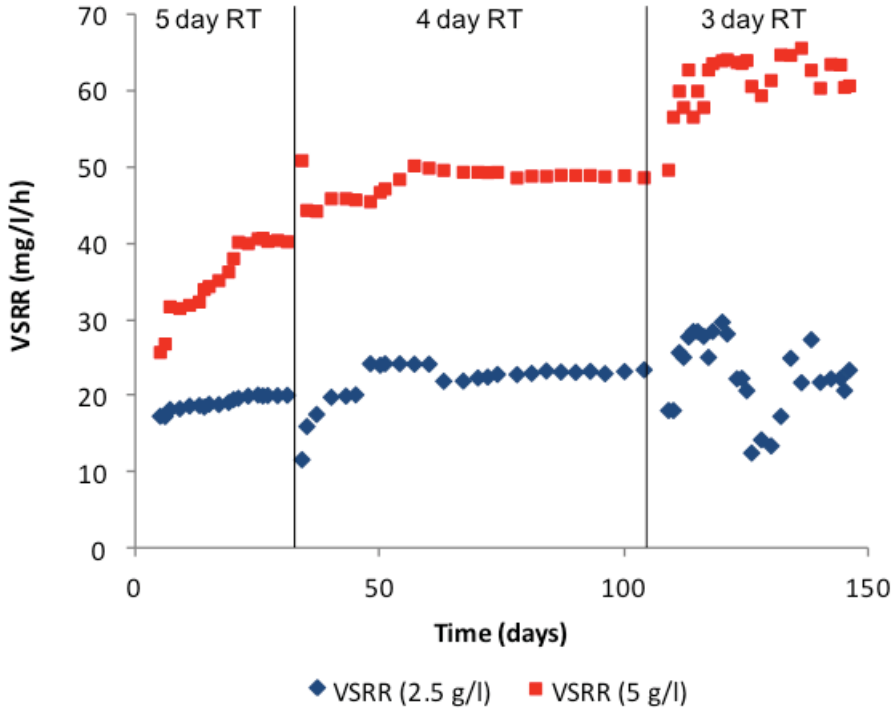

Figure 5: Volumetric sulphate reduction rates achieved in the two CSTRs at five, four and three day hydraulic residence times (RT) (Harrison *et al*., 2015)

The data suggested that consistent, high levels of sulphate reduction could be sustained using digestate from an anaerobic digester as the source of electron donor. It was found that providing organic carbon to the digester at slightly above the optimum organic loading rate, for biogas production, further increased the VFA content of the digestate.

1.6 BIOLOGICAL SULPHIDE OXIDATION

1.6.1 Sulphide chemistry

An efficiently operating sulphate reduction bioreactor produces an effluent with an elevated sulphide concentration. The sulphide may be used to effect metal precipitation, either within the reactor or in a subsequent step, but in many cases there is still residual sulphide. Consequently, a sulphide oxidation unit or similar process is required to remove the sulphide. The partial oxidation of sulphide to sulphur, such as in the SULFATEQ™ process. Such a unit is essential due to the toxic and harmful nature of sulphide.

Sulphides are essentially comprised of three chemical species $H_2S(aq)$, HS^- and S^{2-}. The H_2S that will be dealt with within the experimental system will predominantly occur in an aqueous or dissociated state. The following equations represent the equilibrium between the three species and is strongly

dependent on pH (pH=pK_i ; i = 1,2) (Kuhn *et al*., 1983; Chen and Morris, 1972; Broderius and Smith, 1977).

$$H_2S \rightleftharpoons H^+ + HS^-$$, pK1 = 6.97 - 7.06 (25˚C) Equation 9

$$HS^- \rightleftharpoons H^+ + S^{2-}$$, pK2 = 12.35 - 15 (25˚C) Equation 10

However, the dissociation constant of the second reaction is small (10^{-12}), therefore the possibility of sulphide existing as S^{2-} at the desired pH (7-8) is negligible (Broderius and Smith, 1977).

The partial oxidation of sulphide to elemental sulphur, the desired product in the floating sulphur biofilm occurs within a very narrow redox potential and pH window (Figure 6).

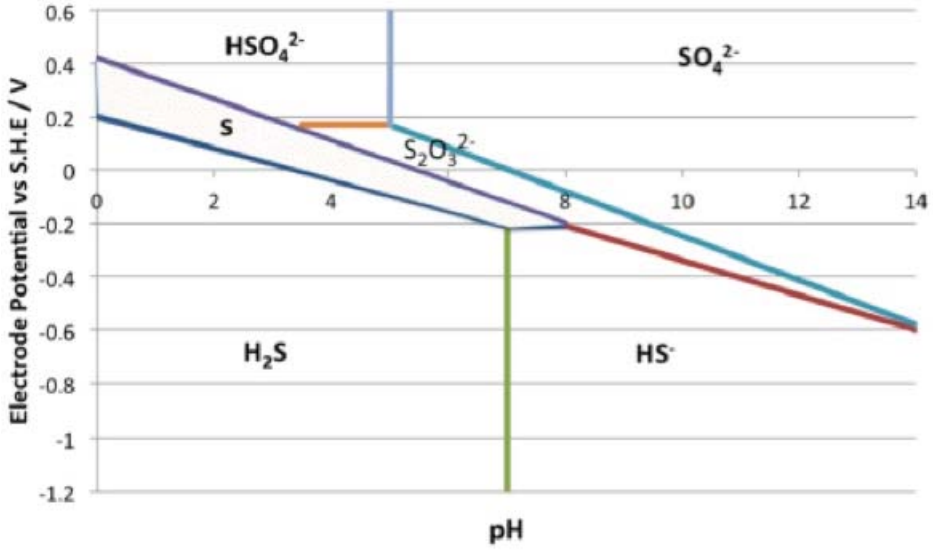

Figure 6: Potential-pH diagram for a sulphur/water system and 298.15K

In addition, the stoichiometric ratio of sulphide to oxygen needs to be maintained 2:1 in order to achieve the desired product. A stoichiometric excess of oxygen will drive the oxidation of both sulphide and elemental sulphur to completion, producing sulphate and acid. From an energetic perspective the complete oxidation of sulphide is far more favourable for sulphur oxidising microbes, so control of oxygen supply is critical.

Sulphide oxidation is a complex process, with competing chemical and biological reactions at play. In addition, these are influenced by pH, redox potential and the presence of other sulphur intermediates.

1.6.2 Chemical sulphide oxidation

Wilmot *et al.* (1988) showed that chemical oxidation played just as significant a role as biological oxidation in the overall total oxidation of sulphides, within domestic wastewater treatment plants. Chemical oxidation accounted for 44-88% of the overall observed sulphide oxidation, with the variations occurring due to the choice of biological substrate influencing biological oxidation. Hence, the following section will highlight the importance of chemical oxidation and how this affects biological sulphide oxidation. The mechanisms of chemical sulphide oxidation have been shown to be dependent on the pH, temperature, sulphide and oxygen concentrations and the presence of neutral salts (Kuhn *et al.*, 1983).

According to the stoichiometry in the following reaction, the required ratio of sulphide to oxygen is 2:1 for chemical sulphide oxidation to produce a sulphur product (Kuhn *et al*., 1983).

$$2HS^- + O_2 \rightarrow \frac{1}{4}S_8 + 2OH^-$$ Equation 11

$$2HS^- + 2O_2 \rightarrow H_2O + S_2O_3^{2-}$$ Equation 12

$$HS^- + 2O_2 \rightarrow SO_4^{2-} + H^+$$ Equation 13

$$HS^- + \frac{3}{2}O_2 \rightarrow HSO_3^-$$ Equation 14

$$SO_3^{2-} + \frac{1}{2}O_2 \rightarrow SO_4^{2-}$$ Equation 15

However, from Equation 12 it is evident that there is the possibility of thiosulphate formation, although this occurs at a low sulphide to oxygen ratio (1:1) and at a neutral or alkaline pH (Janssen *et al*., 1995; van den Bosch, 2008). The ratio of sulphide to oxygen has to be 2:1 or higher in order to limit sulphate formation via Equation 13. Sulphite formation, as an intermediate, is possible from the oxidation of sulphide. However, this is rapidly oxidised to a more stable product such as sulphate (Equations 14 and 15). In most chemical studies, thiosulphate and sulphate are the major stable oxidation products (Amend *et al.*, 2004).

1.6.2.1 Influence of pH

In acidic solutions (pH < 6), H_2S is the dominant sulphide species. However, as the pH increases to 8 so does the solubility of hydrogen sulphide (equation 9). Hydrogen sulphide (H_2S) is not readily oxidised so the rate of chemical oxidation is slow. As the pH increases, to a maximum of 8, so does the oxidation rate due to an increase in HS≠ concentration (Mamashela, 2002; Chen and Morris, 1972). Thereafter there is a three-fold decrease in the oxidation rate at pH 9, followed by a further increase to a second maximum, similar to the first, near pH 11(Chen and Morris, 1972).

The pH also plays a role in the disproportionation of S_0 particles as this leads to formation of HS^- and $S_2O_3^-$ under alkaline conditions, as per equation 16. Additionally at pH values > 9 more thiosulphate and sulphide are formed, due to the low chemical stability of sulphur in oxidation state (S0) (Kleinjan *et al*., 2005a; van den Bosch *et al*., 2008).

$$4S^0 + 4OH^- \rightarrow S_2O_3^{2-} + 2HS^- + H_2O$$ Equation 16

The pH also affects the equilibrium between sulphide and polysulphides. This will be discussed later.

1.6.2.2 Influence of temperature

Millero *et al*. (1987) showed that the oxidation of sulphide is a function of temperature at pH 8. The activation energy (ΔH*) was found to be 56 kJ/mol where, $\Delta H^* = (\frac{dlnk}{dT})RT^2$.

However, at pH 12 the ΔH* was lower at 46 kJ/mol. Zhang and Millero (1993) found that the rate constant increased with increasing temperature from 25-45˚C. This is expected, as the Arrhenius equation $\{k = k_0 \exp(\frac{-E_a}{RT})\}$ is a function of temperature.

1.6.3 Biological sulphide oxidation

In nature sulphur microorganisms play a vital role in the conversion of the various forms of sulphur. Sulphide can be biologically oxidised by denitrifying organisms, colourless bacteria (in the presence of oxygen) or anaerobically by *photosynthetic* bacteria (Buisman *et al*., 1989). Sulphide, polysulphides, thiosulphate, elemental sulphur, polythionates, bisulphite and sulphate are all inorganic sulphur compounds that can be utilised within a microbial community as an electron acceptor. This may occur via dissimilatory or assimilatory pathways (Lens *et al*., 2000).

Sulphide oxidising bacteria are chemoautotrophic and obtain their energy from the oxidation of sulphur compounds. Sulphide oxidising bacteria can be divided into two main groups viz. photosynthetic sulphur bacteria and colourless sulphur bacteria. Photosynthetic sulphur bacteria use sulphide as the electron

donor, CO_2 as the carbon source and the reaction is powered by light (Molwantwa, 2008). Colourless sulphur bacteria generally oxidise sulphide to sulphate, generating more metabolically useful energy that is obtained by partial oxidation to S_0 (Lens & Kuenen, 2001). In order to obtain sulphur as a product, sulphide oxidation must occur under stringent conditions, such as high sulphide loads, controlled redox potential and pH.

1.6.3.1 Ratio of sulphide to oxygen

In order to suppress sulphate production (equations 17 and 18) and promote sulphur formation the ratio of sulphide to oxygen must be strictly controlled. According to reaction stoichiometry two moles of sulphide would be required to one mole of oxygen (equation 19). Sulphate formation is preferred (by SOB) to the formation of elemental sulphur as it yields four times the energy (van den Bosch, 2008).

$$2S^0 + 3O_2 \rightarrow 2SO_4^{2-} + 2H^+ \qquad \text{Equation 17}$$

$$HS^- + 2O_2 \rightarrow SO_4^{2-} + H^+ \qquad \text{Equation 18}$$

$$2HS^- + O_2 \rightarrow 2S^0 + 2OH^- \qquad \text{Equation 19}$$

According to Buisman *et al*. (1990a), in order to minimise sulphate production the sulphide load must be in excess than that of the oxygen concentration. Therefore the ratio of sulphide to oxygen should be 2:1 or higher (equation 19). Janssen *et al*. (1995) demonstrated that when the oxygen supply was increased four-fold the reaction depicted in equation 18 was favoured.

Stefess (1993) and the groups of Buisman *et al*. (1990a) and Janssen *et al*. (1998) all concurred that the sulphide loading rate is an important factor in determining the sulphur production and sulphide oxidation rate; and that a substantial increase in sulphide concentration would inhibit sulphate formation. Additionally the ratio of sulphide to oxygen should be 2:1 or slightly higher. However, the sulphide loading must be controlled as an excessively high sulphide loading would inhibit microbial activity and thus affect sulphide oxidation (Buisman *et al*., 1991).

1.6.3.2 Interaction between chemical and biological sulphide oxidation

A high sulphide loading rate and high sulphide to oxygen ratio is necessary in order to favour elemental sulphur production. However, this can lead to thiosulphate formation via chemical sulphide oxidation. Under oxygen limited conditions the specific biological activity drops, due to a lack of oxygen. Consequently, chemical sulphide oxidation becomes more prominent, resulting in a large amount of sulphide being converted to thiosulphate (Janssen *et al*., 1995; Buisman *et al*., 1990a). Furthermore, the tendency toward thiosulphate formation is increased at low oxygen concentration, exceedingly high sulphide concentration (10 S_{tot}^{2-} : 1.1 O_2) and an alkaline pH 8 (Buisman *et al*., 1990a; Janssen *et al*., 1995; van den Bosch *et al*., 2008; van den Bosch, 2008). Hence, the formation of thiosulphate is inevitable, however if the ratio of sulphide to oxygen is maintained between 2:1 and 2.33:1 it can be minimised.

Gonzalez-Sanchez and Revah (2007) showed that the chemical oxidation of sulphide to sulphide intermediates has a positive effect on biological sulphide oxidation, until the sulphide concentration becomes too high (> 3 mM). A high inlet sulphide and low biomass concentration results in the inhibition of biomass growth and biological sulphide oxidation. The formation of polysulphides and sulphide intermediates also increased biological activity by decreasing the sulphide toxicity. Nonetheless, this was for a particular alkaliphilic sulfoxidising bacterial consortium within an alkaline environment (pH > 9) and might not be true at a neutral pH.

1.6.3.3 Biologically produced sulphur

Elemental sulphur is the element with the largest number of allotropes. Currently there are 30 well characterised sulphur allotropes (Steudel & Eckert, 2003). The most common and stable allotropes are

homocyclic non-polar molecules. This also gives sulphur its hydrophobic nature and very low solubility in water (5 µg/ℓ) (van den Bosch, 2008).

Biologically produced sulphur can be stored as globules within the cell or excreted as globules. In 1887, Winograndsky detailed how living cells such as *Beggiatoa* could contain amorphous sulphur inclusions, which would then disappear once H_2S became limiting. Furthermore, he postulated how these amorphous inclusions would crystallise once the cells died (Kleinjan and de Keizer, 2003). This was proven via X-ray diffraction (XRD), which showed that fresh sulphur globules were amorphous in nature, existed at the submicron scale and were extremely hydrophilic. It was concluded that the particles have high colloidal stability due to biological surface-active polymers/proteins which are secreted by the bacteria (Janssen *et al*., 1999; Kleinjan and de Keizer, 2003). It is assumed that these polymers play a role in the formation of larger sulphur aggregates, by sterical and electrical stabilisation of the colloidal particles (van den Bosch, 2008).

1.7 MICROBIAL FUEL CELLS

A microbial fuel cell (MFC) is an electrochemical device which makes use of the catalytic action of microorganisms to convert chemical energy to electrical energy (Kim *et al.,* 2002; Jang *et al*., 2004; Liu and Logan, 2004; Du *et al*., 2007; Jiang and Li, 2009). The microorganisms oxidise organic biodegradable substrate and recover the electrons to the anode of the MFC instead of a soluble electron acceptor. The electrons then travel through an external circuit and are consumed in a reduction reaction at the cathode electrode. Therefore in the closing of the circuit electricity is produced (Wang *et al.,* 2012, Sevda *et al.,* 2013, Jiang and Li, 2009).

Previously MFCs have typically had two chambers: the anode which houses the bacteria and the cathode, generally aqueous, into which air is bubbled so that oxygen can be reduced. The two compartments are separated by a proton exchange membrane (PEM) (Liu and Logan, 2004; Jang *et al*. 2004; Du *et al*., 2007; Sukkasem *et al*. 2011; Zhu *et al*. 2011).

The anodic chamber must be kept anaerobic in order to keep the microorganisms separated from oxygen and any other terminal electron acceptor other than the anode in order to achieve electrical current generation (Du *et al*., 2007)

Carbon dioxide is produced as a by-product of oxidation, however there is no net carbon emissions as the biomass in the substrate is considered to have been grown using carbon dioxide from the atmosphere (Du *et al*., 2007).

1.7.1 Status of microbial fuel cell development

The transfer of electrons to the anode electrode is often inefficient in terms of the rate of electron transfer seen by the low current generation and the proportion of electrons transferred which is noted in the low Coulombic yields produced. This is partly due to the non-conductive nature of the cell surface structures and previously mediators were often used to aid the transfer of electrons (Kim *et al.,* 2002; Du *et al*., 2007). The study by Kim *et al.* (2002) showed that mediator-less MFC could be operated using electrochemically active microbes capable of using the anode as an electron acceptor (anodophiles) (Du *et al*., 2007) which negated the need for mediators. This has been confirmed in subsequent studies (Liu and Logan, 2004; Du *al*., 2007).

Mediators are often toxic phenolic compounds and expensive (Liu and Logan, 2004; Jang *et al*., 2004; Ghangrekar and Shinde, 2007; Cha *et al.,* 2010) and therefore their use on a large scale is impractical. Significant expenses are also involved with PEMs (Liu and Logan, 2004; Jang *et al*. 2004; Sukkasem *et al*. 2011; Zhu *et al*. 2011) and these factors have contributed to the limited application of the MFCs commercially (Sukkasem *et al*., 2011). Much research has therefore been done on the operation of

mediator-less and membrane-less MFCs configurations for increased power generation and reduced construction and operating costs.

MFC are capable of generating enough electricity for use as small scale batteries and local area electricity generation (Kim *et al*., 2002; Rabaey *et al.*, 2005; Du *et al*., 2007). A prospective way to better utilise the low electricity generated by the cells is to store the electricity in rechargeable devices to be used elsewhere at a later stage once enough has been stored (Du *et al*., 2007). Most MFC studies thus far have been conducted at a laboratory scale with small volumes and expensive and fragile material and would need to developed further for scalability, high power output and low cost for real-world application (Jiang and Li, 2009)

Extensive research has been done into the use of MFC as wastewater treatment methods (Liu and Logan, 2004; Jang *et al*., 2004; Rabaey *et al.*, 2005; You *et al.*, 2007; Clauwaert *et al*., 2007 Ghangrekar and Shinde, 2007; Jiang and Li, 2009; Sukkasem *et al*., 2011; Zhu *et al*., 2011; Wang *et al.* 2012). MFCs are capable of higher chemical oxygen demand (COD) removal than anaerobic treatments with the same retention time (Sukkasem *et al*., 2011) and require less energy than aerobic treatments due to the aeration requirements (Sevda *et al*., 2013). The incorporation of MFCs into existing wastewater treatments, for example after anaerobic treatment, has also been noted (Wang *et al.,* 2012; Sevda *et al.,* 2013). MFCs have also been reported to be able to treat offshore marine sediments as well as sludge (Rabaey *et al.*, 2005; Su *et al*., 2013)

Use of MFCs as biosensors has also been noted (Kim *et al*., 2002; Jang *et al*., 2004; Du *et al.,* 2007) wherein the biological oxygen demand (BOD) of the wastewater can be measure by relating the amount of current produced by the cell and the Coulombic efficiency to the energy content of the wastewater. The sensors are reportedly accurate, stable and capable of good reducibility (Du *et al.,* 2007).

The use of MFC for the production of biohydrogen has been shown. An external potential must be applied in order to increase the cathode potential to combine electrons and protons from the anodic reaction to form hydrogen. However, it is much lower than the potential required for direct electrolysis of water and is a potentially greener method of hydrogen production (Du *et al*., 2007)

The following is a table of the power densities that different MFC configurations are capable of producing. It is noted that the basis on which power density is given is different for different journals and can be either electrode surface area, electrode compartment volume (sometimes given as the net volume) or total MFC volume particularly in the case of single compartment cells. In cases where the basis of the power density is not stated, it has not been specifically stated in the journal.

Table 1: Maximum power densities achieved using different MFC configurations

MFC Type	Maximum Power Density	System Specifics	Reference
Continuous Flow System in Tubular MFCs with GAC cathode	48 Wm^{-3} (NAC)*	$K_3Fe(CN)_6$ catholyte	Rabaey *et al*. (2005)
	65 Wm^{-3} (MFC)**	Air-cathode (Acetate enriched substrate)	Clauwaert *et al*. (2007)
	50.2 Wm^{-3} (NAC)*	Air-cathode	You *et al*. (2007)
Continuous Flow Systems in Tubular MFC with opposite end electrodes	1.3 mWm^{-2}	Glass bead and glass wool packing, aerated cathode	Jang *et al*. (2004)
	33.2 mWm^{-2} (SAC)***	No packing, deoxygenated feed, aerated cathode, up-flow	Zhu *et al*. (20110
	30 mWm^{-2} (SAC)***	No packing, aerated cathode, down-flow	Zhu *et al*. (20110
	10.9 mWm^{-2}	Glass bead and glass wool packing, aerated cathode	Ghangrekar and Shinde (2007)
Batch MFC	28 mWm^{-2} (SAA)****	Single chamber, air-cathode, with PEM	Liu and Logan (2004)
	146 mWm^{-2} (SAA)****	Single chamber, air-cathode, without PEM	Liu and Logan (2004)
	7.2 Wm^{-3}	Single chamber, air-cathode, no PEM, GAC anode	Jiang and Li (2009)
Integrated Systems	16.7 Wm^{-3}	MFC in Aeration Tank	Cha *et al*. (2010)
	6 Wm^{-3}	MFC-MBR	Wang *et al*. (2012)
	4.5 Wm^{-3} (TAC)*	MFC-SBR	Wang *et al*. (2014)

* Total anodic compartment
** Total volume of MFC
*** Surface area cathode
**** Surface area anode

1.7.2 Microbial fuel cell elements

1.7.2.1 Internal resistance

In the study conducted by Jiang and Li (2009) for a single-chamber MFC using granular activated carbon (GAC) as the anode, the internal resistance was found to increase more or less linearly as the electrode distance increased, i.e. the resistance is lower at a smaller distance. However the power density was found to reach a maximum at a distance of about 2cm. This maximum is believed to be due to the diffusion of oxygen from the cathode to the anode which inhibits the anaerobic respiration of the bacteria therefore outweighing the benefits of the continued decrease in resistance.

Jang *et al*. (2004) suggested keeping the electrodes as close as possible to each other to aid proton transfer. It was found that at higher resistance lower current was obtained for the electrode distances tested.

Zhu *et al*. (2011) also found the internal resistance of the cell to decrease as the distance between electrodes decreased, however the diffusion of oxygen to the anode was increased at a small distance which resulted in a maximum power density being achieved at an electrode distance of 10 cm.

Ghangrekar and Shinde (2007) conducted an experiment in which three graphite anodes were present in the anode compartment and distance between each anode and the cathode differed. The highest power density was produced by the anode closest to the cathode which is in agreement with previous studies (Jiang and Li, 2009; Jang *et al*., 2004; Zhu *et al*., 2011).

In the experiments conducted by Jiang and Li (2009), the single-chamber MFC was also run with multiple graphite rod electron collectors. This was done with the assumption that ohmic losses arise from the electrons having to travel from GAC particles far away from the graphite rod. The use of more rods could therefore potentially decrease the resistance in the cell. The multiple rod systems were also used to identify whether the anode or cathode was the limiting factor for power generation. It was found that the combined current produced in a multiple rod system was the same as that produced using only one rod, i.e. in a 4 rod system, each rod collected approximately one quarter of the current produced in a single rod. This indicates that the reduction at the cathode is limiting. The total power production of the cell decreased to approximately one quarter of the power production in a one anode system. It was however noted that the internal resistance of the cell decreased in the multiple rod systems.

1.7.2.2 Continuous flow systems

In the use of MFCs as wastewater treatment methods, it is considered that wastewater is constantly being produced in many applications industrially. If an industrial scale MFC was to be used to treat wastewater, it would be most sensible to use a continuous flow system (Rabaey *et al*., 2005; Wang *et al.,* 2012) as allowance would need to be made for storage if batch systems were used. Batch operation is also typically applied in two-compartment cells in which a PEM used and scale up is difficult (Du *et al.,* 2007)

Much research has been done into continuous flow MFC systems. Jang *et al*. (2004), Zhu *et al*. (2011), Ghangrekar and Shinde (2007), Rabaey *et al.* (2005), Clauwaert *et al*. (2007) and You at al. (2007) all conducted studies on continuous flow systems. In all cases the MFC was tubular in shape and the direction of flow was upwards (up-flow).

In the case of Jang *et al*. (2004) Zhu *et al*. (2011) and Ghangrekar and Shinde (2007), the anode is positioned at the bottom of the tubular MFC and the cathode is positioned at the top. Zhu *et al*. (2011) investigated the effect of downward flow from the cathode to the anode (down-flow) on the performance of the cell.

It was noted that the cell with the down-flow of wastewater produced a higher power output (approximately double) than the cell with up-flow. This was believed to have been due to non-productive oxidation of substrate and reduction of oxygen at the anode due to the DO in the influent at the anode in an up-flow system.

In the case of the fuel cells used in the investigations by Jang *et al*. (2004) and Ghangrekar and Shinde (2007) a packing material of glass beads and glass wool was used to separate the anode and cathode thereby making a MFC with two chambers. In the study conducted by Zhu *et al*. (2011) no packing material is used and the fuel cell consists of a single chamber. In a cell with no packing the organic compounds in the incoming influent are able to diffuse through the cell to be oxidised at the anode regardless of the direction of flow through the cell. In the case of a cell with two chambers it makes little sense to allow the influent to flow into the cathode chamber as the diffusion of the organic compounds would be hindered by the packing material resulting in a limiting step in current generation.

The MFC systems used by Rabaey *et al.* (2005), Clauwaert *et al*. (2007) and You *et al.* (2007) differ from those of Jang *et al.* (2004) Zhu *et al*. (2011) and Ghangrekar and Shinde (2007) in that the tubular cells are packed with a granular activated carbon (GAC) anode and surrounded by the cathode in the form of carbon cloth or felt.

Clauwaert *et al*. (2007) and You *et al.* (2007) make use of carbon felt air-cathodes coated with magnesium oxide and C/Pt powders respectively whereas Rabaey *et al.* (2005) used a ferricyanide catholyte solution. The advantage of having a cathode which surrounds the tubular fuel cell is that that a low internal resistance can be achieved by having a small distance between the anode and the cathode (You *et al*., 2007; Rabaey *et al.*, 2005)

1.7.2.3 Recirculation and accumulation

Rabaey *et al.* (2005) noted that in the MFC operating under continuous flow with recirculation, a significant lag phase in power generation was observed. This was explained by the need for the accumulation of biomass within the reactor. Initially oxygen diffuses through the air-cathode in large enough quantities to lower the anodic potential while at the same time removing COD from the wastewater. Once a biofilm has grown the influx of oxygen can be substantially reduced. It was noted that during the lag phase only about 20% of the removed COD by the cell was related to current which implies that the majority of the COD was removed through alternative electron acceptors or the accumulation of biomass in the reactor. Clauwaert *et al*. (2007) also noticed the lag phase associated with biofilm development,

It is reasonable to assume that if during the start-up of the MFC, it is not operated in batch mode to allow for the growth of the biofilm, recirculation is necessary in order to prevent washout of the inoculum and allow time for the biofilm to grow.

Rabaey *et al.* (2005) also noted that approximately 50% of the reactor volume is taken up by the electrode and at higher loading rates in the case of sludge there is less available space for biomass and the same power density outputs cannot be reached. It is therefore necessary to both remove insoluble organics from the reactor and to increase the specific area of the electrodes without volume losses. The recirculation of substrate may aid the accumulation insoluble organics in the fuel cell and will be a challenge in its continuous operation.

You *et al.* (2007) investigated the effects of recirculation rate on the performance of a tubular flow through MFC. It was noted that at a high COD loading, altering the recycle ratio had almost no effect on the power density produced and the internal resistance of the cell remained almost constant. However, at lower COD loading the power density increased significantly and internal resistance of the cell decreased with an increase in recycle ratio.

It was suggested that in low COD loading the fuel cell behaved like a mixed system with all areas being of similar substrate concentration at a higher a recycle ratio and as a plug flow reactor at low recycle ratios with the substrate being depleted along the length of the reactor. The recommendation is given to operate the cell at higher COD loading in order to reduce the amount of recirculation necessary as the substrate is not depleted along the length of the reactor.

As a result of the slow mass transfer rates of reactants and products, loss of potential due to unequal substrate distribution in the bulk liquid often occurs. The concentration gradient should be reduced by mean of mixing, bubbling or increased flow rate as in recirculation mentioned above. It must be noted however that currently the energy required for pumping fluid through the MFC is considerably larger than the power output of the cell. At present the primary advantage of these fuel cells is therefore wastewater treatment (Du *et al.,* 2007)

1.7.2.4 Aeration and air-cathodes

Zhu *et al*. (2011) attempted to avoid the non-productive oxidation of substrate due to oxygen reduction at the anode by attempting to deoxygenate the wastewater feed for the up-flow cell by purging with nitrogen. This reduced the amount of dissolved oxygen present at the anode and was found to improve the power output. Aeration at the cathode was then done for both the deoxygenated and non-deoxygenated up-flow feeds and found to improve the power output of both by approximately double. This shows the need for anaerobic anode and aerobic cathode conditions.

In MFCs with packing to separate chambers such as those used by Jang *et al*. (2004) and Ghangrekar and Shinde (2007), although there is no separate anolyte and catholyte, the barrier does provide a DO gradient for proper operation of the cell (Du *et al*., 2007)

Jang *et al*. (2004) conducted experiments on a MFC with an aqueous aerated cathode chamber. The aeration rate was altered and current produced was monitored. It was noted that initially there was an increase in the current produced with an increase in aeration rate before becoming almost constant where very little change in current was observed with an increase in aeration rate.

It was however noted that with an increase in aeration rate the COD of the effluent from the cathode compartment decreased significantly whereas the effluent COD of the anode remained reasonably constant. This implied that the organic compounds were oxidised through aerobic bacterial respiration. It was hypothesised that with the critical oxygen concentration of the cathode being significantly higher than that of the aerobic bacteria, the cathode reaction is restricted as a result of oxygen being used by the aerobic bacteria present when the DO concentration is lower than the critical DO concentration of the cathode.

Coulombic yield was very low throughout the experiment which was attributed to the poor cathode reaction. It was noted that if the critical oxygen concentration of the electrode was more comparable to that of the aerobic bacteria, the Coulombic yield might increase. This implies the need for improvement of cathode reaction. In addition these results indicated that a MFC is an efficient wastewater treatment method as a result of the significant removal of COD.

Liu and Logan (2004) state that the main disadvantage of a two-chambered fuel cell is the need to aerate the cathode chamber which is energy intensive. A study was conducted on a cell using an air-cathode with and without a PEM. Liu and Logan (2004) state that the power density achieved by the MFC without the PEM are larger than sediment fuel cells without PEMs and with aqueous cathodes and attribute this to the inefficiency of the aqueous cathode.

You *et al.* (2007) states that as a result of the ability of an air-cathode to use oxygen freely from air, in terms of sustainability and operating costs it is a good option. It is noted that air-cathodes used in tubular reactors where the anode and cathode are placed on opposite ends may be difficult to scale up as a result of the need for the electrodes to remain close to achieve the same electricity production.

Although the performance of a catholyte MFC cannot be matched with an air-cathode, catholyte cathodes are not good for scale-up. Platinum catalyst use on air-cathodes is also to be avoided due to the sensitivity of the catalyst to poisoning as well as the high costs involved (You *et al.*, 2007). This is discussed further below.

1.7.2.5 Chemical oxygen demand (COD) loading

Several studies have tested a range of COD loading values for the MFC influent and its effect on the performance of the cell (Rabaey *et al*. (2005); Clauwaert *et al.* (2007); Jiang and Li (2009); Zhu *et al*. (2011); Sukkasem *et al*. (2011); Wang *et al*. (2014)) It was found in several cases that the power density produced by the cell increases with an increase in COD of the tested substrate for the tested range (Clauwaert *et al.* (2007); Jiang and Li (2009); Zhu *et al*. (2011)) In some cases a maximum power density was achieved before an increase in COD loading resulted in a decrease in power density produced (Rabaey *et al*. (2005); Wang *et al*. (2014))

Rabaey *et al*. (2005), Jiang and Li (2009) and Wang *et al*. (2014) found that Coulombic efficiency decreased with an increase in COD. This was thought to be due to the consumption of substrates for fermentation or bacterial growth instead of electricity generation as much of the suspended bacteria have been found to be non-electricity generating species (Jiang and Li, 2009; Wang *et al*., 2014). It could also be as a result of the use of alternative electron acceptors instead of the anode (Rabaey *et al*., 2005). Jiang and Li (2009) found that the efficiency of COD removal increases with increased COD loading however Wang *et al*. (2014) and Sukkasem *et al*. (2011) found there to be a maximum removal before decreasing with increasing COD loading.

Jiang and Li (2009) and Wang *et al*. (2014) noted the internal resistance of the cell decreased with an increase in COD. Both studies thought this to be as a result of the increase in ionic strength at high substrate concentration which reduces ohmic losses.

1.7.2.6 Proton exchange membrane

The operation of a MFCs with and without a proton exchange membrane has been investigated by Liu and Logan (2004) and Jiang and Li (2009).

Liu and Logan (2004) conducted a study on a single chamber MFC operated with and without a PEM. In the cells with the PEM, the membrane was bonded directly to the platinum coated carbon cloth cathode electrode which was exposed directly to the air.

It was found that the cells with the PEM reached stable power generation much faster than the cells without, however a higher power density was reached for the cell without the PEM. The Coulombic efficiency however was higher for cells with PEMs which Liu and Logan (2004) attribute to loss of substrate due to oxidation and reduction with dissolved oxygen. However, it is mentioned that with oxygen diffusion could potentially be reduced by means of coating the side of cathode exposed to chamber or increased biofilm development.

Jiang and Li (2009) discovered that power density produced in the single-chamber MFC (with no PEM) produced the highest power density which was seven times that of the power density produced by the two-chamber MFC with a PEM. The configuration of the cells did however differ in that an air-cathode was used for the single chamber cells and an aqueous cathode was used in the dual chamber cell. The higher power density was attributed to both the absence of the PEM and the use of the air-cathode.

It is noted that it is sometimes necessary to separate the MFC into two compartments using a PEM in certain case such as cathodes using catholyte and bio-cathodes in which the cathodic bacteria require different conditions to the anodic bacteria

1.7.2.7 Improvements of the cathode reaction

Different electrode materials perform differently as result of having different activation polarisation losses (Du *et al.,* 2007). As a result the slow rates of the reduction reaction which has often been found to be the limiting step in electricity generation (Jang *et al.*, 2004; Du *et al*., 2007; Jiang and Li, 2009; Wang *et al*., 2014), it is often necessary to use catalysts or artificial electron mediators in the form of catholytes (He and Angenent, 2006) to reduce activation losses. Platinum is the most commonly used catalyst but is very expensive and susceptible to poisoning (He and Angenent, 2006; You *et al*., 2007; Rabaey *et al*., 2005)

Transition metals are often used as electron mediators between the cathode and oxygen as a result of the high rates of change between their possible redox states (He and Angenent, 2006) and can be in solid form on the cathode or liquid for as a catholyte. Catholytes such as potassium ferricyanide and potassium permanganate act as liquid-state electron acceptors and are often used. However due to the toxicity and need for regeneration of these chemicals, their use is impractical and unsustainable especially in scale up of the MFC (You *et al*., 2007; Rabaey *et al*., 2005).

Bio-cathodes are also capable of functioning as catalyst to assist in oxygen transfer and can potentially render metal catalysts or artificial electron mediators superfluous. Some aerobic microbes are capable of adopting the cathode as an electron donor and as a result catalyse the oxygen reduction reaction (Clauwaert *et al*., 2007; Cha *et al.,* 2010; Wang *et al*., 2014). Bio-cathodes can be beneficial over abiotic cathodes in terms of the cost of construction operation as sustainability. They are cheap and do not need to be replaced. In some cases microorganisms such as algae are cable of producing oxygen via photosynthesis and therefore eliminate the need for external oxygen supply (He and Angenent, 2006).

Bio-cathodes can be used in aerobic and anaerobic systems. In aerobic systems oxygen is used as the terminal electron acceptor whereas in anaerobic systems compounds such as nitrates, sulphates, iron and manganese an act as terminal electron acceptors. In two chambered fuel cells and anaerobic cathode eliminates the diffusion of oxygen to the anode through the PEM.

Sulphate reduction is considered due to the current work being done on sulphur reducing bacteria (SRB) in anaerobic reactors in the laboratory. It is noted that oxygen has a high redox potential whereas sulphur is far less easy to reduce (He and Angenent, 2006) however the SRB are treating sulphate wastewater and the possibility exists to take advantage of an existing process in which electrochemical reactions are already occurring.

Zhang *et al.* (2012) conducted a study in which the performance of three different cathode types were compared over a period of 400 days, namely a $K_3Fe(CN)_6$ catholyte, an air-cathode and an aerated bio-cathode. The catholyte and bio-cathode cells were dual-chambered cells separated by a PEM whereas the air-cathode cell was a single chamber.

It was noted that from the beginning of the experiment the bio-cathode MFC produced the highest voltage and power density followed by the catholyte and then the air-cathode cells. The voltage and power density produced by the cells with the catholyte and air-cathode decreased over the duration of the experiment whereas both initially increased dramatically for the cell with the bio-cathode before dropping slightly. The same trend occurred for the Coulombic efficiency in all cells. The bio-cathode cell was therefore found to generate the most electricity for the longest amount of time.

This was attributed to the internal resistances of the cells which increased with time for the catholyte and air-cathode cells but decreased for the bio-cathode cell. It was hypothesised that in the case of the catholyte fuel cell, the PEM and cathode were fouled with iron precipitation. In the case of the air-cathode, a biofilm formed on the cathode with overtime would grow. In both cases the diffusivity of protons from anode to cathode would be reduced and therefore increase internal resistance. For the bio-cathode cell the formation of the biofilm had the opposite effect by reducing resistance to charge transfer.

1.7.2.8 Temperature

The importance of maintaining a constant temperature throughout the duration of the fuel cell operation has been noted by several sources. Wang *et al*. (2012) conducted an experiment in which the current produced by the fuel cell fluctuated significantly with time which was attributed to the difference in day and night time temperatures.

Liu and Logan (2004) maintained a constant fuel cell temperature by conducting the experiment in a constant temperature room (30°C). Jiang and Li (2009) conducted experiments in an incubator (30°C). Zhu *et al.* (2011) made use of water bath to maintain a constant fuel cell temperature (30°C). You *et al.* (2007) conducted experiments at constant environmental conditions (25°C) and Ghangrekar and Shinde (2007) conducted experiments at room temperature with minimal fluctuations (29-33°C).

Du *et al*. (2007) propose that the biotransformation of substrate to electrons even at the maximum growth rate of microorganisms is slow as a result of the metabolism of the microorganisms. It is suggested to accelerate the reaction by operating at higher temperatures or using thermophilic microbial species.

When operating a MFC on an industrial scale, the system is most likely to outdoors and the ambient temperature is likely to fluctuate considerably. It is however possible to use insulation or a heating jacket to maintain a reasonably constant temperature.

On a laboratory scale, the size and shape of the fuel cell may make the use of a water bath unfeasible. The length of time for which the experiment will run also means pressure on public areas in the laboratory such as hot rooms. Depending of the heating requirements of the microorganisms in this

experiment, it may be possible to conduct the experiment at room temperature which is maintained reasonably constant by the use of air conditioning.

1.7.3 Integration of MFCs into wastewater treatment systems

1.7.3.1 Systems reported in literature

Wastewater produced in real-world applications contains various types of organic matter and bacteria including methanogens and as a result can disadvantage the electrochemically active bacteria in a MFC due to the complex metabolic process required and methanogenic competition. Pre-treatment of the wastewater may therefore be required (Cha *et al.,* 2010)

The activated sludge process is the most widely used biological wastewater treatment technology today (Wang *et al.,* 2014). An alternative to this process is the use of membrane bioreactors (MBRs) which are a highly efficient wastewater treatment method (Wang *et al.,* 2012; Su *et al.,* 2013). In an attempt to eliminate separate pre-treatment steps, work has been done on the integration of MFCs into current wastewater treatment methods. The construction of the system ultimately results in a bio-cathode which is of interest due to its improved sustainability compared to abiotic cathodes.

Cha *et al.* (2010) conducted experiments in which two single-chamber MFCs were submerged into the aeration chamber in an activated sludge process. In this way the aeration chamber was used as the cathode of the MFC. Each rectangular chamber acting as the anode chambers consisted of two carbon anodes and cathode arrangements on opposite sides of the compartment separated by a PEM with the anode on the inside of the chamber and the cathode on the outside.

The cell was initially run with activated sludge in the anode compartments and distilled water in the cathode compartment. It was found that when activated sludge replaced water as a catholyte the voltage across the cells dropped by almost half. This was attributed to aerobic bacteria using organic substances as electron donors instead of the cathode as expected in the case of a biofilm.

A study by Wang *et al*. (2012) investigated an integrated MFC-MBR system. The aeration chamber was used as a cathode and contained both a nylon membrane module and a non-woven fabric MFC chamber surrounded by activated carbon fibre. Wastewater was allowed to flow through the MFC with the effluent flowing into the aeration tank of the MBR. Initially the MFC was inoculated with anaerobic and activated sludge and submerged in an activated sludge reactor in order to enrich it with electroactive bacteria. Once the system became stable it was transferred to the to the aeration tank of the MBR.

The COD concentration of the effluent of the combined system was found to be considerably lower than for the MFC alone. Cyclic voltammetry was conducted on biofilm on the cathode was performed in order to determine its ability to catalyse oxygen reduction. The reduction peak potential was found to be similar to that of other biocatalysts for oxygen reduction. The peak was found to decrease when the system was sparged with nitrogen and rebound once oxygen was allowed to enter the system again indicating that oxygen reduction was occurring and being catalysed by the microorganisms.

Su *et al.* (2013) investigated a different type of integrated MFC-MBR system. It was noted that the MBR are subject to membrane fouling which is believed to be due to extracellular polymeric substances (EPS). It was hypothesised that these EPSs could be removed in the form of dissolved organic carbon after treatment with a MFC and therefore significantly reduce fouling.

The system consisted of two MBRs operating in parallel and fed with wastewater. The effluent from the system was fed to into a settling pool before being fed into a stack of single chamber MFCs with an anode and air-cathode on opposite sides. The effluent of the MFCs was fed back to the MBR.

It was found that the effective removal of sludge was improved with the addition of the MFC compared to a MBR system alone. Mitigation of membrane fouling was achieved by significantly reducing EPS content with the MFC.

Wang *et al*. (2014) found that in the integrated microbial fuel cell sequencing batch reactor (MFC-SBR) system tested in their experiments that an excess amount of organic material in the aerobic SBR resulted in the growth of heterotrophs which consume large amount of the DO which hinders the reduction of oxygen. It was noted that by increasing the hydraulic residence time (HRT) of the MFC more COD was removed in this portion of the system which has several benefits. These were that electricity generation was improved due to the increased degradation of organics by anodic bacteria, less organics in the SBR favoured the competition of cathode-respiring bacteria over heterotrophs and the sludge yield of the SBR was reduced. The overall effluent quality of the system was also improved in this way.

What is apparent from the studies done into integrated wastewater treatment systems is that many different configurations are possible which ultimately all result in varying degrees of improved water treatment and the electricity production. It may therefore be possible to integrate MFCs with various different types of existing systems. It may also be necessary to compromise on either electricity production or water treatment in order to better the other by altering several system variables.

1.7.3.2 Existing reactors within the laboratory

Work is currently being done in the laboratory on plant biophotovoltaic cells. An element of the work involves a system which uses soil which contains a consortium of unknown bacteria. A plant is grown in the soil which provides the electrochemically active bacteria with organic substrate via rhizodeposition (Helder *et al*., 2012; Timmers *et al*., 2013). The system is anaerobic as a result of it being underground and a liquid medium is necessary in order to transfer electrons to the electrodes which are positioned in the soil on either side of the plant.

Currently in the laboratory several different types of bacteria and reactor systems are being used to treat a variety of types of wastewater.

Rhodospeudomonas palustris is a metabolically versatile phototrophic bacterium which is currently being researched for the production of the polymer poly-β-hydroxybutyrate (PHB), clean fuels such as hydrogen gas and a bioactive substance, *cis*-vaccenic (Carlozzi *et al*., 2006). Currently in the laboratory the use of *R. palustris* in the production of PHB, hydrogen and pigments and most recently and wastewater treatment is being investigated as the potential exists to use *R. palustris* in the treatment of glycerol waste with possible production of useful by-products such as hydrogen.

Xing *et al*. (2008) demonstrated that electricity generation was possible using a strain of *R. palustris* (DX-1) in a single chambered fuel cell with an air-cathode. It was found that as a pure culture of *R. palustris* produced more electricity than mixed cultures. Using complex mixed cultures in MFCs generally allows for a wider consumption of substrate and therefore results in good performance of the cell (Du *et al*., 2007)

It was noted that the *R. palustris* strain ATCC 17001 did not perform to the same extent as strain DX-1. The incorporation of MFC elements into existing *R. palustris* wastewater treatment reactors within the laboratory may therefore be possible. However it is noted that ATCC 17001 is the strain that is currently being investigated in the laboratory.

Currently sulphur reducing bacteria (SRB) are being investigated for the treatment of wastewater from acid rock drainage (ARD). Different reactor configurations are being tested. One is an anaerobic reactor to which sulphate waste water is fed. The effluent is filtered to remove the biomass which is returned to the reactor. The second reactor is a linear flow channel reactor (LFCR) which receives the same influent.

The LFCR is a rectangular Perspex box which is open to the air. Three feed and effluent points are fitted on opposite ends of the reactor. A heating coil controlling the temperature of the reactor is connected between the lowest points, above this attached to the middle points is a strip of carbon fibres. Due to the inability of the bacteria to form a substantial biofilm, carbon fibres are used to support the SRB for better contact of the bacteria with sulphates.

The reactor is aerobic, however sulphate feed entering the reactor from the top port sinks to the bottom of the reactor as a result of having a higher density. Here the bacteria reduce the sulphite to elemental sulphur which floats to the top of the reactor and forms a layer on the top of the liquid. This layer and the sulphur reduction reaction taking place at the bottom of the reactor results in an anaerobic system. Incoming feed then displaces the liquid at the bottom of the reactor and exits through the effluent port on the other side

The potential exist to use the carbon fibres as an electrode in an integrated MFC waste treatment system and allow electrons from the oxidation of substrate to travel through and external circuit before they are used in the reduction of sulphate. Modifications to the existing design would be necessary potentially uncomplicated.

The other reactor systems present in the laboratory are a stirred aerated reactor for the treatment of cyanide wastewater by bacteria and many configurations of reactors for the use of algae to treat wastewater. Both are aerobic systems and the need for the anaerobic operating conditions of a MFC may make the integration of the reactor system with a MFC difficult. They will however their anaerobic operation and potential for integration will be considered.

1.8 PROJECT AIMS

The aims addressed in the project were as follows:

1. To test the digestibility of a number of biomass types to assess their rate of digestion, biogas yield, residual COD and volatile fatty acid profile of the residual COD
2. To assess the effect of temperature on the kinetics and performance of the AD unit, across a range consistent with typical seasonal variations
3. To construct a channel reactor for the simultaneous reduction of sulphate and oxidation of sulphide to elemental sulphur. The channel will contain carbon microfibers for SRB attachment and sulphide oxidation will be achieved in a floating sulphur biofilm at the air-water interface
4. To assess the performance of the system, first using a defined growth medium to support the sulphate reducing community and then using effluent from the AD blended with synthetic ARD and if successful, real ARD
5. To assess the effect of temperature on the sulphate reduction and sulphide oxidation reactions, across a range typical of seasonal variations
6. To optimise the mechanism for harvesting sulphur from the biofilm and characterise the sulphur product
7. To assess the potential of using the sulphate reduction component of the reactor as a microbial fuel cell, quantifying the power and current densities

CHAPTER 2: MATERIALS AND METHODS

2.1 INTRODUCTION

This chapter presents an overview of the algal and microbial cultures used in this research, a description of the individual reactor units and the detail of the routine analyses performed. The specific experimental programme relating to each of the sets of experiments is described in detail in the relevant chapters.

2.2 ALGAL AND MICROBIAL CULTURES

2.2.1 Anaerobic digestion inoculum

A mixed microbial inoculum was prepared using 240 mℓ rumen fluid (obtained from Malmesbury abattoir), 300 mℓ sludge from the anaerobic digester at South African Breweries' Newlands brewery, 300 mℓ suspension from a laboratory-scale anaerobic digester (CeBER) fed *Spirulina* biomass and 60 mℓ mixed sulphate reducing suspension from laboratory stock reactors (CeBER) maintained on different substrates (acetate, lactate, ethanol and a mixture of the substrates). In addition, 0.5 mℓ of 20 g/ℓ molasses and 1.1 ℓ tap water were added to make up a final volume of 2 ℓ. The inoculum was maintained in a modified 2 ℓ Schott bottle in a constant environment room at 37°C. The reactor was placed on a magnetic stirrer and the contents mixed using a stirrer bar. The culture was maintained for 40 days, with periodic addition of molasses from the 20 g/ℓ stock before being used to inoculate the experimental AD reactors.

2.2.2 Sulphate reducing bacteria (SRB) stock culture

The mixed SRB community was obtained from the Department of Microbiology, Biochemistry and Biotechnology at Rhodes University, originally from the anaerobic compartment of a facultative pond at the Grahamstown sewage treatment works, and has been maintained at UCT since 1999. The stock culture has been maintained on modified Postgate B medium consisting of: 0.5 g/ℓ KH_2PO_4, 1 g/ℓ NH_4Cl, 2 g/ℓ $MgSO_4.7H_2O$, 1 g/ℓ Na_2SO_4, 1 g/ℓ yeast extract, 6 mℓ/ℓ 60% sodium lactate solution (Sigma), 0.3 g/ℓ sodium citrate. Previously, the stock culture has been used to generate cultures adapted to ethanol and acetate (Moosa *et al*., 2002; Erasmus 2005).

2.2.3 Sulphide oxidising bacteria (SOB) culture

The SOB culture was obtained from previous studies (van Hille and Mooruth, 2013) on sulphide oxidation conducted within CeBER. The culture was initially selected for by feeding a channel reactor with overflow from a laboratory-scale sulphate reducing column, packed with lignocellulosic material and inoculated with a mixture of the SRB culture described above, rumen fluid obtained from an abattoir and the indigenous community associated with the material used to pack the column (wood chips, grass, primary sewage sludge and leaf mulch). The two cultures were mixed together to inoculate the reactor.

2.3 REACTOR UNITS

2.3.1 Photobioreactors

A portion of the algal biomass used for batch digestion studies was generated in 3.2 ℓ glass and stainless steel, internal loop airlift reactors described fully by Langley *et al*. (2012) and shown in Figure 7. The photobioreactors consisted of a 600 mm high, 100 mm outside diameter (OD) column and a 50 mm OD draught tube. Air, normal or enriched with CO_2, was sparged into the column through a 0.22 µm stainless steel HPLC inlet filter, located at the base of the draught tube. Air and CO_2 flow rates were controlled with a Brooks 5850S Thermal Mass Flow Controller. The two gas streams passed through an inline mixer and were fed to each column at a flow rate of 2 ℓ/min. Light was supplied continuously by three Osram 18 watt cool white fluorescent bulbs at a distance of 3 cm from the column surface, providing 300 µmol/m^2.s PAR.

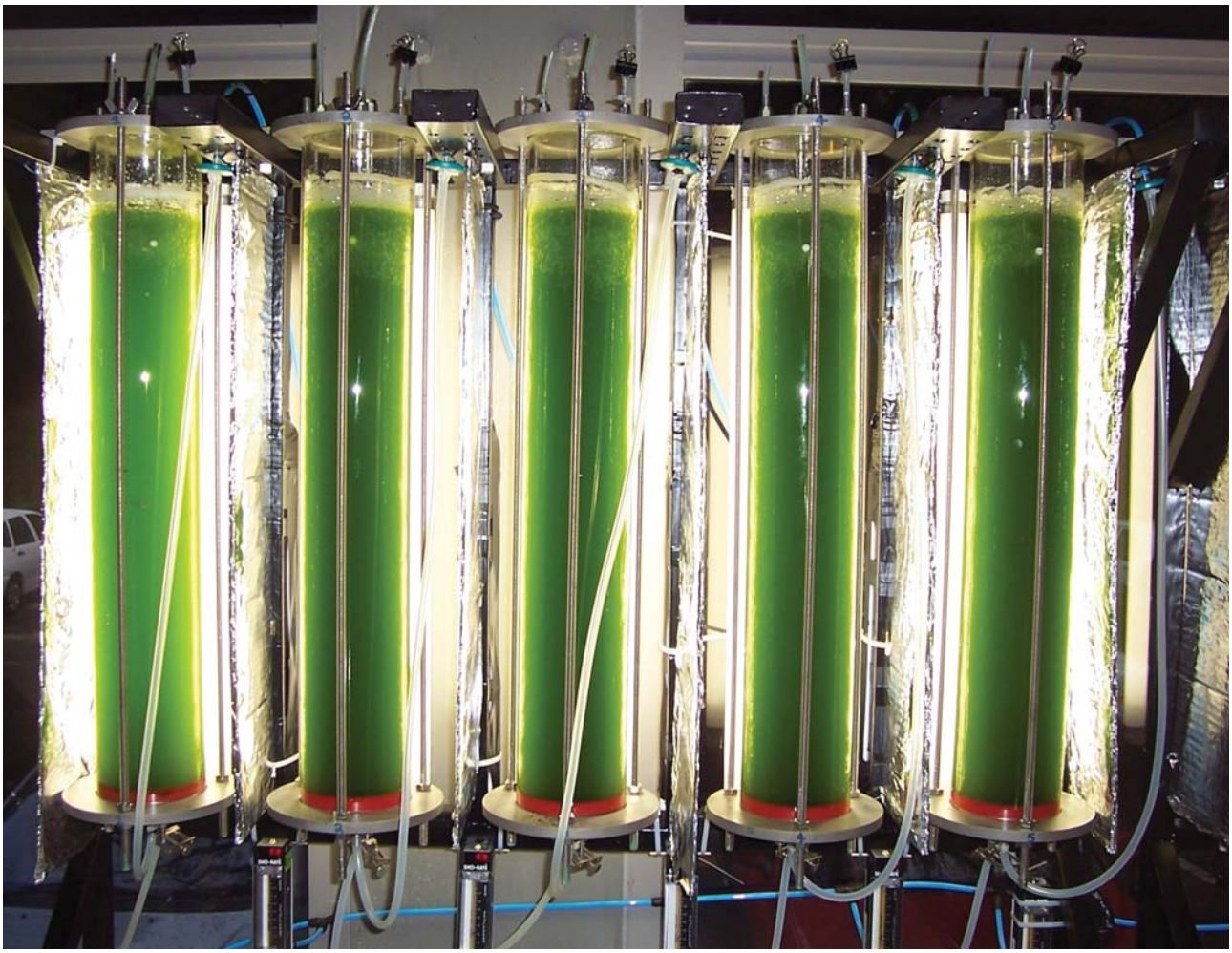

Figure 7: Photograph showing a bank of five airlift photobioreactors used to perform the algal growth experiments

2.3.2 Raceway pond

A 70 ℓ Perspex raceway pond with a paddle wheel was used for larger-scale algal cultivation. Where aeration was required, it was introduced through a 6.35 mm stainless steel tube, with 1 mm holes drilled every 20 cm, positioned on the reactor floor. Circulation of the medium was achieved using a four bladed paddle wheel. The speed could be varied depending on the requirements for the particular algal species. The liquid depth was 10 cm and the total surface area was 0.51 m^2. Six 58 watt and two 36

watt fluorescent bulbs provided continuous light to the cultures. A photograph of the raceway pond is shown in Figure 8.

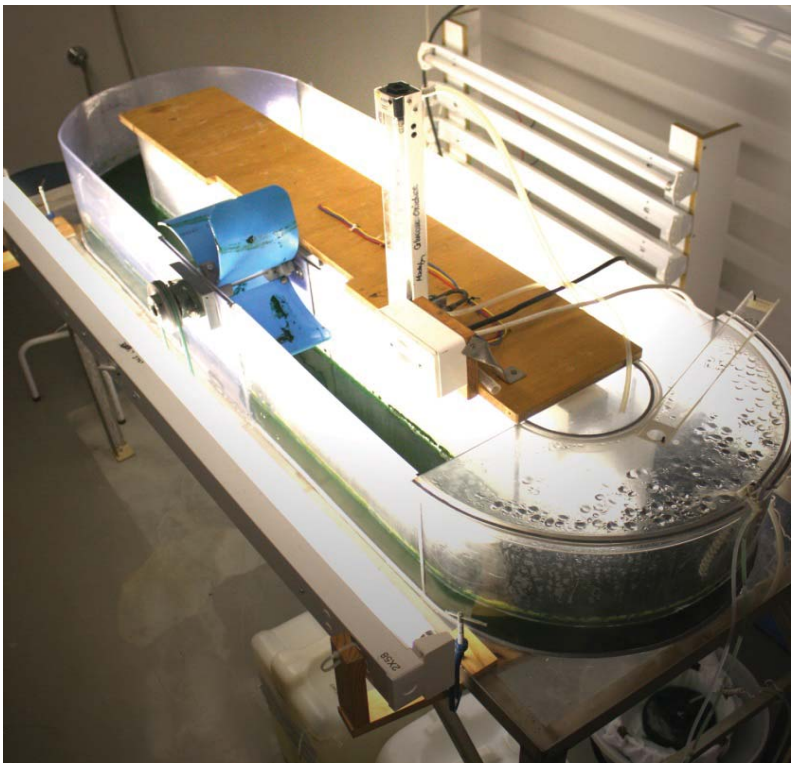

Figure 8: Photograph showing the raceway used for larger-scale algal cultivation

2.3.3 Anaerobic bench-top batch reactors

The digestion experiments were carried out in continuously mixed bench-top batch reactors. The reactors were constructed from 1 ℓ Duran Schott bottles and were operated with minimal headspace. The lid of the reactor was modified to include three ports. The first port was used for biogas collection, the second for liquid sampling and third for biogas sampling to determine composition. The units were placed in a controlled environment room at 37 ± 2 ºC, and were continuously mixed on an orbital shaker (140 rpm). Biogas was collected using water displacement vessels filled with saturated sodium chloride (NaCl) solution to minimise the dissolution of CO_2. To prevent any backflow of NaCl into the reactors, 1 ℓ trap bottles were inserted on all biogas lines. These trap bottles were fitted with a secondary biogas sampling point. The volume of biogas produced was corrected for normal temperature and pressure (STP). The digester pH could be controlled by injecting 5 M sodium hydroxide (NaOH).

2.4 ANALYTICAL METHODS

2.4.1 Biomass concentration using optical density

Algal biomass concentration was determined daily by measuring optical density at 750 nm with a Helios spectrophotometer and converting these to dry mass concentration using a calibration curve. The sample was first diluted to ensure that the absorbance measured did not exceed 1. The final concentration was adjusted using this dilution factor. Bacterial cultures were similarly measured at a wavelength of 660 nm.

2.4.2 Biomass concentration using dry weight

Algal biomass dry weight was measured by filtration of a 5 mℓ sample through a pre-weighed 0.22 µm glass fibre filter paper, which was then dried at 80°C overnight before being re-weighed.

2.4.3 pH and redox potential

The solution pH was measured using a Cyberscan 2500 micro pH meter, fitted with an XS microprobe (6 mm). The meter was calibrated daily using pH 4.0 and pH 7.0 buffers. Redox potential was measured using a Metrohm pH lab 827 redox meter.

2.4.4 Sulphide

Aqueous sulphide was quantified using the colorimetric DMPD method (APHA, 2005). The principle of the method is reaction of aqueous sulphide with N,N-dimethyl-p-phenylenediamine (DMPD), catalysed by ferric ions, to produce methylene blue. An appropriate volume of sample (10-4800 µℓ) is added to 200 µℓ of 1% zinc acetate. The volume is made up to 5 mℓ with deoxygenated water, after which 500 µℓ of 0.4% N,N-dimethyl-p-phenylene diamine (in 6 M HCl) and 500 µℓ of 1.6% ferric chloride (in 6 M HCl) are added. The sample is mixed well and left to react for a minimum of 5 minutes after which the absorbance is read at 670 nm and the concentration determined relative to a standard curve. The assay has a maximum detection limit of just over 1 mg/ℓ so significant dilution is required. This is typically achieved by using a small volume (20-50 µℓ) of sample.

2.4.5 Sulphate

Dissolved sulphate concentrations were measured using the barium sulphate method. Samples (2 mℓ) were centrifuged at 14 000 x *g* for 5 minutes to remove particulate matter. An appropriate volume of supernatant was diluted with deionised water to a final volume of 5 mℓ, to which 0.25 mℓ of conditioning reagent (50 mℓ glycerol, 30 mℓ 32% HCl, 100 mℓ absolute ethanol, 75 g NaCl, 300 mℓ deionised water) was added. A volume (10 µl) of saturated $BaCl_2$ solution was added and the contents of the tube were mixed by vortexing for 15 seconds. The barium reacts with any sulphate present in the sample to produce insoluble $BaSO_4$. The turbidity resulting from the $BaSO_4$ precipitate was measured at 420 nm using a Shimadzu UV spectrophotometer and quantified against a standard curve (0-100 mg/ℓ).

2.4.6 Anions by ion chromatography

Anion (fluoride, chloride, nitrate, sulphate, thiosulphate and phosphate) concentrations was determined by ion chromatography on a Thermo Scientific DIONEX ICS-1600 system equipped with an IonPac AG16 anion column, a 10 µℓ injection loop and a conductivity detector with suppression. A 22mM NaOH solution was used as the mobile phase at a flow rate of 1 mℓ/min. Standard solutions of the respective sodium salts were used to prepare mixed ion standards (100-500 mg/ℓ) and fresh standard curves were generated for each analytical run. Data were analysed using the Chromeleon software package.

2.4.7 Soluble, solid and total COD

All COD measurements were carried out using the Merck reagent test protocol for high (1500-10 000 mg/ℓ) and low (10-150 mg/ℓ) concentrations. The method is based on the oxidation of the sample with a hot sulphuric acid solution containing potassium dichromate, with silver sulphate as the catalyst. The chloride is masked with mercury sulphate. The concentration of unconsumed yellow $Cr_2O_7^{2-}$ ions or green Cr_3^{+} ions is then determined photometrically and used to quantify oxygen demand. The reactions

were performed in glass COD tubes. For the high concentration assay, 2.2 mℓ of COD reagent A and 1.8 mℓ of COD reagent B were added to the tube. The sample (1 mℓ) was added to the reagents in the tube and the contents mixed using a vortex mixer. A blank was prepared using 1 mℓ of deionised water instead of the sample. For the low concentration range 0.3 mℓ of reagent A, 2.3 mℓ of reagent B and 3 mℓ of sample were used. The tubes were heated at 150°C for 120 minutes in a heating block, then allowed to cool to room temperature. The absorbance was measured using a spectrophotometer at 610 nm. To quantify the COD concentrations, standard solutions were prepared using potassium hydrogen phthalate and data used to prepare standard curves.

2.4.8 Volatile fatty acids (VFAs)

A full volatile fatty acids (VFAs) analysis was conducted to quantify the concentration of lactic, acetic, propionic, iso-butyric, butyric, iso-valeric and valeric acids present in all digesters over the duration of digestion. The concentration of each VFA was determined using HPLC on a Waters Breeze 2 HPLC system equipped with a Bio-Rad Organics Acids ROA column and a UV (210 nm wavelength) detector. The system was run isocratically using a mobile phase of 0.01 M H_2SO_4 at a flow rate of 0.6 mℓ/min. The pressure in the column did not exceed 2000 psi. Sample injection volumes of 100 µℓ were used. To quantify the VFA concentrations, standard solutions (100, 200, 300, 400 and 500 mg/ℓ for each acid) were prepared.

2.4.9 Scanning electron microscopy (SEM)

Scanning electron microscopy (SEM) and energy-dispersive X-ray spectroscopy (EDS) were performed at the University of Cape Town Microscopy unit. Samples were fixed using 2 mℓ cold 2.5% glutaraldehyde in 1X phosphate-buffered saline (PBS) solution (pH 7.2) for 24 hours at 4°C. After the primary fixation, the samples were washed twice with 1X PBS solution followed by a sequence of dehydration steps using increasing concentrations of ethanol (30, 50, 70, 80, 90, 95% and 100%), with a 10 minute incubation at each step. Samples were then carefully mounted onto SEM stubs with silver paint. A few drops of hexamethyldisilazane (HMDS) were immediately added onto the samples. More HMDS was added after 5 minutes to ensure a well-dried sample. The dried samples were coated with gold-palladium (60:40) and observed using a FEI NOVA NANOSEM 230.

CHAPTER 3: ANAEROBIC DIGESTION OF COMPLEX SUBSTRATES

3.1 INTRODUCTION

The cost and availability of a suitable carbon source and electron donor has been one of the major constraints that have prevented the widespread application of technologies based on biological sulphate reduction. Recent research (Inglesby, 2011; van Hille *et al*., 2014) has shown that the residue from the anaerobic digestion of *Spirulina*, a cyanobacterium, contained sufficient volatile fatty acids to sustain efficient sulphate reduction when blended with a synthetic circum-neutral ARD stream. The nature of *Spirulina*, specifically its lack of a cellulosic cell wall, makes the biomass particularly suitable for anaerobic digestion. However, the cultivation of *Spirulina* under optimal conditions is expensive due to the requirement for saline and alkaline growth media. The likelihood of water resources suitable for *Spirulina* cultivation occurring in the proximity of ARD impacted environments is low. Therefore, there is a desire to investigate the amenability of a number of other complex organic carbon sources for anaerobic digestions, both from a biogas productivity perspective, but also to characterise the composition of the digestate.

The first two potential substrates investigated were grass and cow manure, due to their availability at the site of the proposed pilot scale application of the integrated process. Microcrystalline cellulose (MCC) was investigated as the third substrate as it is commonly recommended as a reference substrate (VDI, 2006). The selection of MCC is based on the fact that it is completely degradable, but does not ferment too rapidly. Complete degradation, taking into account the formation of new biomass, should yield 740-750 mℓ of biogas per g TS, with a theoretical distribution of CH_4 to CO_2 of 1:1. It is estimated that 80% of this value should be achieved in a control batch reactor (VDI, 2006). Similarly, acetate may be used as a reference substrate if a soluble substrate is desired.

This first part of the chapter focuses on the batch digestion of grass, cow manure and MCC. Algal biomass, both micro and macroalgae, remains a potentially attractive alternative substrate, particularly if it can be cultivated on-site, using available water resources. Therefore, the cultivation of species that do not have the specific media requirements of *Spirulina* was investigated and productivity data are presented later in the chapter.

3.2 MATERIALS AND METHODS

The materials and methods specific to this component of the work are described below.

3.2.1 Anaerobic digester inoculum

A mixed microbial consortium was prepared by targeting a number of environmental enrichments for microorganisms capable of efficient conversion of complex organics to readily metabolisable substrates. A number of manure samples from domestic and game animals, sludge from a working commercial-scale anaerobic digester (AD) treating kitchen waste, cow rumen fluid, sludge and liquid effluent from a *Spirulina*-fed AD and a sample of sludge from the commercial-scale AD reactor at SAB Newlands were obtained. In addition, a compost sample was used to create an independent enrichment, containing cellulolytic microorganisms.

The mixed AD inoculum was built up by gradually drawing and filling the various enrichment cultures and combining the drawn effluent into a 10 ℓ Schott bottle, fitted with a modified lid and sealed with a large nitrile glove as a reservoir for gas produced. The sludge volume within the 10 ℓ inoculum bottle

increased with each additional input of drawn effluent and substrate. Substrates used to feed these inocula included grass, cow manure, Avicel PH-101, waste algal biomass, tissue paper, *Spirulina*-AD effluent and SAB AD effluent. Once an active 10 ℓ inoculum was established the liquid and sludge volume was split into a second 10 ℓ Schott bottle. Following a further period of maintenance and operation of these stock reactors, the volume of liquid and sludge was once again split and used to inoculate a third and more recently a fourth large AD inoculum reactor. The reactors were fed with a combination of the substrates listed above on a bi-weekly basis. The pH was routinely monitored and actively maintained with the range of pH 7.0-8.0.

A further stock inoculum was developed for the AD of complex mixed algal biomass from the mixed AD, described above, supplemented with *Spirulina*-fed AD and a combined feedstock of freshly harvested *Parachlorella hussii*, *Oscillatoria* sp., *Scenedesmus* sp. and *Oedogonium* sp., and waste algal biomass.

The glove attached to the gas vent in the modified lids of the stock reactors inflated due to gas production within the sealed reactor system and was vented 2-3 times per day, or as required (Figure 9). Gas was sampled from the gas reservoirs attached to these reactors and the methane content was analysed by GC, using the standard protocol.

Figure 9: Stock inoculum reactor bottles (10 ℓ) currently maintained on mixed substrates. The one 5 ℓ inoculum reactor bottle maintained on a complex mixed algal substrate is not shown.

3.2.2 Algal cultivation

All algal strains were grown in Bold's Basal Medium (BBM), unless otherwise stated. The BBM consists of 0.25 g/ℓ $NaNO_3$, 0.025 g/ℓ $CaCl_2.3H_2O$, 0.075 g/ℓ $MgSO_4.7H_2O$, 0.075 g/ℓ $K_2HPO_4.3H_2O$, 0.175 g/ℓ KH_2PO_4, 0.025 g/ℓ NaCl, 6 ml/ℓ of PIV metal solution and 1 ml/ℓ vitamin solution. The PIV metal solution was composed of 0.75 g/ℓ Na_2EDTA, 0.097 g/ℓ $FeCl_3.6H_2O$, 0.041 g/ℓ $MnCl_2.4H_2O$, 0.005 g/ℓ $ZnCl_2$, 0.002 g/ℓ $CoCl_2.6H_2O$ and 0.004 g/ℓ $Na_2MoO_4.2H_2O$, while the vitamin solution contained 1.2 g/ℓ thiamine HCl (vit B1) and 0.001 g/ℓ cyanocobalamin (vit B12). The stock cultures were maintained in small (100 mℓ) bottles on 3N BBM growth medium, containing three times the nitrogen of BBM, under

constant aeration. Continuous illumination was provided by two fluorescent bulbs, providing 50-80 µmol/m^2/s photosynthetically active radiation (PAR).

3.2.2.1 Parachlorella hussii

Algal cells were cultivated in 3N BBM medium in a 70 ℓ raceway pond (Section 2.3.2) located in a greenhouse on UCT's Upper Campus. Mixing was provided by a paddlewheel. The increase in biomass was monitored by measuring the optical density (OD) of the cell suspension spectrophotometrically, at 750 nm. The OD was converted to dry weight (DW) using a previously prepared standard curve (DW=0.339 x OD 750nm, R^2=0.95). The volume of the raceway was maintained at 70 ℓ by the addition of water. Nutrients equating to the amount contained in 10 ℓ of 3N BBM were added every two weeks.

3.2.2.2 Filamentous algae

Oedogonium and *Oscillatoria* were cultivated in half strength 3N BBM medium. *Oedogonium* was cultivated in a 25 ℓ Perspex channel reactor (10 ℓ volume) fitted with aeration pipes. Additional silicone tubing was included in the reactor to act as a support matrix for the filamentous algae. *Oscillatoria* was cultured in a similar channel reactor, using a 20 ℓ liquid volume, with the inclusion of aeration pipes and tubing as growth supports. The biomass was harvested using a nylon cloth (mesh size 100 µm).

3.2.2.3 Isolate MPA 34.1 (Chlamydopodium species)

A microalgal species, identified as a high CO_2 assimilating isolate, with a high biomass productivity was selected as a second option for use as an AD substrate. Partial 18S rRNA gene sequencing of the isolate showed the greatest similarity to *Chlamydopodium starrii* (99%). The algae, referred to as isolate 34.1 throughout this study, was cultivated in 3.2 ℓ airlift photobioreactors (Section 2.3.1) under constant illumination (200 µmol photons/m^2/s) provided by three fluorescent bulbs and CO_2 enriched air (10 000 mg/ℓ CO_2) sparged into the reactor at an aeration rate of 0.3125 vvm. The growth rate of the algae was determined by optical density and converted to a biomass DW as detailed for *P. hussii* in section 3.2.2.1. The OD was converted to biomass dry weight using the a predetermined standard curve (DW=0.350 x OD 750nm, R^2=0.98).

3.2.3 Batch anaerobic reactors

The 2 ℓ and 1 ℓ batch reactors were constructed in a similar fashion. The 1 ℓ batch grass reactors were changed to 2 ℓ batch reactors to ensure sufficient headspace and prevent blockages in the outlets. Grass was found to from a "plug" at the liquid surface and that gas build underneath this plug caused the content of the reactor to be sprayed out. The reactors consisted of a Schott bottle with a modified cap, fitted with a metal insert and silicone gasket that held three ports (Figure 10). One of the ports was fitted with a self-sealing septum that allowed for direct sampling of the gas in the headspace using a gas-tight syringe. The second port was connected to a tube submerged into the reactor liquor, allowing the bulk liquid to be sampled. The outside end of the port was connected to a 20 mℓ syringe. The third port provided an outlet for gas generated in the reactor. A tube ran from the gas port into an inverted measuring cylinder allowing the volume of biogas formed to be measured by liquid displacement. The cylinder was placed in a reservoir containing an acidified sodium chloride (NaCl) solution (270 g/ℓ) and a vacuum pump was used to draw the solution up to the 100 mℓ mark. The NaCl and low pH were selected to reduce the solubility of carbon dioxide. The reactor contained a magnetic stirrer bar and was placed on a magnetic stirrer. The speed was set to ensure that the reactor was well-mixed, to achieve complete suspension of the solid substrate.

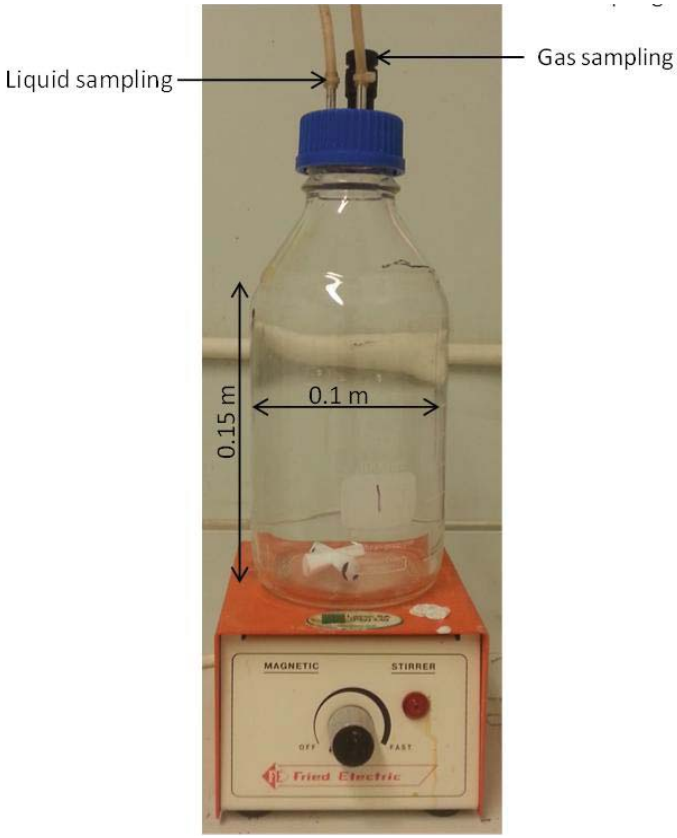

Figure 10: Photograph illustrating the 1 ℓ batch reactor setup

3.2.4 Substrate preparation

The three substrates used during the initial phase of this study were pasture grass (wild-growing, Tokai area), cow manure (obtained from Dreyersdal farm, Bergvliet) and Avicel® PH-101 (Sigma Aldrich, catalogue number 11365), with *Spirulina* (obtained from the raceways in CeBER labs) as a positive control. The reactors loaded with the three primary substrates were set up in duplicate and labelled AD 1 and AD 2 (grass), AD 3 and AD 4 (manure) and AD 5 and AD 6 (Avicel). Two control reactors were prepared, a positive control loaded with *Spirulina* (AD 7) and a negative control, which received the inoculum sludge, but no additional substrate (AD 8). A series of chemical oxygen demand (COD) tests were performed using increasing masses (0.005, 0.01 and 0.02 g) of each of the substrates. The results were used to determine the COD/g of the substrates in the state to which they were added to the reactors, so that a consistent loading of 30 g COD could be achieved. To obtain the desired loading of 30 g COD/ℓ, 22.2 g of grass, 28.6 g of manure, 26.25 g Avicel and 199 g *Spirulina* paste (unwashed *Spirulina* was filtered using a 100 µm Nylon mesh) was added.

The grass was cut with a five blade herb scissor to a size of approximately 3 mm, and a representative 22.2 g was weighed out for each reactor. The manure was homogenised in a Braun kitchen blender prior to taking a 28.6 g representative sample for each reactor. Avicel did not require any pre-treatment since the particle size is approximately 50 µm.

To generate the biomass for the evaluation of algal substrates *Oedogonium* and *Oscillatoria* spp. Biomas was harvested from small-scale growth vessels, while *P. Hussii* was harvested from a 50 ℓ raceway pond. Filamentous algae were harvested and the majority of medium removed by blotting onto tissue paper. Small amounts of the algal biomass were placed into pre-weighed 2 mℓ Eppendorf tubes, using tweezers. The tubes containing wet biomass were weighed to determine fresh weight (FW), before being dried in an oven at 80°C for at least 24 hours to allow the determination of dry weight

(DW), following cooling in a desiccator. The FW to DW ratios of the two filamentous algae, which could not be quantified by optical density, was subsequently used to determine biomass loading for the digesters. For *P. hussii*, algal cells were harvested by centrifugation at 10 000 x *g* for 20 min and the algal biomass dried in a vacuum freeze drier. Elemental analysis was performed on the dried biomass.

The chemical oxygen demand (COD) of a dilution series of the three algal strains was determined. For the filamentous algae, 20 g/ℓ suspensions were prepared using dried and milled algal biomass, prepared as described for elemental analysis. *P. hussii* was obtained directly from the raceway pond as the cells were small enough to produce a homogenous suspension. Data from dilution series was used to determine the COD per g of dry mass for each species.

3.2.5 Analytical methods

The techniques for measuring pH, redox potential, COD and VFAs has been described in Section 2.4). Techniques specific to this chapter are described below.

3.2.5.1 Elemental analysis

Elemental analysis (carbon, nitrogen and hydrogen), giving percentage composition of dried samples was determined at the Chemistry Department (UCT) using a Thermo Flash EA 1112 series elemental analyser.

3.2.5.2 Methane

The methane content of the biogas was determined using flame ionisation gas chromatography (FID GC) on the Perkin Elmer Autosystem gas chromatograph. A Supelco wax column (1.2 mm x 37 m) was used. The FID detector was set at 280°C and the oven temperature at 50°C (Inglesby, 2011). Nitrogen was used as the carrier gas, at a pressure of 400 kPa. Gas-tight Hamilton syringes (50 µℓ and 1000 µℓ) were used extract gas samples from reactors and inject the gas samples into the GC. The column was calibrated with standard gas mixtures containing 25% and 50% methane by volume. Chromatograms were analysed using the Total Chrom software package.

3.2.5.3 Light microscopy

Light microscopy was used to obtain a qualitative assessment of the microbial community, based on visible cell concentration. Reactor samples were observed using an Olympus BX-40 microscope, equipped with phase contrast. Images were captured using a ColorViewII digital camera and the AnalySIS software package. In addition, Gram staining was performed on samples from the reactors, following a 1/10 dilution to reduce cell concentration.

3.2.5.4 Analysis of microbial community structure

The relative proportions of bacteria and archaea in the reactor samples were determined using quantitative real-time polymerase chain reaction (qPCR). DNA was extracted from 0.5 mℓ of reactor sample, rumen fluid or inoculum sample. Reactor samples were allowed to settle for at least 30 min to allow the sampling of the microbial community without transferring large quantities of the solid substrate to the DNA extraction. The DNA extraction was performed using the Roche High Pure PCR template preparation kit, following a modified extraction protocol. Microbial cells were concentrated by centrifugation at 14 000 x *g* for 10 min and re-suspended in 200 µℓ tissue lysis buffer. Lysozyme (1 mg) and 50 µg RNaseA were added and the samples incubated at 37°C for 30 min. After addition of

ProteinaseK (as per manufacturer's instruction), samples were incubated for a further 30 min at 55°C. Following addition of 200 µℓ binding buffer and incubation at 70°C for 10 min, the standard method for DNA binding and elution was followed as per the manufacturer's instruction. Following DNA extraction, the quality and quantity of DNA was analysed using a Nanodrop® 2000 spectrophotometer (Thermo Scientific).

Quantitative polymerase chain reactions (qPCR) were performed using a Rotor-Gene cycler (Corbett Life Sciences) in 15 µℓ reaction volumes with the following constituents: 1x KAPA SYBR master mix, 0.2 µM of each primer and 1 ng of DNA as template. For bacterial quantification a universal bacterial primer set, UniBactF336 (5' gactcctacgggaggcagca 3') and UniBactR937 (5' ttgtgcgggcccccgtcaat 3') was used, while archaea were quantified using a universal archaeal primer set, UniArchF342 (5' acggggigcaicaggcg 3') and UniArchR932 (5' tgctcccccgccaattcc 3'). Cycling conditions were as follows: initial denaturation at 95°C for 5 min, followed by 40 cycles of 95°C for 10 sec, 60°C for 10 sec and 72°C for 20 sec. The relative proportion of bacteria and archaea was calculated after copy number quantification using standards of known copy number.

3.2.6 Experimental programme for evaluation of grass, manure and microcrystalline cellulose

3.2.6.1 Reactor setup

The eight experimental reactors were set up in a constant environment room at 37°C (Figure 11). An aliquot of 600 mℓ of inoculum was added to each reactor and left to settle overnight to obtain a sludge volume of between 200 to 250 mℓ. The substrates (grass for AD 1 and 2, manure for AD 3 and 4, Avicel for AD 5 and 6, *Spirulina* for AD 7) were added to the reactors and tap water was added to the 1000 mℓ mark. Each reactor was loaded with the appropriate mass of substrate to ensure a COD loading of 30 g/ℓ, with the exception of the negative control (AD 8).

3.2.6.2 Reactor monitoring

Each reactor was placed on its own magnetic stirrer and connected to an inverted measuring cylinder to quantify biogas production. Samples were taken three times a week (Monday, Wednesday and Friday). An aliquot of approximately 5 mℓ was removed and placed in a labelled 15 mℓ Falcon tube. The sample volume was replaced with an equal volume of tap water. The pH and redox potential were measured immediately. The sample was mixed on a vortex mixer and a subsample removed to measure total COD. A 2 mℓ subsample was pipetted into an Eppendorf tube and the solid fraction removed by centrifugation (13 000 x *g* for 10 min. The supernatant was used to measure soluble COD and the remainder was centrifuged for 13 000 x *g* for 5 min and filtered through a 0.45 µm membrane filter and retained for VFA analysis. The volume of biogas produced was determined from solution displaced from the inverted measuring cylinder and a gas sample was taken directly from the headspace to measure the methane content.

3.2.6.3 Post-setup adjustments

The two reactors containing the grass (AD 1 and AD 2) experienced operational challenges shortly after inoculation. The substrate material caused a blockage in the gas outlet line, resulting in a pressure build-up, which eventually forced liquid out of the sample port. As a result the two reactors were restarted five days after the initial tests, this time in 2 ℓ reactors. The total volume remained 1 ℓ, resulting in a larger headspace in the reactors. A similar problem occurred with the *Spirulina* reactor, resulting in the loss of approximately 200 mℓ liquid. This reactor was not restarted and was maintained with a

volume of 800 mℓ for the remainder of the experiment. The final experimental configuration is depicted in Figure 11.

Figure 11: Experimental setup for the eight AD reactors. From left to right, *Spirulina* (+ve control; AD 7) reactor, Avicel reactors (AD 6 and AD 5), manure reactors (AD 4 and AD 3), grass reactors (AD 2 and AD 1) and the +ve control reactor with only inoculum (AD 8)

3.2.7 Experimental programme for evaluation of algal substrates

3.2.7.1 Reactor setup and operation

Algal AD reactors consisted of 250 mℓ Schott bottles, with a working volume of 200 mℓ. Each bottle was fitted with an airtight cap containing a metal insert with two ports. The first port contained a stainless steel tube (8 mm ID), the lower portion submerged two thirds of the way into the reactor fluid to allow for the sampling of the digester slurry. The upper portion was connected to a 10 mℓ syringe, allowing the reactor fluid to be sampled. This tube was clamped shut except during sampling periods. The second port was connected to a 50 mℓ syringe to allow for the collection and quantification of any gas produced.

The reactors were loaded with inoculum described in section 3.2.1, such that settled sludge represented 25% of the 200 mℓ reactor volume. The inoculum was allowed to stabilise for three days to deplete any residual substrate, until no further gas production was observed.

The algal biomass used in these experiments was not always available in the required amounts, due cultivation constratints. Therefore, the algal BMP testing was divided into three stages (I, II and III). Stage I consisted of reactors loaded with *Oedogonium* and *P. hussii* as the substrates. Stage II investigated *Oscillatoria* sp., while stage III included repeat tests for *P. hussii* and the MPA 34.1 isolate.

The amount of algal biomass loaded into the digesters was based on the COD of each species. A negative control was included with each set of experiments. This consisted of the algae AD inoculum, at the same loading as the test runs, but without the addition of any algal substrate.

The reactors were maintained in a 37°C constant temperature room. Prior to gas volume measurements and sampling of the AD reactors, the reactors were mixed thoroughly to suspend the

solid material and release any biogas trapped within the algal sludge. Gas volumes were recorded daily, while gas chromatography was performed twice a week to monitor methane concentration. The reactors were initially sampled daily, until gas production slowed down, at which point sampling was reduced to two or three times a week. Sampling involved the removal of 4 mℓ of reactor, liquid using the attached syringe, to measure redox potential, pH and COD (Section 2.4). For total COD measurements a cut-off 1 mℓ pipette tip was used to withdraw the sample, to ensure more representative sampling of particulate matter. A 2 mℓ volume of the sample was centrifuged at 14 000 x *g* to remove the solid fraction prior to soluble COD analysis. The remaining sample volume was centrifuged and the supernatant filtered through a 0.22 µm syringe filter into 2 mℓ Eppendorf tubes for volatile fatty acid analysis (Section 2.4.8). Samples for VFA analysis were stored at -20°C until required.

3.2.7.2 Stage I BMP tests: Spirulina, Oedogonium and P. hussii

The amount of *Oedogonium* biomass available was limited, allowing replicate reactors to be set up with a COD loading to 12 g/ℓ. Therefore, all reactors set up in this stage were operated at a COD loading of 12 g/ℓ to ensure consistency and to allow for comparisons between reactors. Algal BMP tests with the following substrates were initiated during this stage of the study: two *Oedogonium*, three *P. hussii*, one *Spirulina* and one negative control. To confirm the presence of active methanogens within the AD inoculum used, the negative control reactor was spiked with acetate (5 g/ℓ) after two weeks.

3.2.7.3 Stage II BMP tests: Oscillatoria

Oscillatoria was used as the substrate for the second stage of algal BMP tests. The COD loading used for this test was set at 30 g/ℓ to be consistent with previous work at UCT (Inglesby, 2011). The inoculum sludge loading for these experiments was approximately 15%.

3.2.7.4 Stage III BMP tests: P. hussii and isolate MPA 34.1

The stage III experiments examined the effect of partial lysis of the algal cells. Cell lysis was achieved by treating the algal sludge in a microwave for one minute. Partial lysing of cells was confirmed by microscopy. This solution was left to cool and then added directly to the relevant reactor.

The *P. hussii* reactors from the first stage of BMP tests produced poor results, with minimal gas and VFA production. Therefore, the negative control and *P. hussii* BMP reactors from stage I were re-inoculated with fresh algal biomass (30 g/ℓ COD loading) and algal AD inoculum (25% sludge loading). Three replicates for MPA 34.1 and one negative control reactor were also set-up. For the MPA 34.1 tests, reactors one and two were fed with un-lysed algae while reactor three was fed with lysed algal biomass. The experimental design for the *P. hussii* stage III BMP tests is summarised in Table 2.

Table 2: Experimental design for the *P. hussii* stage III algal BMP tests

Old Reactor	Volume retained from stage I (mℓ)	Volume fresh algal AD inoculum added (mℓ)	*P. hussii* sludge added to achieve 30 g/ℓ COD (mℓ)
Negative control	41	70	89
P. hussii reactor 1[1]	111	0	89
P. hussii reactor 2	41	70	89
P. hussii reactor 3[1]	41	70	89

[1]Reactors 1 and 3 were loaded with lysed algal biomass

3.3 RESULTS AND DISCUSSION

3.3.1 Anaerobic digestion of grass, manure and microcrystalline cellulose reactors

The results of the batch biomethane potential tests will be presented by first looking at the basic solution phase data (pH, redox potential) and biogas production across all eight reactors, after which the more detailed data will be presented separately for the different substrate types and the control reactors. The data from the positive control will be discussed with reference to historical data generated as part of a CeBER research programme. The VFA generation data and relationship between VFA concentration and soluble COD will be discussed in some detail, as the primary role of the anaerobic pre-treatment was to assess the potential to generate a digestate containing a suitable mix of VFAs to support efficient sulphate reduction and sulphide oxidation in the downstream channel reactor. Biogas production is considered an additional benefit, but not the primary aim.

The discussion concludes with an assessment of the activity of the microbial community at the end of the experiment and an overall assessment of the implication of the results for the design of the integrated system.

3.3.1.1 Substrate analysis

The elemental analysis of the three substrates and their respective COD values are presented in Table 3. The elemental analysis was performed on dried material, while the COD data represents measured values of the substrates in their native state, meaning that the grass and manure had not been dried. The grass and manure were added to the reactors in their native state, based on measured COD.

Table 3: Elemental composition and COD of the AD substrates

Substrate	**%C**	**%N**	**%H**	**Formula**	**COD (mg/g)**
Grass	36.8	1.17	6.9	$CH_{2.246}N_{0.027}O_{1.13}$	1350.0
Manure	40.7	0.64	6.5	$CH_{1.93}N_{0.0135}O_{0.961}$	1048.9
Avicel	44.3	-	6.2	$CH_{1.67}O_{0.838}$	1142.9

3.3.1.2 pH and redox profiles

The pH data for the eight experimental reactors is summarised in Figure 12. The majority of the reactors follow the same general trend, with a decrease in pH over the first 4-6 days, followed by stabilisation or a slight increase as the experiment progressed. The trend was consistent with expectations, with the release of readily soluble organics and their conversion to VFAs resulting in the observed decrease and their subsequent consumption leading to the stabilisation and marginal increase. The negative control

(AD 8) showed a less pronounced decrease, consistent with the absence of additional substrate, while the limited decrease in the *Spirulina* fed control (AD 7) could be attributed to residual alkalinity from the entrained growth medium and the possible formation of sulphide during the first 8 days.

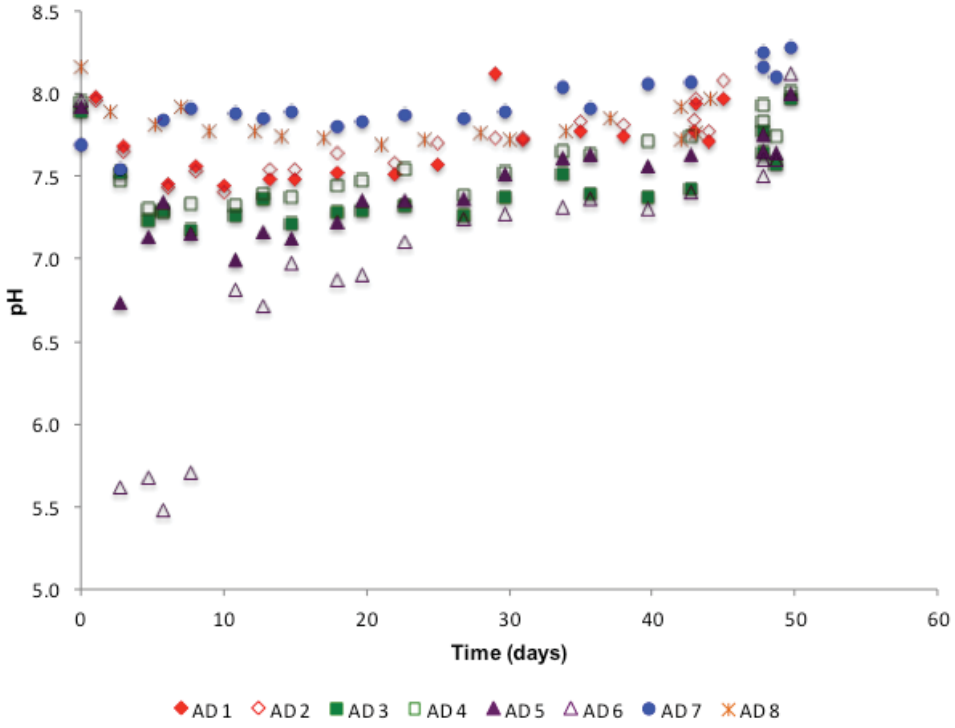

Figure 12: Summary of pH data for the eight batch AD reactors. AD1 and 2 represent grass fed digesters, AD3 and 4 manure, AD5 and 6 Avicel, while AD7 is the *Spirulina* fed control and AD8 the negative control

The most significant pH change was observed in the Avicel fed reactors, particularly AD 6. The detailed analysis of VFAs in solution, presented later in this chapter, confirmed the release of significant concentrations of VFAs, particularly for AD 6. The difference between AD 5 and AD 6 is associated with the degree of hydrolysis observed.

The redox potential data (Figure 13) confirmed that anaerobic conditions were maintained in the reactors for the duration of the experiments. The degree of variation observed can largely be accounted for by the nature of the sampling procedure. A combination of the small sample volume (5 mℓ) and the time taken for the reading to stabilise meant that some oxidation was possible in the time between sampling and obtaining a stable reading. The *Spirulina* fed reactor was characterised by significantly lower redox values during the first week of operation, most likely due to the presence of some soluble sulphide, although this was not confirmed by direct analysis. However, analysis of a parallel fed-batch reactor, maintained on *Spirulina*, showed aqueous sulphide concentration of between 10 and 30 mg/ℓ. The Zarrouk's medium used to cultivate *Spirulina* contains sulphate and the slurry used to feed the digesters contained entrained growth medium.

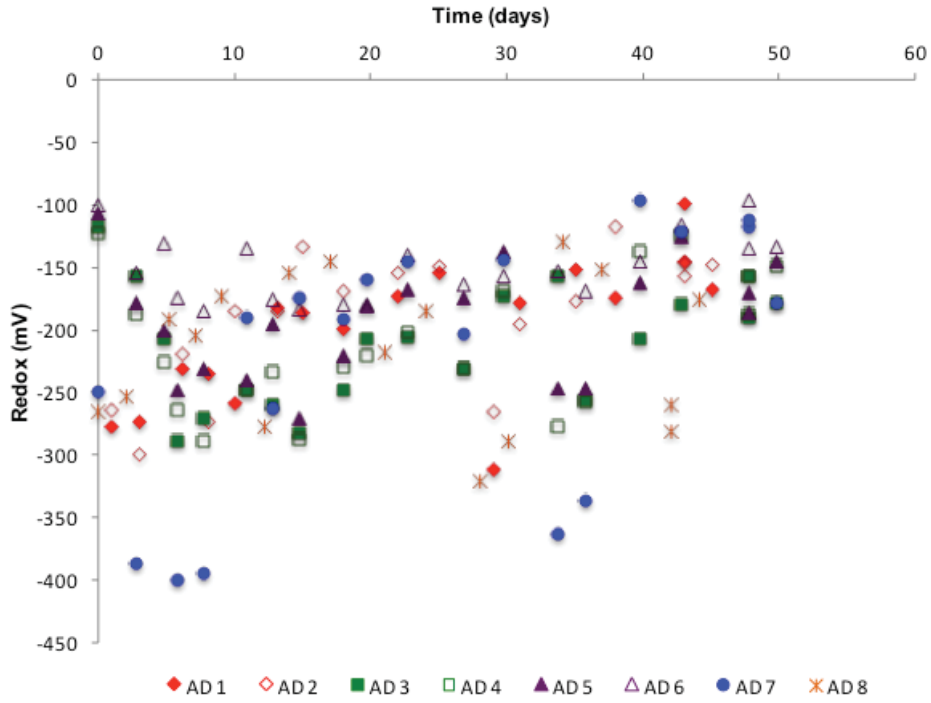

Figure 13: Summary of redox data for the eight batch AD reactors

The total biogas volume recovered from each of the reactors is summarised in Figure 14. The duplicate reactors loaded with grass and Avicel showed similar total biogas production, although there was some variation in the rate of gas production during the first two weeks in the Avicel reactors, which will be discussed in greater detail later. The duplicate reactors fed manure yielded significantly different results with respect to biogas production, with AD 3 producing over 3 ℓ of biogas, while AD 4 showed consistently low levels of activity.

The rate of biogas generation was similar during the first week of operation, after which the grass fed digesters stopped producing gas. The positive control produced gas at a high rate for about seven days, after which gas evolution ceased. The manure reactor that showed high activity (AD 3) continued to produce gas at a slower rate after the first week, while the Avicel fed digesters showed high levels of productivity for approximately two weeks before activity ceased.

The negative control did not produce significant quantities of biogas at any point during the experiment, confirming that the inoculum sludge contained very little metabolisable organic matter.

The most likely reasons for the cessation of biogas production would be the consumption of all biodegradable substrate, the loss of activity of hydrolytic or acidogenic community members, the loss of activity of the methanogenic community or a combination of all three. The residual COD and VFA data will be considered in greater detail in the subsequent sections to try and unpack the data.

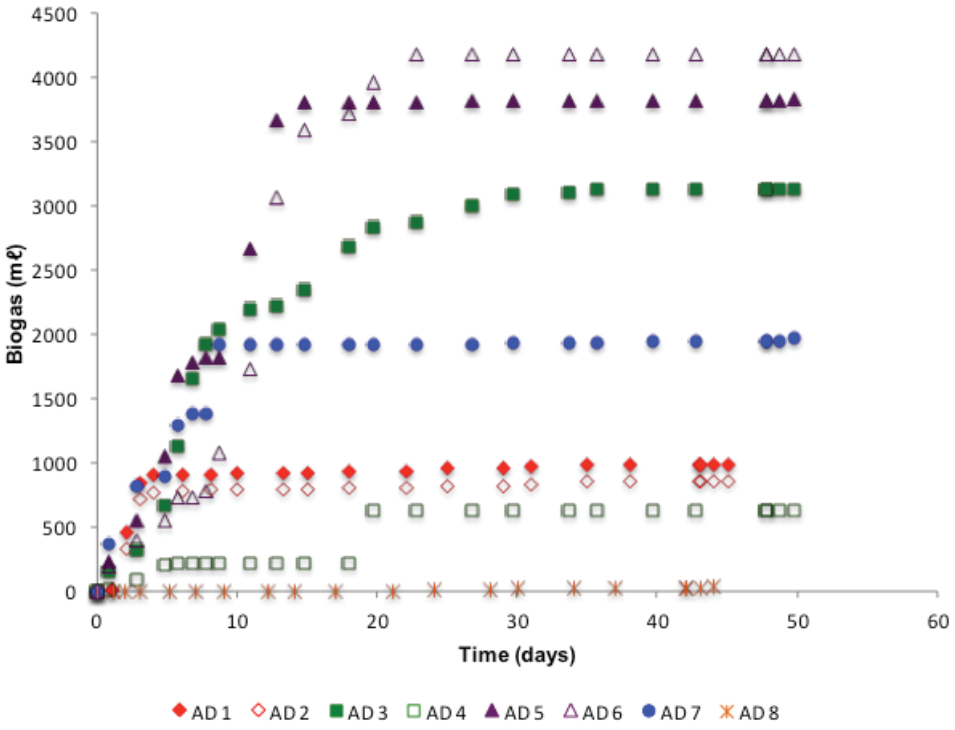

Figure 14: Summary of cumulative biogas production across the eight batch AD reactors

The biogas in the headspace of the reactors was sampled directly to determine the methane fraction by gas chromatography and the relative fractions, measured each time the reactors were sampled, are presented in Figure 15. Stoichiometrically, the conversion of one mole of acetate to biogas should yield one mole of methane and one mole of carbon dioxide. Additional carbon dioxide and hydrogen can be produced via fermentative reactions, such as those presented in Table 4. Hydrogen is typically rapidly consumed, so should not contribute significantly to the measured biogas volume. Similarly, almost all hydrogen sulphide produced by sulphate reducing bacteria would remain as aqueous HS^- at the pH of the reactors.

Table 4: Anaerobic reactions responsible for acetogenesis and methanogenesis (Inglesby, 2011)

VFA	Reaction	Eqn number
Acetate	$CH_3COOH \rightarrow CH_4 + CO_2$	1
Propionate	$CH_3CH_2COOH + 2H_2O \rightarrow CH_3COOH + CO_2 + 2H_2$	2
n-Butyrate	$CH_3CH_2CH_2COOH + 2H_2O \rightarrow 2CH_3COOH + 2H_2$	3
Iso-butyrate	$CH_3(CHCH_3)COOH + 2H_2O \rightarrow 2CH_3COOH + 2H_2$	4
n-Valerate	$CH_3CH_2CH_2CH_2COOH + 2H_2O \rightarrow CH_3COOH + CH_3CH_2CH_2COOH + 2H_2$	5
Iso-valerate	$CH_3(CHCH_3)CH_2COOH + CO_2 + 2H_2O \rightarrow 3CH_3COOH + H_2$	6

The *Spirulina*, Avicel and manure fed digesters were characterised by relatively high methane content during the early part of the experiment, which was indicative of the availability of acetate as a substrate for the methanogens. The methane fraction then decreased in the latter stages of the experiment, which coincided with the decrease in biogas formation. The methane content in the grass fed digesters was initially lower and increased to maximum values by day 7, suggesting that hydrolytic and acidogenic reactions dominated initially. During the initial phase of the experiment the methane content was consistently higher than 50%. This can be accounted for by the mildly alkaline pH in the majority of the reactors. Under these conditions, a fraction of the carbon dioxide generated would remain in solution as bicarbonate (HCO_3^-). The higher the pH the greater the bicarbonate fraction, which accounts for the

high methane fraction in the *Spirulina* fed digester (pH 8) and the relatively lower fraction in the Avicel fed digester (AD 6), for the period when the pH was in the region of pH 5.5 (up to day 11).

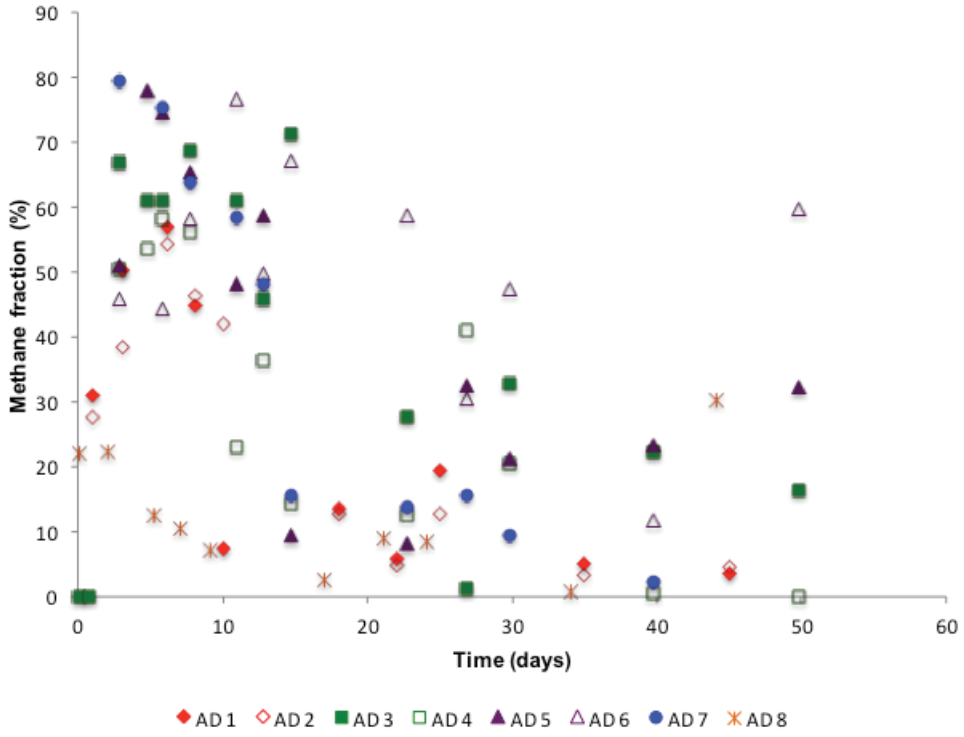

Figure 15: Relative methane fraction (volume %) measured in the headspace of the eight batch AD reactors

3.3.1.3 Negative control – sludge only

The detailed data from the negative control reactor will be discussed first and the data for the remaining reactors need to be considered against the backdrop of measured activity in the negative control. The total and soluble COD data are presented in Figure 16. The data from the positive control will be discussed last and include a comparison with historical data on *Spirulina* digestion.

The total COD data represent the contribution of the biomass in the inoculum as well as any residual suspended organic matter associated with the inoculum sludge. The nature of the inoculum was such that it was anticipated that the non-biomass fraction would not be readily metabolisable and the lack of biogas generation was consistent with that assumption. The nature of the sampling protocol, using a 1 mℓ autopipette tip with the end cut off, and the lack of homogeneity of the suspended particulate matter introduced significant variability in the total COD measurements, particularly for the grass and manure reactors. The negative control data was relatively consistent around 15 g/ℓ.

The soluble COD fraction is comprised of organic matter that was not removed by centrifugation at 13 000 x *g* for 10 minutes, so should exclude most cells and particulate organic matter. The soluble COD is AD 8 was consistently below 1 g/ℓ, with two exceptions. The data point at day 42 was measured after all reactors were spiked with sodium acetate to assess methanogenic activity. A more detailed discussion of this is presented at the end of the chapter.

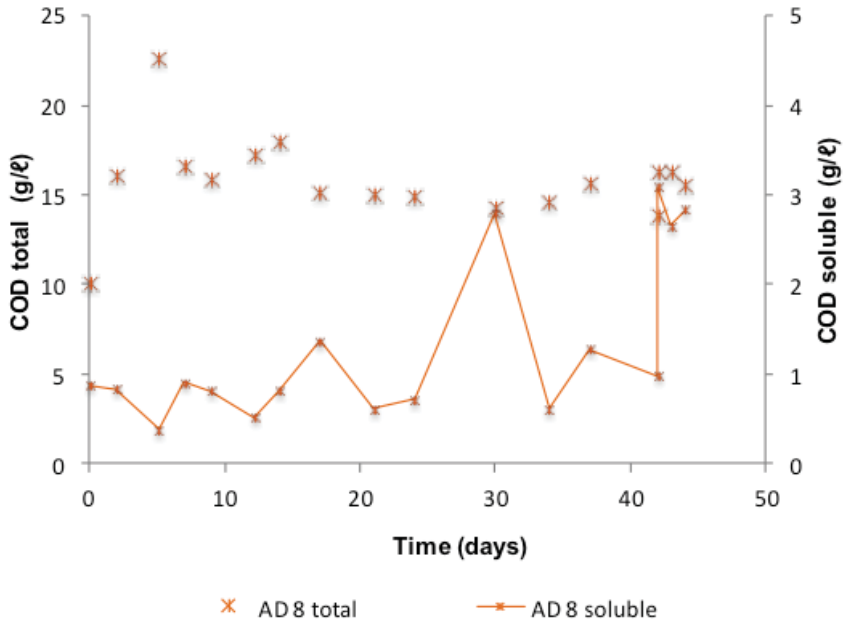

Figure 16: Total and soluble COD data measured in the negative control reactor (AD 8)

The primary aim of the anaerobic pretreatment was to generate VFAs that could be used as a substrate in the SRB/SOB channel reactor. At each sampling event a portion of the sample was filtered through a 0.45 µm membrane filter and analysed by HPLC to determine the VFA profile. The data for the negative control reactor are presented in Figure 17

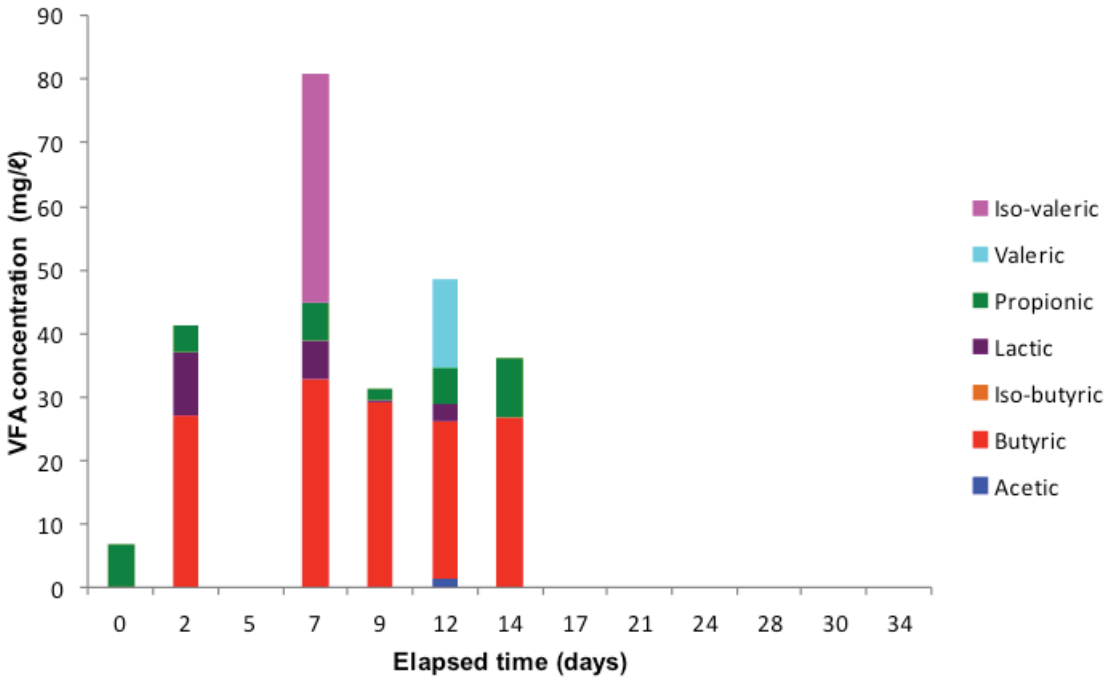

Figure 17: Summarised VFA profile measured in samples from the negative control reactor (AD 8)

The measured VFA concentration was consistently low, with butyric acid making up the bulk of the measured VFAs. From day 17 onwards no discernible peaks were detected on the chromatograms. The relative lack of VFAs, particularly acetate, is consistent with the lack of biogas generation.

3.3.1.4 Grass fed digesters

The reactors loaded with grass produced the lowest amount of biogass, where meaningful biological activity was confirmed (Figure 14), which suggests limited hydrolysis and VFA generation. The grass reactors were the most difficult to measure from a total COD perspective, as the particle size of the cut up grass was still so large that the likelihood of any grass being pulled up into the sample for total COD analysis was remote. The measured total COD values (Figure 18) confirm this, as the values were consistently similar to those obtained in the negative control (Figure 16). The decrease in total COD measured on day 31 is most likely an analytical error as the next two data points are back to around 15 g/ℓ.

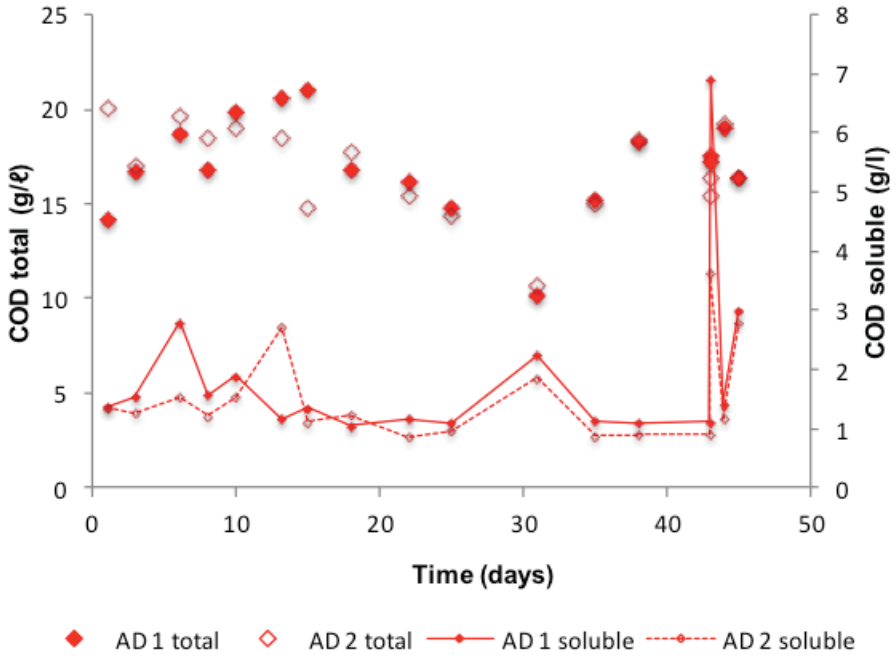

Figure 18: Total and soluble COD data measured in the grass fed reactors (AD 1 and AD 2)

The soluble COD values were typically between 1 and 2 g/ℓ, with the exception of the period following the acetate spike. This is consistent with the VFA profile data for AD 1 (Figure 19) and AD 2 (Figure 20). The measured VFA concentrations were consistently higher in AD 1 than AD 2, particularly between day 8 and day 15. The VFA profile was also significantly different, with the dominance of valeric acid.

The majority of the biogas was produced during the first three days of operation, during which time negligible amounts of VFAs were detected. This suggests an active acetogenic and methanogenic community that was able to convert almost all the liberated VFAs to biogas. The AD 1 reactor did produce more biogas than the AD 2 reactor, which indicates more metabolisable carbon was released. This may account for the higher concentration of VFAs detected between day 8 and 15. A small amount of biogas (40 mℓ) was produced between day 15 and day 25, which could be accounted for by the further metabolism of the valeric acid.

Both digesters showed a spike in VFAs in the day 35 sample, comprised primarily of valeric and iso-valeric acids. The concentration measured in AD 1 was significantly higher than that of AD 2. This increase was not associated with a corresponding increase in soluble COD, which may point to an analytical anomaly, although the proportion of soluble COD accounted for by VFAs was consistently low (Section 3.3.1.8).

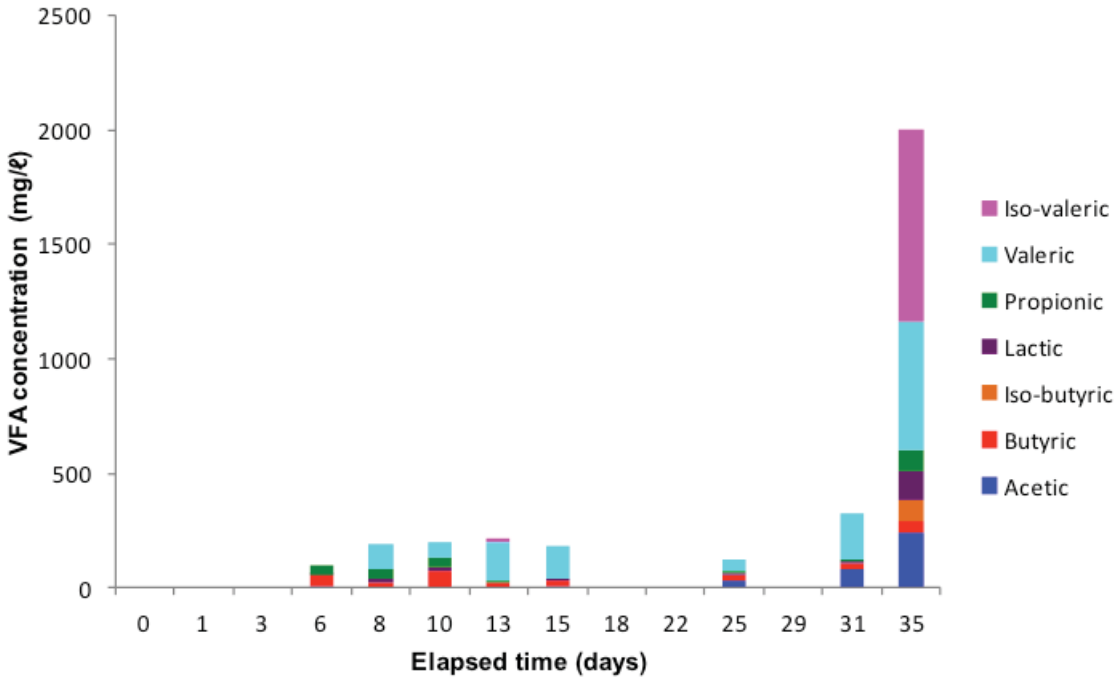

Figure 19: Summarised VFA profile measured in samples from the grass fed reactor (AD 1)

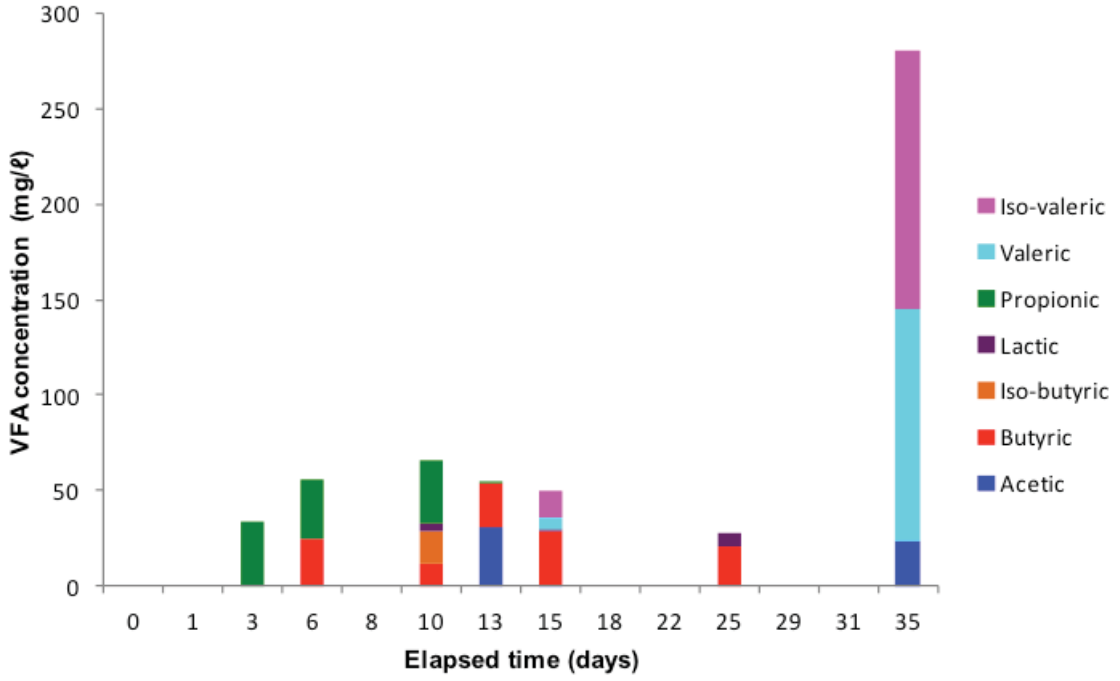

Figure 20: Summarised VFA profile measured in samples from the grass fed reactor (AD 2)

3.3.1.5 Manure fed digesters

The activity in the two manure fed reactors (AD 3 and AD 4) were significantly different, with AD 3 producing over 3 ℓ of biogass, while AD 4 produced just over 500 mℓ. Despite this difference, there was little evidence in the total or soluble COD data (Figure 21) to explain the discrepancy. As with the grass fed digesters, although to a lesser extent, obtaining a representative sample for total COD was difficult. The total COD data for AD 4 appeared to show a greater decrease, but this was not consistent with an

increase in soluble COD or biogas production. There was no significant difference in the soluble COD data between the two replicates, suggesting that the difference in biogas productivity could not be linked to this parameter. The soluble COD profile did differ from that observed in the grass fed reactors, with a steady increase in soluble COD observed over the first two weeks, followed by relative stability in the region of 3 g/ℓ until the addition of the acetate spike. The stable level was almost three times as high as the stable level obtained in the grass fed digesters (Figure 18) and could not be accounted for by VFAs. The colour of the samples prepared for HPLC analysis retained a distinct brown colour, even after filtration and prolonged storage (> 7 days) of the samples resulted in the appearance of a brown precipitate in the tubes. The colour and subsequent precipitate formation suggests the presence of phenolic compounds. Several researchers (Mackie *et al*., 1998; Powers *et al*., 1999; Kayembe *et al*., 2013) have reported on the presence of soluble phenolic compounds in cattle and swine manure, originating from urine and the degradation of manure proteins. Phenol has a COD/VS ratio of 2.38 g COD/g (Wilkie *et al*., 2004), which is significantly higher than that of VFAs and could have contributed to the increased soluble COD.

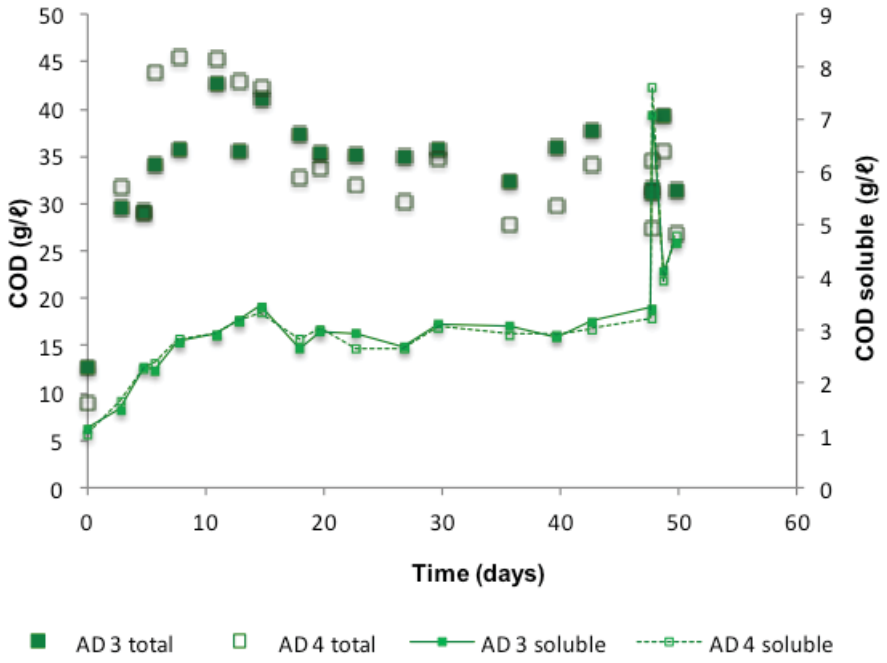

Figure 21: Total and soluble COD data measured in the manure fed reactors (AD 3 and AD 4)

The difference in the biogas production profiles between the two replicates is difficult to explain, given the very similar soluble COD profiles. Low pH is well known to negatively affect methanogenic species, but could not have been the cause in the experiments described, given the similar pH profiles and the fact that the pH in AD 4 was consistently higher than in AD 3 (Figure 22). In addition, inhibition of the methanogens would have resulted in the accumulation of VFAs and this was not observed.

The detailed VFA profiles for AD 3 and AD 4 are presented in Figure 23 and Figure 24 respectively. No VFAs were detected in samples from AD 3 for the first 5 days, during which time approximately 600 mℓ of biogas was formed. From day 6, a relatively low concentration of VFAs was detected, comprising primarily butyric and iso-butyric acid. No residual acetate was detected, suggesting that the rate of methanogenesis was higher than the rate of acetogenesis. Between day 6 and day 23 the residual VFA concentration decreased to the point where none could be detected, coinciding with a slowdown in biogas production.

The increase in soluble COD observed during the first 6 days cannot be accounted for by accumulation of VFAs, further supporting the hypothesis of the accumulation of phenolic compounds.

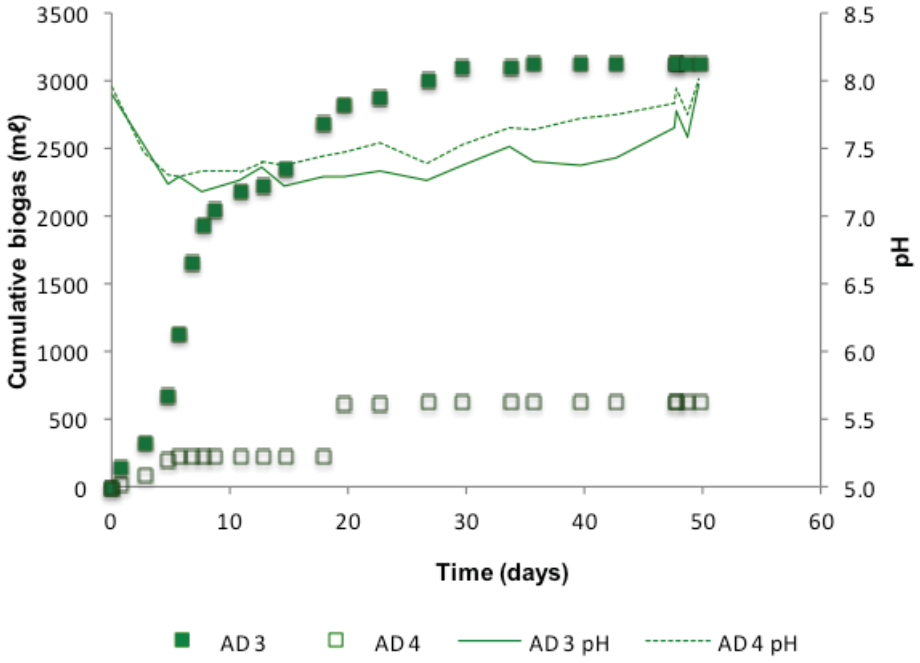

Figure 22: Relationship between pH and biogas generation in manure fed digesters (AD 3 and AD 4)

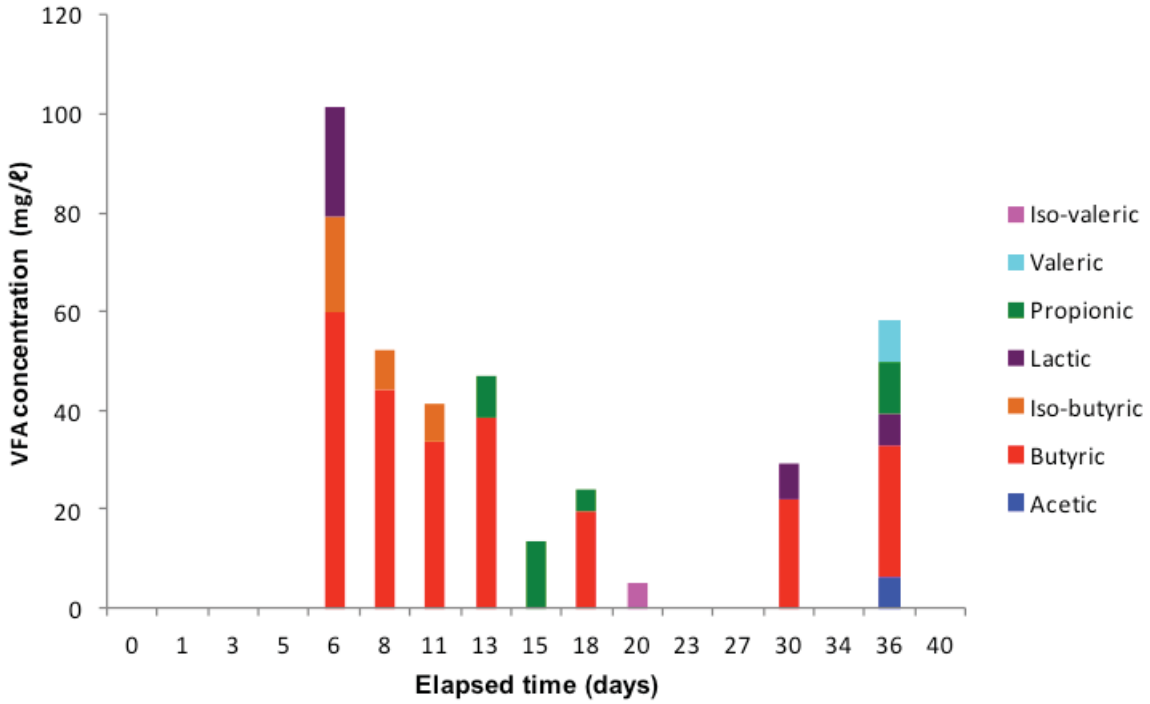

Figure 23: Summarised VFA profile measured in samples from the manure fed reactor (AD 3)

Analysis of the samples from AD 4 showed the absence of detectable VFAs for most of the first 30 days, despite the increase in soluble COD. This suggests inhibition on acidogenesis and possibly hydrolysis. The presence of low molecular weight phenolics has been shown to reduce the performance of anaerobic digestion (Kayembe *et al.*, 2013; Gonçalves *et al.*, 2012), although much of the research has focussed on the digestion of olive mill wastewater. In addition, the phenolic compounds have been shown to have a greater effect on the methanogens than the acidogenic community, so the poor performance of AD 4 cannot be explained with confidence.

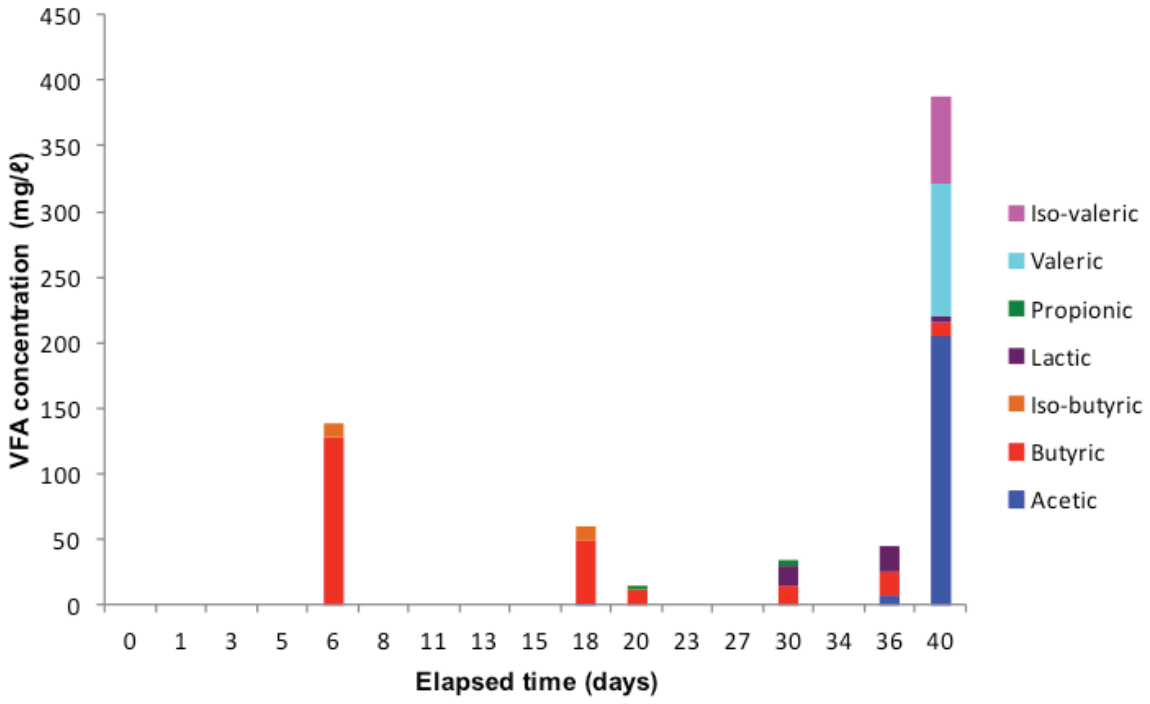

Figure 24: Summarised VFA profile measured in samples from the manure fed reactor (AD 4)

3.3.1.6 Avicel fed digesters

The Avicel fed reactors provided the best opportunity to study the performance of the inoculum. The particle size (< 50 µm) and density were such that complete suspension should have been possible in the reactors, allowing the accurate analysis of both total and soluble COD. As such, monitoring the hydrolysis of Avicel should have been possible, allowing for a full material balance across the batch system.

However, in reality there were still inconsistencies in the total COD data (Figure 25). Based on the data from the negative control, the initial total COD should have been in the range of 45 g/ℓ, but the actual measured values were lower. The variability in the measured values was particularly significant during the initial phase for AD 6. Despite the variability, a clear trend of decreasing total COD was observed in both reactors for the first four weeks. While the decrease in total COD was relatively similar between the duplicate reactors, the soluble COD data were very different, with soluble COD values as high as 6 g/ℓ recorded for AD 6, while remaining consistently below 1 g/ℓ in AD 5.

This can be attributed to the significant difference in pH between the reactors during the first week of operation (Figure 26). The pH in AD 6 decreased from pH 7.6 at the start of the experiment to below pH 5.7 within the first three days, which is consistent with efficient hydrolysis and acidogenesis. The low pH would have inhibited methanogenic activity, resulting in the lower biogas production observed as well as the reduced methane content (Figure 15).

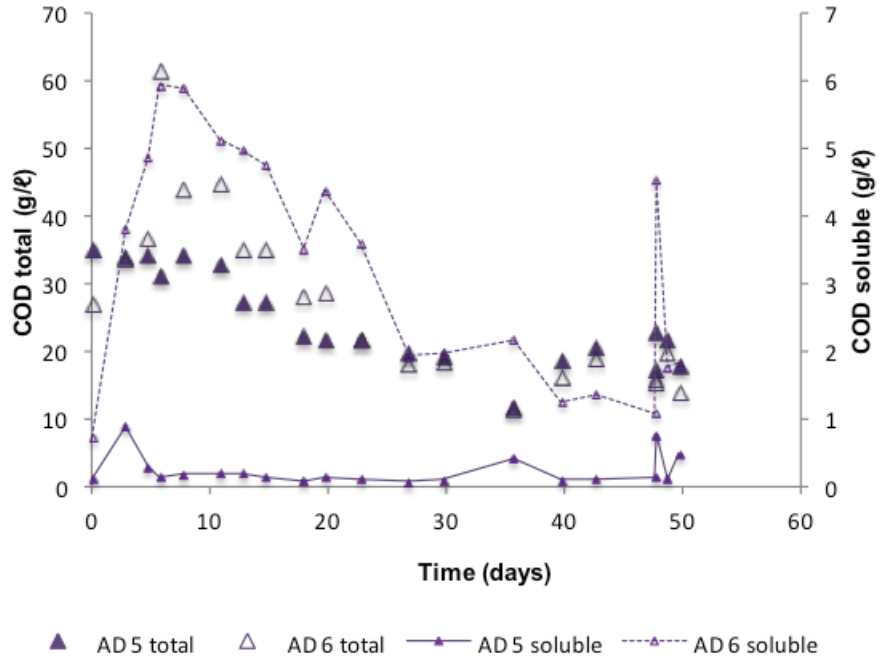

Figure 25: Total and soluble COD data measured in the Avicel fed reactors (AD 5 and AD 6)

The pH in AD 6 increased to above pH 6.5, where methanogenesis would no longer be inhibited, by day 10 and this was accompanied by an increase in biogas production and the methane content. By day 20 the biogas volume exceeded that produced in AD 5, but no further biogas was produced after day 21, suggesting either the depletion of bioavailable substrate or the loss of microbial activity. The fact that complete digestion of MCC has been reported suggests the latter.

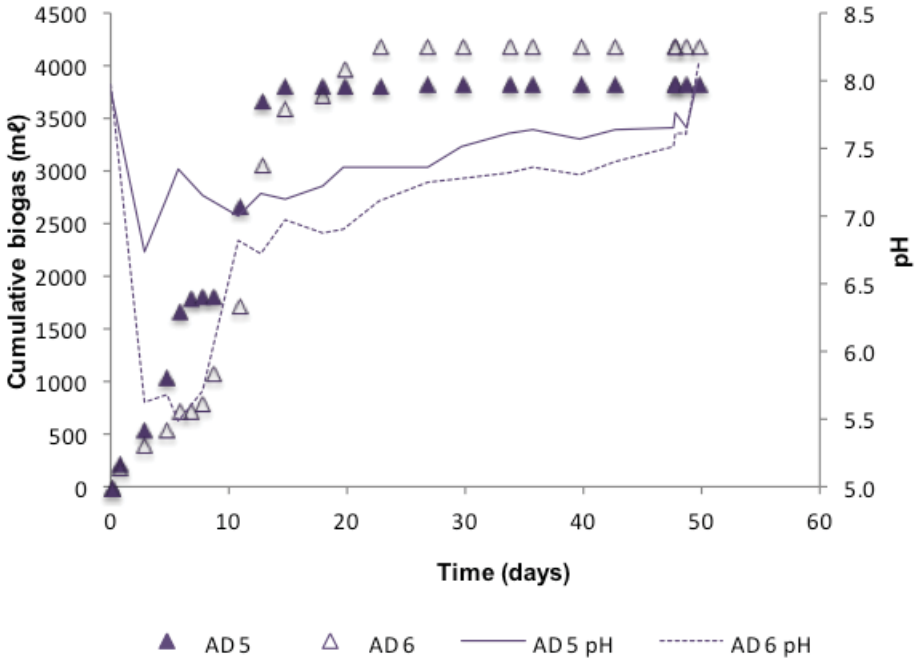

Figure 26: Relationship between pH and biogas generation in Avicel fed digesters (AD 5 and AD 6)

The VFA profile and the relationship between pH and the accumulation of VFAs for the two Avicel fed reactors are illustrated in the figures below. Significant acetate accumulation was observed on day 3

in AD 5 (Figure 27). This was not observed in either the grass or manure fed reactors, suggesting that the rate of hydrolysis of the Avicel and subsequent acidogenic and acetogenic reactions were faster than the conversion of acetate to methane. The VFA accumulation resulted in a decrease in pH from pH 8 to pH 7, which was still within the optimum range for methanogenesis. Almost all the acetate had been consumed by day 5, resulting in the formation of over 1.5 ℓ of biogas and an increase in pH of 0.5 units (Figure 28).

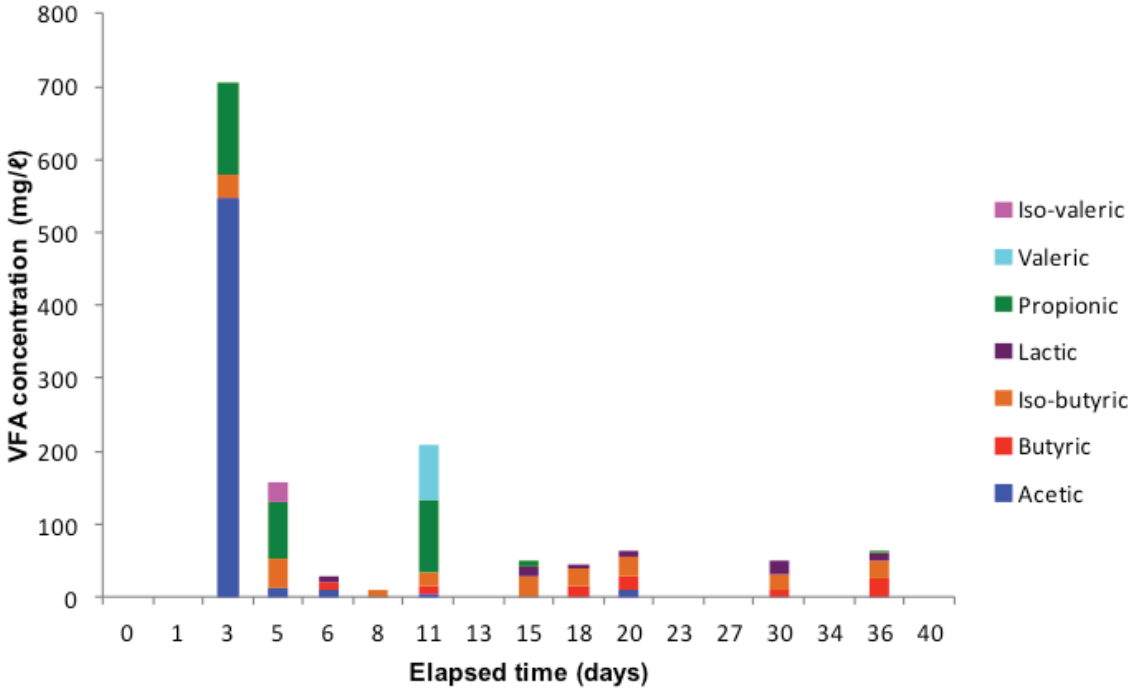

Figure 27: Summarised VFA profile measured in samples from the Avicel fed reactor (AD 5)

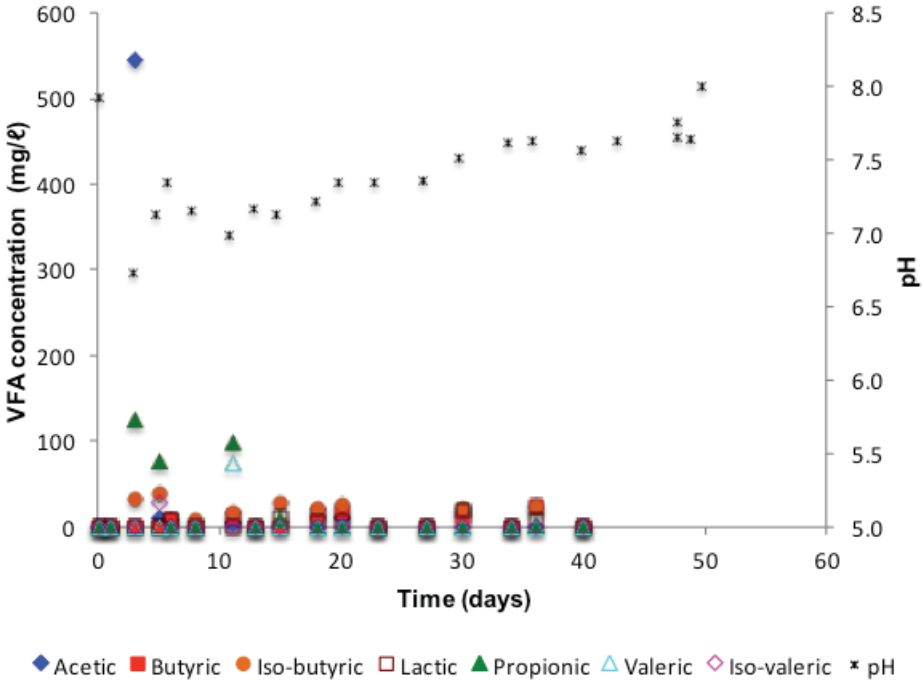

Figure 28: Relationship between pH and VFA concentration in the Avicel fed reactor (AD 5)

The pH remained above pH 7 for the remainder of the experiment and there was no further accumulation of VFAs, which was consistent with the low soluble COD values.

By contrast, the accumulation of VFAs in AD 6 was several times higher, with over 2 500 mg/ℓ of acetate measured on day 3 (Figure 29). The high concentration of acetate reduced the pH in the reactor to below pH 5.7, which reduced methanogenic activity. Therefore, the acetate was not rapidly consumed and biogas production remained relatively low. Significant acetate consumption, coupled with biogas generation, was observed from day 8 and by day 15 almost all the acetate had been converted to biogas. This was followed by the slower metabolism of propionic acid, most likely according to Equation 2 (Table 4). The conversion of propionic to acetic acid produces additional carbon dioxide which would account for the decrease in the methane fraction of the biogas to below 50% at this time. By day 27 the propionic acid had been consumed and valeric acid became the dominant VFA. Valeric acid had not previously been accumulated at such significant concentrations and this suggests a shift in microbial community structure or dominant metabolic pathway. In addition to the valeric acid peak another large peak was observed at around 41 minutes, which did not correspond to any of the available VFA standards. Hypotheses regarding the nature of the peak are presented in Section 3.3.1.8.

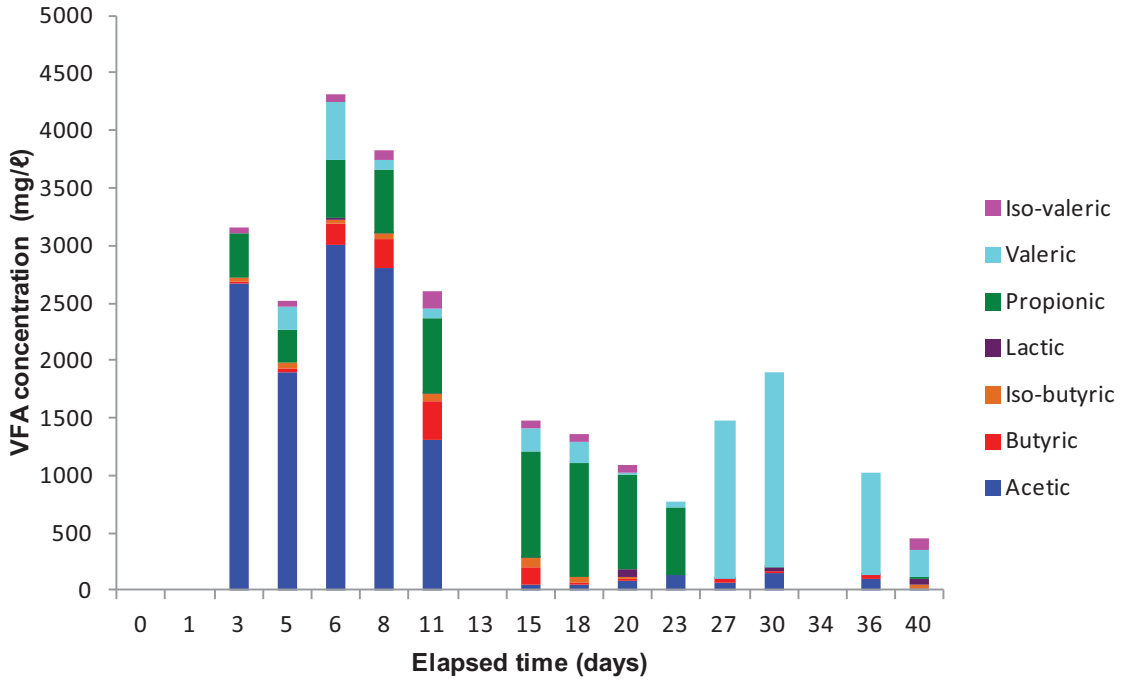

Figure 29: Summarised VFA profile measured in samples from the Avicel fed reactor (AD 6)

The relationship between VFA concentration and pH is highlighted in Figure 30. The influence of acetic acid on the pH is clearly visible. The pKa of acetic acid is 4.75, which accounts for the low pH up to day 8. By day 11 the pH had increased to around pH 6.8. Valeric acid has a similar pKa (4.82), but the accumulation of almost 2 g/ℓ was not sufficient to reduce the pH to below pH 7. Between day 30 and day 40 the majority of the valeric acid appears to be consumed, but this is not accompanied by an increase in either acetic or butyric acid (Equation 5, Table 4) or additional biogas production. It is possible that the valeric acid peak may have been misidentified or that the gas collection system was not perfect, resulting in significant biogas leakage when the gas production rate was low.

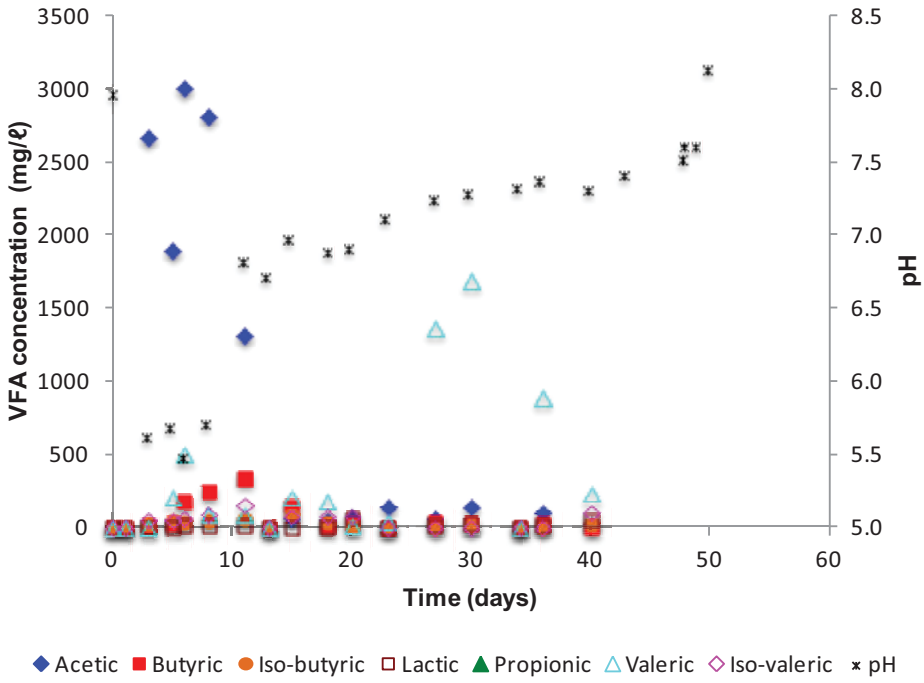

Figure 30: Relationship between pH and VFA concentration in the Avicel fed reactor (AD 6)

3.3.1.7 Positive control – Spirulina

Spirulina was selected as the substrate for the positive control as previous batch tests, conducted in a similar fashion, showed that it could be effectively digested, with good VFA liberation and biogas production (Inglesby, 2011). The current experiment was set up in almost identical fashion, with the exception that the *Spirulina* was not slurried with water prior to addition and a different inoculum was used.

The *Spirulina* in the current experiment reacted differently to what was previously observed, with biomass aggregation observed in the reactor. As with the grass and manure this made obtaining a representative sample for the total COD assay difficult. The nature of the inoculum may have contributed to this. Inglesby's inoculum was predominantly planktonic and did not contain the particulate sludge used in the current experiment.

The soluble COD did increase significantly, from 2 to almost 5 g/ℓ over the first three days (Figure 31) and this was associated with VFA accumulation (Figure 32). There were, however, several important differences between the current experiment and replicate experiments performed during Inglesby's work (2011). These will be highlighted in the subsequent discussion and possible reasons for the differences proposed.

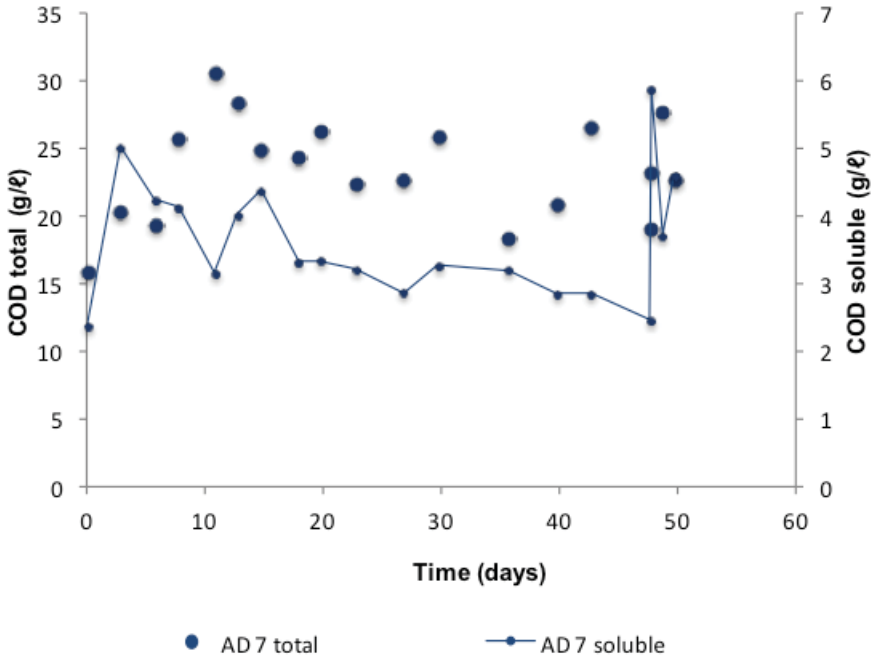

Figure 31: Total and soluble COD data measured in the *Spirulina* fed reactor (AD 7)

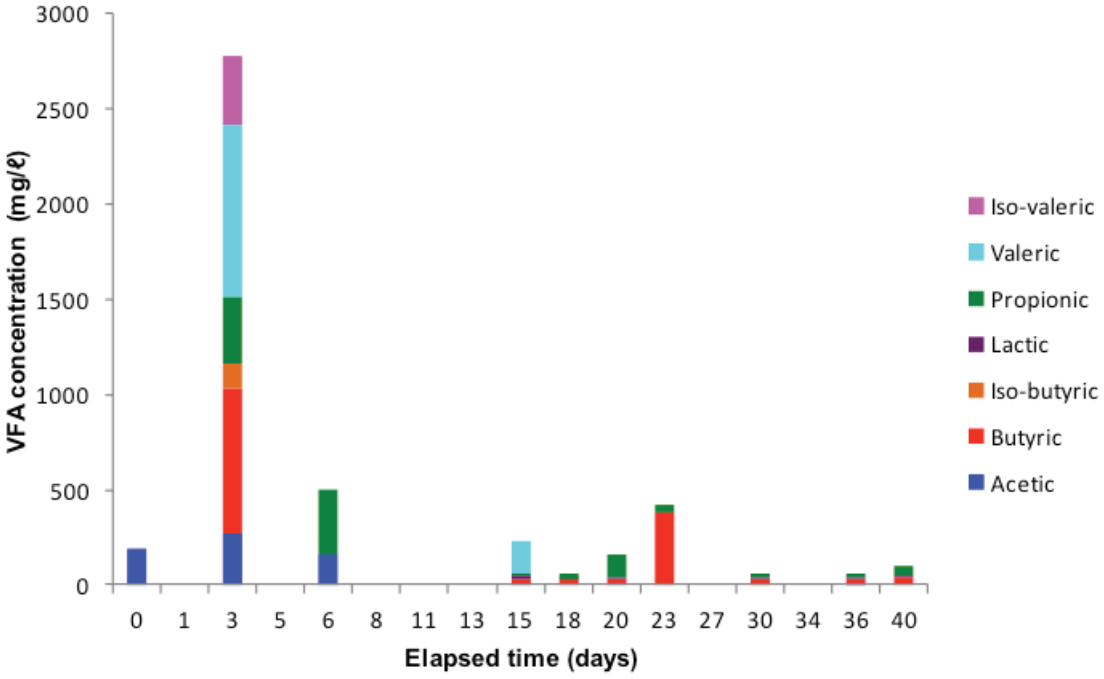

Figure 32: Summarised VFA profile measured in samples from the *Spirulina* fed reactor (AD 7)

The first major difference is the degree of solubilisation observed during the first days of the experiment. In Inglesby's experiments the total COD decreased from approximately 30 g/ℓ to below 15 g/ℓ within the first 24 hours, accompanied by an increase in soluble COD from 8 g/ℓ to almost 16 g/ℓ (Figure 33b). Light microscopy revealed almost complete disintegration of the *Spirulina* filaments during the first 24 hours. The initial soluble COD value was also almost four times higher. The fact that the harvested biomass was added as a premixed slurry rather than a wet filter cake may have accounted for this. *Spirulina* is cultivated in Zarrouk's medium, which has a high salt content (conductivity > 20 mS/cm).

Preparing a slurry in fresh water likely induced osmotic shock, resulting in spontaneous cell lysis. Cell lysis was so extensive that there was almost no difference in the COD and VFA profiles observed between the studies conducted with whole cells and those using *Spirulina* that had been pre-treated by high pressure homogenisation. By contrast, the degree of liberation of soluble COD and VFAs for homogenised *Scenedesmus* was almost double that of whole cells (Inglesby, 2011)

Following the large decrease in the first 24 hours the total COD continued to decrease for the next 30 days, before stabilising at approximately 4.5 g/ℓ. This was not observed in the current study (Figure 33). The presence of the inoculum sludge would have contributed to the measured total COD, but based on the data from the negative control this would account for approximately 15 g/ℓ.

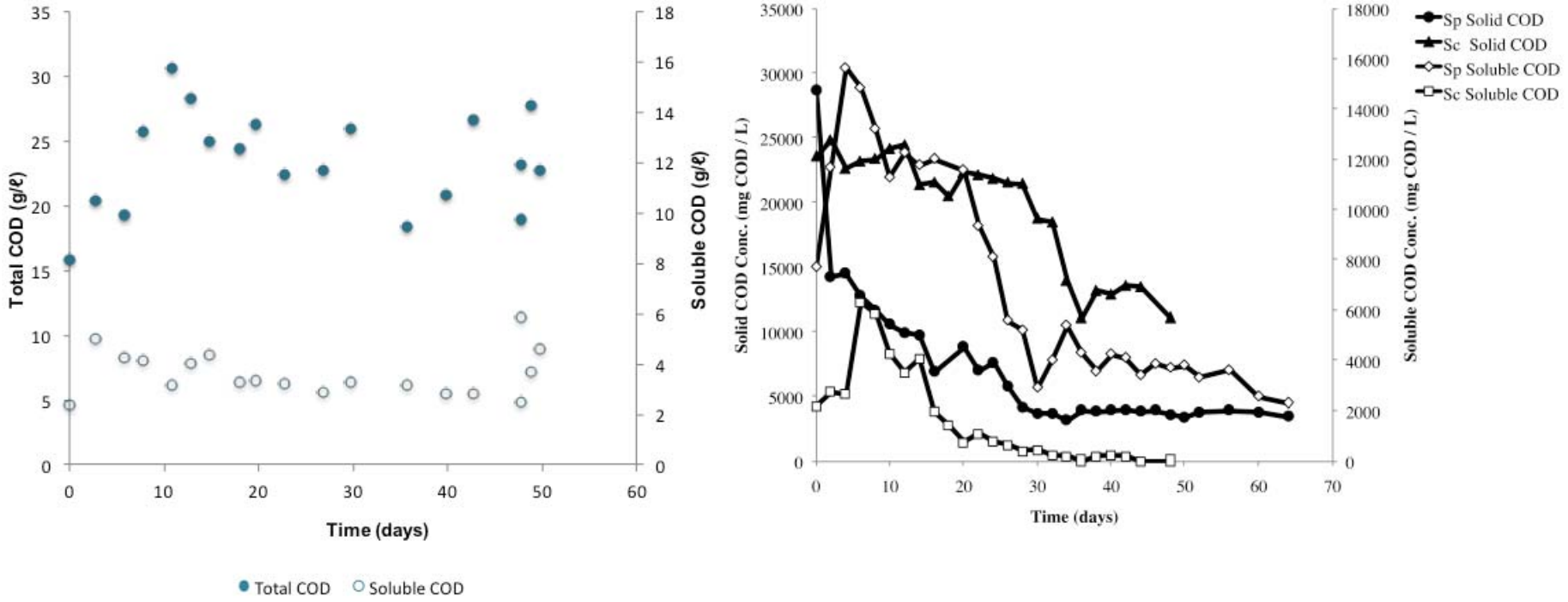

Figure 33: Comparison of total and soluble COD data between current and historical (Inglesby, 2011) studies. Sp refers to *Spirulina* and Sc to *Scenedesmus*

The VFA profiles for the two sets of data are very different, although broadly consistent with the soluble COD. The high soluble COD values from the original experiments could largely be accounted for by VFAs, with the acetate concentration remaining around 4 000 mg/ℓ for almost 20 days, before rapidly decreasing (Figure 34). The steady decrease in the total COD over that period pointed to continued hydrolysis of the remaining cells and cell fragments, replenishing the VFAs that had been consumed during biogas production. The data from the current study show no accumulation of acetate, indicating that any acetate released into solution was rapidly consumed.

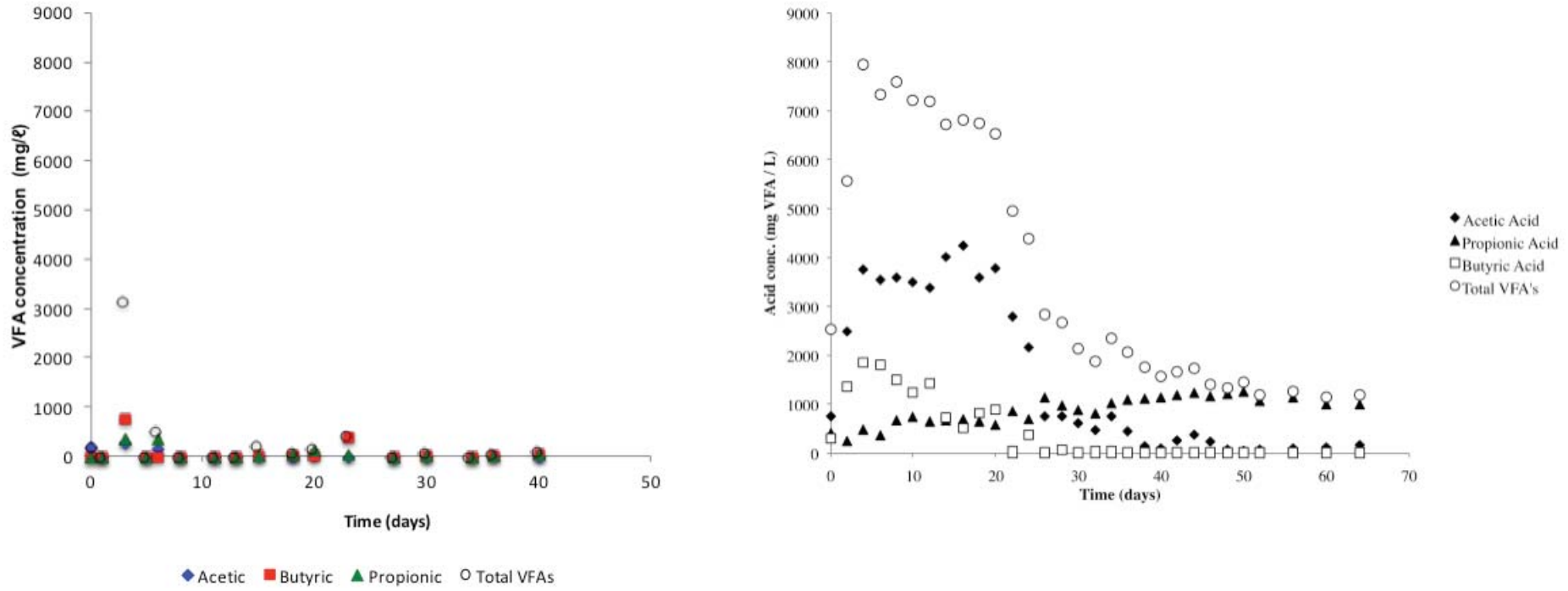

Figure 34: Comparison of primary VFAs between current and historical (Inglesby, 2011) studies where whole *Spirulina* was used as the substrate

A similar trend was observed for the indicator VFAs (Figure 35). Inglesby's data showed an increase in iso-valeric and iso-butyric acids during the phase of rapid hydrolysis, followed by a clear preference with respect to the further metabolism of the indicator VFAs. Significant metabolism of the iso-butyric acid only occurred after the concentration of iso-valeric acid had decreased by almost 80%.

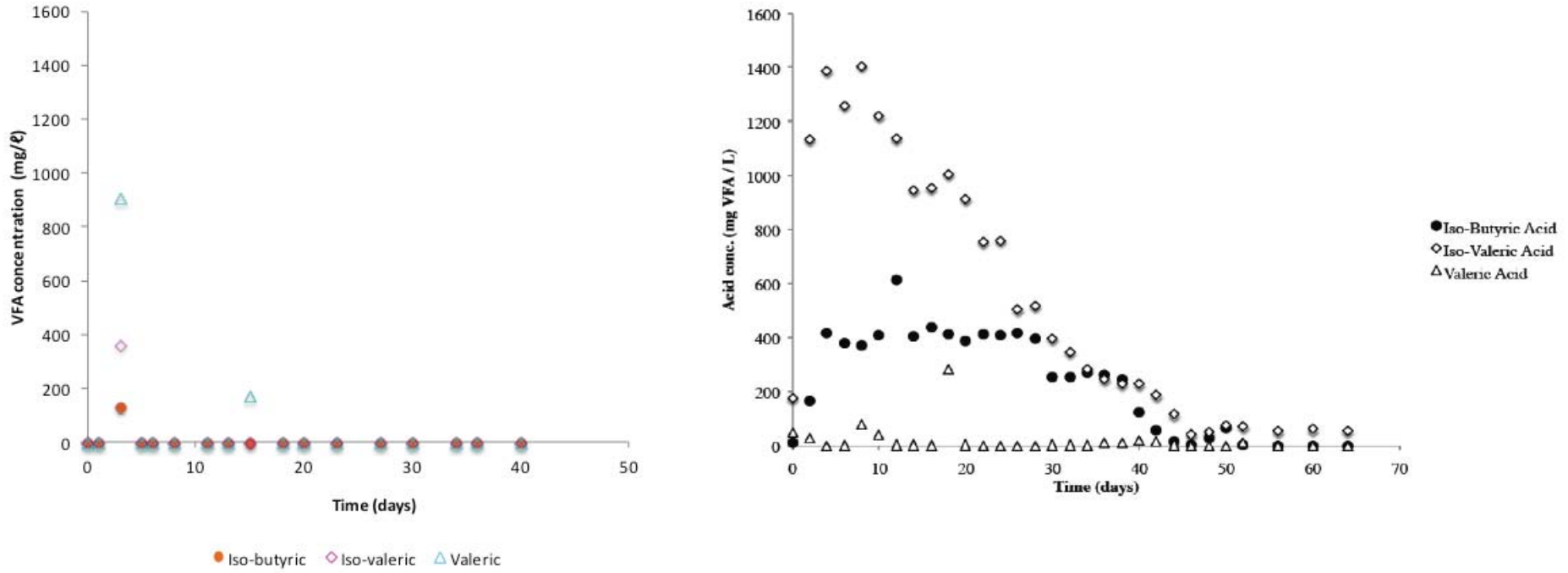

Figure 35: Comparison of indicator VFAs between current and historical (Inglesby, 2011) studies

A comparison of the biogas production (Figure 36) and methane content (Figure 37) between the two studies is revealing and suggests differences in the predominant metabolic pathways, possibly caused by differences in the microbial consortia. Both sets of data showed significant biogas generation during the first days of the experiment, but the methane concentrations are very different. In the current study, the methane content peaked around 80% at the start of the experiment and steadily declined, along with the biogas productivity. This indicates a high level of methanogenic activity and a relatively high pH, to account for the elevated methane content. This is consistent with the limited decrease in total COD, suggesting limited hydrolytic and acidogenic activity. By contrast, the methane content in the previous study was low (< 20%) during the first days of the experiment, despite the high biogas productivity, suggesting a predominance of carbon dioxide, associated with hydrolysis and acidogenic reactions. The accumulation of VFAs caused the pH to decrease to pH 6.1 (data not shown), which would have inhibited methanogenic activity. There was limited biogas formation for almost two weeks, during which time some active pH control was required to achieve a pH > 6.5. Biogas productivity increased from around day 16, as did the methane content, indicating a shift towards methanogenesis as primary metabolic pathway. The consumption of accumulated VFAs further increased the pH, leading to the increase in methane content to around 80%.

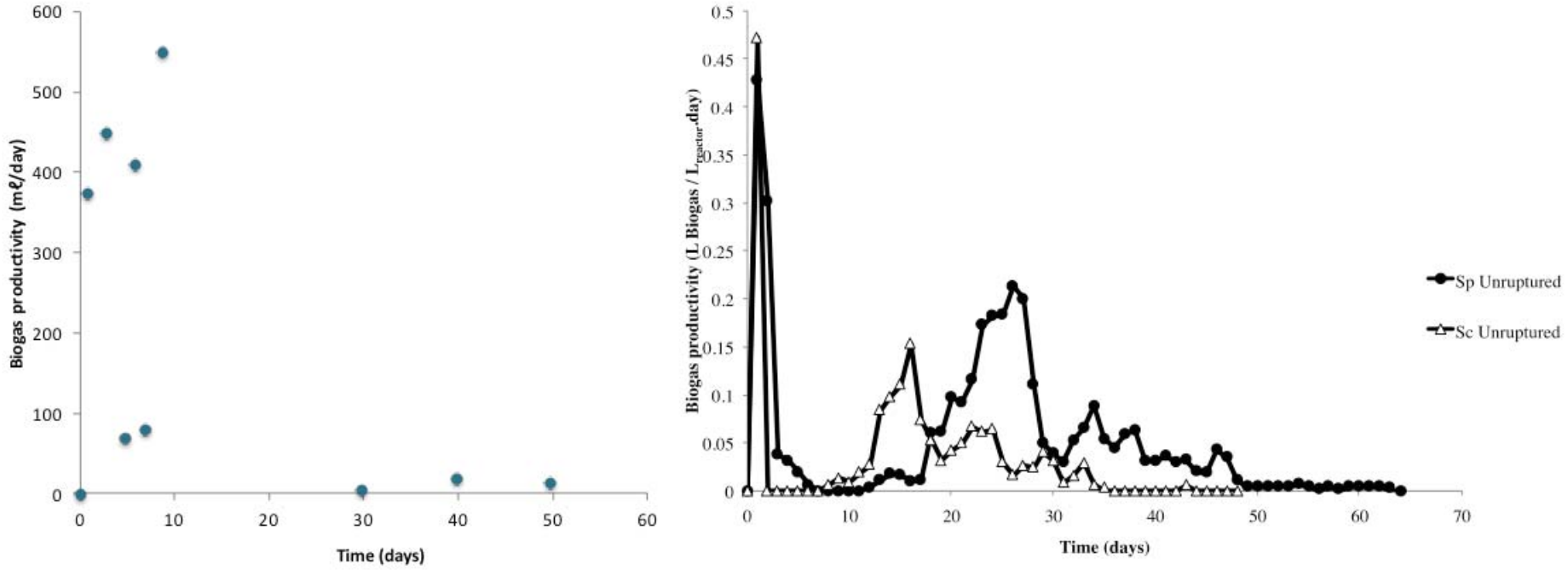

Figure 36: Comparison of biogas productivity between current and historical (Inglesby, 2011) studies

The absence of the secondary phase of biogas production in the current study is consistent with the limited hydrolysis and acidogenesis indicated by the COD and VFA data. The reasons may be associated with the way the *Spirulina* inoculum was prepared. The addition of unwashed biomass in the current study resulted in the transfer of salts from the Zarrouk's medium entrained in the wet filter cake. As a consequence the salinity in the *Spirulina* digester, measured as electrical conductivity, was significantly higher (15.8 mS/cm) than the rest of the reactors (8-9 mS/cm). This may have had two important consequences. Firstly, reduced osmotic shock which could account for the lack of spontaneous cell lysis and secondly, some inhibition of the microbial community.

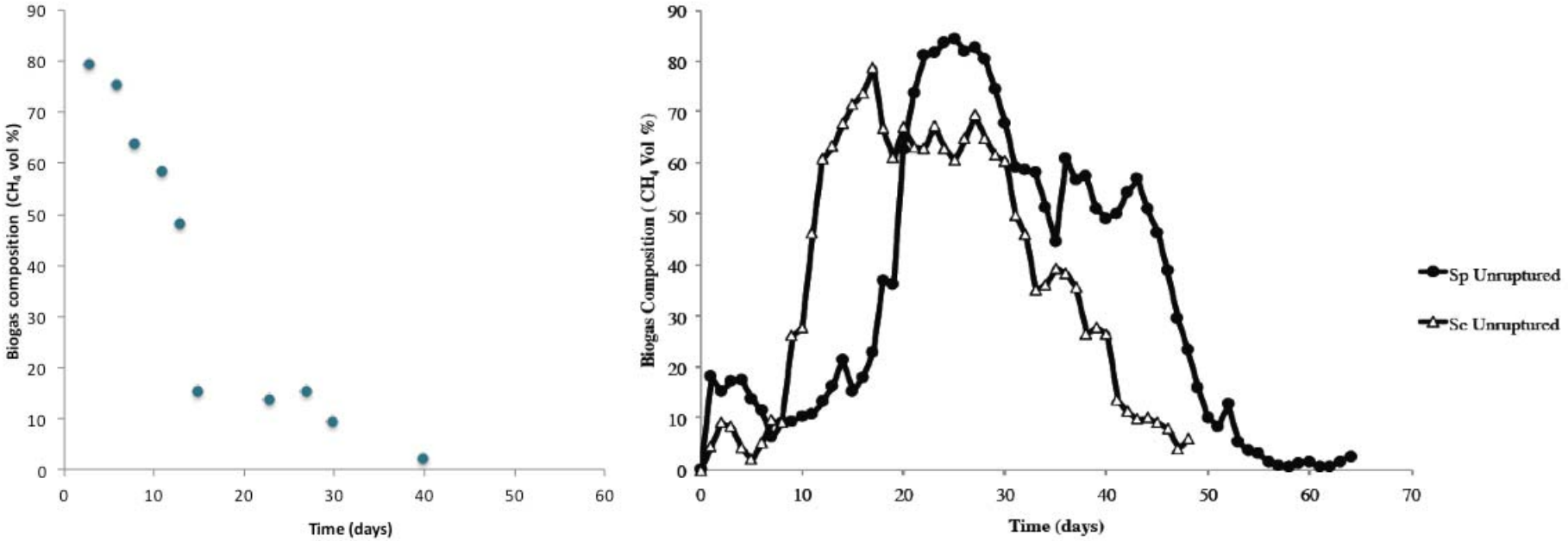

Figure 37: Comparison of biogas composition between current and historical (Inglesby, 2011) studies

3.3.1.8 Relationship between soluble COD and VFAs

The primary aim of the anaerobic reactor in the overall integrated process is the hydrolysis of the complex substrate and the generation of VFAs that can be used as the electron donor and carbon source for the sulphate reducing and sulphide oxidising communities in the channel reactor. As such, the production and accumulation of VFAs in the reactors are key parameters. Historical data (Inglesby, 2011) on the digestion of *Spirulina* and *Scenedesmus* sp showed that between 50 and 90% of the soluble COD could be accounted for by measured VFAs, across the duration of the batch experiments. These data served as motivation for the current study, investigating a wider range of substrates.

Plots of soluble COD against the sum of measured VFAs for the five sets of experimental reactors are presented in Figure 38 to Figure 42. The data consistently show that VFAs account for only a small proportion of the soluble COD, with the exception of the AD 6 Avicel reactor (Figure 41) where the contribution of the VFAs is similar to that previously reported.

At this stage it is not clear what type of molecules are accounting for the majority of the soluble COD, but the persistence of stable values for long periods in most of the reactors suggests that they are not easily degradable. There is some evidence to suggest phenolic compounds could be present in the manure fed reactors and this has been discussed above.

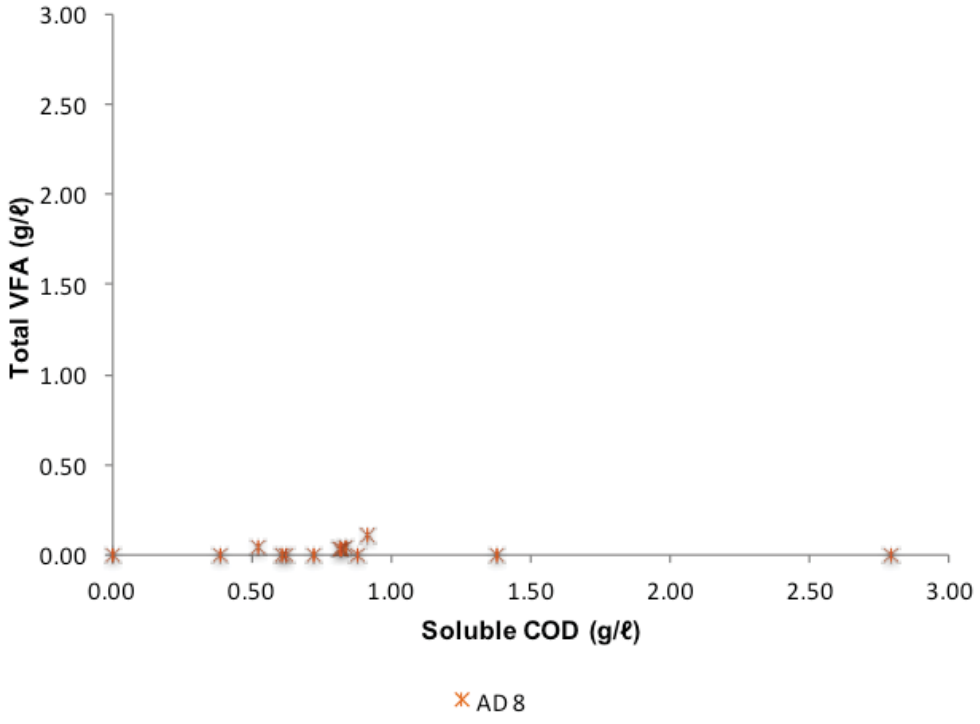

Figure 38: Relationship between soluble COD and total VFA concentration for the negative control (AD 8)

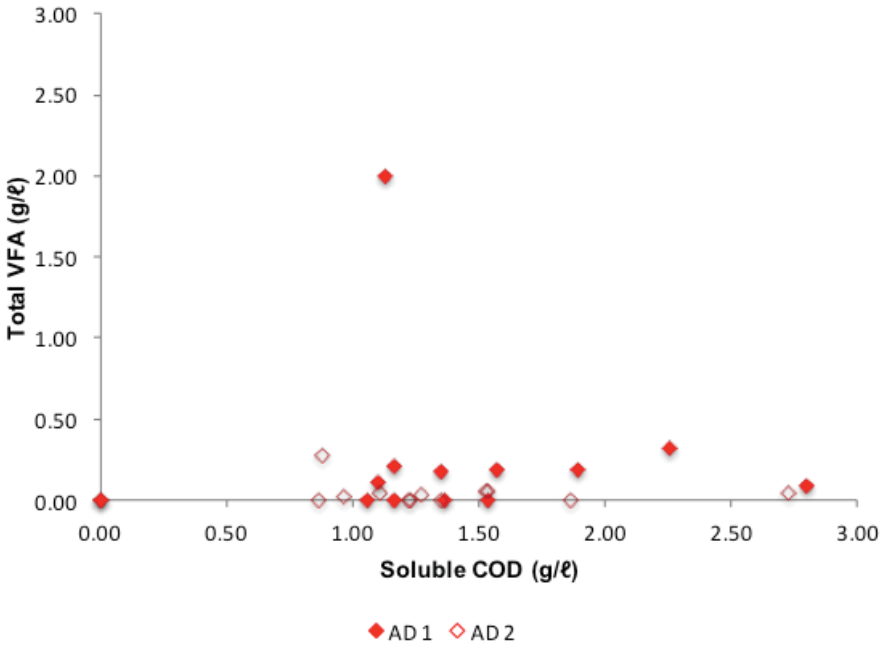

Figure 39: Relationship between soluble COD and total VFA concentration for the grass fed reactors (AD 1 and AD 2)

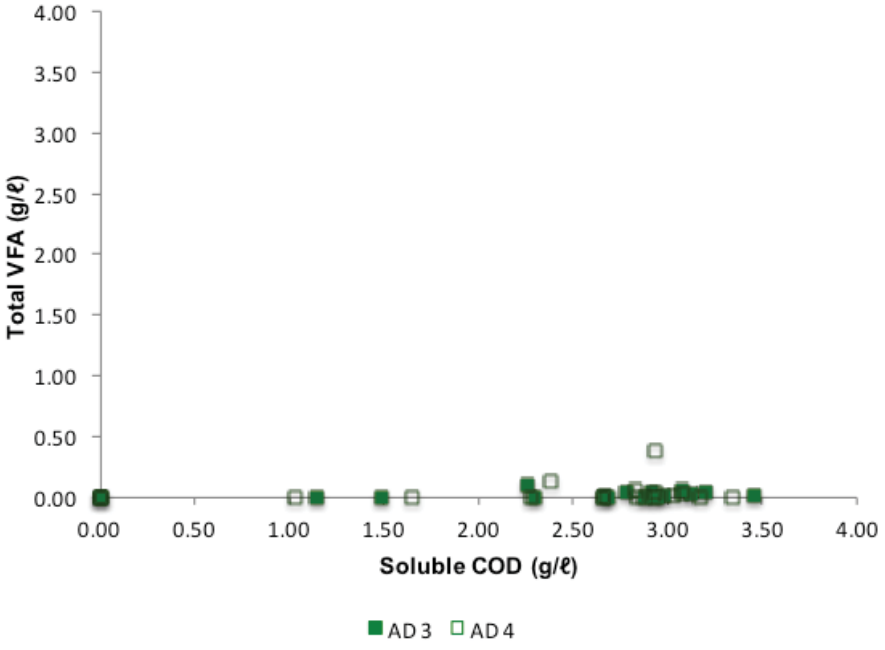

Figure 40: Relationship between soluble COD and total VFA concentration for the manure fed reactors (AD 3 and AD 4)

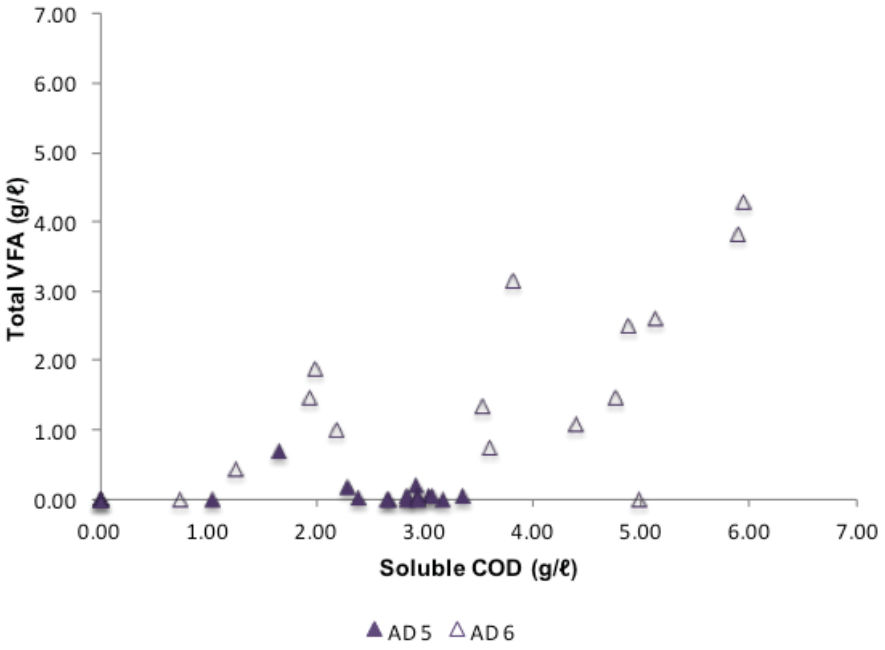

Figure 41: Relationship between soluble COD and total VFA concentration for the Avicel fed reactors (AD 5 and AD 6)

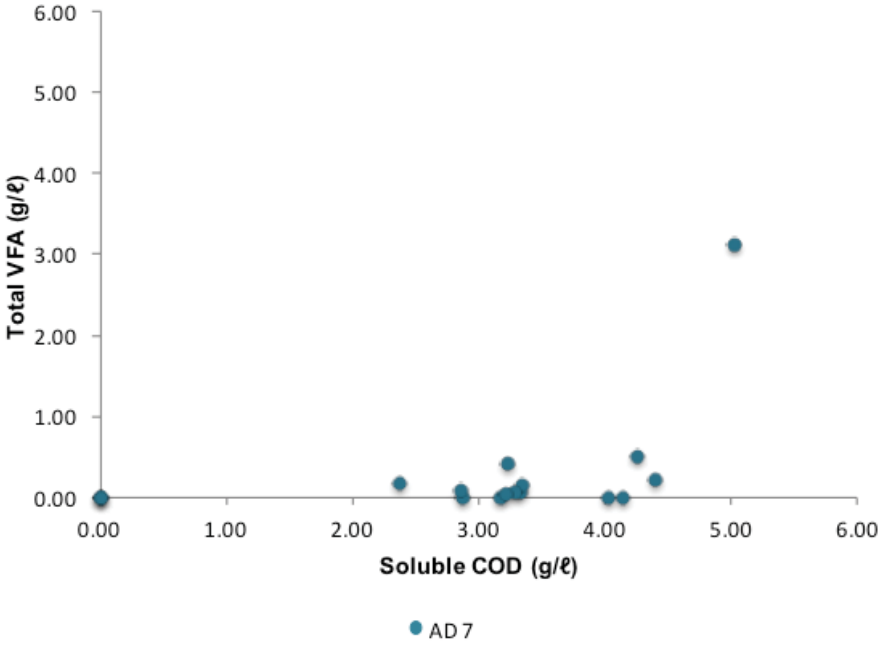

Figure 42: Relationship between soluble COD and total VFA concentration for the positive control (AD 7)

The HPLC chromatograms obtained during the study did occasionally contain peaks that did not correspond to the retention times of the seven VFA standards (Figure 43) used. Samples from the Avicel fed reactors occasionally showed a peak between the lactic and acetic acid peaks, which was subsequently identified as formic acid, but this was not significant.

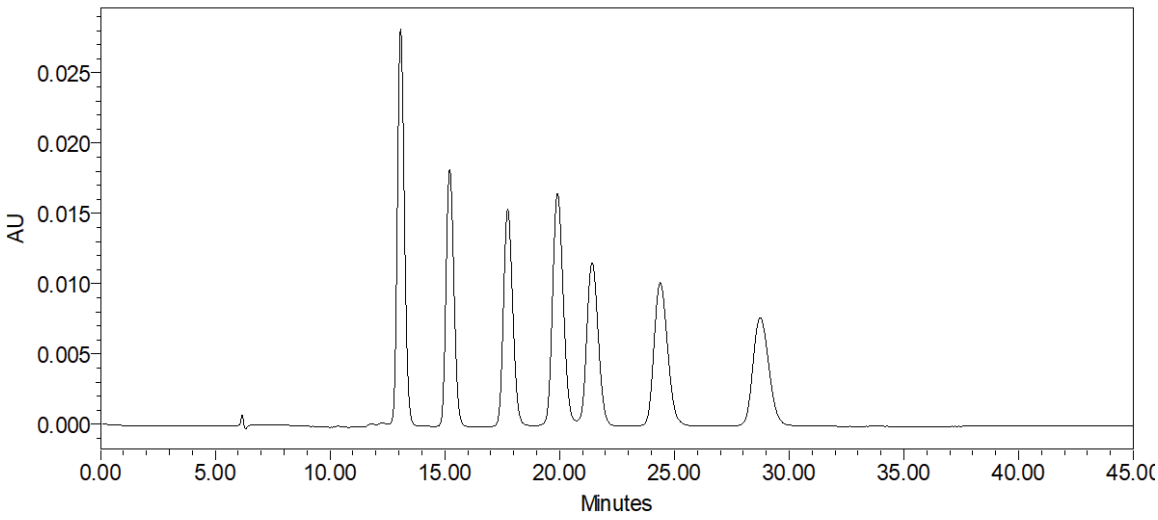

Figure 43: HPLC chromatogram showing the mixed standard at 300 mg/ℓ for each VFA. Peaks and retention times, in order are: lactic (12.98), acetic (15.19), propionic (17.73), iso-butyric (19.90), butyric (21.40), iso-valeric (24.38) and valeric (28.73)

A more significant peak was observed in a number of samples at a retention time of just over 41 minutes. The peak was particularly significant in the reactors fed with Avicel, *Spirulina* and grass, but was not detected in the manure fed reactors or the negative control. In many cases the peak area was significantly greater than those of the seven standard VFAs. The shape, consistency and fact that the peak area changed as the experiments progressed suggest that it is not a contaminant coming off the column, but an actual metabolite.

An example of the peak, showing the decrease in area over a period of nine days is shown in Figure 44. During this period a total of 550 mℓ of biogas was produced, without any other VFAs being detected. The decrease in peak area suggests that it represents a compound that is being metabolised.

A review of literature, as well as reference chromatograms for the specific HPLC column suggests that the peak may represent caproic (hexanoic) acid. Research by Kenealy and co-workers (1996) reported on the production of caproic acid by cellulolytic rumen bacteria and *Clostridium kluveri* when grown on substrates including cellulose. Similar findings have been reported by Sauer and associates (2012) and others (Pakarinen *et al*., 2008).

At the time the research was conducted a standard for caproic acid was not available. It is recommended that subsequent work should attempt to confirm whether or not the observed peak can be attributed to caproic acid. If it is confirmed, the proportion of soluble COD that can be attributed to VFAs would increase significantly for the grass, Avicel and *Spirulina* digesters. It would also be valuable to investigate the metabolism of caproic acid in greater detail, both from an AD/biogas production perspective and for the generation of substrate for the integrated process.

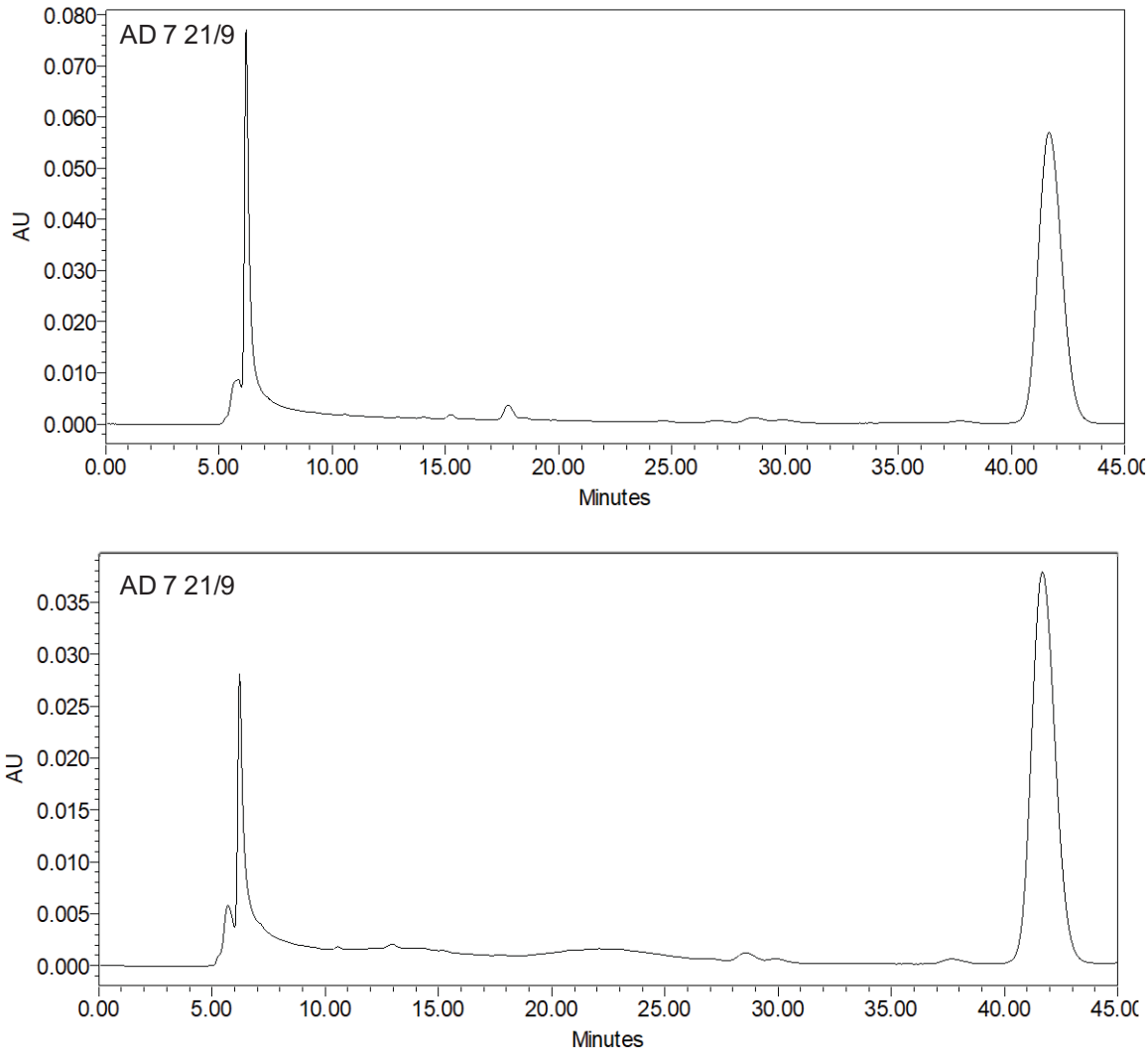

Figure 44: Presence of an additional peak at 41.8 minutes in the positive control reactor showing the decrease in peak height between 21 September (day 6) and 30 September (day 15)

3.3.1.9 Effect of acetate supplementation

Biogas production had essentially ceased in all the reactors by day 26. Therefore, a decision was taken to supplement each of the reactors with a dose of sodium acetate to assess the viability of the methanogenic community, ahead of a potential second round of biomass addition. A concentrated sodium acetate solution (188 g/ℓ) was prepared and 10 mℓ added to each digester on day 48. The total and soluble COD were measured prior to and one hour after the acetate addition. Based on the amount added, the soluble COD was expected to increase by approximately 1.89 g/ℓ. The actual values ranged from -0.37 to 7.20 g/ℓ and there was little consistency between replicate reactors. The samples analysed 24 hours later showed a decrease of between 0.66 and 5.20 g/ℓ, although again with no consistent trend. Notwithstanding the variation in the COD measurements, the theoretical biogas volumes associated with the measured decrease in soluble COD, assuming conversion of acetate to biogas, ranged between 330 and just over 4 000 mℓ under the experimental conditions. However, only between 5 and 10 ml of gas formation was observed across the range of reactors and the methane content remained low. This strongly suggested that the methanogenic activity within the microbial consortium had been severely compromised and as such the experiments were terminated shortly afterwards.

3.3.2 Anaerobic digestion of algal biomass

The large-scale cultivation of algae is considered as a possible method of offsetting carbon emissions associated with electricity generation by coal-fired power stations. Certain species may be able to grow on mining-impacted or effluent water, improving water quality and generating a biomass product that may provide commodity or high value products. Therefore, the cultivation and digestion of a range of algal species was considered for this work.

3.3.2.1 Cultivation of algae for use as anaerobic digester substrate

The growth of *P. hussii* in the 70 ℓ raceway pond was traced over a period of 227 days (Figure 45).

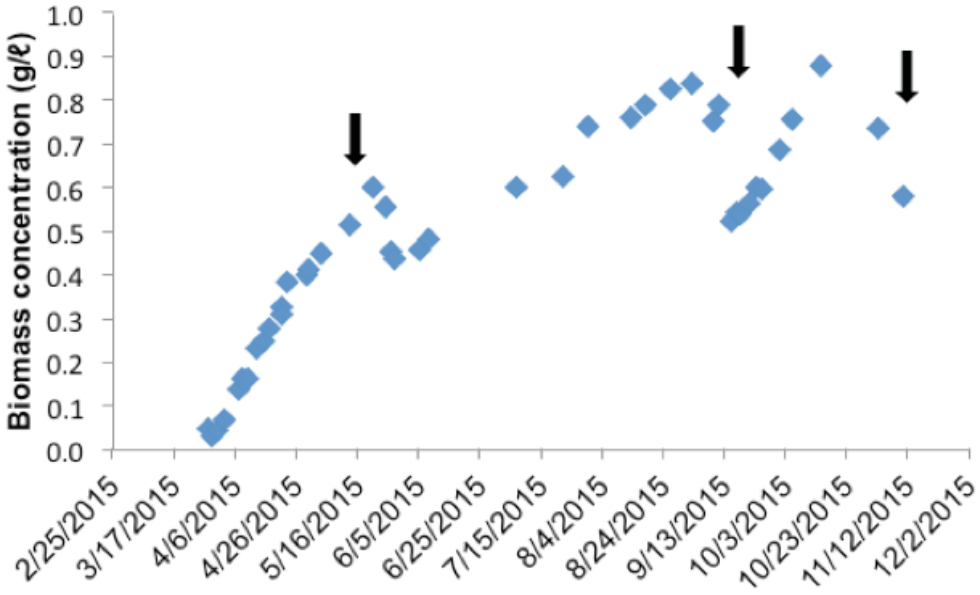

Figure 45: Increase in cell concentration of *Parachlorella hussii* cultivated in a 70 ℓ raceway. Arrows indicate time of partial biomass harvest (10 ℓ for first harvesting point and 15 ℓ for subsequent two)

At the times indicated by the black arrows, 10 ℓ of the raceway was harvested. Late winter and early spring conditions appeared to favour *P. hussii* growth as biomass concentrations of 0.9 g/ℓ were achieved in the outdoor raceway reactor. These concentrations are similar to those achieved in aerated Erlenmeyer flasks and airlift reactors, when cultivated in 3N BBM medium (BBM supplemented with three times the normal nitrogen concentration). Unfortunately, no previous data are available for the growth of this algae in outdoor raceway ponds.

Spirulina had previously been cultivated in the 70 ℓ raceway pond situated in the greenhouse during the month of May in 2014 and achieved a biomass concentration of 1 g/ℓ within 15 days of cultivation. The temperature of the pond was maintained at an average of 29°C for the duration of the *Spirulina* growth, with a maximum of 30°C and minimum of 26.5°C. For the cultivation of *P. hussii* the pond temperature was not controlled. However, the culture exhibited sustained biomass growth, regardless of temperature, during the onset of winter. A biomass concentration of greater than 0.9 g/ℓ was achieved in the outdoor raceway pond during late winter and early spring, marked by moderate temperatures. However a decrease in biomass concentration was observed as the temperature of the greenhouse increased and pond temperatures of over 30°C were measured. Similar biomass concentrations have been generated for *P. hussii,* cultivated in airlift photobioreactors on 3N BBM medium aerated with ambient air at 0.625 vvm. Other microalgal species, such as *Chlamydomonas debrayana*, are able to reach biomass concentrations of 1.2 g/ℓ in airlift reactors under the same conditions, although

C. debrayana appeared to be more susceptible to clumping making it difficult to cultivate. When the air was supplemented with 10 000 mg/ℓ CO_2, the biomass concentration of *P. hussii* increased to 1.2 g/ℓ (unpublished data). *P. hussii* productivity was similar to that achieved for the similar sized *C. vulgaris* (0.9-1.6 g/ℓ; Griffiths *et al*. 2012).

A microalgal isolate identified as having a high CO_2 assimilation rate was cultivated under similar conditions in airlift reactors and achieved maximum biomass concentrations greater than 2.9 g/ℓ (Figure 46). This is higher than that achieved for *Scenedesmus* and *C. debrayana* under similar conditions. *Scenedesmus* achieved maximum biomass concentrations of 2.27 to 2.61 g/ℓ (Griffiths *et al*., 2012; Jones and Harrison, 2014), while *C. debrayana* was able to achieve 2.6 g/ℓ.

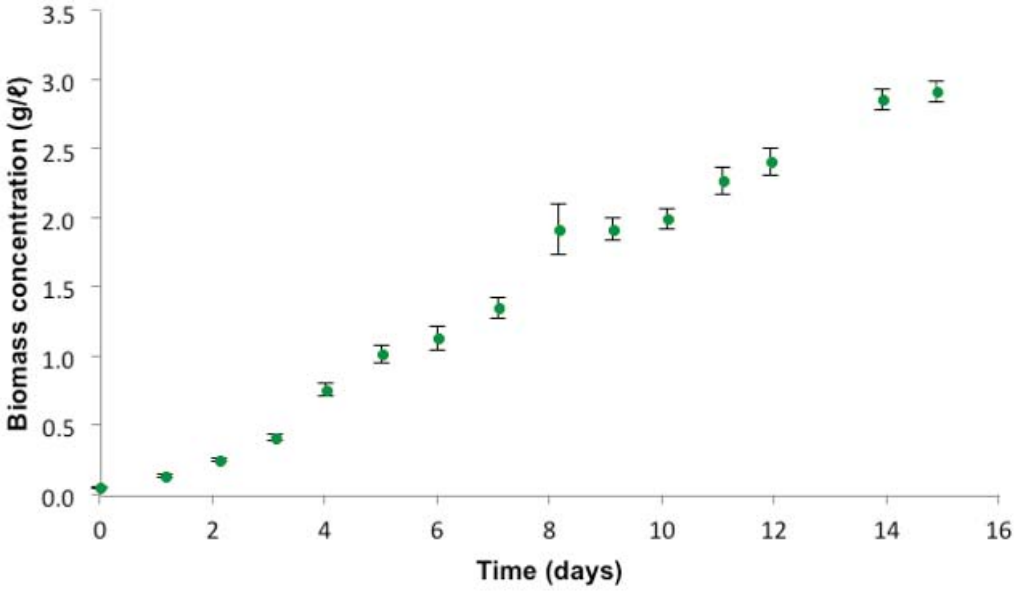

Figure 46: Biomass concentration vs time for isolate MPA 34.1, cultured in a 3.2 ℓ airlift photobioreactor aerated with 10 000 ppm CO_2 enriched air at an aeration rate of 0.3125 vvm

Isolate 34.1 demonstrated high productivity and after draining approximately 95% of the airlift volume the remaining biomass could reach maximum biomass concentrations within 7 days after the reactor was refilled with dH_2O supplemented with a full suite of 3N BBM nutrients.

The growth of several microalgal species, including isolate MPA 34.1, in the CeBER airlift reactors and outdoor raceway pond, where data is available, are compared in terms of productivity in Table 5.

Table 5: Comparison of productivities of micro-algae cultivated in airlift reactors and raceway ponds under similar conditions (this study, Griffiths *et al*. 2012; Jones and Harrison, 2014)

	Productivity (g/ℓ/day)	
Algal species	Airlift reactor	Raceway pond
Tetraselmus suecica	0.49	
Spirulina platensis	0.29-0.34	0.025-0.05 (Jan-Apr)
Scenedesmus sp.	0.25-0.36	
Chlorella vulgaris	0.24-0.28	
Parachlorella hussii	0.10	0.011-0.014 (Apr-June)
MPA 34.1 (Chlamydopodium sp.)	0.21	

The biomass productivities of the two filamentous species, *Oscillatoria* and *Oedogonium,* were determined from small-scale cultivation systems. The small-scale reactors consisted of Erlenmeyer flasks (2 ℓ) for *Oedogonium* and a fish tank (10 ℓ) for *Oscillatoria*. The productivity of *P. hussii* was

determined from the 70 ℓ raceway pond (Figure 47). The productivity of the filamentous algae *Oscillatoria* was approximately two times higher than that achieved for *P. hussii* and *Oedogonium* (Table 6).

Table 6: Biomass productivities of *Parachlorella hussii*, *Oscillatoria* sp. and *Oedogonium* sp.

Species	Culture volume (ℓ)	Cultivation time (d)	Growth vessel	Biomass productivity (g/ℓ.d)
Parachlorella hussii	70	54	Raceway with paddlewheel	0.0111
Oscillatoria sp.	10	14	Aerated fish tank	0.0235
Oedogonium sp.	4	14	Aerated Erlenmeyer flasks	0.0116

Larger scale growth trials were conducted on the two filamentous algae in 25 ℓ channel reactors (Figure 47 B). Filamentous species are theoretically easier to harvest, particularly if the algae can be cultivated on support matrices that can be removed from the growth medium. Initial trials were performed by cultivating *Oedogonium* in a 10 ℓ volume, on plastic meshing as depicted in Figure 47 C, while structures made of plastic sheeting were constructed for the cultivation of *Oscillatoria* (Figure 47 D). The nature of the plastic mesh made it difficult to harvest the *Oedogonium* biomass from the channel reactor, so a second set of experiments was conducted using silicon tubing as the support matrix. The biomass proved easier to remove from the tubing. *Oscillatoria* failed to attach to the plastic sheeting used as initial support matrix, however silicon tubing proved efficient for this species too. Similar to *Oedogonium*, the *Oscillatoria* biomass was easily harvested from the tubing.

Figure 47: Larger scale reactors used for the cultivation of algal biomass. (A) *Parachlorella hussii* in a 70 ℓ raceway, 25 ℓ channel reactor for *Oedogonium,* (B and C) and *Oscillatoria* (D)

Elemental analysis of the algal biomass indicated that *P. hussii* and *Oedogonium* contained similar amounts of C, approximately 43%, whereas *Oscillatoria* had a slightly lower C content, approximately 39% (Table 7). The H content in *P. hussii* and *Oscillatoria* was similar at 7.8 and 7.6% respectively, while H was slightly higher in *Oedogonium* (8.4%). *Oedogonium* also had the highest N content, 6.4%,

which was 5.6 and 4.9% for *Oscillatoria* and *P. hussii* respectively. No elemental analysis has been performed for isolate MPA 34.1.

Table 7: Percentage composition of algae cultivated in high nitrogen medium

Species	C	H	N	C:N ratios	Empirical formula[1]	Reference
Parachlorella hussii	43.3	7.8	4.9	8.8	$CH_{2.17}N_{0.097}O_{0.76}$	This study
Oscillatoria sp.	38.9	7.6	5.6	6.9	$CH_{2.34}N_{0.12}O_{0.92}$	This study
Oedogonium sp.	43.1	8.4	6.4	6.7	$CH_{2.34}N_{0.13}O_{0.73}$	This study
Scenedesmus	48.2	7.1	9.4	5.1	$CH_{1.76}N_{0.17}O_{0.55}$	Griffiths
Chlorella vulgaris	46.1	7.4	4.1	11.3	$CH_{1.94}N_{0.07}O_{0.69}$	Griffiths
Spirulina	41.0	6.1	7.7	5.3	$CH_{1.78}N_{0.16}O_{0.83}$	Griffiths

[1]Excluding P and S

The elemental composition of the three algae cultivated during this study is similar to those achieved for *Scenedesmus* sp., *Chlorella vulgaris* and *Spirulina* previously analysed. In general the C:N ratios (determined using % DW composition) range between 5.1 and 11.3 for all the algae, with *Chlorella vulgaris* having a value of 11.3. These are lower than the optimal ratios (20-25) proposed for AD and found to prevent ammonia accumulation and inhibition of methanogens (Yen and Brune, 2007). However, both Spirulina and *Scenedesmus* has successfully been used as substrates for AD with maximum methane yields of 113 m^3 CH_4/ton volatile solids (VS) and 55 m^3 CH_4/ton VS being reported for the two algal spp. respectively (Inglesby, 2011). These results suggest that algae with similar composition may also be suitable substrates for AD. Furthermore, it has been demonstrated that successful AD can be achieved at higher N levels through use of an altered AD consortium utilising an alternative metabolic pathway (Ekama, personal communication).

Although *C. vulgaris* has a higher C:N ratio than those reported for the other algal species, it is more difficult to cultivate in large-scale bioreactors and appears to be more susceptible to catastrophic failure. This has been confirmed through the substantial data presented on the ATP[3] testbed facilities across seven sites in the USA (Knoshaug *et al*., 2015). For this reason *P. hussii* and/or isolate MPA 34.1 may be the ideal choice as an AD substrate as it can be cultivated with relatively little maintenance. The choice of growth medium may further be optimised to generate *P. hussii* biomass with a C:N ratio more desirable for AD. The potential to influence algal C:N ratio through medium composition, while not affecting the biomass productivity of the algae would need to be tested experimentally.

The COD of the algal biomass was determined to assess the amount of biomass that would be required to obtain a 30 g/ℓ COD loading for anaerobic digestion. *P. hussii* had a higher COD than the filamentous algae (Table 8). Assuming *P. hussii* can achieve a maximum biomass concentration of 0.9 g/ℓ in the raceway reactor, by harvesting 13 ℓ of the 70 ℓ raceway pond a total of 12 g DW *P. hussii* can be obtained. The biomass concentrations achieved for the filamentous algae were 0.162 and 0.329 g/ℓ for *Oedogonium* and *Oscillatoria* respectively. These concentrations are quite low and it is expected that higher concentration could be achieved in the larger reactors.

Table 8: Chemical oxygen demand obtained from a g DW/ℓ of *Parachlorella hussii*, *Oscillatoria* and *Oedogonium* biomass

Species	**COD (g/ℓ)**	**g DW algae for 30 g/ℓ COD loading[1]**
Parachlorella hussii	2.56 ± 0.07	12
Oscillatoria sp.	0.55 ± 0.04	55
Oedogonium sp.	0.81 ± 0.03	37

[1]Assuming a 1 ℓ anaerobic digestion reactor is used

The higher COD value achieved for *P. hussii* may be a result of the high lipid content of these cells, up to 23.5% DW lipid content for stationary phase cells (unpublished data). However, values as high as

35.7% has been reported in literature for *P. hussii* cells cultured in waste water (Osundeko *et al*., 2013). *P. hussii* shows great promise as an AD feedstock as it is appears to be more robust than *C. vulgaris* and *Scenedesmus* for outdoor cultivation and may be suitable for year round cultivation.

3.3.2.2 Biomethane potential tests

The suitability of using the algal biomass, cultivated during this study, as the substrate for anaerobic digestion was tested by performing small-scale (200 mℓ) biomethane potential (BMP) tests. The volume or mass of the harvested biomass required for these tests are shown in Table 9 and was dependent on the COD of the algal biomass and the water content of the sludge created during harvesting or following centrifugation of the algal cells. Partially lysed algae were also used in certain reactors to test the effect that more readily available substrates may have on the BMP.

Table 9: COD of algal biomass sludge and mass or volume of sludge required to obtain desired COD loading

Algal species	COD loading of algal sludge (g/mℓ or g/g)	Volume or mass of sludge for desired COD loading	BMP test
Oedogonium sp.	0.045 g/mℓ	269 mℓ	Stage I (12 g/ℓ COD loading)
P. hussii	0.041 g/mℓ	293 mℓ	
Spirulina	0.16 g/g	76 g	
Oscillatoria sp.	0.30 g/g	100 mℓ	Stage II (30 g/ ℓ COD loading)
P. hussii	0.068 g/mℓ	291 mℓ	Stage III ((30 g/ ℓ COD loading)
MPA 34.1	0.10 g/mℓ	442 mℓ	

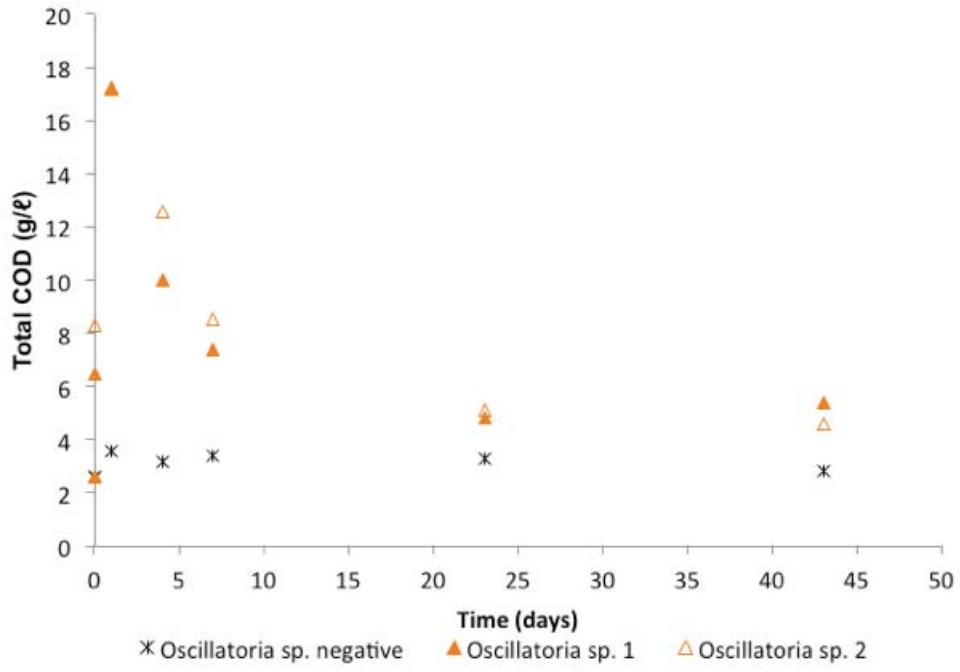

Figure 49: Total COD measurements expressed as g/ℓ of algal AD reactors included in the stage II BMP tests. The COD loading of the substrate for these experiments was 30 g/ℓ, and 0 g/ℓ for the negative control

The total COD values from reactors set up during all three stages of the algal BMP tests followed the same general trend, with an initial high total COD which gradually decreased throughout the experimental runs (Figure 49, and Figure 50). This trend is expected in a system releasing methane and CO_2 in the form of biogas, resulting in a decrease in total COD of the system. The total COD following addition of the algal biomass did not reach the expected values when considering the COD of the algal substrate added. This may be attributed to the difficulty in obtaining a homogeneous reactor sample for COD testing especially in the case of the filamentous algal substrates. The total COD of the *Spirulina* BMP increased by 15 g/ℓ upon introduction of the algal biomass, this was close to the targeted 12 g/ℓ theoretically determined from the COD of the algal biomass following substrate addition (Figure 48). This suggests that for the other reactors the discrepancies between the calculated and measured COD values were probably due to the difficulties associated with obtaining a homogenous sample from the reactor. This effect was less evident for the stage III BMP tests where microalgae were used as substrates (Figure 50).

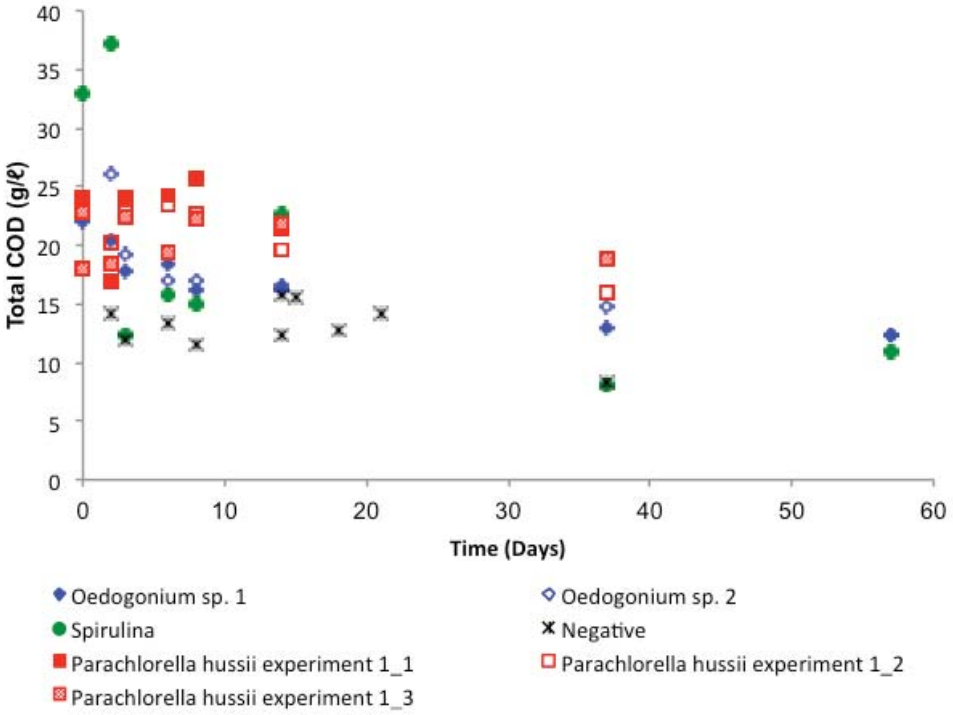

Figure 48: Total COD measurements expressed as g/ℓ of algal AD reactors included in the stage I BMP tests. The COD loading of the substrate for these experiments was 12 g/ℓ, and 0 g/ℓ for the negative control. Acetate (1 g) was added to the negative control on day 14 of the experiment

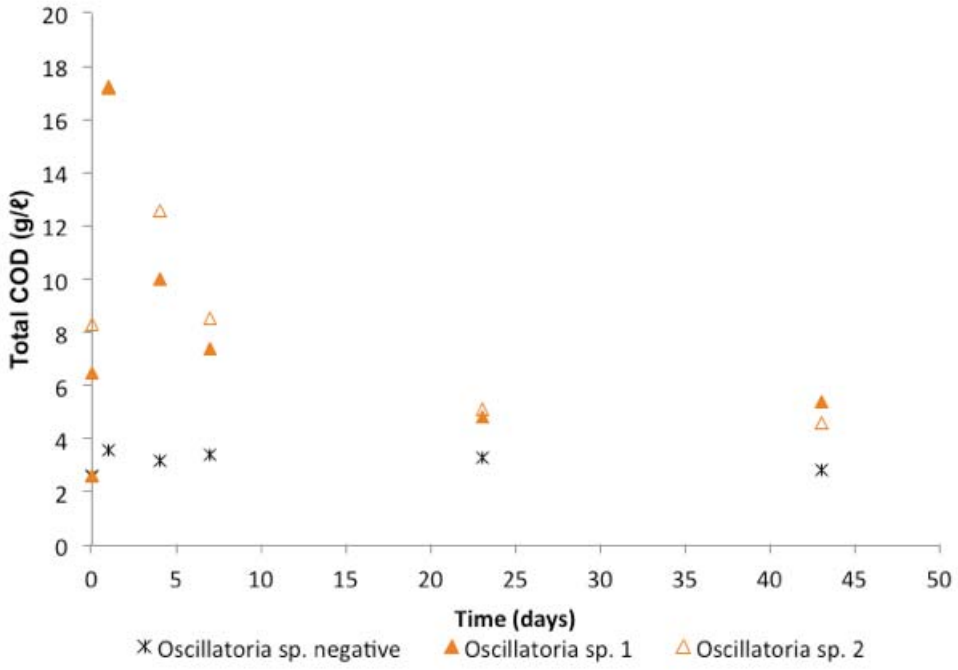

Figure 49: Total COD measurements expressed as g/ℓ of algal AD reactors included in the stage II BMP tests. The COD loading of the substrate for these experiments was 30 g/ℓ, and 0 g/ℓ for the negative control

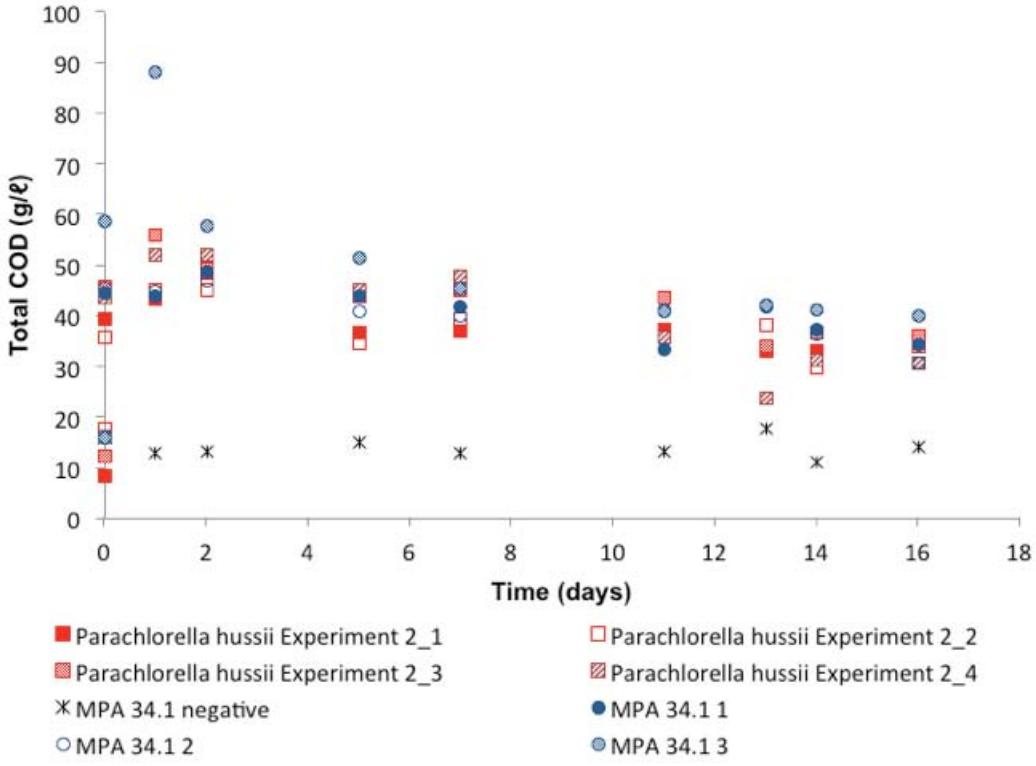

Figure 50: Total COD measurements expressed as g/ℓ of algal AD reactors included in the stage III BMP tests. The COD loading of the substrate for these experiments was 30 g/ℓ, and 0 g/ℓ for the negative control

In the stage I algal BMP tests the *Oedogonium* and *Spirulina* reactors initially had high soluble COD values (Figure 51). The soluble COD decreased to close to 0 within 14 days after the initiation of the BMP tests. The *P. hussii* algal biomass added to the reactor had a very low soluble COD content, which was evident from the lack of increase in the soluble COD of the reactor after addition of the

biomass. However, during the course of the experiment the soluble COD content of the *P. hussii* reactors increased to 2.27 g/ℓ by day 37. This may be indicative of the hydrolytic activity of microorganisms within the AD inoculum; however the lack of soluble COD decrease may indicate that the methanogenic activity of the inoculum had decreased. To test this, the negative control reactor was supplemented with 1 g of acetate to test the methanogenic activity of the inoculum. Even after 14 days of 'starvation' the culture was active enough to decrease the soluble COD to close to 0 within 23 days of introducing the acetate (Figure 51). The initial increase and then decrease of the soluble COD was as expected for a substrate being broken down and releasing VFAs before the hydrolysis process ceased due to a depletion of degradable substrate (Cheng, 2010; Chynoweth & Isaacson, 1987). The point at which soluble COD stopped being released within the BMP reactors did not correlate to the substrate being used up, as shown by high total CODs, which indicated that the anaerobic community may not be able to fully degrade the algal substrates. The *Parachlorella hussii* reactors all had thick, highly viscous supernatants throughout experimental runs and this could have been indicative of compounds, such as polysaccharides, being present within the reactor fluid. These compounds would have resulted in high soluble CODs without the soluble COD necessarily being usable by the methanogenic community.

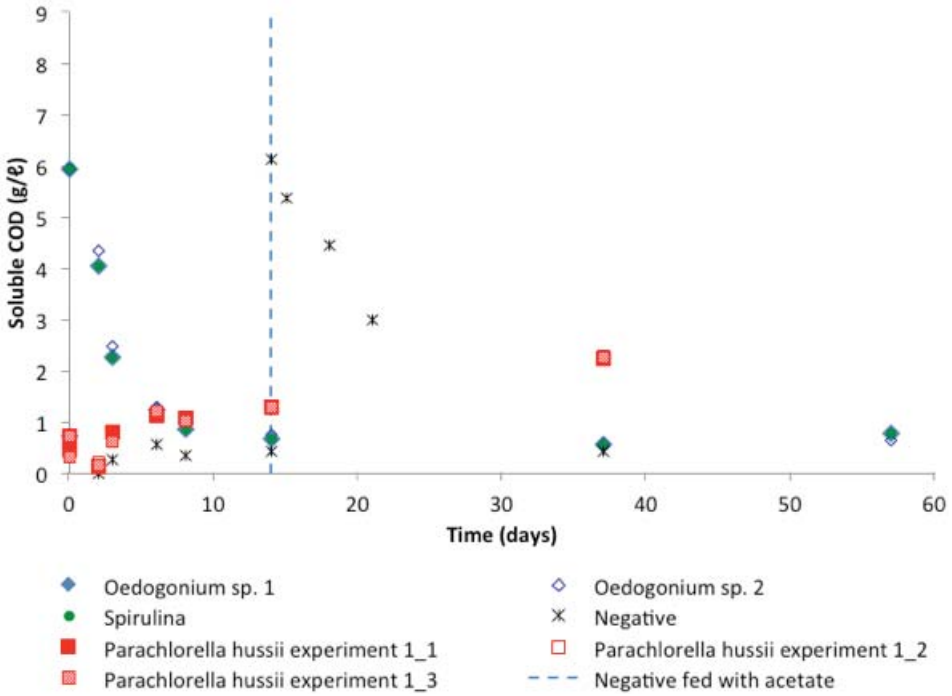

Figure 51: Soluble COD of stage I algal BMP tests expressed as g/ℓ. A COD loading of 12 g/ℓ was achieved for the algal reactors and 0 g/ℓ for the negative control. On day 14 of the experiment 1 g of acetate was added to the negative reactor.

Oscillatoria biomass proved to be very recalcitrant to microbial hydrolysis, with poor liberation of soluble COD from the substrate (Figure 52). The inoculum loading was also lower, 15% compared to the 25% sludge loading, in these stage II BMP tests which may have influenced the number of hydrolytic microorganisms available for substrate hydrolysis. A slight increase, from 0.3 g/ℓ to 1 g/ℓ COD, was however observed for the soluble COD of *Oscillatoria*.

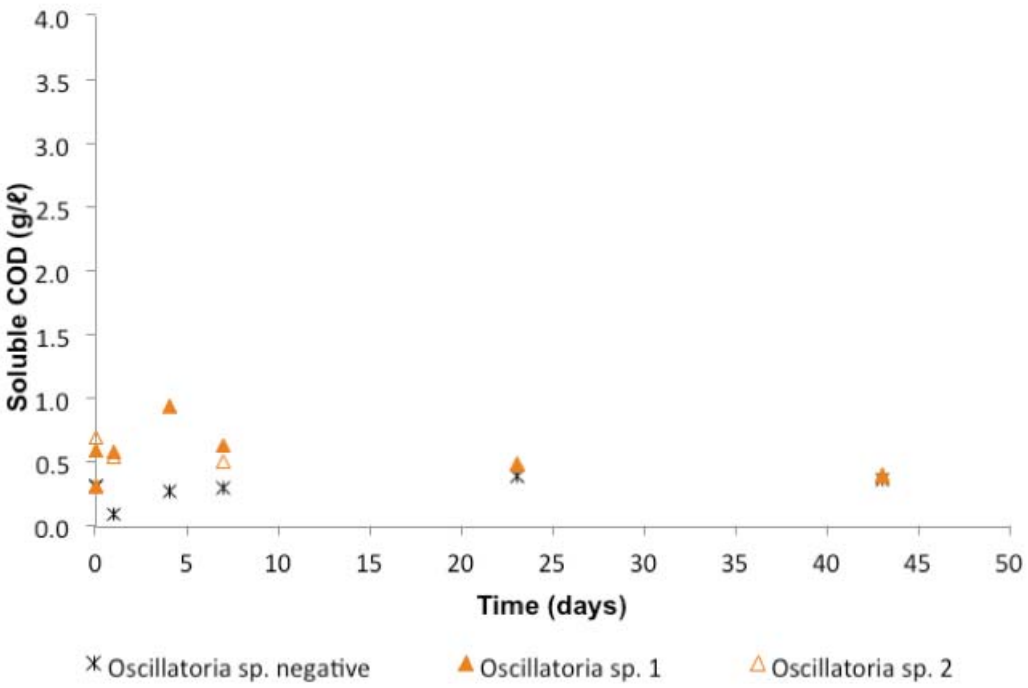

Figure 52: Soluble COD of stage II algal BMP tests expressed as g/ℓ. A COD loading of 30 g/ℓ was achieved for the *Oscillatoria* algal reactors and 0 g/ℓ for the negative control

The initial soluble COD values were higher in experimental runs conducted using partly lysed *P. hussii* and MPA 34.1 algal cells (Figure 53).

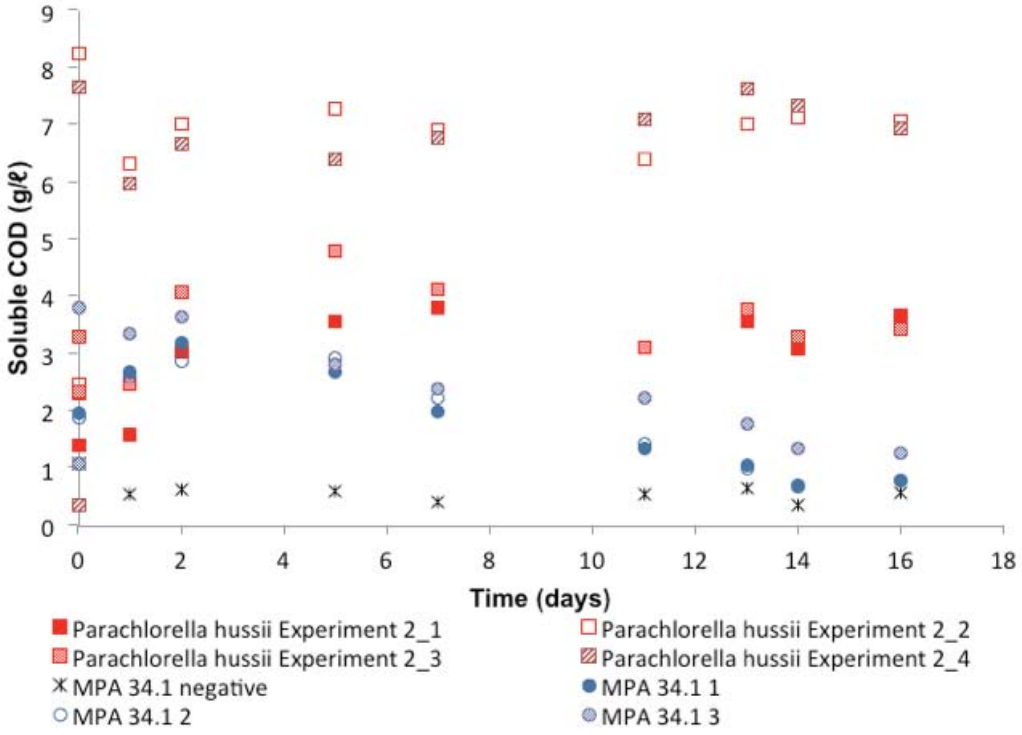

Figure 53: Soluble COD of stage III algal BMP tests expressed as g/ℓ. A COD loading of 30 g/ℓ was achieved for the algal reactors and 0 g/ℓ for the negative control

This is as a result of the release of the cell contents during the microwave treatment. The partially lysed algal experiments also resulted in the soluble COD remaining at a consistently higher level for a longer time period, possibly explained by the partial lysis increasing access for the hydrolytic microorganisms to the remaining algal substrate. The results achieved from the stage III algae AD BMP tests were, in general more, promising than the previous two stages. The fact that the algal anaerobic digester inoculum had been adapted to complex algal feedstocks for seven weeks more than when it was used for the first BMP tests may have contributed to this. This may have resulted in a microbial community structure with a greater number of hydrolytic organisms to assist in the breakdown of algal cell walls.

The biogas volumes obtained were consistent with the measured soluble COD values. The *Oedogonium* sp. and *Spirulina* reactors produced the largest biogas during stage I of BMP testing (Figure 54). The biogas produced by the negative control reactor (126 mℓ) also confirmed that the methanogenic community was capable of producing biogas even after 14 days of 'starvation', suggesting the presence of a robust methanogenic community. This was less than the 860 mℓ of biogas that should theoretically have been produced by the addition of 1 g of acetate. The reasoning for this was not clear although the negative control reactor had been at a pH of over 8 for two weeks prior to this feeding. Therefore, the methanogenic community may have been inhibited by the elevated pH for an extended period; as the optimal pH for the culture of methanogenic microbes is between pH 6.5 and 8 (Cheng, 2010; Chynoweth and Isaacson, 1987).

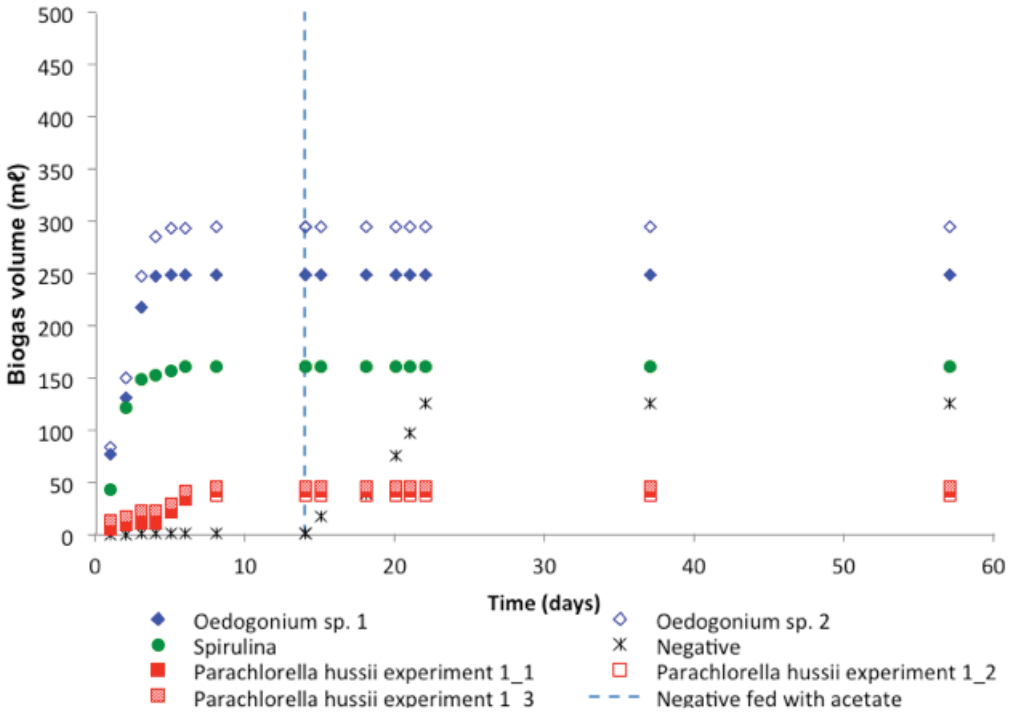

Figure 54: Biogas volumes produced from stage I algal AD BMP tests. Substrates were introduced at a 12 g/ℓ COD loading and 0 g/ℓ for the negative control. On day 14 of the experiment 1 g of acetate was added to the negative reactor

The *Oscillatoria* reactors produced very little biogas which matched the low soluble CODs obtained throughout the experimental testing (Figure 55).

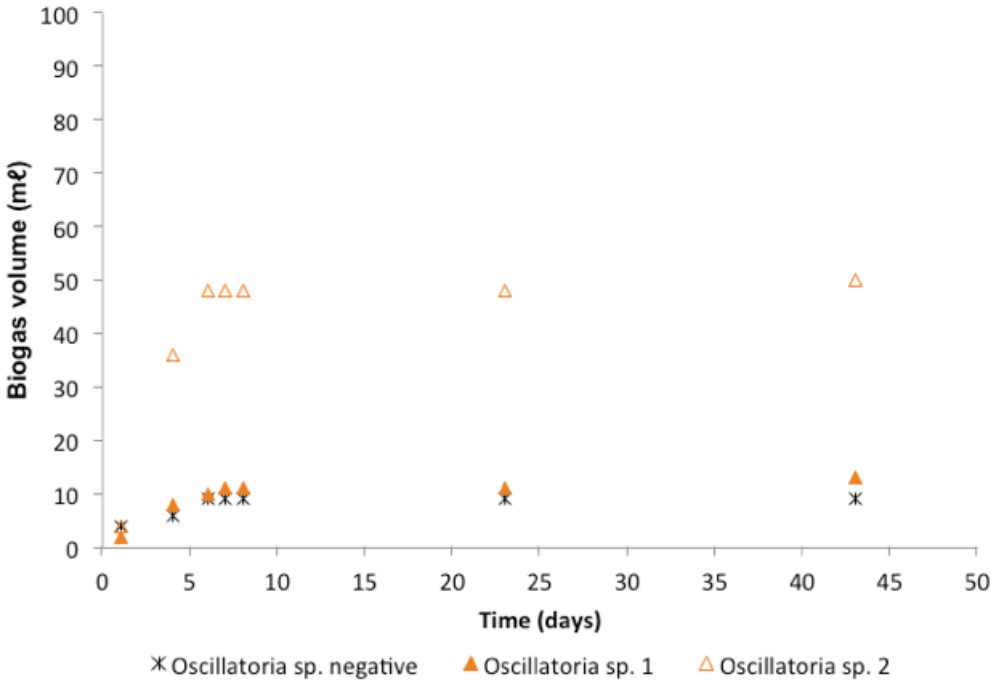

Figure 55: Biogas volumes produced from stage II algal AD BMP tests. *Oscillatoria* was introduced at a 30 g/ℓ COD loading and 0 g/ℓ for the negative control

The stage III BMPs with *P. hussii* as feedstock produced large volumes of biogas as was expected from the high soluble CODs obtained (Figure 56).

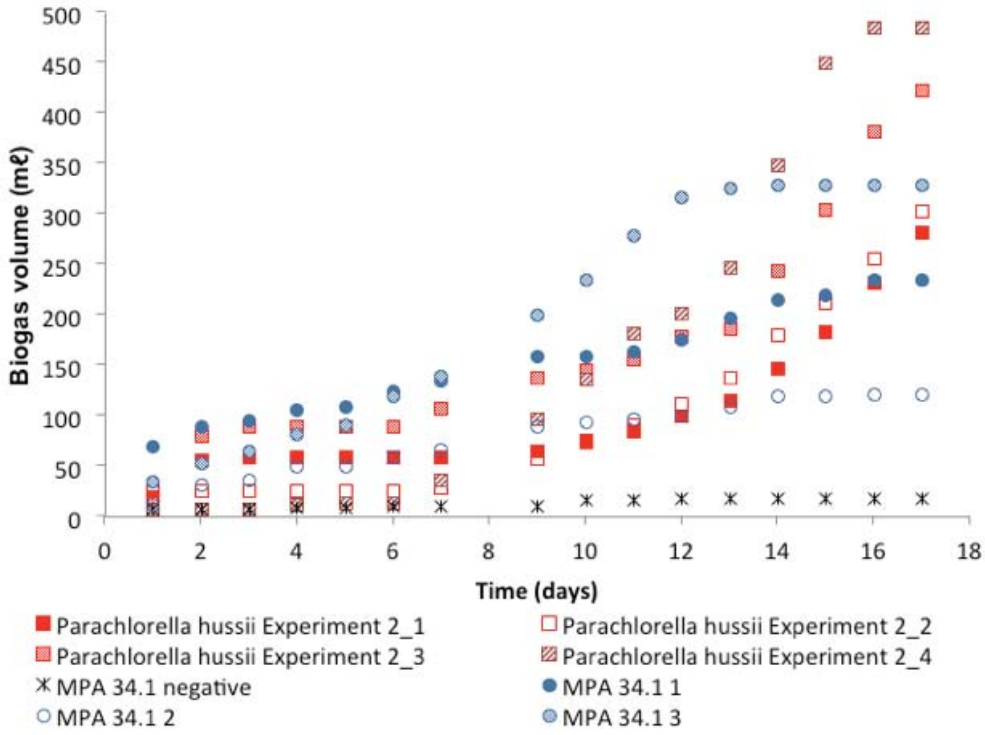

Figure 56: Biogas volumes produced from stage III algal AD BMP tests. Algal biomass was introduced at a 30 g/ℓ COD loading and 0 g/ℓ for the negative control

The two *P. hussii* reactors from the stage I BMP tests that were inoculated with both fresh inoculum and substrate produced the highest gas volumes to date (Figure 56). This increase in biogas production

may indicate that the further development of the inoculum has resulted in a microbial community which is more effective at breaking down the algal substrate and obtaining soluble compounds for biogas production. The MPA 34.1 fed reactors produced less biogas than the reactors fed with *P. hussii* as substrate. The MPA 34.1 reactors had lower soluble COD values and the soluble COD reduced quickly within these systems (Figure 53). The MPA 34.1 reactor fed with partly lysed algal cells produced more biogas than the reactor fed with un-lysed cells (Figure 56).

The methane production was calculated using the biogas volumes and the methane composition data. This allowed for the calculation of the methane production per gram of initial COD loading as shown in Table 10. The results matched the biogas volume data presented above with the *Oedogonium* sp., *Spirulina, Parachlorella hussii* and partly lysed MPA 34.1 reactor systems producing the highest methane per gram of initial COD loading. These algal systems also had the highest soluble COD values, which may suggest the presence of soluble VFAs utilised by methanogens for the production of biogas (Cheng, 2010; Chynoweth and Isaacson, 1987; Kwietniewska and Tys, 2014).

The redox potential of all fed reactor systems remained at below -300 mV for the duration of the experimental period where biogas was produced suggesting the anaerobic microbial community was active. The redox of the first stage reactors increased to approximately -100 mV more than a month after the initiation of the experiments, once the microbial community had been starved for an extended period. The methane concentration within the biogas changed throughout the course of the experimental runs with the peak concentrations of more than 50% achieved during peak gas production. This peak in gas and methane production correlated with the peak soluble COD concentrations.

Table 10: Methane production per gram of initial COD loading for all experimental runs

Experiment	Methane production (mℓ/g total COD loading)
Oedogonium sp. 1	13.0
Oedogonium sp. 2	17.0
Spirulina	7.4
P. hussii Experiment 1_1	0.6
P. hussii Experiment 1_2	0.6
P. hussii Experiment 1_3	0.5
Oscillatoria sp. 1	0.2
Oscillatoria sp. 2	0.6
P. hussii Experiment 2_1	2.6
P. hussii Experiment 2_2	3.1
P. hussii Experiment 2_3	5.5
P. hussii Experiment 2_4	10.0
MPA 34.1 1	2.3
MPA 34.1 2	1.1
MPA 34.1 3	4.7

3.3.2.3 COD balances and theoretical methane production

Total COD balances were performed on each reactor system to determine the theoretical amount of methane that should have been produced within the reactor system assuming that COD is conserved within a batch reactor system. This principal assumes that any total COD change within the reactor would be as a result of methane production. This is an oversimplification, given that many of the fermentation, acidogenic and acetogenic reactions result in CO_2 formation. The COD of any organic compound can be calculated using the full oxidation chemical formula to calculate the number of moles of oxygen required to complete the oxidation of the compound. Using this first principal calculation the

COD of methane is known to be 64 g/mol and hence the expected volume of methane was could be calculated. The results of this analysis are given in Table 11.

The results indicated that the experimentally measured methane volumes were considerably lower than the theoretical volumes expected, especially in the stage I *P. hussii*, stage II *Oscillatoria* and stage III MPA 34.1 2 algal BMP tests. Various factors could have contributed to the poor methane yield observed. Accurate total COD values were difficult to obtain due to the nature of the algal biomass used as feedstock. The algal biomass tended to form clumps, especially in the case of filamentous algae, so achieving total homogeneity within the small volume extracted for sampling was challenging. The sampling method of drawing the sludge through a relatively narrow outlet port would have amplified this error as larger pieces or clumps would have been left behind within the reactor. It was also noted that the algal sludge formed large deposits on the outer walls of the reactors that were not dislodged during daily shaking. All of these factors would have contributed to the sludge tested for total COD being not fully representative of the reactor system and potentially resulting in the overestimate of the total COD decrease. Any error within the total COD measured would also significantly influence the theoretical methane yield calculated as a 1 g/ℓ under or over estimation of the COD within the reactor represents 74 mℓ of methane. This error could be minimised by doing full, destructive, sampling of each final reactor system and blending all reactor liquid to achieve near full homogeneity (Boyles, 1997).

Table 11: Total change in the COD measured within the reactor systems used to calculate the theoretical methane production compared to the experimentally observed values

Experiment	Total COD removed (g/ℓ)	Theoretical methane production (mℓ)	Observed methane production (mℓ)	Percentage of theoretical
Oedogonium sp. 1	5.6	418	152	36
Oedogonium sp. 2	5.8	430	202	47
Spirulina	10.0	760	89	12
Negative	5.6	415	0	0
P. hussii Experiment 1_1	2.5	187	7.8	4.2
P. hussii Experiment 1_2	3.3	245	6.6	2.7
P. hussii Experiment 1_3	1.0	76	6.2	8.1
Oscillatoria sp. 1	1.1	81	5.3	6.6
Oscillatoria sp. 2	3.7	272	19	6.9
P. hussii Experiment 2_1	4.2	303	79	26
P. hussii Experiment 2_2	1.9	135	93	69
P. hussii Experiment 2_3	10.0	703	165	23
P. hussii Experiment 2_4	13.0	924	286	31
MPA Negative	5.0	359	0	0
MPA 34.1_1	7.4	534	68	13
MPA 34.1_2	9.1	660	33	5.1
MPA 34.1_3	17.0	1252	140	11

Regular sampling was required to obtain reactor fluid for VFA analysis to allow for the tracking of VFA concentrations throughout the experimental run. The calculations performed to determine the theoretical methane yield from the reduction of the total COD took into account the removal of 2% of the reactor volume with each sampling performed. However, the regular sampling could have introduced oxygen into the reactors, especially in cases where produced gas volumes were low, which would have disrupted the anaerobic nature of the reactors resulting in the oxidation of substrates. This oxidation would have lowered the measured COD as some compounds contributing to the total COD

could have then been fully oxidised resulting in a measured COD of 0. Maintenance respiration of the microorganisms within the AD reactor resulting in a decrease of the soluble COD without methane production, could have also have influenced the results obtained. These factors could explain the reason that the negative reactor systems had total COD reductions of over 5 g/ℓ without the production of methane being observed. A better indication of BMP could be obtained by performing COD measurements only at the beginning and end of the experiment, thus preventing volume loss from the reactor and excluding oxygen (Esposito *et al.*, 2012; Hamilton, 2015).

3.3.2.4 VFA Analysis

VFA analysis of the reactor liquid is shown for the initial stages of each reactor where soluble COD values were highest. The VFA concentrations within the two *Oedogonium* sp. reactors were initially very high with a wide range of VFAs present (Figure 57 and Figure 58). However, the concentration of VFAs decreased rapidly, with no VFAs present in the reactor by day six. This trend matched the soluble COD trend and the fact that gas production had completely ceased by day six (Figure 51 and Figure 54). The acetate concentration decreased significantly between day 0 and day 3 which was expected as the methanogenic community utilise acetate to form methane and this process is considerably faster than the hydrolysis of more complex substrates (Cheng, 2010; Chynoweth and Isaacson, 1987). The high initial VFA concentrations, even on day 0, indicated that the algal substrate was already partly hydrolysed when it was added to the reactors. This indicated that the initial VFAs present were used up with no additional VFAs released through the hydrolysis of any of the remaining algal substrate.

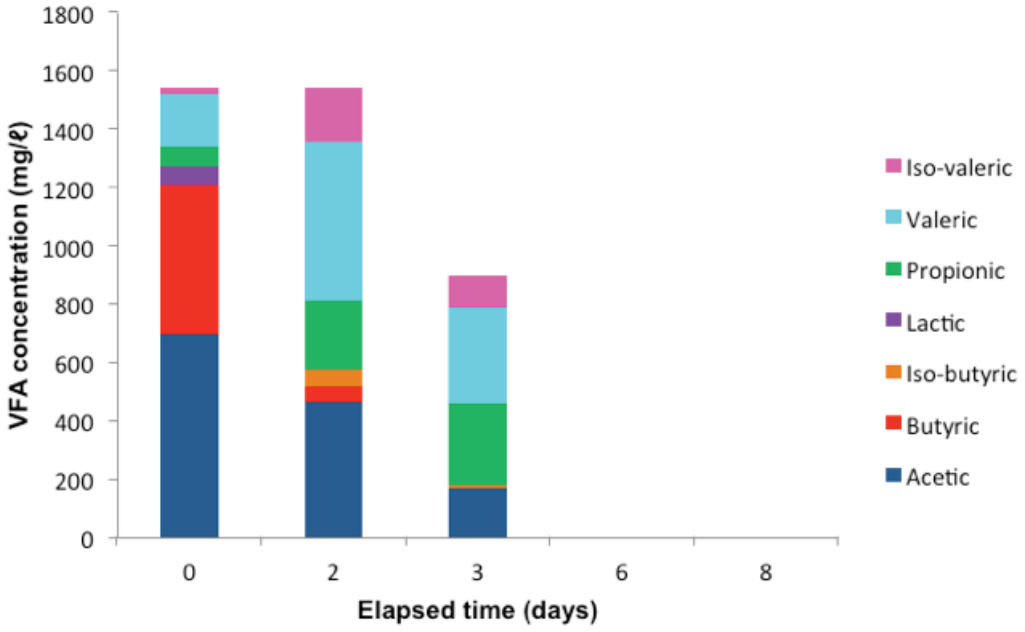

Figure 57: Concentrations and composition of VFAs present within the *Oedogonium* reactor 1 included in the stage I algal AD BMP tests

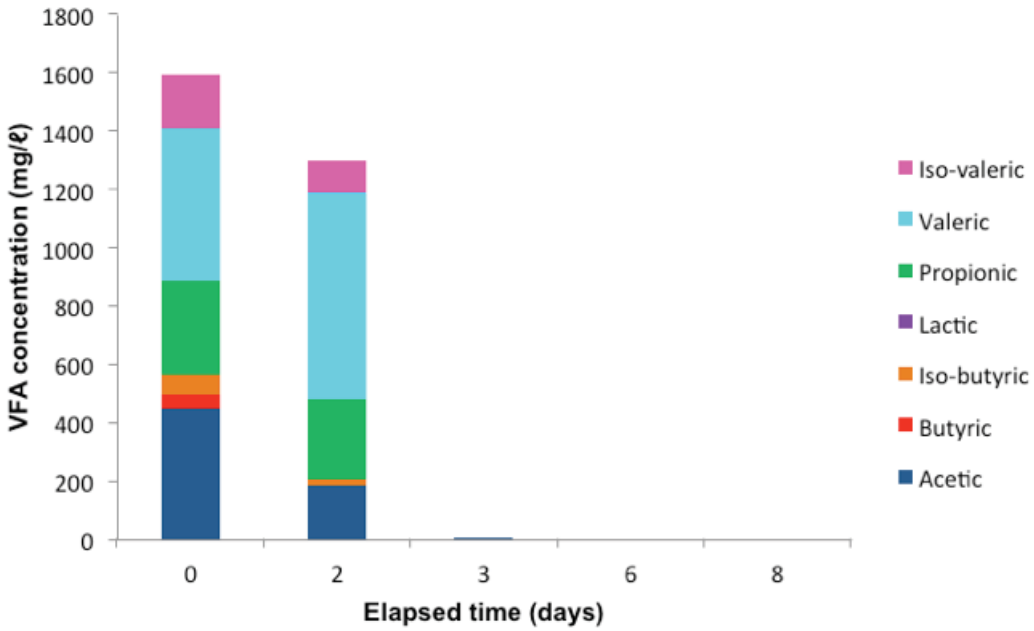

Figure 58: Concentrations and composition of VFAs present within the *Oedogonium* reactor 2 included in the stage I algal AD BMP tests

This trend was repeated across the remaining reactors during stage I and II, with the VFA concentrations for the *P. hussii* reactors the lowest (< 100 mg/ℓ), indicating limited hydrolysis of the algal biomass and rapid utilisation of the available VFAs.

A wide range of VFAs was present within the soluble fraction of the reactors with *P. hussii* as substrate during the stage III algae AD BMP tests (Figure 59, Figure 60, Figure 61 and Figure 62). The two reactors fed with untreated algal sludge initially had low VFA concentrations that increased and peaked on day five, before they decreased by day seven (Figure 60 and Figure 61).

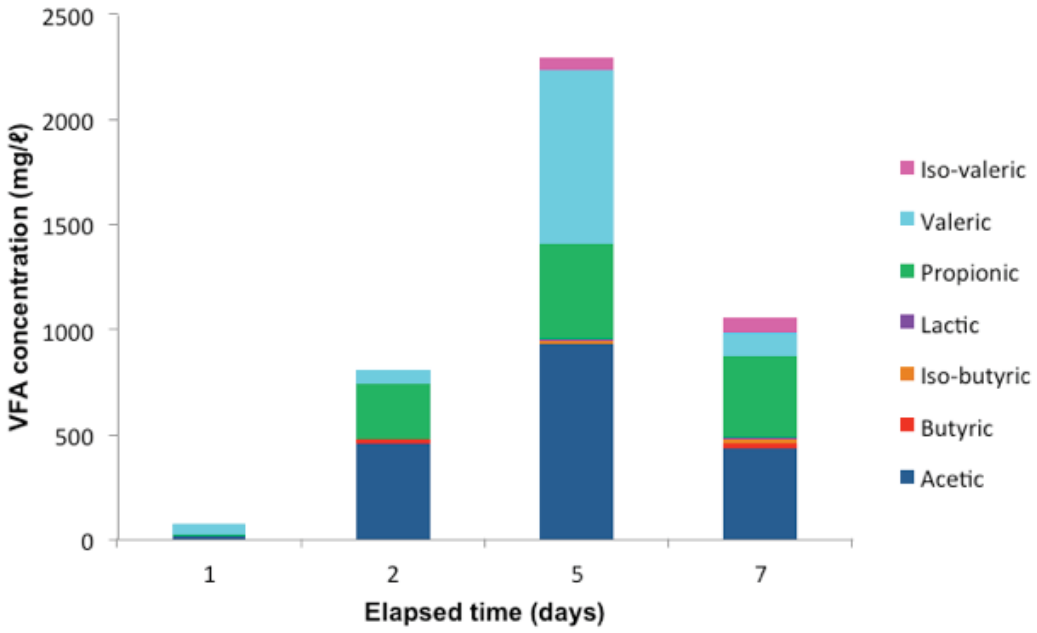

Figure 59: Concentrations and composition of VFAs present within the stage III *P. hussii* AD reactor fed with fresh inoculum and un-lysed *P. hussii biomass* to achieve a 30 g/ℓ COD loading (negative control reactor from stage I)

This indicated that the microbial community hydrolysed a certain portion of the substrate, resulting in the increase in VFAs. However, VFA concentrations reduced once the easily degradable substrates had been depleted. The reactors fed with the partly lysed algal sludge had a higher initial VFA concentration and the total VFAs within solution remained high, indicating that new VFAs were being released into solution. This suggested that partial lysis of the substrate made it possible for the microbial community to access a greater proportion of the substrate for hydrolysis.

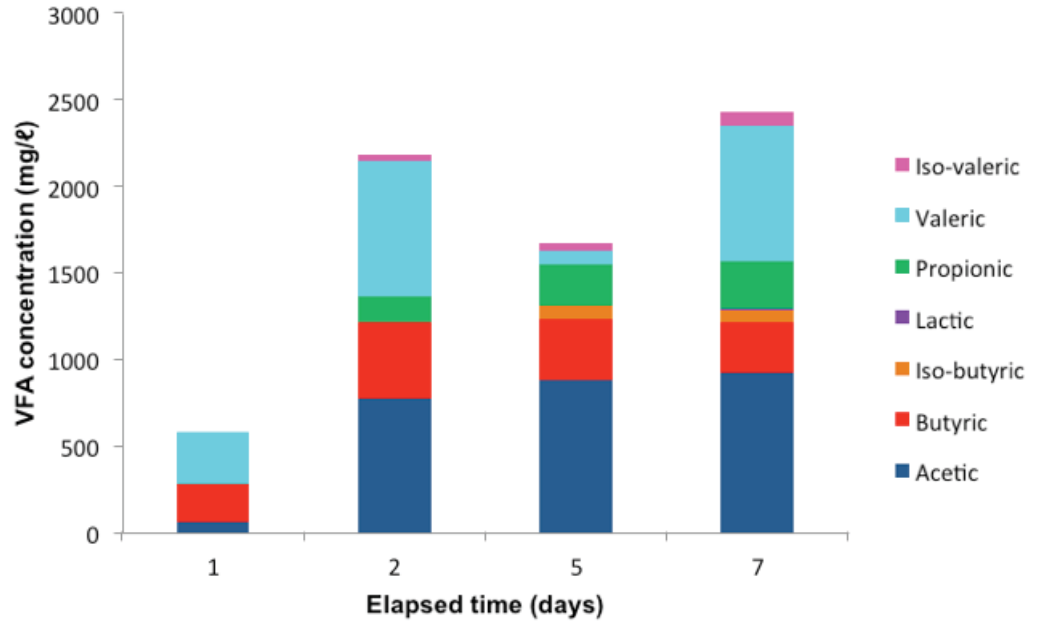

Figure 60: Concentrations and composition of VFAs present within the stage III *P. hussii* AD reactor 1 fed with fresh partially lysed *P. hussii biomass* to achieve a 30 g/ℓ COD loading

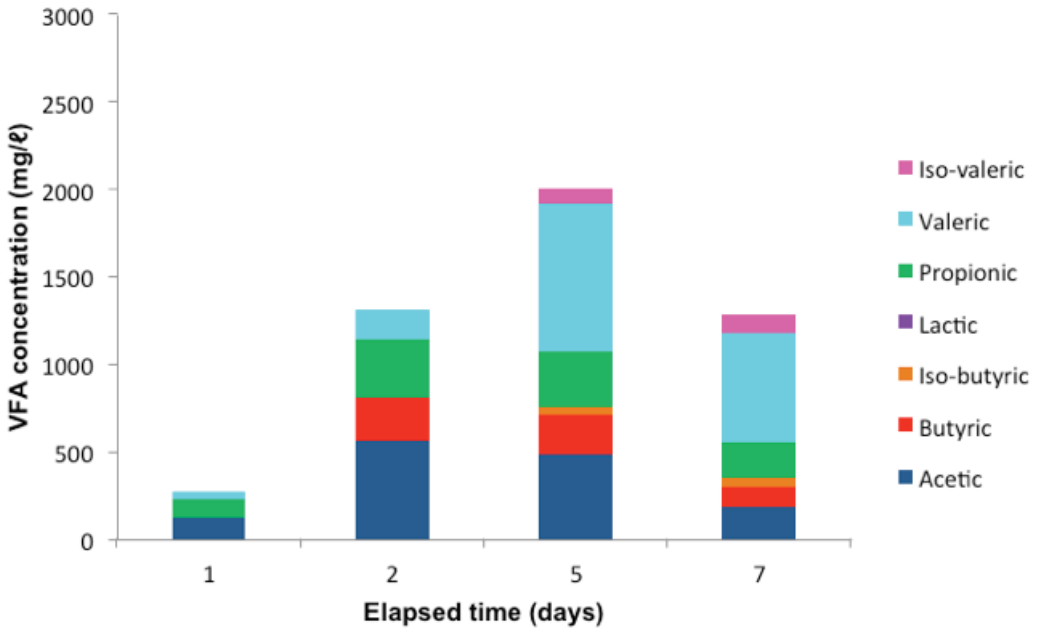

Figure 61: Concentrations and composition of VFAs present within the stage III *P. hussii* AD reactor 2 fed with fresh inoculum and un-lysed *P. hussii biomass* to achieve a 30 g/ℓ COD loading

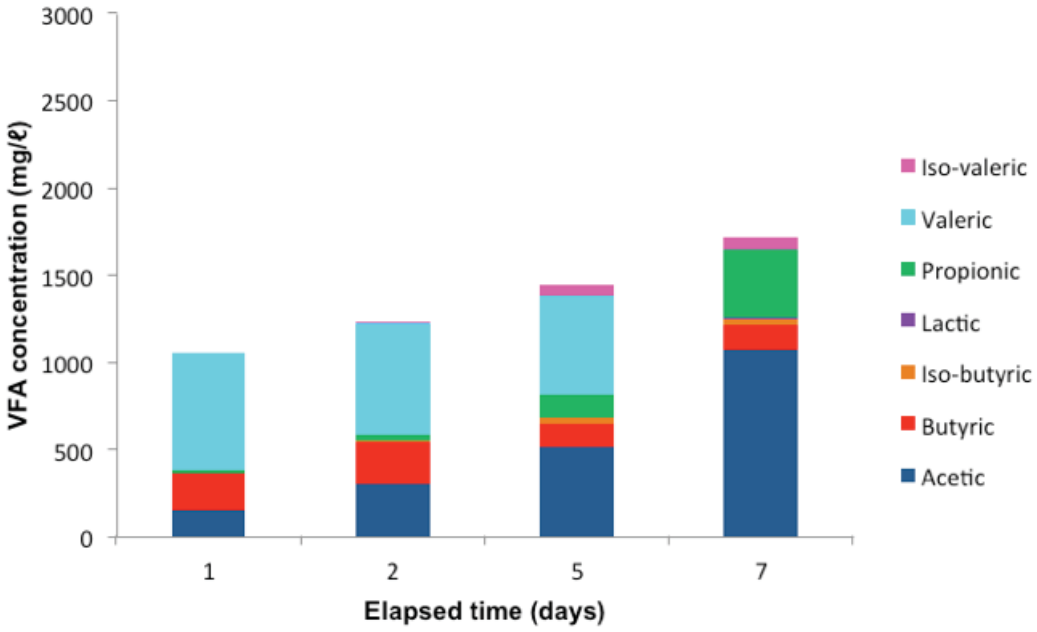

Figure 62: Concentrations and composition of VFAs present within the stage III *P. hussii* AD reactor 3 fed with fresh inoculum and partially lysed *P. hussii biomass* to achieve a 30 g/ℓ COD loading

All reactor systems inoculated with MPA 34.1 as the substrate showed high VFA concentrations. Interestingly, the un-homogenised reactor systems had almost all VFAs in the form of acetate and propionate (Figure 63 and Figure 64), while the reactor with partially lysed algae had a wider range of VFAs present (Figure 65).

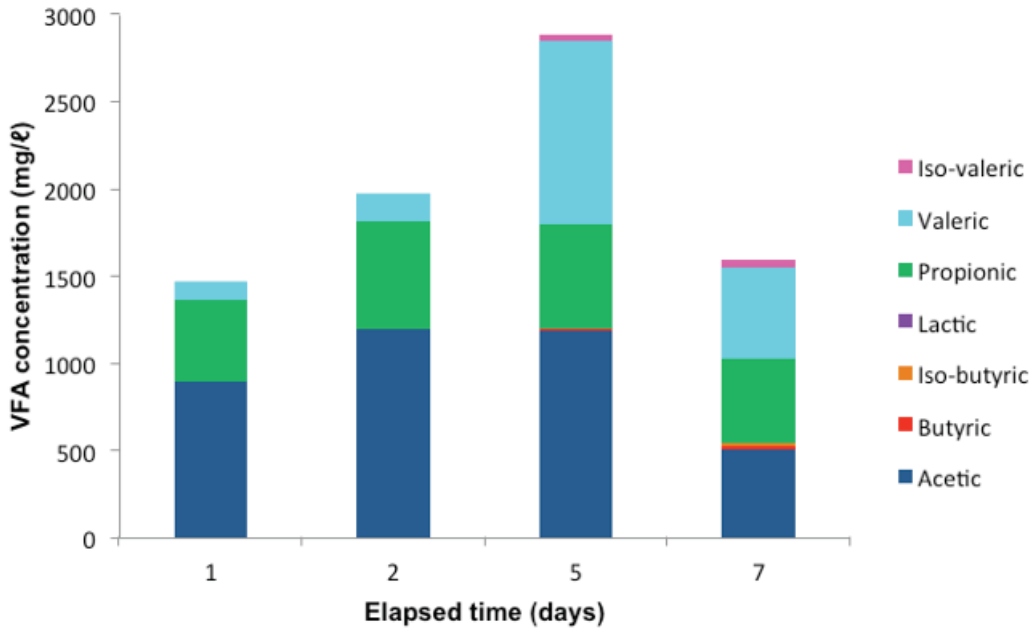

Figure 63: Concentrations and composition of VFAs present within the stage III MPA 34.1 AD reactor 1 fed with un-lysed MPA 34.1 biomass to achieve a 30 g/ℓ COD loading

The acetate concentration within this reactor was also lower than the un-homogenised reactor, indicating the potential that a certain fraction of the acetate was volatilised during the microwave treatment. All the reactor systems appeared to have a peak in VFA concentration between days 2 and 5, which decreased by day 7. This indicated that the easily degradable biomass was hydrolysed first and then the hydrolysis slowed down. However, the decrease was slower than that witnessed during the *Oedogonium* sp. or un-homogenised *Parachlorella hussii* experiments, suggesting that hydrolysis was still occurring as some VFAs were still being released. This also correlates to the gas production observed (Figure 56).

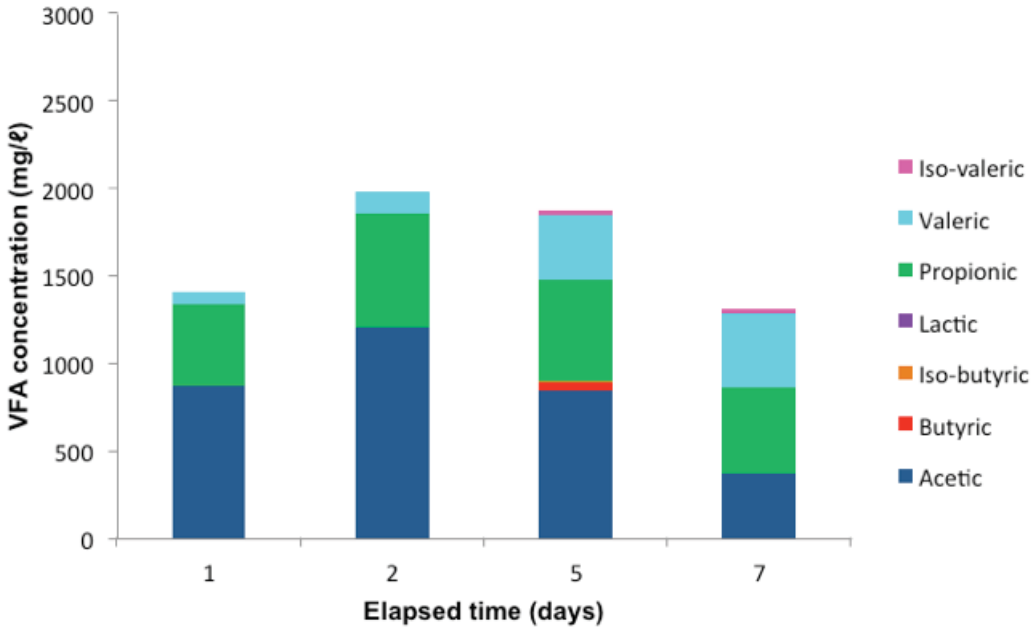

Figure 64: Concentrations and composition of VFAs present within the stage III MPA 34.1 AD reactor 2 fed with un-lysed MPA 34.1 biomass to achieve a 30 g/ℓ COD loading

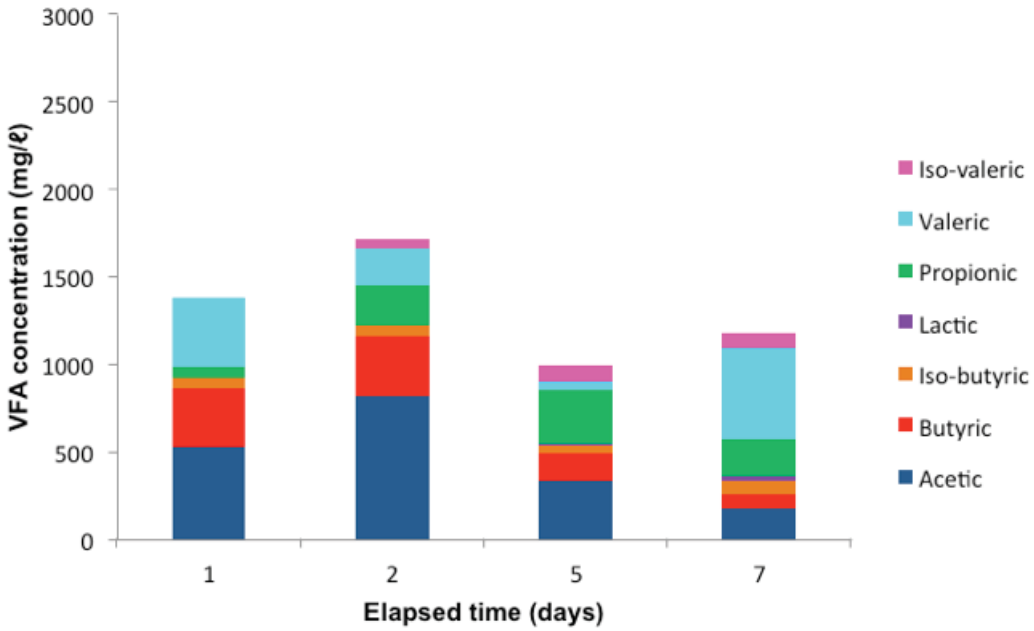

Figure 65: Concentrations and composition of VFAs present within the stage III MPA 34.1 AD reactor 3 fed with partially lysed MPA 34.1 biomass to achieve a 30 g/ℓ COD loading

During the stage I and II tests the acetate present at the start of the test was rapidly consumed, suggesting the rate of acetate consumption was faster than acetate generation, or no acetogenesis was taking place. A different acetate concentration profile was observed for the stage III BMP tests, where the acetate concentration increased and reached a peak before it decreased, suggesting that acetate was actively being released from the biomass substrates at a rate exceeding that of consumption by methanogens (Figure 66). For the stage I and II BMP tests the decrease in acetate concentration correlated to the time points at which biogas production ended (Figure 54 and Figure 55). This may be a consequence of the lack of acetate available for methanogens to utilise for methane production (Cheng, 2010; Chynoweth and Isaacson, 1987; Kwietniewska and Tys, 2014). Stable acetate concentrations above 800 mg/ℓ are considered a sign of digester failure (Kwietniewska and Tys, 2014). It can therefore be assumed that the microbial community within the AD test reactors contained an active population of methanogens, but that hydrolysis, acidogenesis and acetogenesis were not effective.

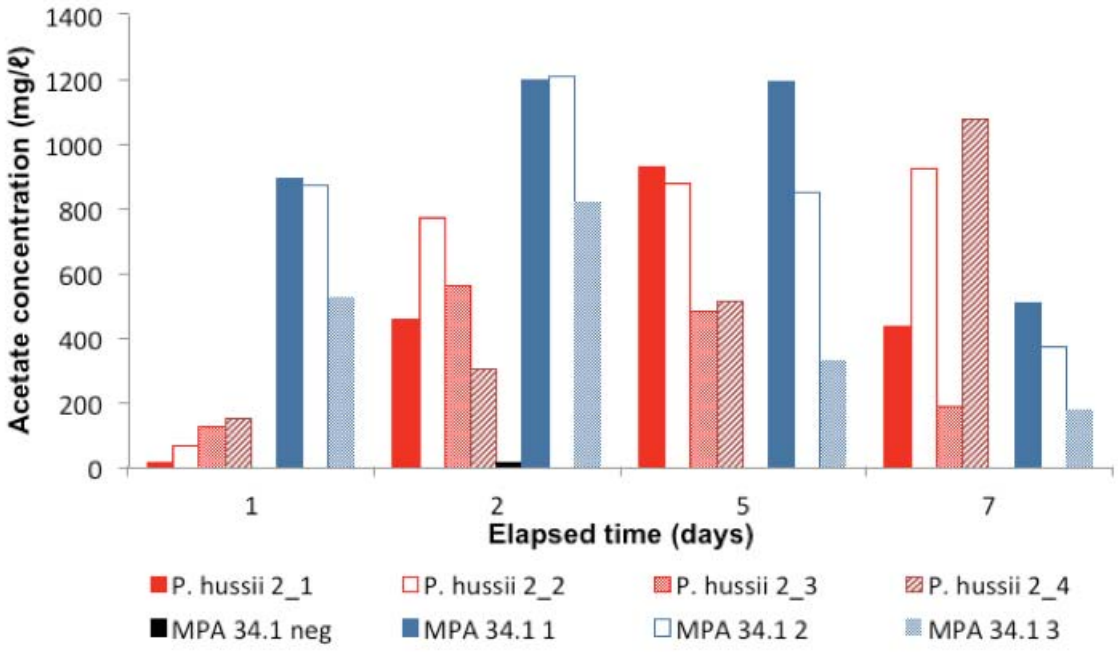

Figure 66: Acetate concentrations for various algal substrate used during stage III algal AD BMP tests

Stage I, II and III algal BMP reactors showed similar trends in the measured propionate concentrations, with an increase to peak between day 2 and 5, followed by a decrease. It has been suggested that propionate to acetate ratios of greater than 1.4 are a sign that the anaerobic community is not functioning effectively (Kwietniewska and Tys, 2014). Therefore, the fact that the propionic concentration decreased, while the propionate to acetate ratio was maintained below 1.4 may indicate that a healthy microbial AD community was present within the algal AD BMP test reactors.

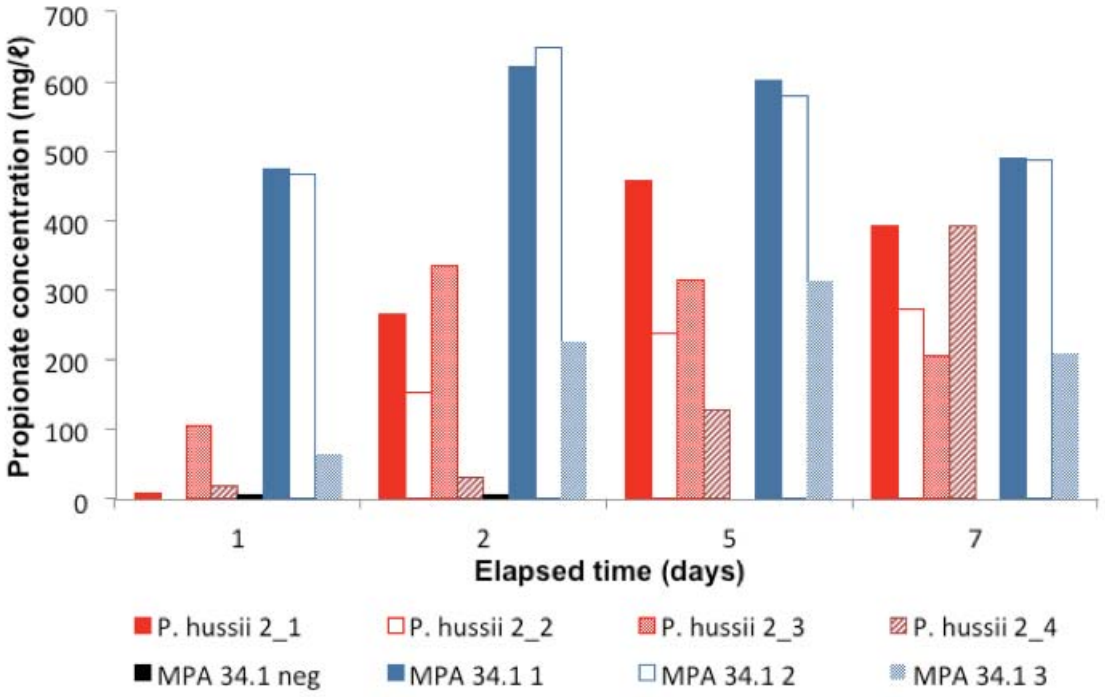

Figure 67: Propionic concentrations for various algal substrate used during stage III algal AD BMP tests

A similar trend to that observed for the propionic acid was observed also observed for butyric acid in the stage III BMP tests. A build-up of butyric acid, exceeding concentrations of 6 500 mg/ℓ, is

considered inhibitory to the microbial community (Kwietniewska and Tys, 2014). Therefore, the decrease in butyric acid concentration observed may also be indicative of a well-functioning AD system.

The soluble CODs measured during the course of the experiments were compared with the theoretical CODs achieved from the measured VFA concentrations. The COD of each VFA was calculated using the first principal calculation and these results are shown in Table 12. The comparison between the calculated and theoretical COD (indicated by a grey trend line) is shown in Figure 68.

Table 12: Theoretically CODs of various VFAs calculated using first principal calculations

Volatile fatty acid	COD (g/g)
Lactic	1.07
Acetic	1.07
Propionic	1.51
Iso-butyric	1.82
Butyric	1.82
Iso-valeric	2.04
Valeric	2.04

The percentage of the soluble COD that can be attributed to VFAs varied considerably with algal species and sampling time, although on average VFAs contributed 56% of the soluble COD (Figure 68). The remaining soluble COD is probably composed of other soluble organic compounds (Boyles, 1997). MPA 34.1 had the highest fraction of soluble COD that could be accounted for by VFAs (76%) while *P. hussii* had the lowest with only 41%. In general, a higher soluble COD value corresponded to a higher VFA concentration for all the algae used as AD substrates. This was very different from the data for the grass, manure and Avicel substrates.

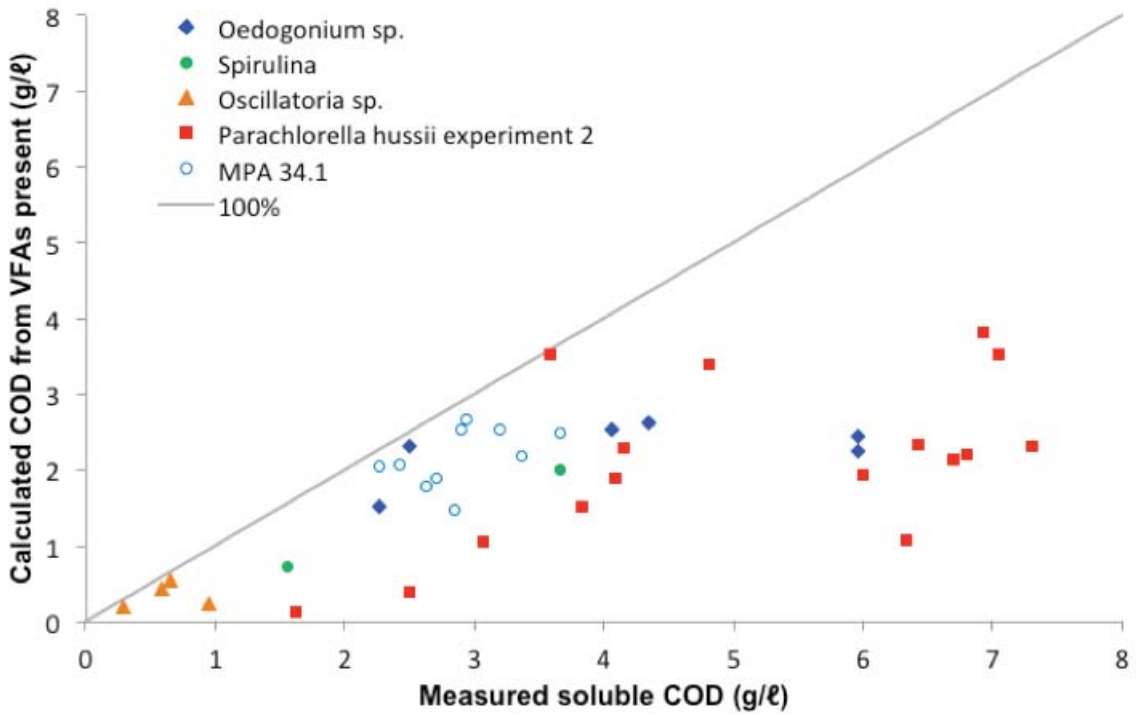

Figure 68: Comparison between the measured soluble CODs and the calculated COD from the VFAs present

A key objective of this study was to assess whether algal biomass can be used for the production of high concentrations of VFAs, to be used as electron donors for processes involved in sulphate reduction and sulphide oxidation. It is therefore important to be able to compare results between different types

of algal biomass, especially where different COD loadings were applied. The total COD loading within anaerobic digesters influences the methane and VFA production. However, the production of each has been found to be proportional to initial COD loadings within batch reactors (Raposo *et al.*, 2006; Erguder *et al*., 2001; Raposo *et al*., 2011; Costa *et al*., 2012; Frigon *et al*., 2013). However, this does not apply for very low COD loadings, where a lack of nutrients may limit the productivity and at very high COD loadings, where the VFAs are produced by the breakdown of substrates faster they can be utilised by methanogens (Raposo *et al*., 2006; Raposo *et al*., 2011). Erguder *et al*. (2001) demonstrated proportionality between the COD loading rate and product formation for COD loadings up to 22.5 g/ℓ , which was their highest COD loading tested. For the current study it was assumed that the VFA production was proportional to the loading rate up to 30 g/ℓ to allow for the scaling up of the 12 g/ℓ COD loading applied in the stage I BMP tests. Table 13 gives a comparison of the expected VFA concentrations from the different algal AD BMP tests if a 30 g/ℓ COD loading was applied to all reactors.

Table 13: Maximum VFA concentrations and soluble CODs for all experimental runs

Experiment	Maximum VFA concentration assuming 30 g/ℓ COD loading (g/ℓ)	Maximum soluble COD assuming 30 g/ℓ COD loading (g/ℓ)
Oedogonium sp. 1	3.9	10
Oedogonium sp. 2	4.0	11
Spirulina	2.9	9.1
P. hussii Experiment 1_1	0.09	3.2
P. hussii Experiment 1_2	0.19	3.2
P. hussii Experiment 1_3	0.22	3.2
Oscillatoria sp. 1	0.28	2.4
Oscillatoria sp. 2	0.29	2.4
P. hussii Experiment 2_1	2.3	3.8
P. hussii Experiment 2_2	2.1	8.3
P. hussii Experiment 2_3	1.8	4.8
P. hussii Experiment 2_4	1.6	7.7
MPA 34.1_1	2.9	3.2
MPA 34.1_2	2.0	2.9
MPA 34.1_3	1.4	3.8

The *Oedogonium*, *Spirulina* and partly lysed *P. hussii* AD reactors produced the highest maximum soluble COD loadings and highest maximum VFA concentrations. Therefore, the highest VFA concentrations would have been produced by the *Oedogonium* reactors followed *Spirulina* and the MPA 34.1 and *Parachlorella hussii* reactors. The suitability of using *Oscillatoria* as a substrate for VFA production in an AD reactor will need to be further investigated, as the inoculum used for the stage II BMP tests had a lower sludge loading that the stage I and III tests.

The experiments using algae as a substrate appeared to yield more promising data than the grass and manure, from a VFA liberation perspective. However, the results need to be considered in the context of the requirements for sustaining the proposed semi-passive treatment system. A typical application may seek to treat 10 000 ℓ per day of mining-impacted water, with a starting sulphate concentration of 2000 mg/ℓ to a target level of 500 mg/ℓ sulphate. Assuming an ideal COD to sulphate ratio of 0.7, this would require 10.5 kg of COD per day. Taking the most promising *P. hussii* data from Table 13 (Experiment 2_2), achieving 8.3 g/ℓ of soluble COD from a loading of 30 g/ℓ after two days, or 4.15 g COD/ℓ.day. This computes to the generation of 0.138 g soluble COD per g of algae per day, so a required loading of 76.1 kg of algae per day. Using the maximum volumetric growth rate of 0.0111 g/ℓ.d

for *P. Hussii* and a 100% harvesting efficiency it would take the processing of 6.85 Mℓ of algal suspension per day to produce sufficient COD.

3.4 CONCLUSIONS

The provision of a cheap, reliable carbon source and electron donor for biological sulphate reduction and sulphide oxidation remains the most significant obstacle to the widespread application of the technology. This chapter focussed on the potential for using the digestate from the anaerobic digestion of grass, manure and a range of algal species, by assessing AD performance and residual VFA concentration in batch reactors.

The main conclusions that could be drawn from the research are:

- The anaerobic digestion of grass and manure was not effective, primarily due the slow rates of hydrolysis achieved under the experimental conditions. The amount of biogas generated was significantly lower than the theoretical maximum, based on the initial COD loading.
- The majority of the biogas production in the grass and manure reactors occurred during the first seven days, after which gas production ceased or slowed down considerably.
- There was no substantial accumulation of VFAs in the reactors loaded with grass or manure, even during the first seven days when the rate of biogas generation was highest. This indicates that VFA consumption was faster than the rate of VFA generation. There was no consistent decrease in the total COD and the soluble COD remained relatively stable at a low concentration. These data indicate limited hydrolysis of the solid substrate and the presence of some recalcitrant soluble organics.
- The Avicel reactors provided some interesting data, with one of the two reactors showing relatively high levels of hydrolysis initially. This was coupled to a significant decrease in pH, indicating that the hydrolytic organisms were more active at low pH (pH <6). During this period biogas generation was suppressed and VFA accumulation to over 3 g/ℓ was observed. This suggests that the microbial community contained distinct hydrolytic and methanogenic populations, with different pH optima.
- Once the pH increased to above pH 6.5 biogas generation increased significantly, coupled with the consumption of the accumulated acetate.
- The *Spirulina* reactor, set up as a positive control, was not able to replicate historical data. This was largely attributed to the way the biomass was prepared. The unwashed biomass resulted in a substantially higher salinity in the AD reactor, which may have inhibited the un-adapted microbial community and reduced the osmotic shock to the *Spirulina*, leading to less disruption of the filaments.
- A number of unicellular and filamentous algal species were successfully cultivated and tested as substrates in batch biomethane potential tests. Data suggest that an extended adaptation period significantly improves the performance of the hydrolytic and methanogenic populations in the community.
- The algal biomass showed a similar overall trend to the other complex carbon sources, with hydrolysis and acidogenesis becoming the rate limiting reactions after a relatively short period of time. Once the rate of VFA consumption exceeds that of VFA generation the system is no longer suitable for generating substrate for the downstream components of an integrated system.

- Using the most promising algal digestion data and a best-case scenario for algal cultivation and harvesting, the analysis points toward the cultivation and digestion of algae as part of an integrated treatment system for mining impacted water not being viable.
- Data from the one Avicel reactor suggests that operation of a dedicated pre-treatment reactor under acidic conditions, which suppress methanogenesis, could facilitate the generation of a VFA-rich stream as part of an integrated treatment system.

CHAPTER 4: ACCELERATED HYDROLYSIS OF GRASS

4.1 INTRODUCTION

The conceptual design of the integrated system provided for an anaerobic digestion unit, generating renewable energy in the form of biogas and a digestate with sufficient residual COD to sustain the downstream sulphate reducing and sulphide oxidising communities. The intention was to use organic substrates that were abundant in the proximity to the target site, preferably waste or by-products, to avoid the cost of buying and transporting substrates.

The previous chapter describes experiments aimed at evaluating the anaerobic digestion of a range of complex organic substrates. The experiments were conducted at near neutral pH to facilitate biogas production, as the intention of the research was to integrate localised renewable energy production with remediation of the minewater. The results of the experiments were not particularly encouraging and indicated that the initial hydrolysis of the complex carbon sources was the rate-limiting stage. There was no significant accumulation of volatile fatty acids (VFAs) and biogas production dropped off significantly after the first few days, as the acetate supply became limiting.

An exception to the general trend was observed in one of the reactors loaded with microcrystalline cellulose (Avicel), where hydrolysis and subsequent fermentation to VFAs was significant during the initial period, resulting in a decrease in pH to below the optimal range for methanogenesis. The inhibition of methanogenesis led to the accumulation of up to 4 g/ℓ of VFAs, predominantly acetate. This prompted a shift away from operating conditions that favoured biogas formation to those that favoured hydrolysis, with the intention of optimising hydrolysis in a separate reactor.

Grass was selected as the substrate of choice due to its availability in the areas impacted by coal mining. Grass is used extensively as a cover during the initial stages of land rehabilitation. The potential of grass as a direct substrate for sulphate reducers has been investigated in the past, with the CSIR playing a leading role (Greben *et al.,* 2009; Mulopo, 2016).

This chapter presents data on the characterisation of grass and a series of batch tests to assess the liberation of organic carbon under a number of controlled conditions, as well as a series of preliminary batch experiments using statistical design tools to assess the significance of potential control parameters on the degradation of the biomass and release of soluble organic material.

4.2 MATERIALS AND METHODS

4.2.1 Grass cuttings

The availability and composition of grass can vary seasonally, so in an attempt to ensure the most consistent substrate for the experiments *Poa annua* was selected. *Poa* is commonly used for the greens of golf courses, where it is consistently irrigated and cut regularly. For experiments performed in Cape Town grass was obtained from the Clovelley Golf Club, while grass for the experiments conducted at Wits was obtained from the Eagle Canyon golf club. Due to the nature of grass on greens and the type of mower used the cuttings were generally below 3 mm in size with a relatively narrow size distribution (Figure 69) so were not processed further.

Figure 69: Photograph of the grass cuttings used, indicating the small particle size and relatively narrow size distribution.

4.2.2 Anaerobic inocula

A mixed microbial consortium was prepared by targeting as described in section 2.2.1.

The mixed AD inoculum was built up by gradually drawing and filling the various enrichment cultures and combining the drawn effluent into a 10 ℓ Schott bottle, fitted with a modified lid and sealed with a large nitrile glove as a reservoir for gas produced. The sludge volume within the 10 ℓ inoculum bottle increased with each additional input of drawn effluent and substrate. Substrates used to feed these inocula included grass, cow manure, Avicel PH-101, waste algal biomass, tissue paper, *Spirulina*-AD effluent and SAB AD effluent. Once an active 10 ℓ inoculum was established a sample of the sludge and liquid fraction was used to inoculate a 2 ℓ reactor, which was subsequently maintained on grass cuttings. A second reactor (1 ℓ) was inoculated with the same mixture, but the pH was reduced to pH 4.5 using sulphuric acid to select for the hydrolytic organisms. Both reactors were periodically loaded with 10 g of freshly grass cuttings.

4.2.3 Batch anaerobic reactors

The AD and hydrolytic cultures were maintained in a 2 ℓ and 1 ℓ batch reactor respectively. The reactors are described in section 2.3.3.

The batch experiments were performed in either 1 ℓ or 500 mℓ Schott bottles, without the modified lid.

4.2.4 Substrate characterisation

The COD of the fresh grass cuttings was determined by accurately (4 decimal points) weighing out a small (0.0010-0.0200 g) mass of material. The grass was added to a COD digestion tube along with 1 mℓ of deionised water. A minimum of four replicates was performed for each batch of grass. In parallel, the moisture content of the grass was determined by drying at 70˚C for 48 hours in an aluminium crucible. The moisture content was used to determine the COD equivalent per g of dry mass.

4.2.5 Analytical methods

The analytical methods have been described in detail in section 2.4, in chapter 2.

4.2.6 Experimental procedure

4.2.6.1 Abiotic tests with sulphuric acid

The experimental reactors (1 ℓ Schott bottles) were set up by adjusting the pH of 1 ℓ of deionised water with sulphuric acid across a range from pH 2 to pH 5, at 0.5 unit increments. Each bottle was loaded with 15 g (wet mass) of freshly cut grass and sealed. The reactors were not inoculated with an active culture, but the grass was not sterilised prior to addition. The reactors were maintained in an air-conditioned laboratory (24 ± 2˚C) and manually agitated for 10 s twice per day. The pH and redox potential were measures daily. A 2 mℓ sample was removed each day, centrifuged at 14,000 rpm and filtered through a 0.45 µm membrane filter and stored at -20˚C prior to HPLC analysis. The COD and acidity/alkalinity were measured at intermediate intervals during the experiment.

The experiment was replicated using grass dried at 70˚C for 48 hours to determine whether the freshness of the substrate has an impact. The moisture content of the grass was determined and the mass adjusted to ensure the same COD equivalent was added.

4.2.6.2 Abiotic tests with sulphuric acid and a metabolic inhibitor

The results of the initial abiotic tests showed that the reactors were rapidly colonised by anaerobic bacteria, most likely associated with the grass cuttings. To eliminate the effect of bacterial action the abiotic tests were repeated in the presence of 50 mM sodium azide. Sodium azide releases ammonia when dissolved, which increased the pH of the solutions, so they needed to be adjusted back to the initial range (pH 2-5) before the addition of the grass cuttings. The sampling and analytical protocols were as described above.

4.2.6.3 Abiotic tests with acetic acid

A second set of experiments was conducted to determine whether the presence of acetic acid had a catalytic effect on the hydrolysis of grass. The 1 ℓ reactors were loaded with a dilute acetic acid solution (1 g/ℓ) and the pH adjusted with sodium hydroxide to achieve the initial range between pH 2 and 5 prior to the grass addition. Reactors were maintained and sampled as described above for the sulphuric acid reactors.

4.2.6.4 Effect of biomass loading

Based on the observations from the first set of sulphuric acid tests, the effect of biomass loading was assessed for the most acidic conditions (pH 2 and 2.5). Experiments were performed in 500 ml Schott bottles, loaded with deionised water adjusted to pH 2 and 2.5 with sulphuric acid. One set of reactors was loaded with 10 g/ℓ fresh grass, a second with 15 g/ℓ and the third with 20 g/ℓ. The reactors were maintained and sampled as described above.

4.2.6.5 Batch tests using mine water

Mine water was obtained from the site of the pilot scale investigation, an active coal mine in the Mpumalanga region of South Africa. The raw mine water had been partially treated by a lime addition

step, although the efficiency of the treatment process has historically been inconsistent. The process was designed to increase the pH to above pH 5.5, to ensure the removal of the majority of the iron. Data from the past three years (2014-2016) indicated a pH range between pH 2.3 and 5.8, with the majority of the samples returning pH values below pH 3.5. Over the same period iron concentrations in the effluent ranged from 3 to 1050 mg/ℓ.

Fresh mine water was obtained from the site on two occasions (November 2016 and May 2017). The first sample was used to assess the effect of adding fresh grass cuttings (10 g/ℓ and 20 g/ℓ) in 500 ml batch reactors. The reactors were sampled periodically to determine pH, redox potential, sulphide (soluble and colloidal precipitate) and sulphate. The presence of iron in the mine water led to the formation of amorphous iron sulphide precipitates, a fraction of which remained in suspension after agitation. The strong acids used to prepare the reagents for the sulphide assay dissolved the iron sulphide precipitate, leading to the quantification of that fraction of sulphide. To measure only the aqueous sulphide, a 2 mℓ sample was centrifuged at 14 000 x *g* for 5 minutes and the supernatant assayed. An additional 10 g of fresh grass cuttings were added to the 20 g/ℓ reactor on two occasions (day 111 and day 186).

On day 168 a fraction of the culture (100 mℓ) was removed and used to inoculate a second 500 ml reactor. This was replaced with 0.74 g of Na_2SO_4 dissolved in 100 mℓ tap water.

The inoculum was used to start up a second 500 ml reactor, loaded with 400 ml of mine water (May 2017 sample) and 10 g fresh grass cuttings. The intention was to compare the performance of an uninoculated system with one that was inoculated with active culture (20% v/v). The second reactor was monitored using the same protocol.

4.2.6.6 Evaluation of 8 ℓ channel reactor for pre-treatment

The tests conducted using the mine water as a substrate confirmed that effective microbial sulphate reduction did not occur until the pH of the medium had increased to around pH 6.5. Historical data from the pilot site showed that the pH of the partially treated minewater was typically in the region of pH 3.5, so some pre-treatment would be required to increase the pH.

An 8 ℓ channel reactor was evaluated as a potential pre-treatment reactor, for contacting the acid minewater with fresh grass cuttings. In addition, the experiment was designed to investigate whether a sulphate reducing bacterial population could be established, as had occurred in the batch reactor.

The standard 8 ℓ channel reactor was modified by removing the carbon fibres. The reactor was loaded with 160 g of fresh grass cuttings (Figure 70) and 8 ℓ of acidic, high sulphate solution prepared by blending mine water with acidified solutions of sodium and magnesium sulphate. The solution has a pH of 3.21 and a sulphate concentration of approximately 2500 mg/ℓ. The reactor was not inoculated with microbial culture.

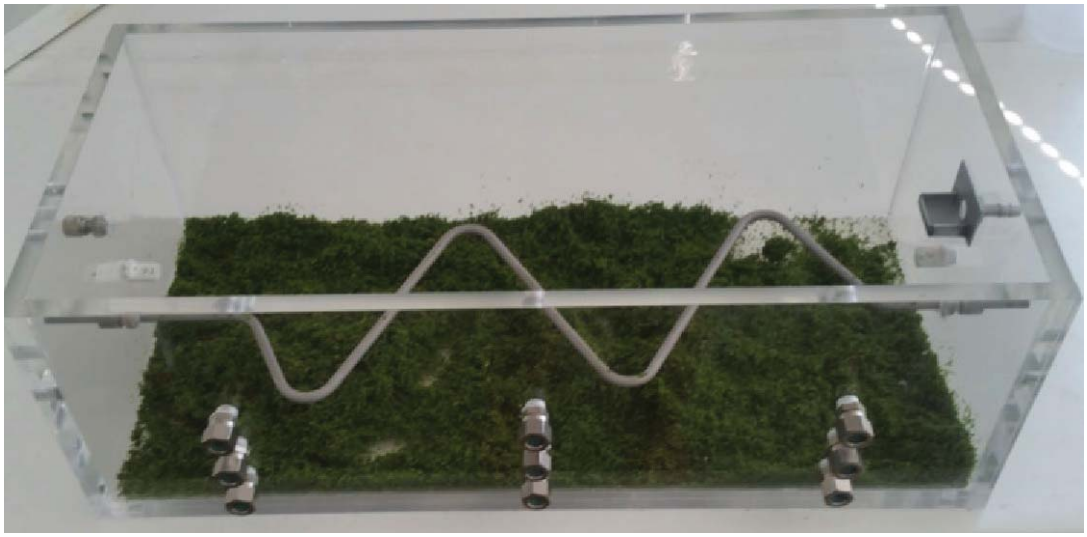

Figure 70: Image showing the channel reactor loaded with grass cuttings

The system was operated in batch mode and sampled every 2-3 days by extracting 7 mℓ from the top, middle and bottom sampling ports using a syringe and hypodermic needle. A fraction was immediately used to measure sulphide (soluble and colloidal). The remaining sample was used to measure pH and redox potential. A 2 mℓ fraction was centrifuged at 14000 x *g* for 5 minutes. The supernatant was used to measure aqueous sulphide, sulphate and COD. A second 2 mℓ sample was centrifuged, then filtered and retained for VFA analysis by HPLC.

4.3 RESULTS AND DISCUSSION

4.3.1 Substrate analysis

The elemental analysis was performed on dried material, while the COD was measured using fresh material. The moisture content of the grass was determined each time fresh material was collected, with values ranging from 65 to 73% (mean 68.2 ± 3.4). The mean COD data presented in the table has been corrected for the moisture content.

Table 14: Elemental composition and COD of the AD substrates

Substrate	%C	%N	%H	Formula	COD (mg/g)
Grass	36.8	1.17	6.9	$CH_{2.246}N_{0.027}O_{1.13}$	1110 ± 88

4.3.2 Abiotic tests with sulphuric acid

The intention of the batch tests was to assess the extent to which weak acid could achieve cellulose hydrolysis at ambient temperatures and to what extent free acidity was consumed in the process. There is a substantial amount of published work on cellulose hydrolysis using weak acid at elevated temperatures (150-270˚C), but very little data on lower temperatures.

The addition of fresh grass resulted in a change in the colour of the solution phase within the first 24 hours (Figure 71). The colour became increasingly light as the initial acid concentration increased, most likely as a result of a reaction between the free acid and the leached pigment molecules.

The presence of the grass cuttings resulted caused the pH in all the reactors to increase during the first 24 hours. The measured change was most significant in the reactors that started at pH 3 and above, increasing to between pH 5.9 and 6.7 (Figure 72). The reactor that started at pH 2 did not show a

significant increase in pH during the first seven days of the experiment, but by day 33 the pH had increased to above pH 5.5 (Figure 73). The increase could be attributed to biological activity.

Figure 71: Photograph showing effect of initial pH on the appearance of the liquid phase (24 hours after grass addition)

The reactor that started at pH 2.5 did show a more significant increase during the first 24 hours and the pH continued to climb steadily for the next six days, while the pH in the remaining reactors decrease slightly between 24 and 48 hours before remaining relatively stable. This suggests that the components leached out of the grass, or the hydrolysis products, presented sufficient buffering capacity to consume the free acidity.

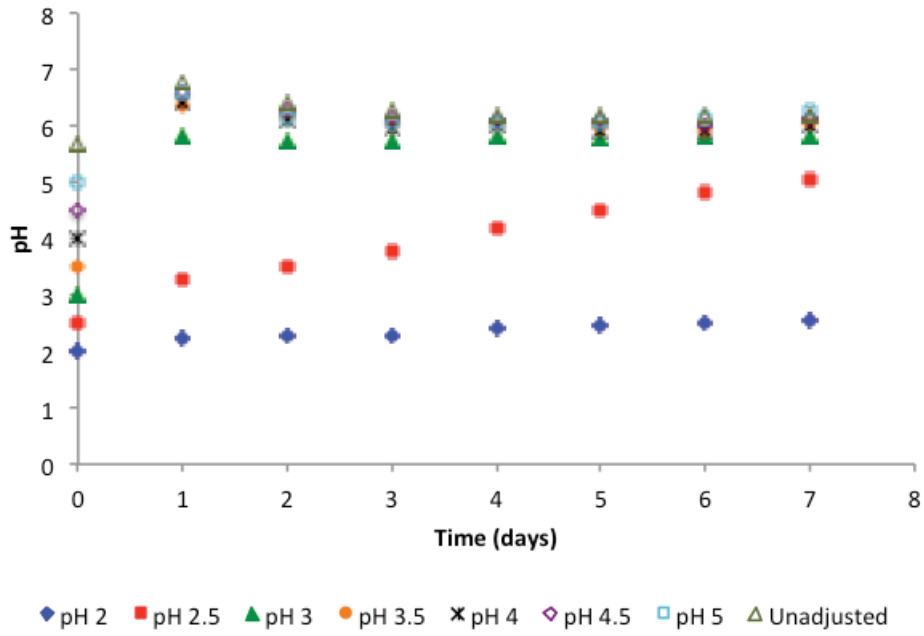

Figure 72: Change in solution pH during the first seven days of the experiment

While the reactors were not deliberately inoculated, clear evidence of microbial activity became apparent within the first seven days. This could be attributed to microbes that were introduced with the grass cuttings. This was confirmed by light microscopy, which showed a greater number and diversity

of bacteria in the higher pH reactors. The presence of the microbes coincided with a substantial decrease in the redox potential, indicating that the reactors changed from aerobic to anaerobic as the experiment progressed. No significant gas production was observed in the reactors, suggesting that methanogenic archaea were not present in large numbers. When the same grass was added to the methanogenic stock reactor biogas production was observed within the first 24 hours. The low starting pH in reactors could account for the limited biogas formation.

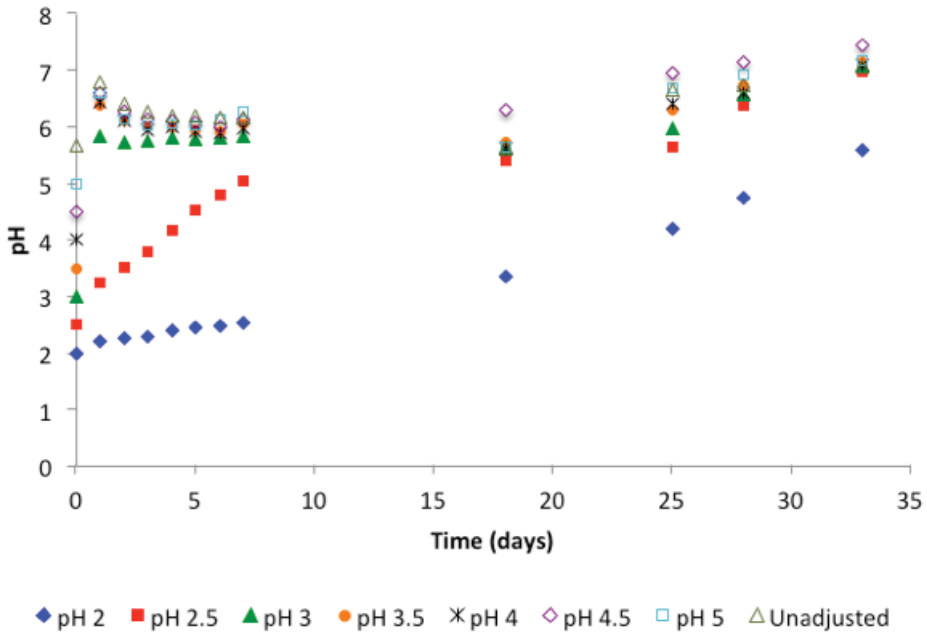

Figure 73: Change in solution pH following contact between fresh grass and dilute sulphuric acid

The results for acidity and alkalinity as a function of time and initial pH are summarised in Table 15. The day 0 data represent the initial acidity as a result of the sulphuric acid added to achieve the desired starting pH. By day 3 it was clear that the addition of the grass had resulted in major changes in the solution chemistry. The pH in the most acidic reactor had increased from pH 2 to pH 2.39, but this had coincided with the consumption of over 250 mg/ℓ of acidity. A smaller change was observed in the pH 2.5 reactor, but for all the other reactors the total acidity had actually increased, suggesting the leaching of organic acids into solution. Between day 3 and day 7 the acidity continued to increase for all the reactors, with the exception of the pH 2 reactor where the acidity decreased further.

Table 15: Acidity and alkalinity values measured for the reactors measured by titration using 0.02 N NaOH (acidity) and 0.01 N H_2SO_4 (alkalinity)

	Acidity (mg/ℓ $CaCO_3$ equivalents)			Alkalinity
Initial pH	Day 0	Day 3	Day 7	Day 28
Unadjusted	0.1	115.0	175.0	362.5
5	1.8	115.0	170.0	312.5
4.5	3.0	105.0	150.0	337.5
4	7.0	130.0	242.5	317.5
3.5	18.0	110.0	165.0	335.0
3	63.0	155.0	212.5	320.0
2.5	223.0	155.0	175.0	237.5
2	816.0	555.0	490.0	15.0

By the end of the experiment the pH in all but the most acidic reactor was higher than pH 6, suggesting the presence of alkalinity. This was confirmed by titration, suggesting that the degradation of organic matter and subsequent microbial metabolism had generated alkalinity. Initially the process was abiotic, but after the first few days was likely driven by biological action.

Samples from the reactors were taken at specific time intervals for analysis by HPLC (section 2.4.8). The technique allowed the separation and quantification of nine volatile fatty acids (Figure 74).

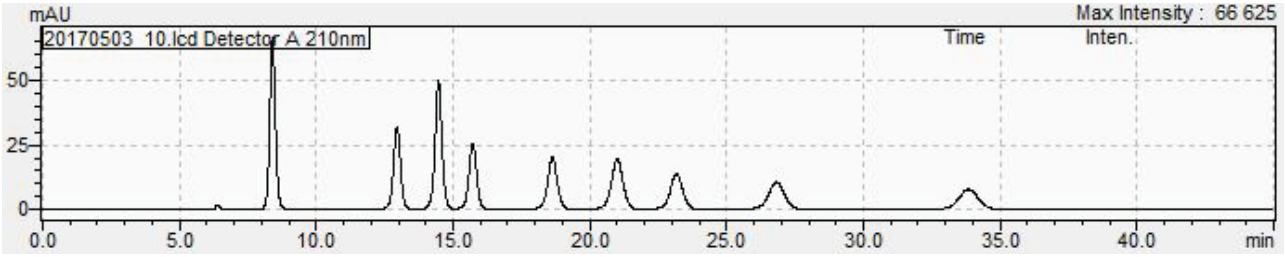

Figure 74: Chromatogram showing separation of the nine VFA standards (500 mg/ℓ). In order: citric acid, lactic acid, formic acid, acetic acid, propionic acid, iso-butyric acid, butyric acid, iso-valeric acid and valeric acid

Samples for VFA analysis were taken on day 1,3,5,7,18 and 28. Analysis of the data showed significant changes in the VFA profile as a function of pH and time. The samples taken on day 1 contained very few VFAs with acetate concentrations between 5 and 25 mg/l measured across the pH range and no other VFAs detected. The chromatograms did show a number of large peaks that did not correspond to any of the VFA standards. The most significant peaks had retention times of 6.4, 11.2 and 22.2 minutes respectively. The peak at 6.4 minutes was the most substantial, particularly in the reactors at pH 2 (Figure 75) and pH 2.5, where the peak areas were 900,000 and 840,000 respectively. The analysis of the yeast extract presented in a subsequent chapter showed a large peak with the same retention time, suggesting a common compound. The peak areas for the samples from the remainder of the reactors could not be accurately quantified because of the appearance of a second, smaller peak (Figure 76). However, the height of the larger peak was much lower (see relative y-axis scale) so it can be inferred that the area would be less. This suggests a relationship between initial pH and liberation of the compound.

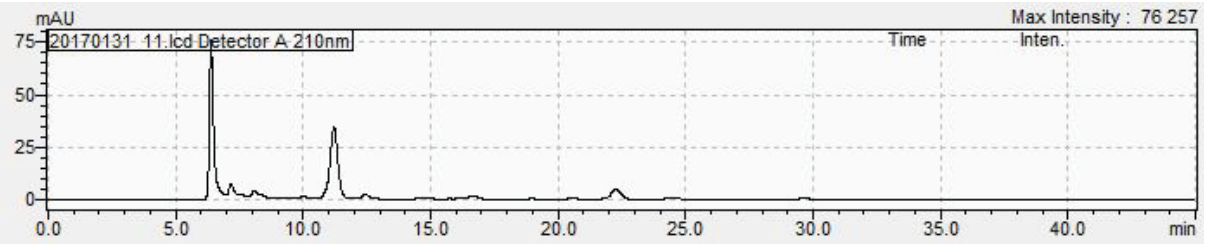

Figure 75: Chromatogram showing peaks detected in the day 1 sample from the reactor at pH 2

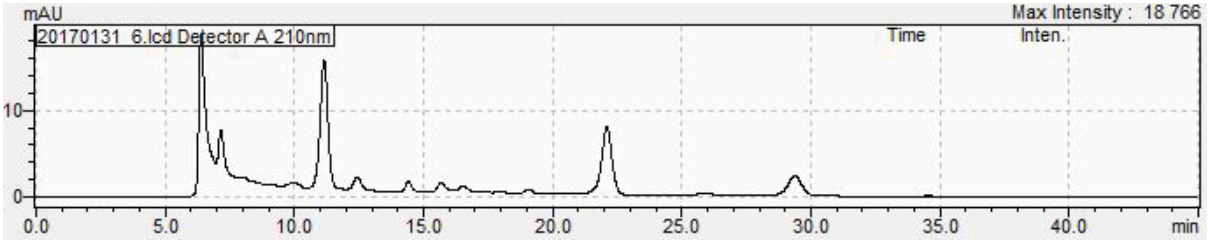

Figure 76: Chromatogram showing peaks detected in the day 1 sample from the reactor at pH 4.5

The profile of peaks on the chromatograms changed as the experiment progressed, providing evidence for the metabolism of compounds present following the initial contact between the grass cuttings and the acidified water. An example of this progression for the pH 4.5 reactor is presented in Figure 77. Between day 1 and day 7 there was a significant reduction in the peaks at 11.2 and 22.5 minutes, while the peak at 6.4 minutes increased slightly in magnitude. In addition, the acetate concentration increased from 25 to 141 mg/ℓ.

Between day 7 and day 28 there was a further reduction in the number and magnitude of most of the peaks. The peak at 7.1 minutes, which was still present after seven days had disappeared, along with the peak at 22.5 minutes. The small peak at 29.5 minutes was still present, along with a residual amount of acetate (18 mg/ℓ). The magnitude of the large peak at 6.4 minutes had decreased slightly, although the peak area was still around 750,000.

Assuming the peak at 6.4 minutes is the same compound present in the yeast extract, the results suggest that the microbial communities are different, given the persistence of the compound. The results show a clear progression in the metabolism of the soluble organic compounds, with the appearance and subsequent disappearance of a number of peaks. From a volatile fatty acid perspective, acetate was the most prominent, with concentrations peaking at around 300 mg/ℓ between day 7 and day 18. The accumulation of acetate was significantly lower in the reactors started at pH 2 and pH 2.5, where the pH increased more slowly and the redox potential remained higher, implicating fermentative bacteria in the generation of acetate. Of the other volatile fatty acids, propionate concentrations peaked at around 100 mg/ℓ and butyrate concentrations at 60 mg/ℓ, also between day 7 and day 18.

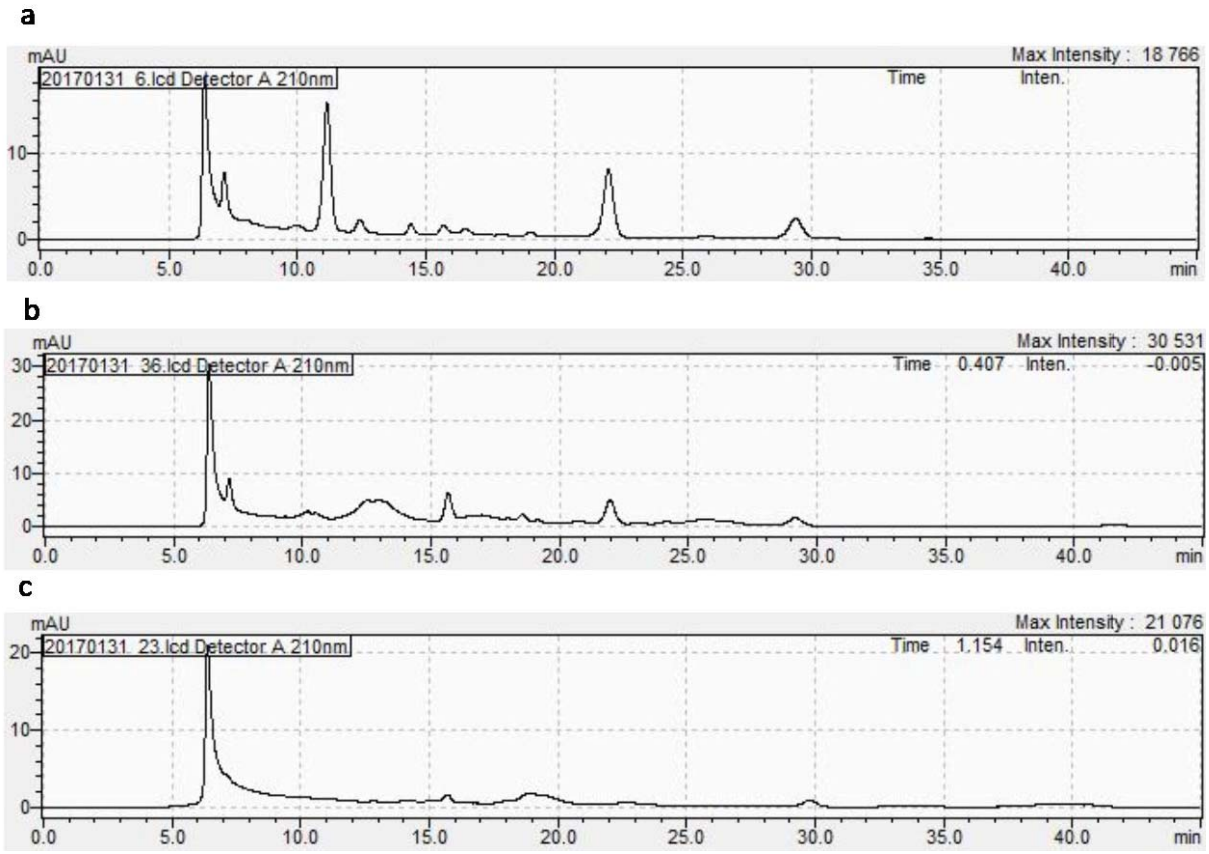

Figure 77: HPLC chromatograms for samples taken from the pH 4.5 reactor on (a) day 1, (b) day 7 and (c) day 28.

The results confirm that it is possible to generate VFAs from grass cuttings in an anaerobic pre-treatment reactor, but suggest that a higher biomass loading is required to generate the concentrations required to sustain meaningful sulphate reduction. Acetate appears not to be a preferred substrate for the fermentative community, only being consumed toward the end of the experiment. Very limited amounts of biogas were produced in any of the reactors, indicating that a methanogenic community had not been selected.

4.3.3 Abiotic tests with sulphuric acid and a metabolic inhibitor

The presence of 50 mM sodium azide completely inhibited microbial activity. Samples were observed using light microscopy at the end of the experiment, which confirmed the absence of bacteria. The pH data (Figure 78) did show some increase in pH, particularly over the first 48 hours, but the magnitude of this increase was significantly lower. In the presence of microorganisms the pH for most of the reactors rapidly converged, stabilising around pH 6. This did not occur in the absence of microbial activity.

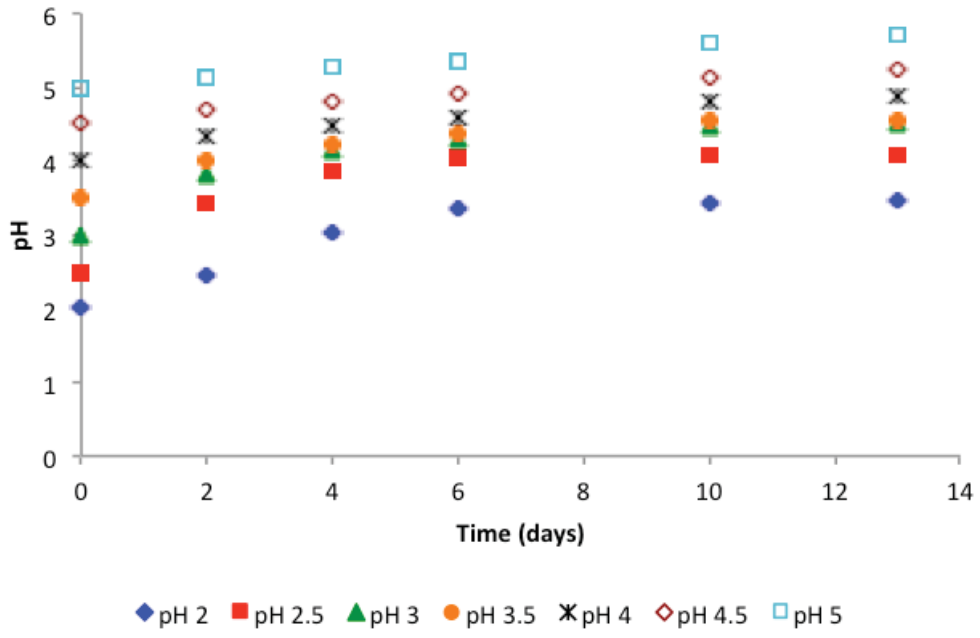

Figure 78: Change in pH in the presence of sodium azide

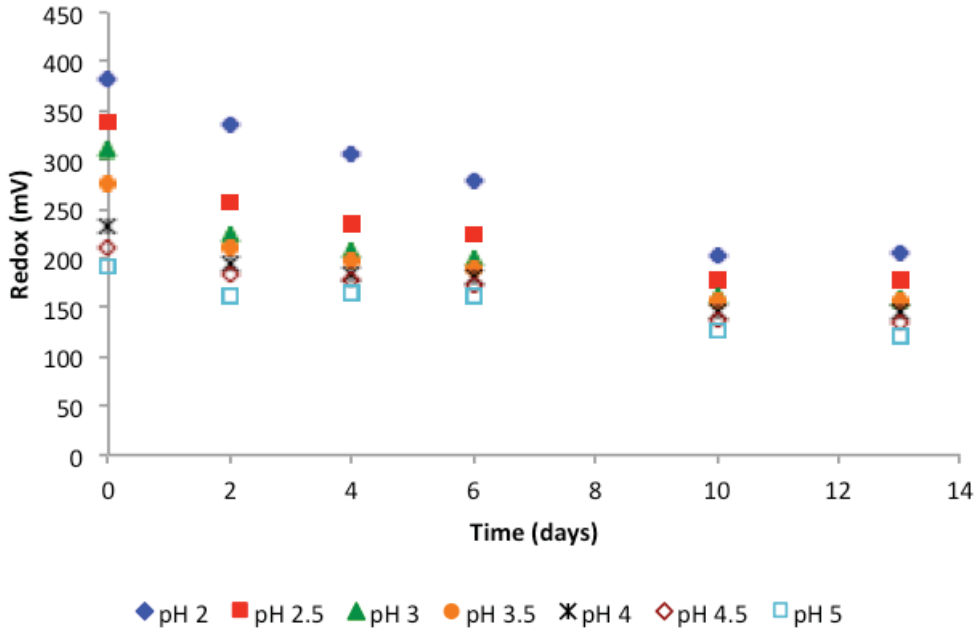

Figure 79: Change in redox potential in the presence of sodium azide

Further evidence for the absence of microbial activity is provided by the redox potential data (Figure 79). As with the pH, there was a gradual change in the redox potential, but at no point did the potential drop below 130 mV in any of the reactors, even after 13 days

The results for acidity and alkalinity as a function of time and initial pH are summarised in Table 16. The day 0 data represent the initial acidity as a result of the sulphuric acid added to achieve the desired starting pH. The table compares the data from day 7 between the experiments conducted in the presence and absence of sodium azide. The data between the two experimental systems are very different after 7 days. In the absence of sodium azide there was acid consumption in the low pH reactors, presumably due to the reaction with organic compounds within the grass or the protonation of

soluble organic acids. For the reactors with an initial pH of 3 and higher there was nett acid generation, with soluble organic acids again the most likely explanation.

Table 16: Comparison of acidity values measured on day 7 for inhibited and uninhibited experiments

	Acidity (mg/ℓ $CaCO_3$ equivalents)			
	No azide		Azide added	
Initial pH	Day 0	Day 7	Day 7	H_2SO_4 adjusted
Unadjusted	0.1	175.0		
5	1.8	170.0	223.3	221.5
4.5	3.0	150.0	486.7	483.7
4	7.0	242.5	810.0	803.0
3.5	18.0	165.0	1140.0	1030.7
3	63.0	212.5	1340.0	1122.0
2.5	223.0	175.0	1690.0	1277.0
2	816.0	490.0	1846.7	1467.0

The azide treated reactors exhibited significantly higher acidity values at day 7, even when the contribution of the sulphuric acid initially added to reduce the pH to the desired values was accounted for. The 50 mM azide solution has a pH of 9.66, so would not contribute to the acidity. It is possible that that the additional acid that was required to reduce the pH back to the desired value after azide addition contributed to the measured acidity, suggesting the azide acted like a buffer. A second possibility is that the absence of bacterial activity allowed greater accumulation of organic acids during the 7 days and that this was relative to the initial pH.

4.3.4 Abiotic tests with acetic acid

Acetic acid has been shown to catalyse the hydrolysis of lignocellulosic biomass under abiotic conditions (Trzcinski and Stuckey, 2015), attributed to an increase in pore size related to the removal of hemicellulose. Previously, the microbial degradation of microcrystalline cellulose resulted in an accumulation of acetic acid, prompting the experiments to assess the impact of pH and acetic acid in combination.

A similar range of initial pH values was tested, but at a concentration of 1 g/ℓ acetic acid. The presence of the acetic acid resulted in a different pH profile to that observed in the sulphuric acid experiments. While the addition of grass did increase the pH, the change was not as dramatic, particularly in the reactors where the starting pH was pH 3 or greater (Figure 80). In the absence of the additional acetic acid the pH in those reactors converged within 24 hours and remained similar for at least the first seven days of the experiment. By contrast, in the presence of the acetic acid the pH values did not converge.

The redox potential data were also very different to that observed in the sulphuric acid experiments, with a distinct progression from positive to negative as a function of the initial pH (Figure 81). The redox potential in the pH 5 reactor became significantly negative within the first 24 hours, while the reactor that started at pH 2.5 only became reducing after six days. The reactor at pH 2 maintained a positive redox potential for the duration of the experiment.

The shift from an oxidising to reducing environment is thought to be a consequence of microbial activity and the data suggest that the presence of protonated acetic acid may have inhibited the activity of the microbial community that was introduced with the grass cuttings. Acetic acid has a pKa of 4.75 so the majority would have been deprotonated in the reactors that started at pH 4.5 and 5 after 24 hours of

contact. The results were very different from the previous experiments, where even the pH 2 reactors showed negative redox potential values within three days.

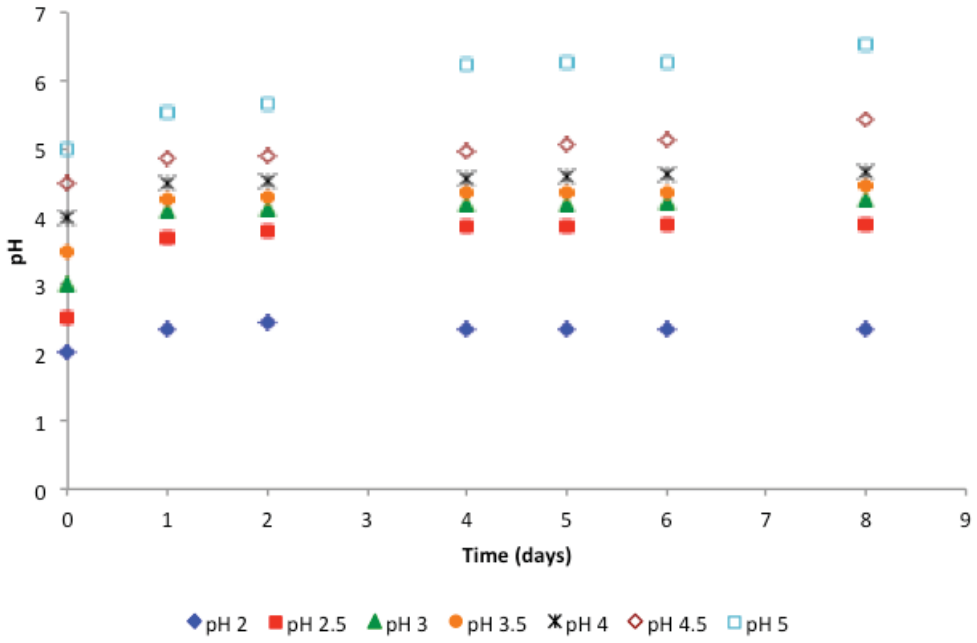

Figure 80: Change in solution pH following contact between fresh grass and dilute acetic acid

Light microscopy was used to assess the microbial community in each of the reactors at the end of the experiment and the observations were consistent with redox data. The pH 2 reactor showed very low microbial numbers (< 2.5 x 10^6 cells/mℓ) and no diversity with respect to cell morphology. The cell concentration and diversity increased as a function of initial pH, with the pH 5 reactor exhibiting several different morphologies (cocci, rods, spirals and chains) and a cell concentration of over 1 x 10^9 cells/mℓ. The microbial community from the active reactors was used to inoculate enrichment cultures that will be used in subsequent experiments.

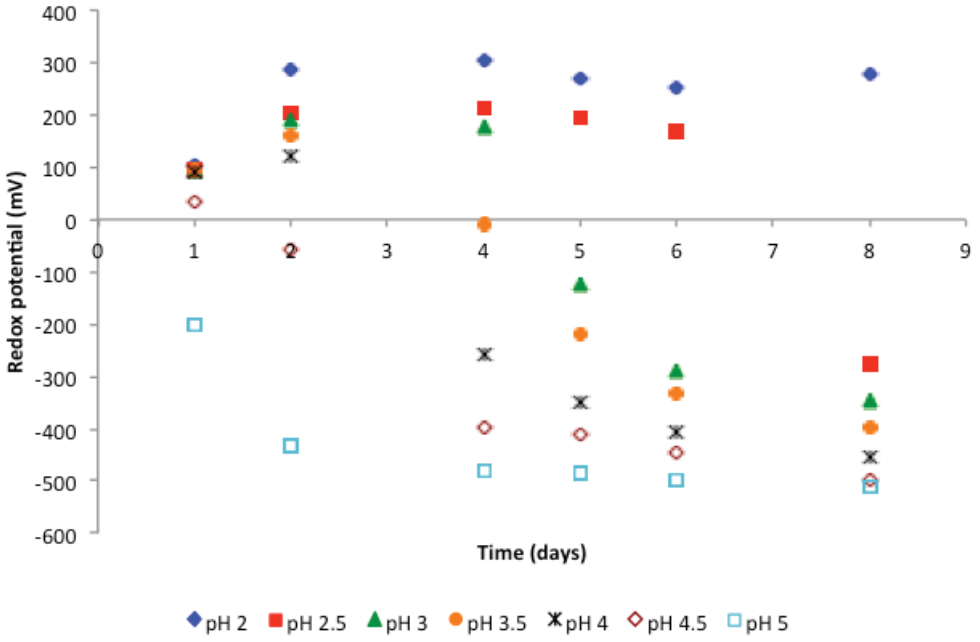

Figure 81: Change in redox potential following contact between fresh grass and dilute acetic acid

4.3.5 Effect of biomass loading

The initial set of experiments were performed using a mass loading of 15 g/ℓ and showed that contact between the grass cuttings and acidified water did result in an increase in pH and consumption of acidity when the initial pH was below pH 2.5. To test the effect of biomass loading the experiments at the two lowest pH values were repeated using three different mass loadings. The results (Figure 82) clearly show a consistent relationship between the mass of grass added and the change in pH.

The mass loadings were selected to maintain a level of consistency with the historical experiments, given the measured COD value for the grass of 1.1-1.3 g COD/g dry material. The data presented below indicates that at a loading of 20 g/ℓ, free acidity can be reduced from 220 mg/ℓ to below 10 mg/ℓ within 48 hours, increasing the pH from 2.5 to just below pH 4.5. However, data on the release of organic carbon suggests that a higher biomass loading will be necessary to provide sufficient substrate for sulphate reduction.

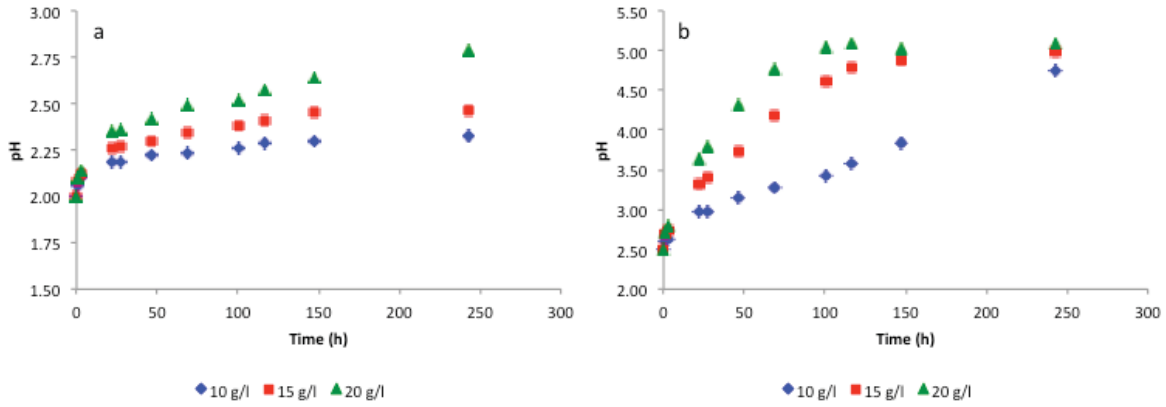

Figure 82: Change in solution pH as a function of grass mass at an initial pH of (a) pH 2 and (b) pH 2.5

4.3.6 Batch tests using minewater

The results from the initial batch tests showed that the addition of grass cuttings was able to increase the pH of acidic solutions, even before any significant microbial activity. The integrated process depends on the activity of sulphate reducing bacteria, so is limited to applications where the pH of feed water is above pH 6 or where the reactor generates sufficient alkalinity during the sulphate reduction process to neutralise the incoming acidity. Pre-treatment of the minewater in a grass reactor could have the dual benefit of consuming acidity and generating soluble organic carbon to sustain the sulphate reduction and sulphide oxidation processes. The retention time in such a pre-treatment reactor would need to be relatively low to keep the reactor size manageable.

Minewater was obtained from the pilot site, after the lime treatment step. Despite the lime addition the water had a pH of 3.22, which would most likely inhibit the sulphate reducing culture. Batch experiments were set up to contact the minewater with fresh grass at 10 and 20 g/ℓ loadings. The pH was measured regularly over the initial 24 hour period (Figure 83).

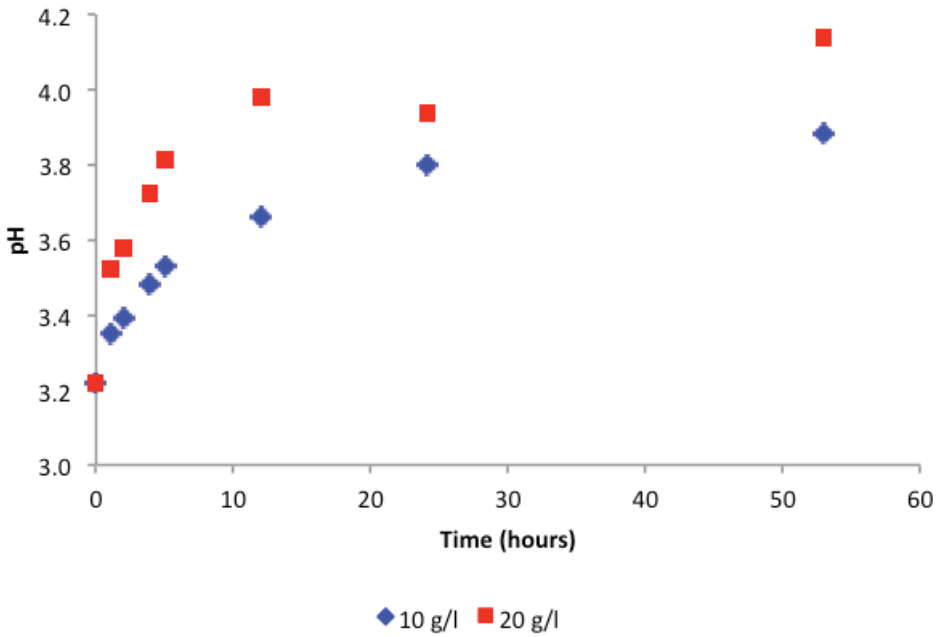

Figure 83: Change in solution pH following addition of increasing mass of fresh grass cuttings to raw mine water

A noticeable increase in pH was observed over the first 12 hours, with the magnitude of the increase a function of the mass loading. In the 20 g/ℓ reactors the pH had increased to just below pH 4. The pH did continue to increase, although more slowly, after the first 12 hours.

The reactors were maintained for a longer period and after about three weeks the reactor loaded with 20 g/ℓ had changed colour (Figure 84) suggesting some sulphate reducing activity and subsequent iron precipitation. No change was observed in the reactor loaded with 10 g/ℓ of grass. Samples taken on day 25 showed that the pH in the 20 g/ℓ reactor had increased further to pH 5.6 and 20 mg/ℓ of aqueous sulphide was detected, confirming sulphate reducing activity. By day 43 the pH had increased to pH 6.2 and the sulphide concentration to 93 mg/ℓ. The sulphate concentration had decreased from 3273 to 2782 mg/ℓ. Based on the amount of sulphate reduced the expected sulphide concentration would be 163 mg/ℓ, but it was clear that some of the sulphide had reacted with iron in the minewater.

Figure 84: Evidence of sulphide generation following contact of fresh grass cuttings with raw mine water for 20 days

The experiment was extended to over 200 days, with regular monitoring. By day 80 the redox potential had decreased to -400 mV (Figure 85), consistent with an active sulphate reducing culture. The sulphide concentration increased to 180 mg/ℓ, with the reduction of just over 500 mg/ℓ of sulphate (Figure 86).

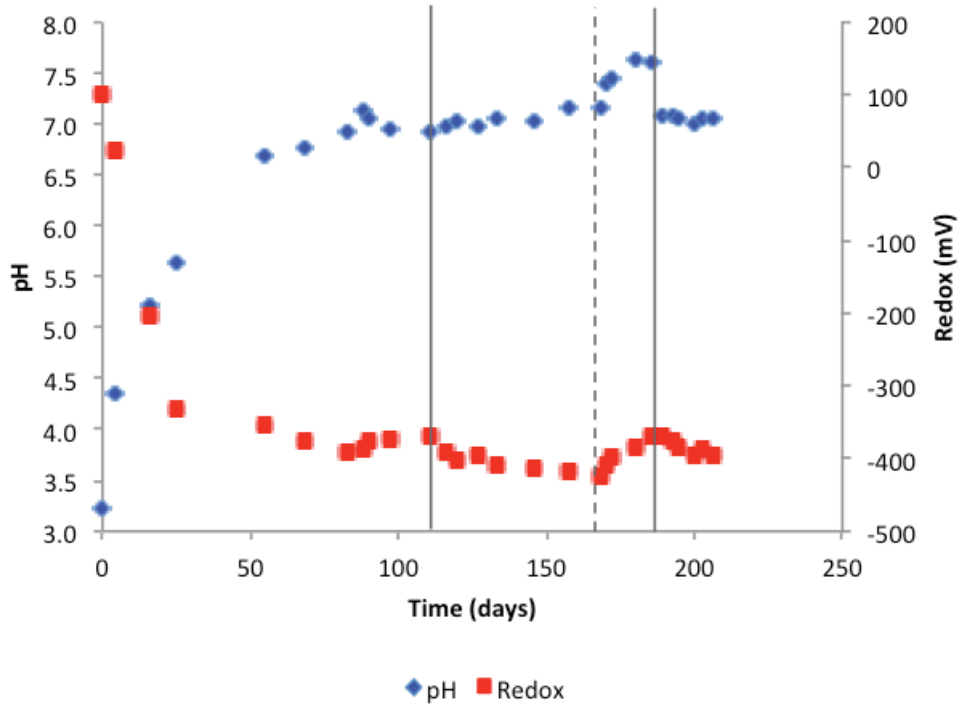

Figure 85: pH and redox potential for experiment contacting 20 g/ℓ grass cuttings with minewater Vertical lines (solid) indicate the addition of 10 g of fresh grass cuttings or (dashed) 500 mg of sulphate

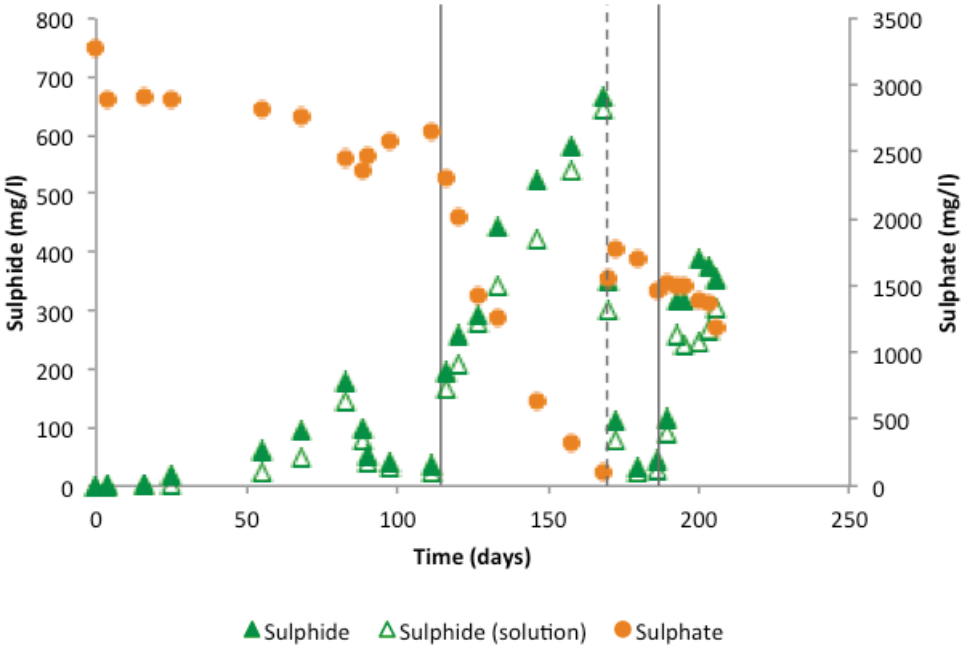

Figure 86: Sulphate and sulphide data for experiment contacting 20 g/ℓ grass cuttings with minewater. Vertical lines (solid) indicate the addition of 10 g of fresh grass cuttings or (dashed) 500 mg of sulphate

Between day 80 and day 100 the sulphide concentration decreased steadily, falling back to below 30 mg/ℓ and there was an increase in sulphate concentration, indicating re-oxidation of some of the sulphide. This trend suggested that the organic substrate had been exhausted, with autotrophic sulphide oxidation becoming dominant. The absence of VFAs was confirmed by HPLC. Some oxygen was introduced into the system each time it was sampled.

In response to the substrate limitation an additional 10 g of fresh grass cuttings were introduced on day 111, with an almost immediate resumption of sulphate reduction.

Following the resumption of the sulphate reduction it progressed steadily, with a volumetric sulphate reduction rate of 3.18 mg/ℓ.h. The rate is significantly lower than has been achieved using lactate as a substrate, but was dependent on the liberation of organic carbon from the grass and its subsequent fermentation to VFAs. Complete sulphate reduction was achieved, albeit over an extended period of time, with sulphide concentrations increasing to around 650 mg/ℓ.

On day 168 a 20% volume of the culture was removed to inoculate a second minewater reactor. The volume was replaced with a sodium sulphate solution, introducing another 500 mg of sulphate, but no additional organic substrate. This perturbation resulted in a rapid decrease in aqueous sulphide, coupled to an increase in pH and redox potential. The most likely cause for this was the introduction of oxygen during the sub-culturing and illustrates the sensitivity of the culture to oxygen, even though the redox potential remained below -370 mV.

Over the following 18 days the culture showed only limited signs of activity. Again, a reduction in organic substrate may have contributed to this, so on day 186 another 10 g of fresh grass cuttings were added, which resulted in an immediate improvement in performance.

By contrast, the reactor inoculated with 10 g/ℓ grass cuttings was not able to elevate the pH above pH 4.3 and did not show any signs of active sulphate reduction. This experiment was terminated after 60 days.

The experiment described above was not inoculated with any microbial culture, with both the fermentative and sulphate reducing species originating from the grass cuttings or minewater. Once complete sulphate reduction had been achieved the active culture was used to inoculate a second reactor, using fresh minewater. It was anticipated that an active culture would significantly reduce the time taken to treat the minewater.

Using a 20% inoculum resulted in a higher initial pH (pH 4.87) and lower redox potential (-200 mV), theoretically creating a more conducive environment for the sulphate reducers. The pH has continued to increase, reaching pH 6 by day 30, but the redox potential did not decrease rapidly as was observed in the previous experiment. In fact, the most recent data points show an increase in the redox potential.

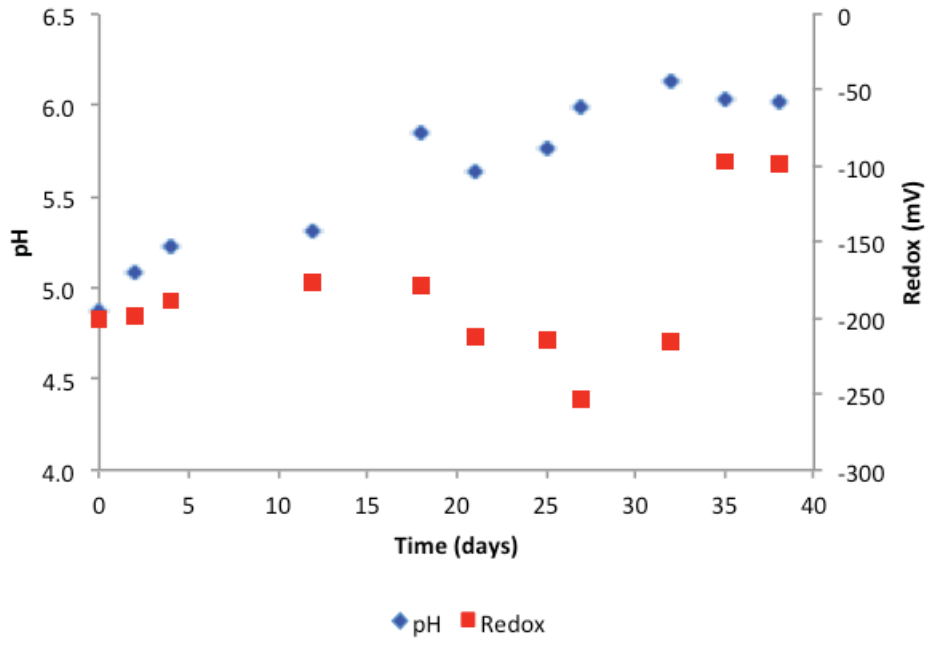

Figure 87: pH and redox potential data for the minewater treatment experiment using active inoculum

Based on the sulphide in the culture used as the inoculum the initial sulphide concentration in the new reactor should have been 133 mg/ℓ, but it was significantly lower than this due to the formation of iron sulphide precipitates (Figure 88).

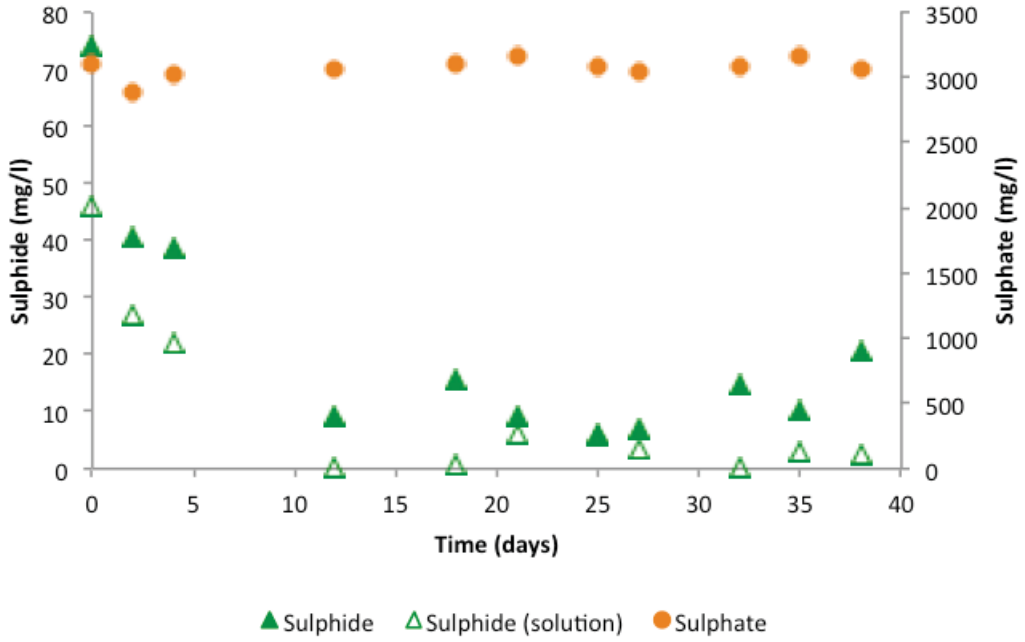

Figure 88: Sulphate and sulphide data for the minewater treatment experiment using active inoculum

The difference between the soluble sulphide (open symbol) and total sulphide is due to the measurement of some of the sulphide trapped within the iron sulphide precipitates. The reactor was not actively agitated, so the amount of iron sulphide in suspension was relatively low, particularly as the experiment progressed, accounting for the convergence of the two values.

The sulphate data show that there has essentially been no active sulphate reduction over the first 37 days, which was not expected. The most likely explanation relates to the pH, which has not increased as quickly as it did in the original experiment. Significant sulphate reduction began after the pH increased above pH 6.5. Thus, the increase in pH in that experiment and the other batch experiments has been attributed to the action of fermentative bacteria and part of this community may have been lost or inhibited once the sulphate reducers became established, possibly due to the high sulphide concentration. If this is the case, it points toward the necessity of keeping the pre-treatment and sulphate reducing stages separate.

4.3.7 Evaluation of 8 ℓ channel reactor for pre-treatment

There are three 2000 ℓ channel reactors available at the pilot site and the laboratory data suggest that two in series should be sufficient for the sulphate reduction and sulphide oxidation, with the third being available as a pre-treatment option. To assess the potential for this, a laboratory scale unit was set up to treat a blend of real and synthetic minewater.

Within 24 hours a biofilm had started to form on the reactor surface and this biofilm became complete within four days. The biofilm appeared to consist of a number of bacterial and fungal morphologies, with mould-like fungi prominent (Figure 89). The biofilm was sticky, rather than brittle and there was no evidence of sulphur deposition or the crystallisation of salts.

Figure 89: Top view of channel reactor showing establishment of bacterial and fungal biofilm

The reactor was sampled from the middle set of sample ports (top, middle and bottom). The pH and redox potential data (Figure 90) confirmed that there was no significant vertical stratification in the reactor.

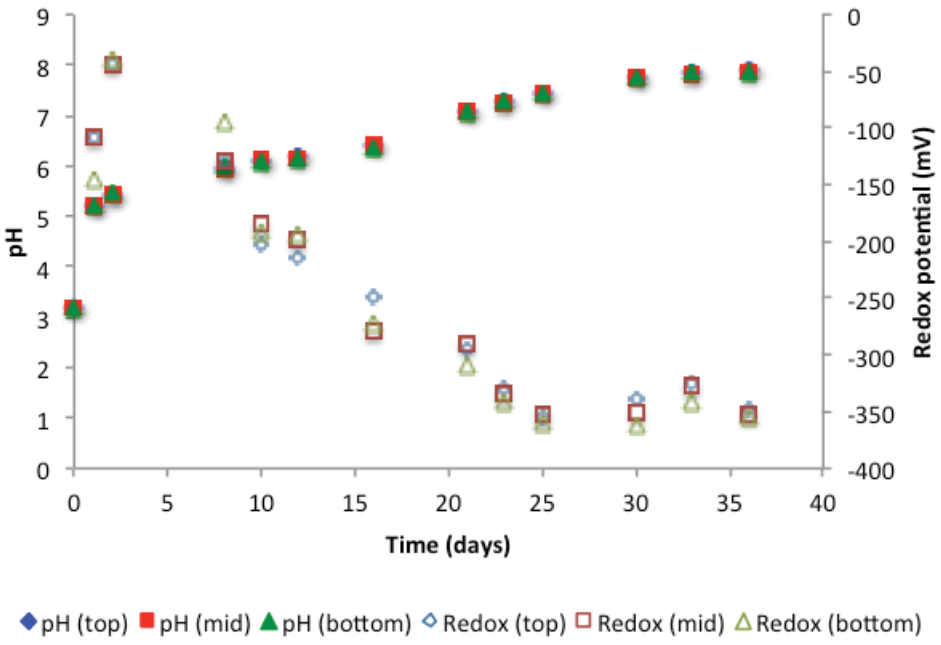

Figure 90: pH and redox potential data for the 8 ℓ channel reactor

The data are consistent with the results from the smaller batch reactors, showing a rapid increase in pH over the first 48 hours, followed by a more gradual increase thereafter, reaching values between pH 7.5 and 7.7 by day 35. The redox potential decreased steadily before stabilising around -350 mV.

There was some evidence for sulphide generation, with the bulk liquid in the reactor showing evidence of iron sulphide precipitation after day 10. The aqueous sulphide analysis (Figure 91) showed the presence of low concentrations of sulphide after day 10, primarily in the non-centrifuged sample, which confirmed the presence of sulphide precipitates. The sulphide concentration did not increase beyond those levels and the concentration in the centrifuged fraction never exceeded 5 mg/ℓ. The sulphate concentration remained stable, confirming the lack of sustained sulphate reduction.

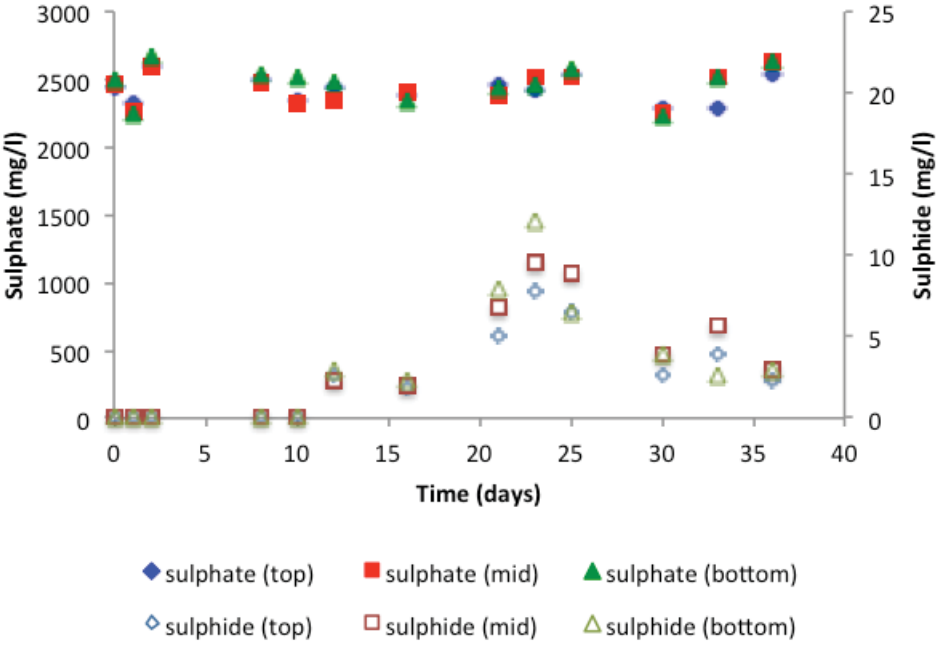

Figure 91: Sulphate and sulphide data for the 8 ℓ channel reactor

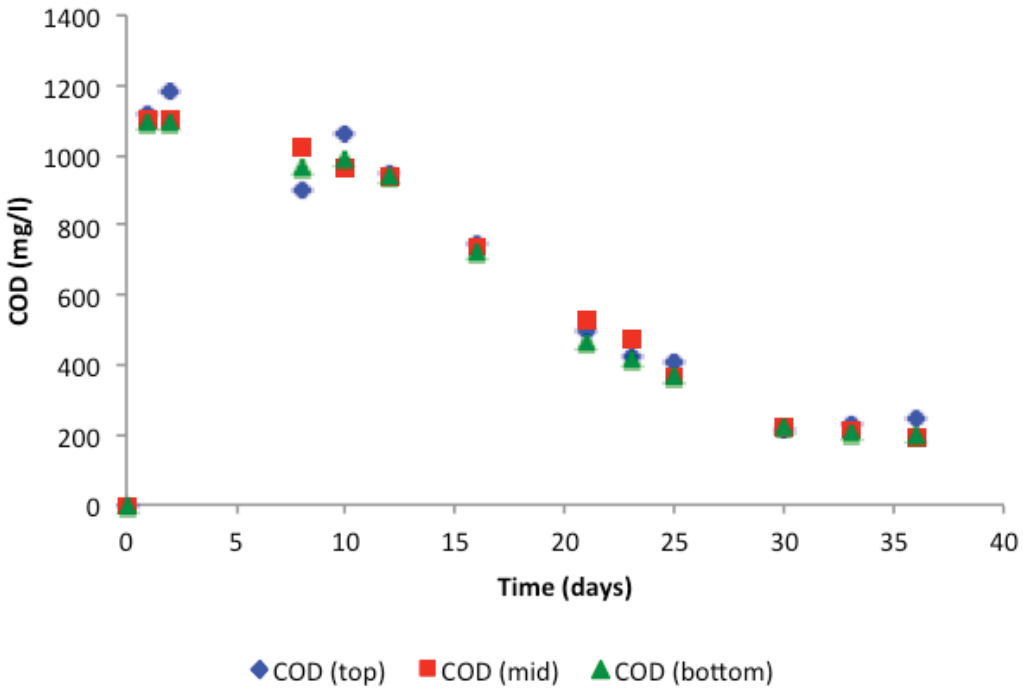

Figure 92: Soluble COD data for the 8 ℓ channel reactor

Soluble COD was measured on the centrifuged samples and this showed concentrations in excess of 1 g/ℓ over the first three days (Figure 92), after which the COD began to decline steadily, finally stabilising between 250 and 300 mg/ℓ.

4.4 CONCLUSIONS

Based on the experimental data, the following conclusions can be drawn:

- Freshly cut grass is able to modify the aqueous chemistry of synthetic acid solutions and acidic mine water samples, consuming acidity and releasing compounds which buffer the system around pH 6.
- During the first 24 hours the impact is predominantly abiotic, after which microorganisms present on the grass begin to change the aqueous environment. Significantly, the environment changes from oxidising to reducing. This occurred more rapidly at a higher pH.
- Exposing grass cutting to an acidic environment induced the release of organic material, with the magnitude and profile seemingly affected by pH. During the first 24 hours the release of VFAs was insignificant.
- The unknown compounds appeared to be metabolised under anaerobic conditions, with some VFA generation, particularly acetate.
- The inclusion of a metabolic inhibitor, sodium azide, prevented the environment from becoming reducing. The absence of microbial activity reduced, but did not eliminate the increase in pH.
- Undissociated acetic acid appeared to have a strong inhibitory effect on the microbial flora associated with the grass, which slowed down the microbial activity and largely inhibited it when the solution pH remained below pH 2.3.
- Sulphate reduction was observed in reactors where grass cuttings were contacted with partially treated mine water from the pilot site, indicating the presence of sulphate reducers on the grass or in the mine water. Complete removal of the sulphate was achieved, but over a long period of time. Sulphate reduction was strongly inhibited under acidic conditions (pH < 6), even when reactors were inoculated with active culture from a grass-fed SRB reactor.

- Exposure of mine water to grass cuttings in a pre-treatment reactor did result in neutralisation, the generation of a reducing environment and the release of soluble organic carbon. The system still requires significant optmisation.

The experiments conducted on the cellulosic feedstock have shown that grass cuttings can be effectively used to neutralise the acidity in the mine water from the pilot site and create a suitable reducing environment for subsequent sulphate reduction. In addition, complete remediation of the mine water using grass cutting as the sole carbon source has been demonstrated, but over an excessively long time.

CHAPTER 5: DEVELOPMENT AND EVALUATION OF THE HYBRID LINEAR FLOW CHANNEL REACTOR

5.1 INTRODUCTION

The application of the floating sulphur biofilm (FSB) technology for sulphide oxidation in mine water treatment was first described in the Integrated Managed Passive (IMPI) process developed by Pulles, Howard and de Lange. The process involved the use of degrading packed bed reactors (DPBRs) for biological sulphate reduction and linear flow channel reactor units downstream for partial sulphide oxidation via FSB (Molwantwa *et al*., 2010). The demonstration plant faced a number of challenges, particularly the sulphide oxidation component, which did not perform as expected (van Hille *et al*., 2011). Since then a detailed study conducted by Mooruth (2013) has led to further optimisation in design and operational parameters of the linear flow channel reactor (LFCR). The study demonstrated the feasibility of obtaining high partial oxidation rates in an LFCR through FSB formation.

Efficient bacterial sulphate reduction is dependent on maintaining a high biomass concentration and can be a challenge in flow through systems due to the relatively slow growth rate of anaerobic SRB. Therefore, biomass retention in these reactors plays a critical role in defining the treatment capacity of the system, where efficient sulphate removal can be achieved at high loading rates. Support matrices for biomass attachment within the reactor have been used to promote biomass retention, to facilitate the decoupling of the hydraulic residence time and biomass retention time (Baskaran and Nemati, 2006; Sheoran *et al*., 2010). A study by van Hille *et al*. (2015) demonstrated the potential application of carbon microfibers as support matrices for biological sulphate reduction within a closed LFCR, providing a high surface area for biomass retention without significantly reducing effective reactor volume, as many bulky packing materials do. The study achieved high sulphate reduction efficiency of 85-95%. When operated at a feed sulphate concentration of 1 g/ℓ and a dilution rate exceeding the maximum specific growth rate (0.083/h) the LFCR maintained a VSRR approximately 20% higher than that obtained in a continuously stirred tank reactor (CSTR). During the study, complete elimination of oxygen was not possible and there was evidence of partial sulphide oxidation and the establishment of a floating biofilm. This was similar to that observed in the dedicated sulphide oxidation reactor (Mooruth, 2013). This suggested that partial sulphide oxidation could be coupled with sulphate reduction within a single LFCR configuration.

This section describes the design and proof of concept evaluation of a hybrid reactor that integrates biological sulphate reduction and partial sulphide oxidation. It was hypothesised that the inclusion of carbon microfibres would facilitate the attachment and retention of a sulphate reducing microbial community within the bulk volume of the reactor, while the particular hydrodynamic properties (Mooruth and van Hille, submitted) would establish discrete anaerobic and microaerobic zones, the latter facilitated by the biofilm at the air-liquid interface, creating a suitable microenvironment for partial sulphide oxidation by sulphur oxidising bacteria.

The intention of the proof of concept study was to assess the performance of the hybrid channel reactor, in terms of sulphate reduction efficiency, sulphide removal efficiency and the potential for recovery of elemental sulphur, demonstrating that the hybrid LFCR could be evaluated at larger scale for the treatment of sulphate-rich, mining impacted water as part of a semi passive process.

5.2 MATERIALS AND METHODS

5.2.1 Microbial cultures

The sulphate reducing and sulphide oxidising communities were obtained from the stock reactors described in section 2.2

5.2.2 Hybrid linear flow channel reactor

A modified LFCR, with an operating volume of 2 ℓ, was set-up for the proof of concept evaluation of the hybrid reactor (Figure 93). It was constructed from Perspex (11 mm thickness) and had internal dimensions of 250 mm (l) x 10 mm (w) x 15 mm (h). The front facing side of the reactor was fitted with six sampling ports, allowing the bulk reactor volume to be monitored across the length and at different heights. The reactor design was based on the original 25 ℓ LFCR described by (Mooruth, 2013). The hybrid LFCR was fitted with a plastic strip (10 mm wide) holding carbon microfibers as a microbial support matrix and a heat exchanger (4 mm ID) for temperature control. A harvesting screen, made of plastic mesh fixed to an aluminium frame, was designed to lie 5 mm below the liquid surface to facilitate biofilm harvesting. Reactor feed was pumped in continuously through the uppermost inlet port on the left side of the reactor while the effluent flowed from the equivalent exit port on the right side of the reactor.

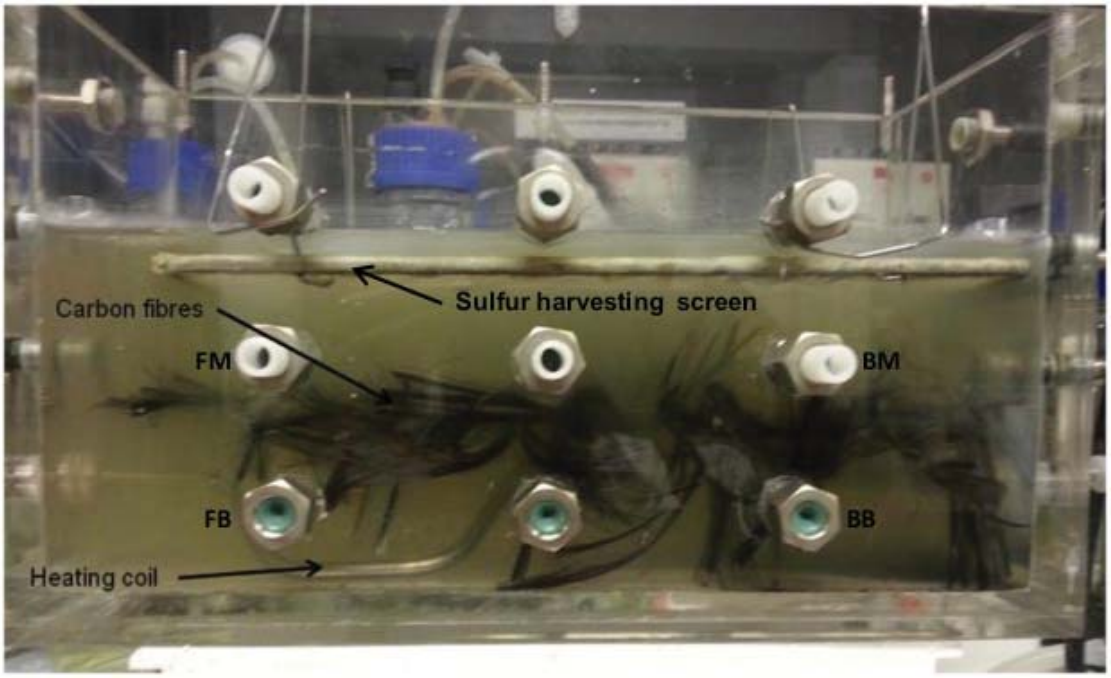

Figure 93: Photograph of the hybrid linear flow channel reactor showing the position of the heating coil, carbon fibres, sulphur harvesting screen and the location of the sampling ports (FM, FB, BM, and BB)

5.2.3 Analytical methods

The pH, redox potential, sulphate, sulphide and VFA analyses were performed as described in 2.4.

Samples of planktonic and attached SRB as well as sections of the FSB were prepared for SEM and EDX analysis as described in 2.4.9.

5.2.4 Hydrodynamic study

The LFCRs were constructed from Perspex to allow for easy visualisation of the hydrodynamic mixing patterns. A dye tracer experiment was conducted by filling up the LFCR with a sodium hydroxide (0.002 M) solution to which ten drops of phenolphthalein was added to achieve a uniform pink colour. Hydrochloric acid (0.042 M) was pumped into the reactor at a predetermined flow rate. When the neutralisation reaction occurred the liquid within the reactor turned colourless, thus demonstrating the fluid's path. The experiment was performed at ambient temperature (22.4°C) and conducted over a range of HRTs (4, 3, 2, 1, and 0.5 days). The duration of each experiment varied based on how long it took for the entire reactor fluid volume to turn colourless. This was monitored photographically at intervals throughout each experimental run.

5.2.5 Proof of concept

To test the proof of concept, a 2 ℓ LFCR was inoculated with a mixture of the SRB and SOB cultures and fed, by speed controlled peristaltic pump, with modified Postgate B medium (1 g/ℓ SO_4^{2-}) at a rate equivalent to a 4 day HRT (dilution rate: 0.104/h). The temperature was controlled at 30˚C. Samples (2 mℓ) were removed daily from the middle and lower sample ports in the first and third rows (FM, FB, BM, BB), as well as from the effluent port. The pH and sulphide concentration were measured immediately, after which the remainder of the sample was prepared for chromatographic analysis (VFAs and anions). Biofilm formation was observed visually and once a thick, stable biofilm had been formed it was periodically collapsed and harvested.

The FSB was collapsed by physically disrupting the biofilm and allowing the fragments to settle on the harvesting screen. Following disruption, the biofilm reformed to cover the entire surface of the reactor within 24 hours. The sulphur product was recovered by removing the harvesting screen and removing the accumulated biofilm. The biofilm was dried at 37°C for 48 hours, prior to weighing and elemental analysis.

5.2.6 Effect of biofilm collapse

To assess the short-term effect of biofilm removal, the reactor was operated for three residence times after which the floating sulphur biofilm (FSB) was disrupted. Once collapsed, samples were collected and analysed at hourly intervals over 24 hours. The reactor was run for an additional three residence times and upon completion the biofilm was harvested.

5.3 RESULTS AND DISCUSSION

5.3.1 Hydrodynamic study

A phenolphthalein tracer study was conducted to evaluate the fluid mixing profile in the LFCR as a function of hydraulic residence time. The mixing profile was consistent across the experiment and an example, for a 2 day HRT, is presented in Figure 94.

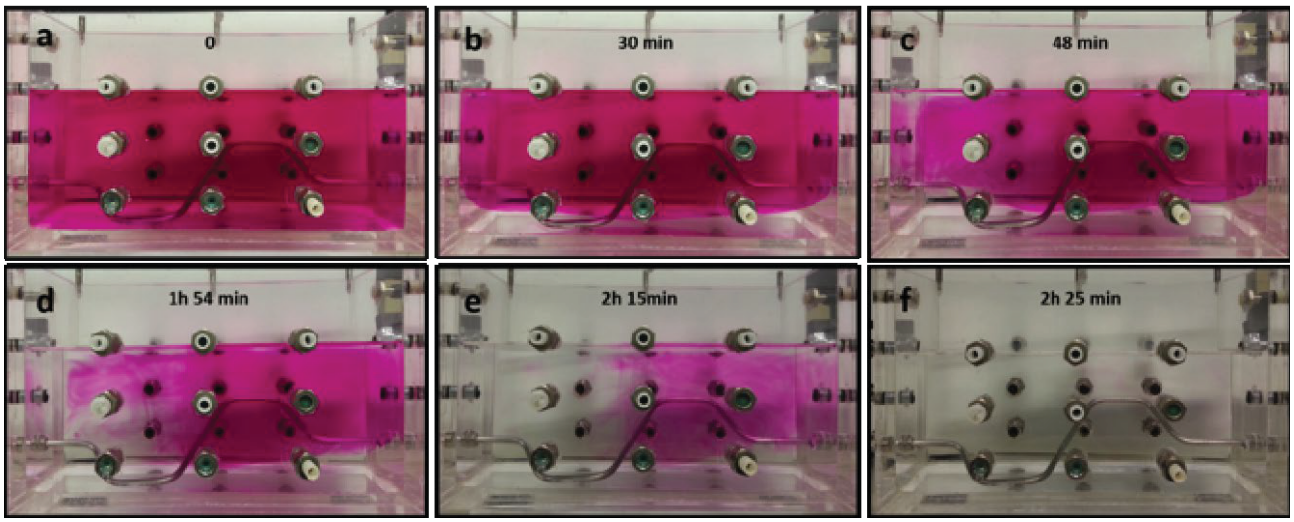

Figure 94: Photographic images showing the progression of mixing in the hybrid LFCR operated at a feed rate equivalent to a 2 day HRT

Results showed that the mixing in the LFCR was initially governed by the liquid velocity at the inlet point (advective transport), which caused some turbulent eddies in the bulk volume. The slightly denser feed then sank to the bottom of the channel. Back mixing, which occurred in the front corner of the reactor was characterised as a dead-zone. The fluid then proceeded to move forward along the floor of the reactor, with a laminar parabolic velocity profile (Figure 94b and c). After 30 minutes the feed front reached the back wall of the reactor and the fluid collided with the wall resulting in the vertical displacement of the HCl layer. Similarly, the mixing observed at the back corner resulted in a second dead-zone with movement of some of the HCl back towards the entrance. As time progressed, convection (a combination of advective and diffusive transport) transport became predominant (Figure 94d and e) at the front corner directed towards the surface and effluent port until the entire bulk volume turned colourless. This observed mixing profile in the LFCR was consistent across all HRTs tested.

The study concluded that the fluid dynamics in the LFCR is primarily governed by passive mixing through a combination of advective and diffusive transport with elements of laminar parabolic flow. This supports the conceptual fluid dynamic model previously described by Mooruth, 2013. Additionally, the study revealed that the LFCR achieved macro-mixing times that were significantly shorter than that of the overall hydraulic residence time across all scenarios tested. Results obtained from a saline tracer study revealed that the LFCR resembles a similar residence time distribution (RTD) profile to that of a CSTR, which further supports the findings that the LFCR can be considered a relatively well-mixed system.

The fluid dynamics observed in the LFCR demonstrated the suitability of the reactor design for the desired application as it facilitates complete mixing within the bulk volume of the reactor with limited turbulence at the surface, promoting ideal conditions for sulphate reduction and the formation of the floating sulphur biofilm at the air-liquid interface.

5.3.2 Proof of concept

The hybrid LFCR was inoculated with an active SRB culture with an initial sulphide concentration at approximately 230 mg/ℓ. The sulphide concentration decreased rapidly over the initial 24 hours as a result of unimpeded oxygen mass transfer across the liquid surface resulting in sulphide oxidation.

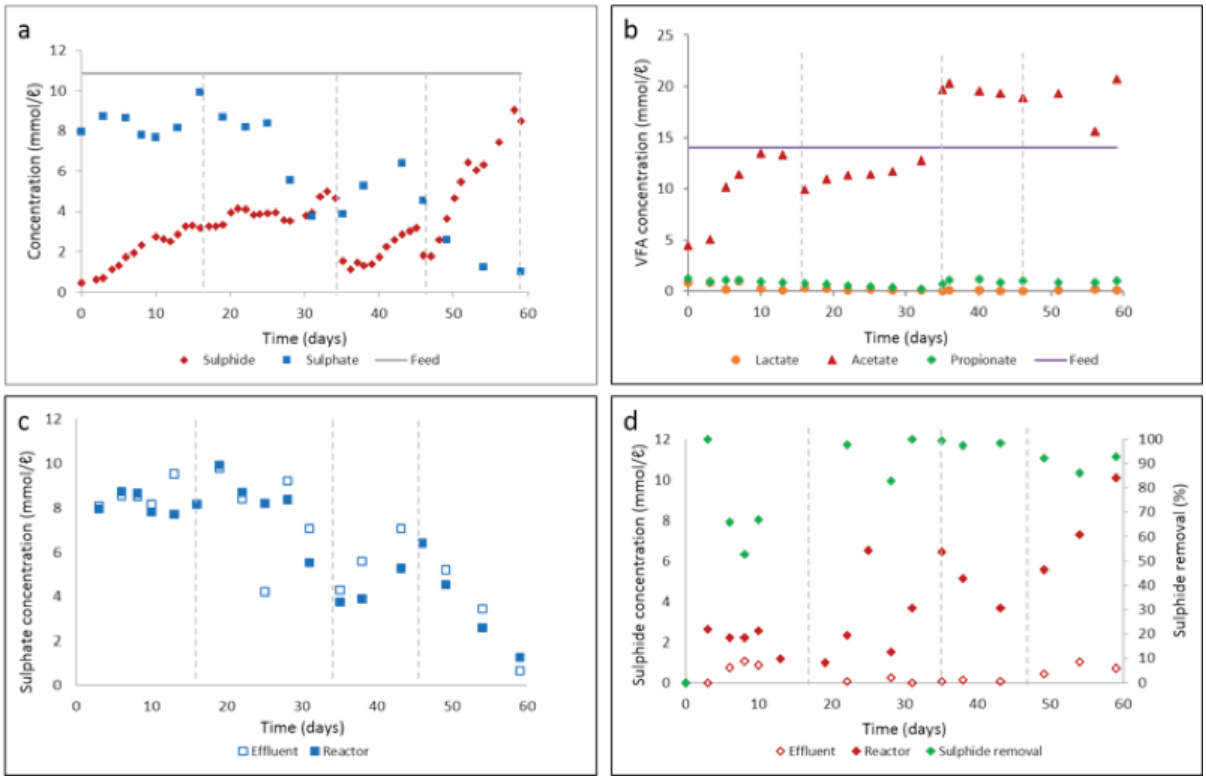

Figure 95: a) Residual sulphate and dissolved sulphide concentration profiles during the initial colonisation of the LFCR and demonstration of the integrated process, vertical dotted lines indicate biofilm disruption. b) The measured volatile fatty acid concentration and sulphate conversion c) dissolved sulphide removal d) biofilm performance and sulphur recovery efficiency

Within 24 hours a thin, but complete biofilm was observed covering the entire surface. Once the biofilm had formed the dissolved sulphide concentration in the bulk liquid began to increase steadily (Figure 95a) from around 16.5 mg/ℓ to 152 mg/ℓ by day 34. This was an indication of SRB activity, which was further confirmed by the residual sulphate data where feed sulphate concentration decreased from 1042 mg/ℓ to 373 mg/ℓ (Figure 95a and c) by day 34, corresponding to a sulphate conversion of 64%. On day 34 a controlled biofilm collapse and harvest resulted in the rapid decrease in sulphide concentration and slight increase in residual sulphate concentration. As the floating sulphur biofilm regenerated at the air-liquid interface the sulphide concentration increased to 106 mg/ℓ by day 45 after which the biofilm was collapsed. As the biofilm develops and matures it acts as a barrier, impeding oxygen mass transfer across the air-liquid interface. The inoculum acclimatised and colonised the carbon fibres, leading to an increased biomass concentration. By day 60 the residual sulphate concentration (Figure 95c) decreased to 96 mg/ℓ, reaching a VSRR and sulphate conversion of 10.56 mg/ℓ.h and 96% respectively.

The residual sulphate concentration (figure 3c) measured in the reactor and effluent was consistent throughout the study. Sulphide removal (figure 3d) was efficient, with low concentrations measured in the effluent. The average removal efficiency, between day 30 and 60, was over 90%. Thiosulphate remained below detection limits for the duration of the experiment. Together, these findings strongly suggest that partial sulphide oxidation to elemental sulphur was favoured throughout the study, with negligible complete oxidation of sulphide to sulphate in the effluent.

The LFCR maintained anoxic conditions within the bulk volume of the reactor with an average redox potential measured between -350 to -410 mV, an optimal range for sulphate reducing activity. The effluent samples were variable and exhibited increased ORP measurements. This was expected since the effluent is exposed to the aerobic zone at the surface as it flows through the exit port of the reactor. The ability of the LFCR to maintain anoxic conditions within the bulk volume, despite the surface being

open to atmosphere, was a critical factor necessary to achieve simultaneous sulphate reduction and partial sulphide oxidation.

The pH (Figure 96) increased initially in the bulk volume of the reactor (pH 7-7.5) with an additional increase observed in the effluent sample (pH 7.5-8). The initial pH increase was attributed to SRB activity as a result of alkalinity (bicarbonate) production while the additional pH increase observed in the effluent was attributed to partial sulphide oxidation, where hydroxyl ions are released as a by-product. While the experiments were conducted using neutral feed, these results confirm the generation of alkalinity and highlight the potential of the system to neutralise acid wastewater streams.

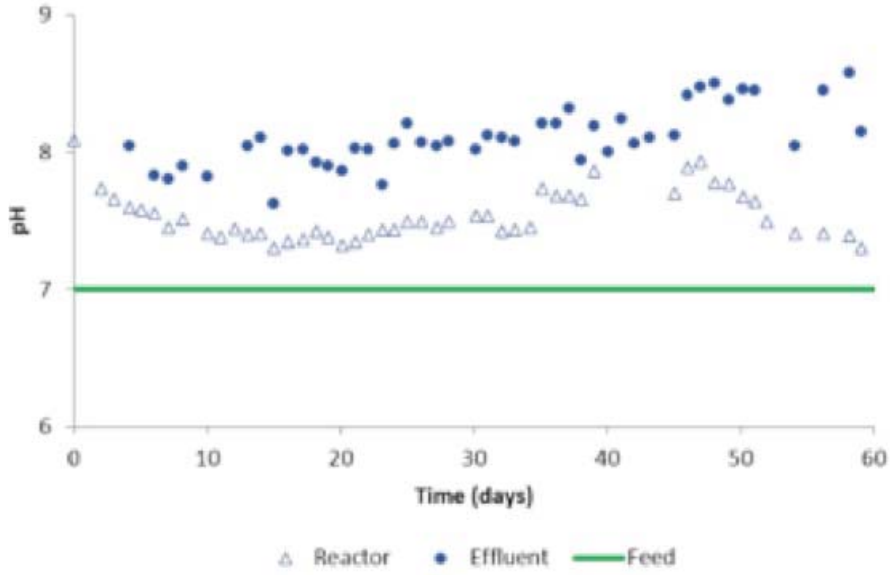

Figure 96: Graph showing pH as a function of time for the bulk reactor volume and effluent

Throughout the experiment, the residual lactate concentration was below the detection limit. Acetate was accumulated as the main by-product, while propionate concentrations were consistently low. This indicates that incomplete lactate oxidation was the dominant metabolic pathway. The low propionate concentration suggests very little fermentation occurred throughout this study. These results were consistent with previous studies that investigated the VFA concentration profile in sulphate reducing reactors fed with lactate as a carbon source (Oyekola *et al*., 2012; Bertolino *et al*., 2012). Measured acetate concentrations exceeded the theoretical values based on reaction stoichiometry (amount of lactate supplied in the feed) from day 30 (Figure 95b) and was attributed to the metabolism of yeast extract and citrate. Citrate metabolism is described in literature and acetate is a possible reaction product (Stams *et al*., 2009). Yeast extract is primarily added as a source of nitrogen, vitamins, and trace metals. However, it also contains carbon, in the form of carbohydrates (4-13 %), which can be broken down to acetate (EURASYP, 2015). The accumulation of acetate means that it is unlikely that complete lactate oxidation took place.

The performance of the hybrid reactor is summarised in Table 2. The study achieved a sulphate conversion of 96% with a corresponding VSRR of 10.56 mg/ℓ.h (0.11 mmol/ℓ.h), when operated at a 4 day HRT. These results are consistent with data obtained using the same microbial community in conventional CSTRs under similar operating conditions (Oyekola *et al*., 2012). Complete sulphide removal (95-100%) was achieved with recovery of approximately half the added sulphur as elemental sulphur by harvesting the biofilm. The fraction of sulphur that was not recovered in the biofilm was suspended in solution. This can be recovered by gravity sedimentation, which is a standard procedure used in conventional sulphur recovery treatments (i.e. Thiopaq process)(Cai *et al*., 2017).

Table 17: Summary of performance during the proof of concept study

HRT	Dilution rate	VLUR	VSRR	SO_4^{2-} conversion	HS^- removal	S recovery
Days	h^{-1}	mmol/ℓ.h	mmol/ℓ.h	%	%	%
4	0.0104	0.12	0.11	96	95-100	45[1]

[1] Sulphur recovery from the FSB between day 45 and 60

The progression of the floating sulphur biofilm development at the air/liquid interface before and after disruption is illustrated in Figure 97.

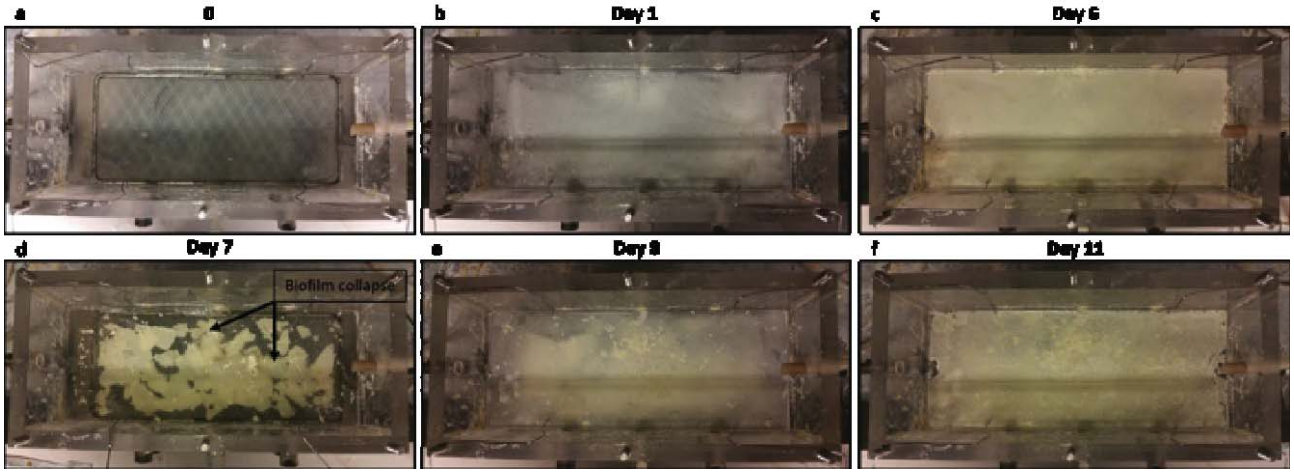

Figure 97: Photographic recording of the floating sulphur biofilm formation at the air-liquid interface over time with a biofilm disruption event occurring on day 7

After 24 hours a thin layer of biofilm covered the surface and thereafter continued to develop as the biomass and elemental sulphur content increased. The reactor configuration and operating conditions in the modified LFCR promoted the development and maintenance of two reactive zones. The conceptual model for the FSB was described by Mooruth (2013). Heterotrophic bacteria lay down an organic carbon matrix at the air-liquid interface, which supports the retention of autotrophic sulphur oxidisers. As the biofilm develops it becomes a barrier to unimpeded oxygen mass transfer, creating a microaerobic zone within the biofilm where pH and redox conditions favour partial oxidation of sulphide to sulphur. If sufficient sulphide is delivered from the bulk volume into the biofilm complete consumption of oxygen is achieved and the bulk volume remains anoxic, favouring sulphate reduction. Attachment of SRB to the carbon fibres supports biomass retention and increased sulphate reduction rates, ideally ensuring that there is sufficient aqueous sulphide in the bulk volume to consume oxygen that penetrates in the time between biofilm harvesting and the establishment of a new biofilm.

5.3.3 Effect of biofilm disruption

Most BSR systems are operated in closed reactors under anaerobic conditions due to the sensitivity of SRBs to oxygen exposure. The collapse and harvesting of the biofilm removes the barrier to oxygen mass transfer into the bulk volume, until the biofilm reforms. This could negatively affect the SRB activity, resulting in a decrease in performance or complete collapse of the system. Data from the initial demonstration (Figure 95a) showed that FSB collapse had significant implications on the sulphide concentration with a notable decrease over 24 h. A study was conducted to evaluate the effect of biofilm collapse on the performance of the integrated process. This involved hourly monitoring of the reactor performance over the 24 h period after FSB collapse.

The biofilm was disrupted on day 7. The removal of the biofilm resulted in a rapid decrease in dissolved sulphide concentration, from 148 mg/ℓ to 82.5 mg/ℓ within 12 hours, after which the concentration stabilised. A similar trend was observed in the effluent. Approximately 20 hours after collapse the aqueous sulphide concentration began to increase again, corresponding with the reforming of the biofilm. After 24 hours a distinct thin layer of biofilm was observed (Figure 97). The rapid decrease in dissolved sulphide concentration observed after biofilm collapse (Figure 98a and b) can be attributed to the increased oxygen mass transfer into the bulk liquid in the absence of the biofilm at the surface. The oxygen is rapidly consumed through the oxidation of sulphide. As the biofilm reforms and matures at the surface, oxygen mass transfer into the bulk liquid is impeded and the rate of sulphide generation exceeds the sulphide oxidation rate resulting in the observed increase in aqueous sulphide (Figure 98a). Critically, the residual sulphate concentration remained stable during this period (Figure 98b) indicating that sulphate reduction was not adversely affected during the 24 h period after biofilm collapse. It is clear that if there is sufficient residual aqueous sulphide to react with all the oxygen that crosses the surface in the absence of biofilm it is possible to maintain anoxic conditions in the bulk volume. This was confirmed by redox potential measurements.

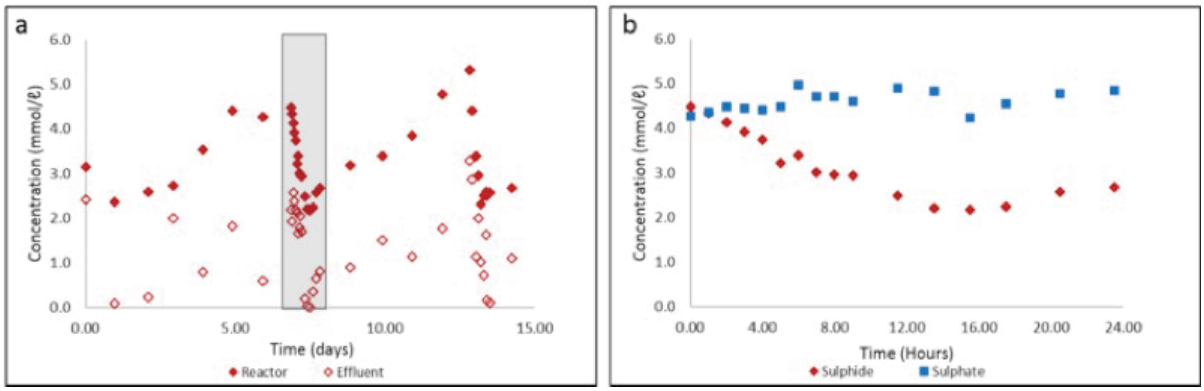

Figure 98: Effect of biofilm collapse showing a) dissolved sulphide concentration over 15 days and b) residual sulphate concentration over 24 h after FSB collapse, grey box outlines the 24 h period

The decrease in sulphide was predominantly attributed to sulphide oxidation rather than the evolution of H_2S gas. This is consistent with the data from Mooruth (2013) who assessed H_2S (g) liberation to account for mass balance discrepancies in a similar system and concluded that the liberation of H_2S (g) from the LFCR surface was negligible. This can be accounted for by the absence of turbulent mixing and the fact that most of the sulphide is present at HS^- at the operating pH. This is important from an aesthetic and safety perspective, due to the toxicity of hydrogen sulphide gas.

Sulphide oxidation, with the generation of partially oxidised sulphur species such as colloidal sulphur, thiosulphate, polysulphides, or complete oxidation to sulphate may occur abiotically or catalysed by microbes. For abiotic oxidation, the thermodynamics associated with the initial transfer of an electron for sulphide and oxygen reveal that the reaction is unfavourable as an unstable superoxide and bisulphide radical ion would need to be produced (Luther *et al*., 2011). Alternatively a two-electron transfer is favourable, with the formation of a stable S_0 and peroxide. However, the partially filled orbitals in oxygen that accept electrons prevent rapid kinetics. Due to these constraints the abiotic oxidation of sulphide is relatively slow. Alternatively, biologically mediated sulphur oxidation by photolithotrophic and chemolithotrophic microbes rely on enzymes that have evolved to overcome these kinetic constraints to allow rapid sulphide oxidation (Luther *et al*., 2011). A study by Luther and co-workers (2011), demonstrated that biologically mediated sulphide oxidation rates are three or more orders of magnitude higher than abiotic rates due to the thermodynamic and kinetic constraints. Furthermore, a study by Mooruth (2013) investigated the extent of abiotic and biotic sulphide oxidation in a LFCR similar to that used in the current study. The study revealed that abiotic sulphide oxidation played a minor role in the overall observed oxidation rate. This was based on a combination of kinetic

constraints, poor oxygen diffusion, mixing (hydrodynamics) and convective mass transport found within the LFCR. The biologically mediated oxidation of sulphide in the bulk volume following biofilm harvesting is critical. If the process relied on slower, abiotic oxidation it is likely that oxygen concentration in the bulk volume would increase to the point where sulphate reduction was inhibited.

As the biofilm reforms oxygen mass transfer into the bulk liquid is impeded and sulphide oxidation occurs exclusively within the biofilm. As the biofilm continues to mature and thicken at the surface, oxygen penetration through the biofilm slows to the point where it becomes limiting, resulting in significantly reduced partial sulphide oxidation activity and an increase in dissolved sulphide concentration in the effluent, which is undesirable. Therefore, there is a need to optimise the FSB harvesting frequency to ensure maximum sulphur recovery and consistent sulphide removal.

5.3.4 SEM and EDS

The anaerobic and aerobic zones within the reactor promoted the development of two separate microbial communities. Examples of the different cell morphologies, visualised by SEM, are shown in Figure 99. These images confirmed biomass attachment and colonisation of the carbon microfibres. Previous studies have reported on the enhanced VSRR that can be achieved through increased biomass retention within a LFCR fitted with carbon microfibres as support matrix (van Hille *et al*., 2015).

Additionally, SEM-EDS analysis (Figure 100) of the FSB confirmed partial sulphide oxidation, with the presence of highly concentrated elemental sulphur deposits detected. Sulphur deposits were also observed on the outer membranes of the sulphur oxidising bacteria (Figure 99a). This mechanism of sulphur excretion in SOBs has been previously documented (Cai *et al*., 2017).

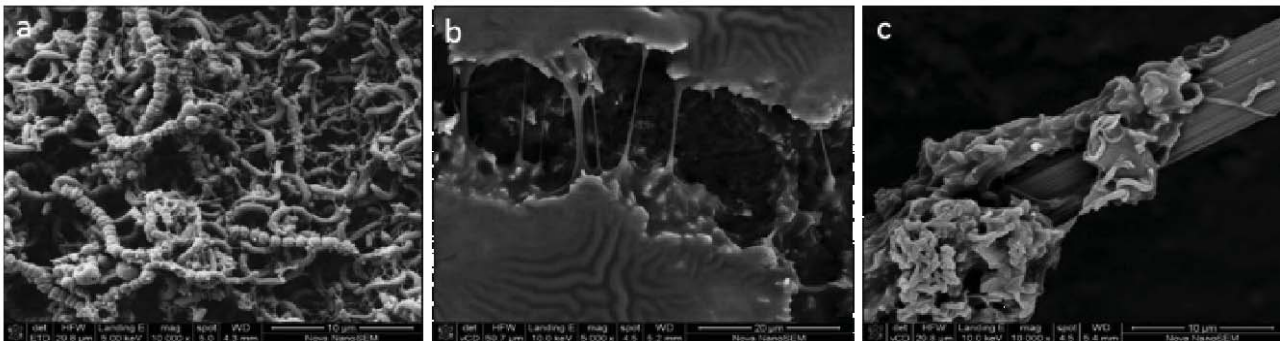

Figure 99: SEM images of the a) floating sulphur biofilm microbial community, b) pores within the biofilm structure and c) biofilm attached on a carbon fibre

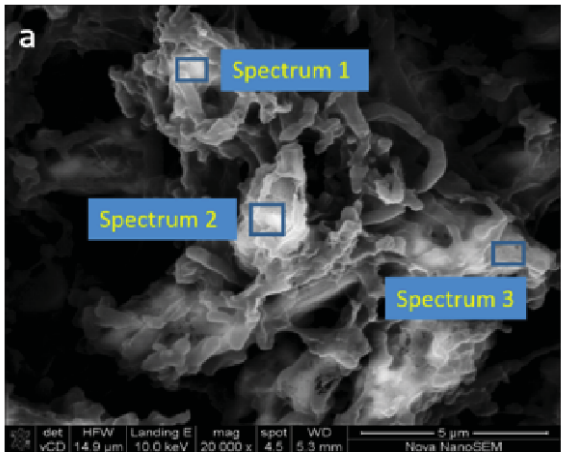

Spectrum	In stats.	C	O	S	Total
Spectrum 1	Yes	0	0	100	100
Spectrum 2	Yes	0	0	100	100
Spectrum 3	Yes	0	0	100	100

*All elements analysed (normalised)

Figure 100: SEM image with EDS analysis of selected regions, illustrating the presence of elemental sulphur

5.3.5 Development of conceptual model

The data presented in this chapter show that it is possible to achieve efficient biological sulphate reduction and partial oxidation of sulphide to sulphur in a single reactor that is open to the atmosphere. A conceptual model for how this is achieved is presented below and summarised in Figure 101.

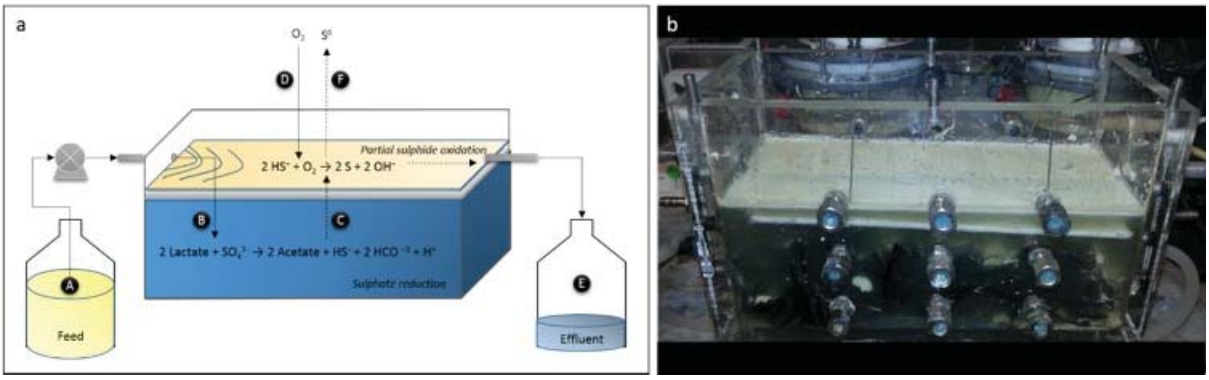

Figure 101: a) Conceptual model of the integrated semi-passive bioprocess b) colonised LFCR with a floating sulphur biofilm at the surface

Feed solution (A), containing sulphate and sufficient organic carbon to sustain sulphate reduction and the heterotrophic component of the biofilm is pumped into the reactor. Biological sulphate reduction occurs within the anaerobic bulk volume of the reactor (B). Microbial attachment and subsequent colonisation of the carbon fibres facilitates biomass retention and an increased sulphate reduction rate. The absence of turbulent mixing ensures limited loss of gaseous hydrogen sulphide, ensuring good odour control, while the fluid flow pattern ensures delivery of sulphide to the biofilm. The floating biofilm is formed, initially by heterotrophic species that produce an extracellular carbon matrix at the air-liquid interface. Autotrophic sulphur oxidisers colonise the biofilm. The biofilm results in an oxygen concentration gradient, creating a zone where the pH and redox environment favours microbially catalysed partial oxidation of sulphide to elemental sulphur. As the biofilm thickness and sulphur deposition increases, oxygen mass transfer is impeded to the point where the sulphide oxidation rate becomes slower than the sulphide generation rate and the sulphide concentration in the effluent increases. At this point, biofilm collapse or harvesting is necessary. Collapsing the biofilm removes the barrier to oxygen mass transfer so oxygen from the atmosphere (D) diffuses into the bulk volume, where it is used by planktonic SOB to oxidise sulphide within the bulk volume. This leads to a rapid decrease in sulphide concentration, but critically ensures that the bulk remains anoxic and sulphate reduction is not inhibited. The biofilm begins to reform almost immediately and within 24 hours oxygen

mass transfer is reduced to the point where the aqueous sulphide concentration increases again. Treated effluent flows from the reactor (E) out of a port at the liquid surface and is characterised by low residual sulphate and sulphide. The biofilm is recovered by removing the harvesting screen (F) that lies just below the air-liquid interface.

5.3.6 Analytical inconsistencies and the role of yeast extract

The data presented in Figure 95b show that from around day 35 the molar concentration of acetate in the reactor is higher than the molar concentration of lactate in the feed. The phenomenon was widely observed in subsequent experiments where lactate was used as the electron donor and suggested that the yeast extract was being metabolised, with acetate as one of the resulting products. To assess this, samples of feed before and after the addition of yeast extract were analysed by HPLC (Figure 102).

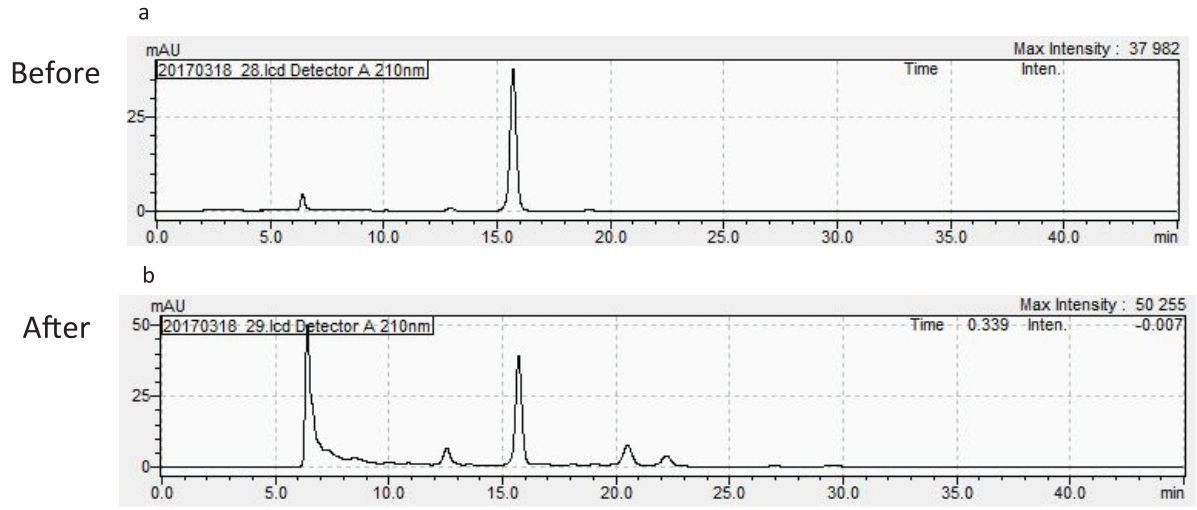

Figure 102: HPLC chromatograms showing VFA profile of acetate-based feed before (a) and after (b) yeast extract addition

Prior to the addition of yeast extract a single large peak, representing acetate was observed. A small peak at 6.4 minutes could also be seen that did not correspond to any of the VFA standards. The addition of yeast extract did not affect the acetate concentration, but did introduce small amounts of lactate (12.5 minutes), butyrate and iso-butyrate. Most notable, however, was the very large increase in the magnitude of the peak at 6.4 minutes. A similar peak was observed in the chromatograms for the acid-treated grass (Figure 77), which persisted for the duration of that experiment, suggesting the compound was not metabolised by microbial community. Attempts to identify the compound using LC-MS were not successful.

To assess the possible metabolism of yeast extract a number of 500 mℓ batch reactors were set up, using modified Postgate medium, with no VFA added and inoculated with 2 mℓ of SRB stock culture, maintained on acetate-based media. The cultures were incubated at room temperature and sampled periodically.

Within 48 hours the culture became murky, suggesting substantial microbial growth, which was confirmed by light microscopy. An HPLC analysis of a sample withdrawn after 6 days of incubation showed a substantial reduction in the area of the unknown peak, an increase in the concentrations of butyrate and iso-butyrate and the appearance of peaks corresponding to acetate and propionate (Figure 103). This confirmed that the metabolism of yeast extract could account for the additional acetate observed in the proof of concept experiment, particularly if the butyrate and iso-butyrate were further metabolised to acetate.

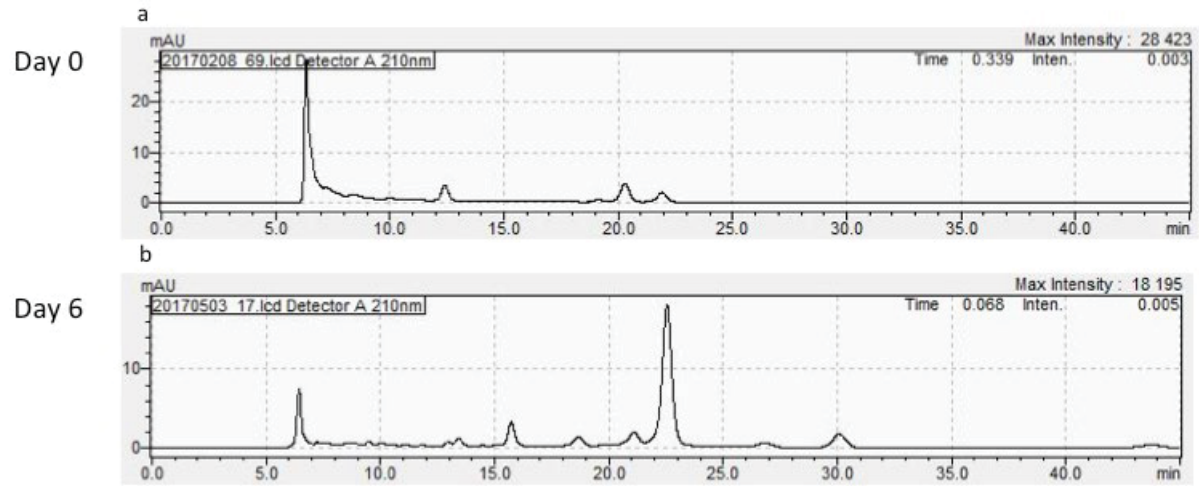

Figure 103: HPLC chromatograms showing the metabolism of yeast extract

The second interesting observation is that the area of the unknown peak decreased substantially, while the compound persisted, with no apparent metabolism, in the earlier grass hydrolysis experiments. This suggests that the compound is metabolised by community members present in the SRB consortium, but not in fermentative/hydrolytic community. However, despite the clear evidence of microbial growth and metabolism of the unknown compound there was no evidence of sulphate reduction or sulphide formation, suggesting that the metabolism is performed by a non-SRB member of the community.

5.4 CONCLUSIONS

The data presented in this chapter show the successful integration of sulphate reduction and partial sulphide oxidation within a single LFCR unit, achieving high volumetric sulphate reduction rates and sulphide removal efficiencies, with elemental sulphur recovery. The reactor was operated as an open system, but despite this, evolution of hydrogen sulphide gas was insignificant. The biofilm is an excellent odour control barrier. Technically, the hybrid reactor has the potential to be incorporated as part of an integrated semi-passive system to treat mining impacted water with high sulphate concentrations.

The reactor was able to maintain sulphate reduction rates equivalent to those achieved in active, stirred tank reactors using a simple reactor geometry and no energy input.

The successful demonstration of the proof of concept opens the way for additional research to evaluate the potential of the reactor from a performance perspective.

The sulphate reducing and floating sulphur biofilm communities are complex, but most likely depend on the presence of a smaller subset of species for structural and functional integrity. A microbial ecology study to identify these key species will significantly aid the understanding of structure-function relationships.

CHAPTER 6: EFFECT OF HYDRAULIC RESIDENCE TIME AND TEMPERATURE ON HYBRID LFCR PERFORMANCE

6.1 INTRODUCTION

The previous chapter described the successful demonstration of the proof of concept of the hybrid LFCR, showing that simultaneous sulphate reduction and partial sulphide oxidation could be achieved in a single, open reactor. The sulphate reduction rate achieved at a four-day hydraulic residence time was similar to that previously shown in continuously stirred tank reactors, despite the lack of active mixing. The floating sulphur biofilm could be harvested to recover the sulphur product by removing the harvesting screen from the reactor.

The next step in the development of the integrated system was to evaluate the effect of hydraulic residence time and temperature on performance and to assess the potential for scale up.

6.2 MATERIALS AND METHODS

6.2.1 Microbial cultures

The sulphate reducing and sulphide oxidising cultures used in this study have been described in section 2.2.

6.2.2 Reactor units

6.2.2.1 Original linear flow channel reactor

The original design of the hybrid LFCR has been described in detail in section 5.2.2.

6.2.2.2 New linear flow channel reactor

The ultimate intention of the research is to evaluate the system at pilot scale, with a 1000-fold increase in reactor volume. Initially, the dimensions of the pilot scale LFCR were based on scaling up the original hybrid LFCR. However, following the decision to construct the pilot scale LFCRs out of a transparent material and the constraints this imposed, it was decided to construct slightly larger laboratory scale reactors with relative dimensions similar to the pilot scale units. The reactors were constructed from Plexiglass (10 mm), with internal dimensions of 450 mm (l) x 200 mm (w) x 150 mm (h). Operating at liquid height of 100 mm the working volume would be approximately 8 ℓ. The location of the sample ports are shown in Figure 104.

The left and right side walls each contained three tapped (1/8" BSP) holes (Figure 105). The uppermost holes were used as the feed and effluent ports, while the middle and lower holes were used as attachment points for rod supporting the carbon fibres and the inlet and outlet points for the heat exchanger respectively.

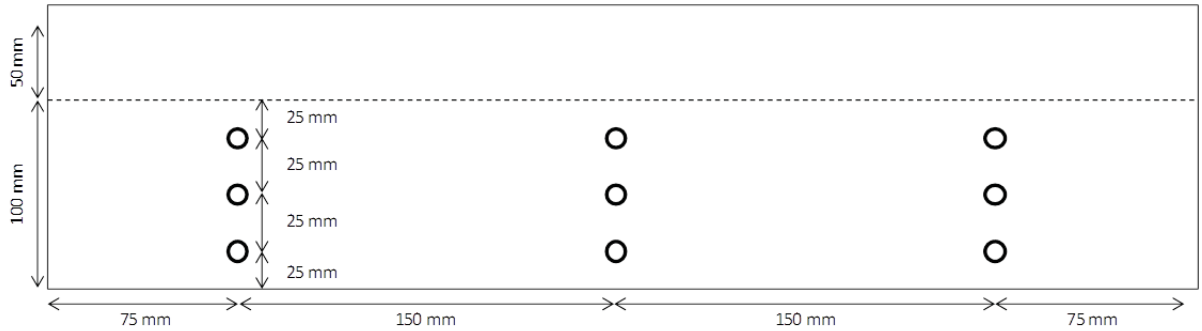

Figure 104: Schematic diagram of the new LFCR showing positions of the sample ports in the front wall.

The sulphur harvesting screen was help in position, just below the liquid level, using wire hooks (Figure 106).

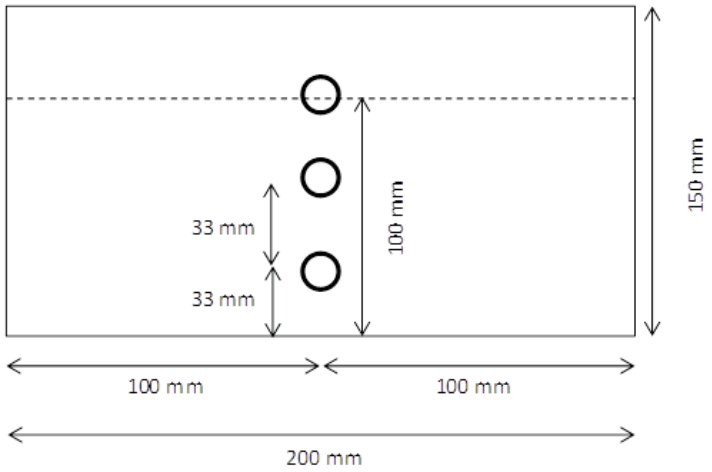

Figure 105: Schematic representation of the left and right side walls of the new LFCR showing location of feed/effluent port as well as the positioning of the carbon fibre support rod and heat exchange pipe.

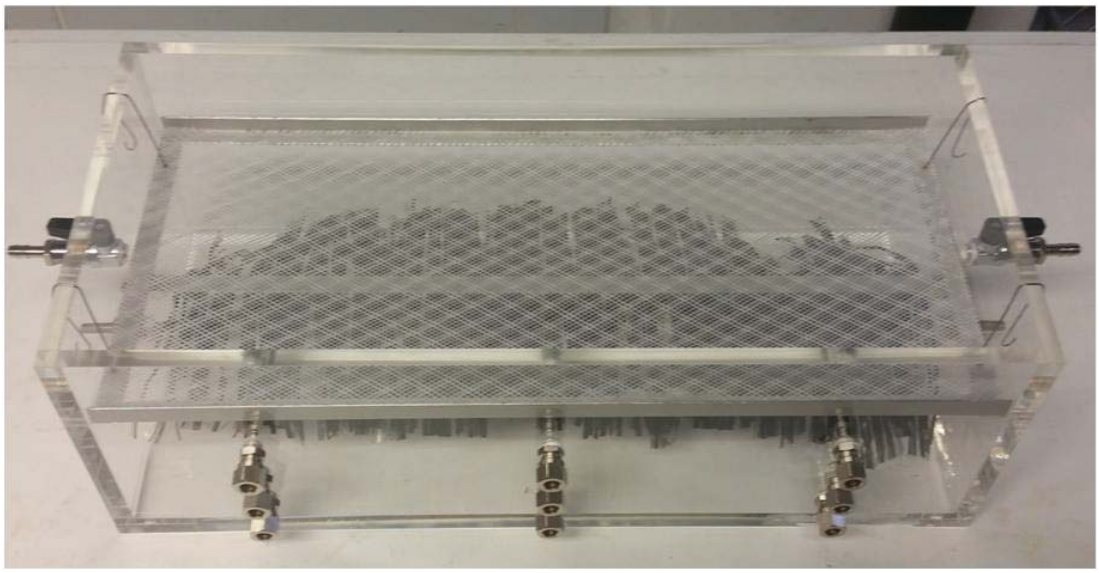

Figure 106: Photograph of the new LFCR prior to inoculation

6.2.2.3 Pilot scale reactor units

The initial intention for the pilot scale reactor was to modify pre-existing concrete channels located at an abandoned wastewater treatment plant on the mine site. However, for a number of reasons, including accessibility and safety concerns, it was decided to construct new reactors that would be housed in a barn on the mine site. The design and construction of the pilot scale reactors are described below.

Channel dimensions

The pilot scale channel reactors were constructed of Plexiglass (15 mm thickness). The maximum dimensions of standard Plexiglass sheets is 3 050 mm x 2 050 mm, which constrained the length of the channel to an internal length of 3 000 mm. Longer sheeting required specialised fabrication, which would significantly increase the cost. To maintain the desired volume of 2 025 ℓ, at a working depth on 500 mm, the width needed to be increased from 1 230 mm in the original design to 1 350 mm. A schematic diagram showing the overall dimensions is presented in Figure 107.

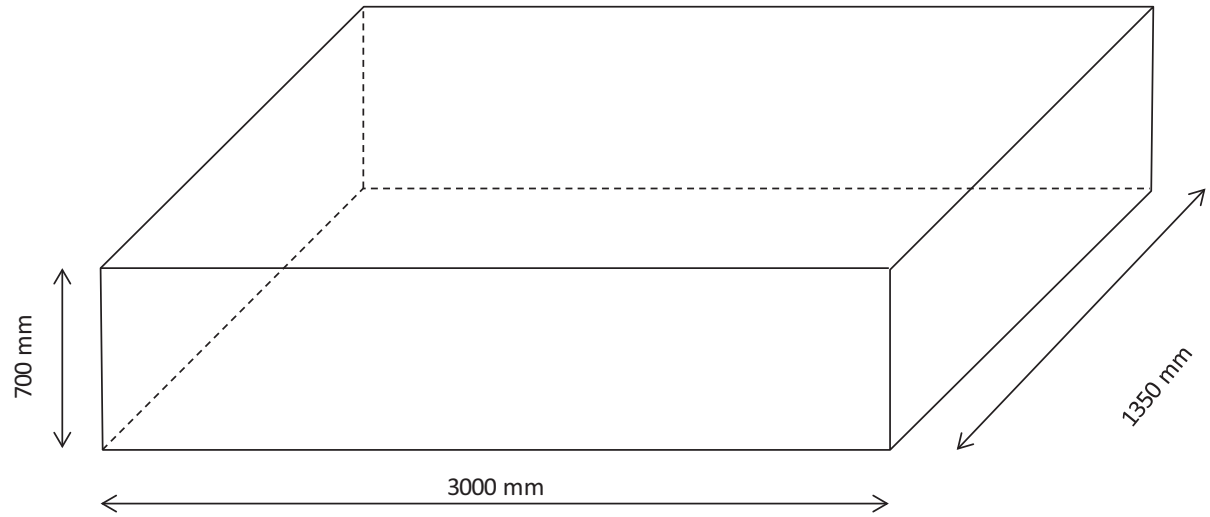

Figure 107: Overall dimensions of the channel reactor. Measurements reflect internal values

The advantages of constructing the reactors from Plexiglass include that the reactor internals (carbon fibres and harvesting screen) will be clearly visible and it will be possible to include sampling ports similar to those in the laboratory scale reactor. The front wall of the reactor was fitted with 15 potential sampling points (Figure 108).

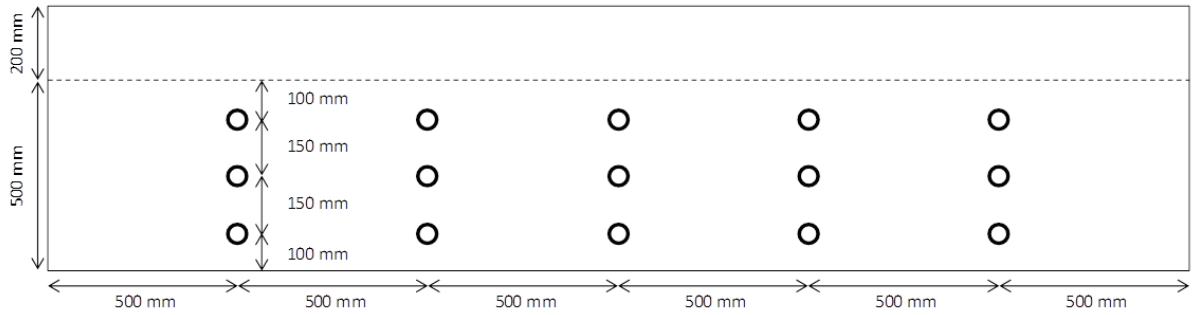

Figure 108: Schematic representation of the front wall of the pilot scale reactor showing the location of sample ports

The left and right side walls contained a single port (30 mm diameter) for fresh feed and effluent outflow (Figure 109).

The reactor contained three parallel beams, manufactured from two pieces of aluminium angle between which the carbon fibres were held. The fibres extended approximately 200 mm from each side of the beam. The beams rested on a 10 mm wide Plexiglass ledge fixed on the inside of the left and right walls at a height of 240 mm above the base. The sulphur harvesting screen was constructed of aluminium square tubing which created a frame that held the same plastic mesh as shown in the laboratory scale reactor (Figure 106).

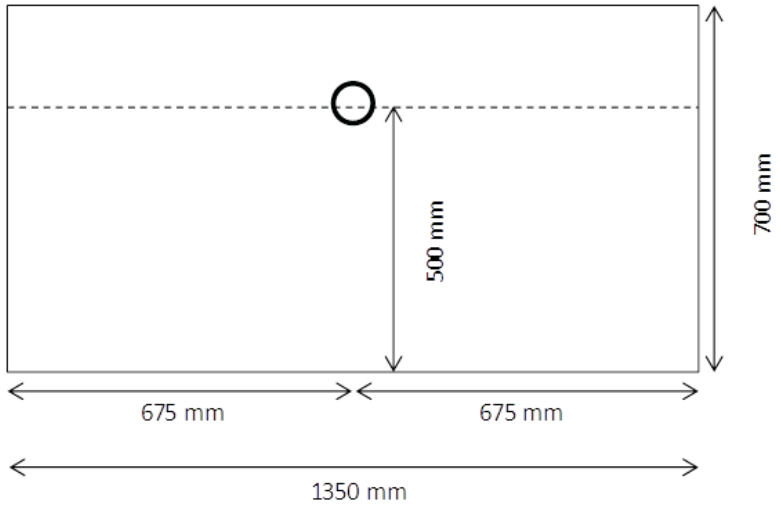

Figure 109: Schematic representation of the left and right walls of the reactor showing the location of the feed/effluent port

The constructed pilot scale LFCR, fitted with the carbon fibre beams and harvesting screen and loaded into the support stand at the pilot site is shown in Figure 110. Each of the three reactors is supported by a custom designed and constructed stand to provide additional structural support when the reactors are filled. The stand height varies from 120 to 60 cm, to the base of the reactor, to support gravity flow between the reactors connected in series.

Figure 110: Image illustrating the pilot scale LFCR reactor on site, prior to inoculation

6.2.3 Analytical methods

The analytical methods used during this phase of the research have been described in section 2.4.

6.2.4 Hydrodynamic study on new reactor

The new LFCR design was both longer and wider that the original. The hydrodynamic flow in the original LFCR had been characterised using a visual tracer and the macromixing time determined. It was important to perform a similar study on the new reactor to assess any changes in fluid flow or macromixing time. The fluid flow in the reactor was characterised using a visual tracer method to determine the flow pattern and macro-mixing time for each of the HRTs tested (4, 3, 2, 1 and 0.5 d). The reactor was filled with a dilute (0.002 M) sodium hydroxide solution and 10 drops of phenolphthalein indicator were added and mixed to produce a uniform pink colour. Hydrochloric acid (0.042 M) was pumped in at the relevant flow rates and the pattern of discoloration recorded photographically. The macro-mixing time was determined when the last of the pink colour disappeared, indicating neutralisation of the alkalinity. Experiments to assess the impact of HRT were performed at ambient temperature (22.4 ± 1°C), in triplicate.

A second series of hydrodynamic tests were performed to assess the effect of temperature (10-40˚C) on the mixing regime and macromixing time.

6.2.5 Effect of hydraulic residence time on performance

The initial proof of concept was demonstrated at a hydraulic residence time of 4 days, so the next step was to assess the performance of the hybrid LFCR at reduced HRTs to compare with more traditional reactor configurations. The reactor was initially operated at a 4 day HRT, on the modified Postgate B medium with a feed sulphate concentration of 1 g/ℓ, until the residual sulphate concentration across the reactor was reduced to below 100 mg/ℓ. The FSB was then disrupted and harvested and the feed rate increased to achieve an HRT of 3 days. Samples were withdrawn on a daily basis and analysed using the standard suite of analyses. After three residence times the FSB was disrupted, with complete harvesting after a further three residence times. The feed rate was then increased again to achieve a 2 day HRT and the cycle repeated. This was done twice more to collect data at residence times of one day and 12 hours.

6.2.6 Effect of temperature on reactor performance

The original intention was to assess the performance of the system across a temperature range from 35˚C down to 10˚C, across both the 2 ℓ and 8 ℓ reactor configurations and on the lactate and acetate based feeds.

At the start of the experiment there were three continuously fed reactors in operation, one 2 ℓ on each of the growth media and an 8 ℓ reactor on the lactate based feed. The reactors were maintained at a constant temperature of 30˚C. Before the temperature study was initiated the HRT of each of the reactors was reduced to 2 days and an effective steady state established, based on the sulphate reduction performance. At this point the temperature of the water bath was increased to raise the temperature in the reactors to 35˚C.

The performance of the reactors was monitored by daily sampling from four of the sample points along the side of the reactor (FM, FB, BM and BB) and the effluent. Samples were analysed by measuring the pH, aqueous sulphide and sulphate concentrations.

The experimental design required the establishment of steady state conditions and 35˚C. Once steady state had been achieved the reactors would be operated for three HRTs, at which point the biofilm would be disrupted, but not harvested. The biofilm would be allowed to reform and after an additional three HRTs the film would be collapsed again, but this time the biofilm would be harvested and analysed to determine the sulphur content. At this point the temperature would be reduced by 5˚C and the process repeated, with the experiment finishing following the collection of data at 10˚C.

However, the increase in temperature appeared to induce substantial changes in the structure and composition of the biofilm, which had a significant negative effect on the overall performance of the system. The structure and appearance of the biofilm changed significantly, with the sulphur content of the biofilm decreasing, particularly as the biofilm matured. These will be discussed at the end of the chapter. A number of interventions, including reducing the magnesium and yeast extract in the feed and trying to manage the evaporation rate were tried, but ultimately the decision was taken to restart the experiment at 30˚C and omit the 35˚C operating temperature.

Prior to restarting the study all reactors were adapted to function at a 2 day HRT at 30˚C. The 2 day HRT was chosen based on optimum performance in the preceding residence time study. Once “steady state”, based on stable sulphate reduction, was achieved the reactors were run for 6 HRTs, after which the biofilm was physically disrupted and allowed to reform. After an additional 6 HRTs the biofilm was harvested by removing the mesh plate. Harvested biofilm was dried at 50˚C for 48 hours, weighed and analysed to determine sulphur content (elemental analysis). Selected biofilm samples were acid digested for more complete elemental analysis.

Each reactor was sampled at least once per HRT to determine pH, sulphate and sulphide. Selected samples were prepared for VFA analysis by HPLC.

After 12 HRTs at 30˚C the temperature in the reactors was reduced by 5˚C by adjusting the temperature of the water bath pumping water through the heat exchanger. The same 24 day (12 HRT) regime was followed at 25˚C after which the temperature was again reduced. This was repeated at 20˚C, 15˚C and finally 10˚C.

6.2.7 Assessing the impact of yeast extract

The modified Postgate B medium contains 1 g/ℓ yeast extract. The yeast extract is a necessary requirement in the presence of an “incomplete” substrate, such as oxamate, but only provides moderate stimulation in the presence of a “complete” substrate, such as lactate (Postgate, 1979). On this basis, the relatively high concentration of yeast extract in Postgate B medium is surprising. The selection of Postgate B medium is historical and the particular culture has been maintained on it for over 15 years.

To assess whether the yeast extract could account for the discrepancies in the carbon balance, a number of analyses and experiments were performed. The first was HPLC analysis of the lactate and acetate-based media before and after the yeast extract addition, as well as the complete media before and after autoclaving.

To assess whether the yeast extract could be used as the sole carbon source and electron donor for sulphate reduction or other microbial species within the consortium reactors (1 ℓ batch) were prepared that contained the 800 mℓ of basal salts, sulphate (1 g/ℓ) and yeast extract (1 g/ℓ) in the absence of lactate or acetate. The reactors were inoculated with 200 mℓ of active culture from either the lactate or acetate SRB stock reactors. The reactors were maintained at 23˚C and sampled daily to determine pH, redox potential, sulphate and sulphide concentration.

In addition, a series of 1 ℓ reactors were set up to assess the performance of the sulphate reducing consortia on standard media (lactate and acetate-based) with lower levels (50% and 10%) of yeast

extract. A 20% inoculum of active culture was used in each case. The reactors were maintained at 23˚C and sampled as described above.

6.2.8 Inoculum scale-up and pilot plant inoculation

While the focus of this study was on developing the fundamental understanding of the system the ultimate goal was to assess the potential at larger scale, so the initial inoculation of the 2000 ℓ reactor is described in this report. The microbial inoculum, containing the sulphate reducing and sulphide oxidising consortia, was scaled-up in order to inoculate the 2 000 ℓ pilot scale reactors. Inoculum build-up was started at laboratory scale in a series of 10 and 15 ℓ glass containers, maintained in batch mode on an acetate based medium with an initial sulphate concentration of 3 500 mg/ℓ. The sulphide concentration was monitored regularly as a measure of SRB activity. The final analysis prior to shipping revealed sulphide concentrations between 680 and 1 170 mg/ℓ. Stock cultures from these reactors were blended into four 25 ℓ plastic drums, such that each drum had a sulphide concentration of approximately 400 mg/ℓ. These drums were transported to the mine site.

Subsequent analysis at the pilot site on 24 September 2015, approximately one month after they were packed at UCT, revealed additional activity in two of the four drums. The sulphide concentration in these drums increased to 790 and 1 012 mg/ℓ respectively, while the remaining two remained near 400 mg/ℓ. Three of the 25 ℓ drums were used to inoculate two 210 ℓ drums containing raw mine water. The first drum (Inoc 1) was inoculated from 25 ℓ drums 1 and 4, while the second (Inoc 2) was inoculated with 25 ℓ from drum 2. The sulphate concentration of the minewater was not known. Each 210 ℓ drum was supplemented with 500 g of sodium acetate and 100 g of yeast extract.

The contents of the 210 ℓ drums was analysed again on 2 November 2015. The pH in Inoc 1 and 2 were pH 7.71 and pH 8.12 respectively. The first drum contained an aqueous sulphide concentration of 735 mg/ℓ and a residual sulphate concentration of 16 mg/ℓ. The second drum was less active, with a sulphide concentration of 340 mg/ℓ and a residual sulphate concentration of 1 670 mg/ℓ.

The first of the 2 000 ℓ channel reactors was filled with raw minewater, with a sulphate concentration just over 4 000 mg/ℓ. This was higher than desired, so about half the volume was pumped out and replaced with tap water. The reactor was inoculated from the two 210 ℓ inoculum drums on 3 November 2015 and initial measurements were taken from nine of the sampling points. About 190 ℓ could be pumped from each inoculum drum, which was then filled with fresh minewater and supplemented with sodium and ammonium acetate and yeast extract.

6.3 RESULTS AND DISCUSSION

6.3.1 Hydrodynamic study in new LFCR

The hydrodynamic profile, based on the visual tracer studies, observed for the new LFCR was very similar to that of the original reactor, despite the differences in the aspect ratio. Once again, the flow pattern was characterised by very limited turbulent mixing, with vertical stratification based on minor density differences observed (Figure 111).

The additional length and width of the reactor did result in more diffusive mixing. In the smaller reactor the acid front (zone of clearing) reached the far end of the reactor well before significant decolouration was observed in the upper portion of the reactor near the feed port. This was not the case in the larger reactor (Figure 111b). The flow pattern was consistent across repeat experiments performed at the different hydraulic residence times.

Critically, the changes to the reactor configuration did not have a significant effect on the macromixing times. These remained substantially smaller than the overall HRT, so the reactor contents could be considered well mixed and performance data across the different reactor configurations can be compared going forward. The macromixing times for the different HRTs across the two reactor configurations are compared in Table 18.

The effect of temperature on the flow pattern and macromixing time within the 8 ℓ channel was evaluated at a constant feed rate equivalent to that of a two day HRT. The temperature of the bulk liquid was adjusted using the heat exchanger filled with either heated or cooled water. Temperature had a profound effect on the macromixing time, but not in the expected way.

Table 18: Macromixing times as a function of HRT for the original and new LFCR. Values represent the mean and standard deviation of three replicates

	Original LFCR (2 ℓ)				
	0.5 day HRT	1 day HRT	2 day HRT	3 day HRT	4 day HRT
Mean ± SD (min)	67 ± 3	90 ± 5	146 ± 5	228 ± 18	283 ± 15
	New LFCR (8 ℓ)				
Mean ± SD (min)	0.5 day HRT	1 day HRT	2 day HRT	3 day HRT	4 day HRT
	73 ± 3	107 ± 3	148 ± 3	213 ± 16	307 ± 21

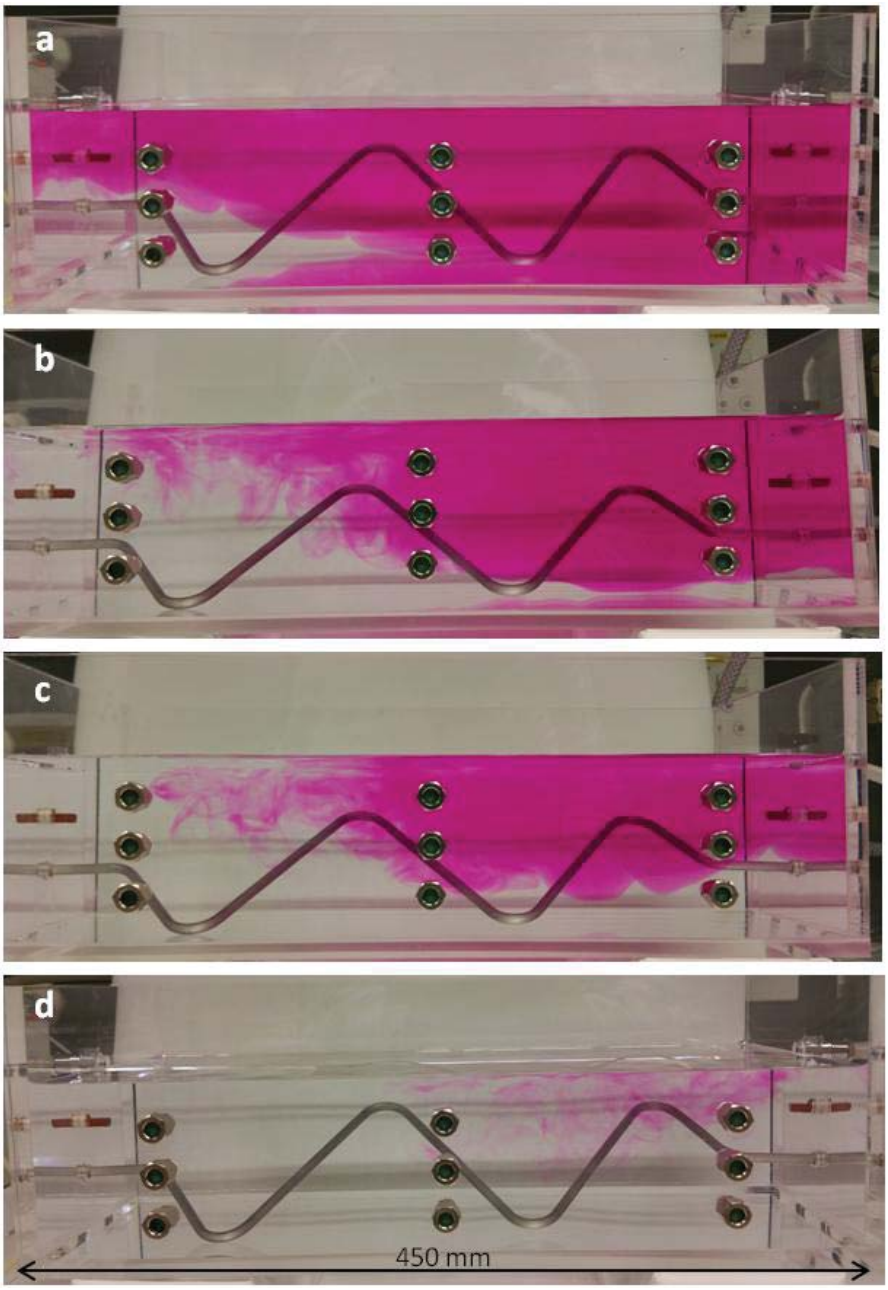

Figure 111: Images from hydrodynamic tracer study conducted at a 2 day hydraulic residence time at ambient temperature. Photographs taken at a) 54 min, b) 70 min, c) 85 min and d) 98 min

The macromixing time data are summarised in Figure 112 and show that the mixing times observed at 20˚C were similar to the ambient temperature runs at the two day HRT described above. As expected, the macromixing times increased as the temperature decreased, accounted for by slower rates of diffusion. Unexpectedly, a similar trend was observed at the higher temperatures, with incrementally longer mixing times recorded at 30, 36 and 40˚C.

Selected images showing the mixing patterns for the study at 10˚C (Figure 113) and 40˚C (Figure 114) are shown below. A consistent pattern has been observed in all previous studies conducted at ambient temperature, irrespective of the reactor dimensions, with the acid feed entering the reactor then sinking to the bottom before moving in a horizontal direction. The distinctive mixing pattern is shown in Figure 111.

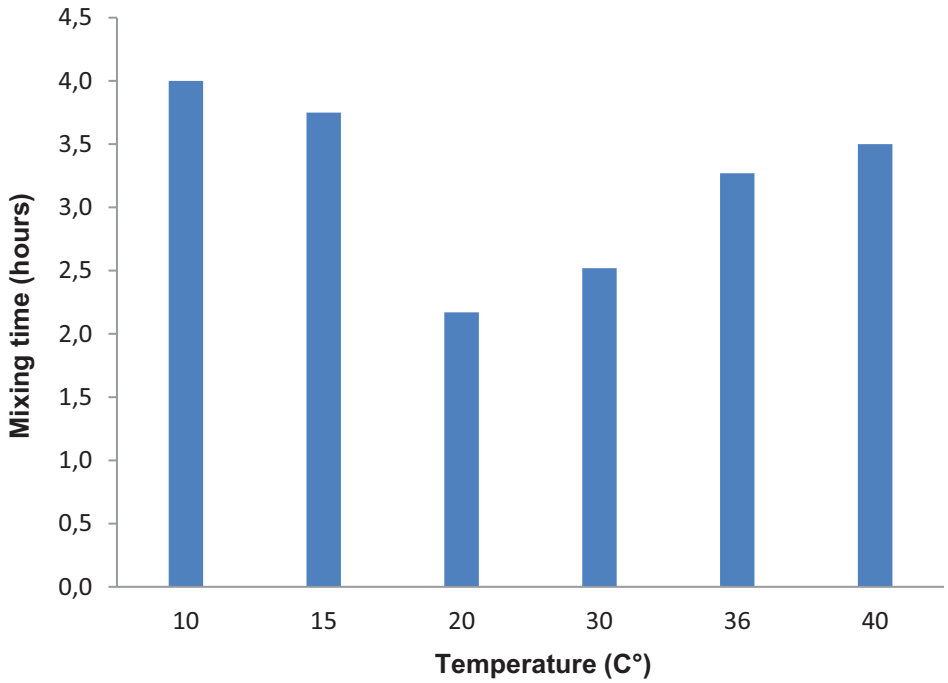

Figure 112: Summary of macromixing times as a function of temperature for the new LFCR

The mixing pattern at 10˚C was very different, with the zone of clearing initially observed near the top of the reactor. This is most likely due to the effect of the temperature differential, between the feed and the bulk liquid, on the relative density of the feed. After 146 minutes (Figure 113b) the zone of clearing remained confined to a narrow zone near the air liquid interface. By contrast, complete mixing had occurred by this stage during the previous study conducted at ambient temperature.

The effect of temperature on mixing is likely to be amplified in the pilot scale reactors as the greater liquid depth results in more significant vertical temperature gradients than observed in the laboratory scale reactors. The temperature gradients were confirmed during measurements taken at the pilot site.

The experiments conducted at temperatures above ambient showed more rapid diffusion during the early part of the tracer study, but while the majority of the reactor volume was neutralised, a number of “dead zones” remained. These resulted in the time required for complete mixing to be longer than that observed at ambient temperature. As with the experiments conducted at the lower temperatures there was a temperature differential between the feed, which was at ambient temperature, and the bulk liquid, which was heated. Attempts were made to minimise this effect by keeping the acid feed reservoir on a heating block. While this did reduce the temperature differential the relatively slow feed rate meant that the feed continued to lose heat in the time between being pumped out of the reservoir and entering the reactor.

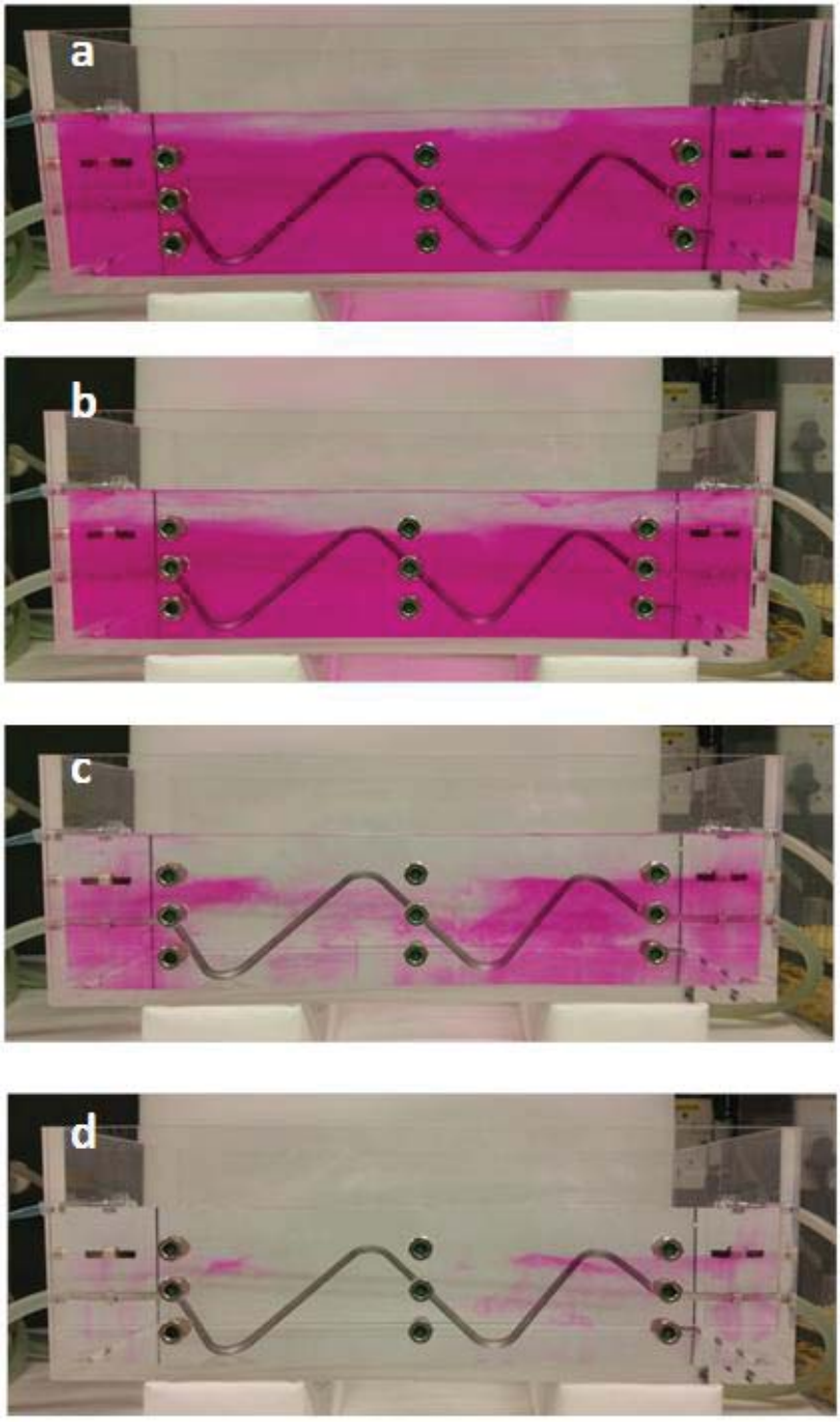

Figure 113: Images from hydrodynamic tracer study conducted at a 2 day hydraulic residence time at a temperature of 10˚C. Photographs taken at a) 34 min, b) 146 min, c) 215 min and d) 240 min

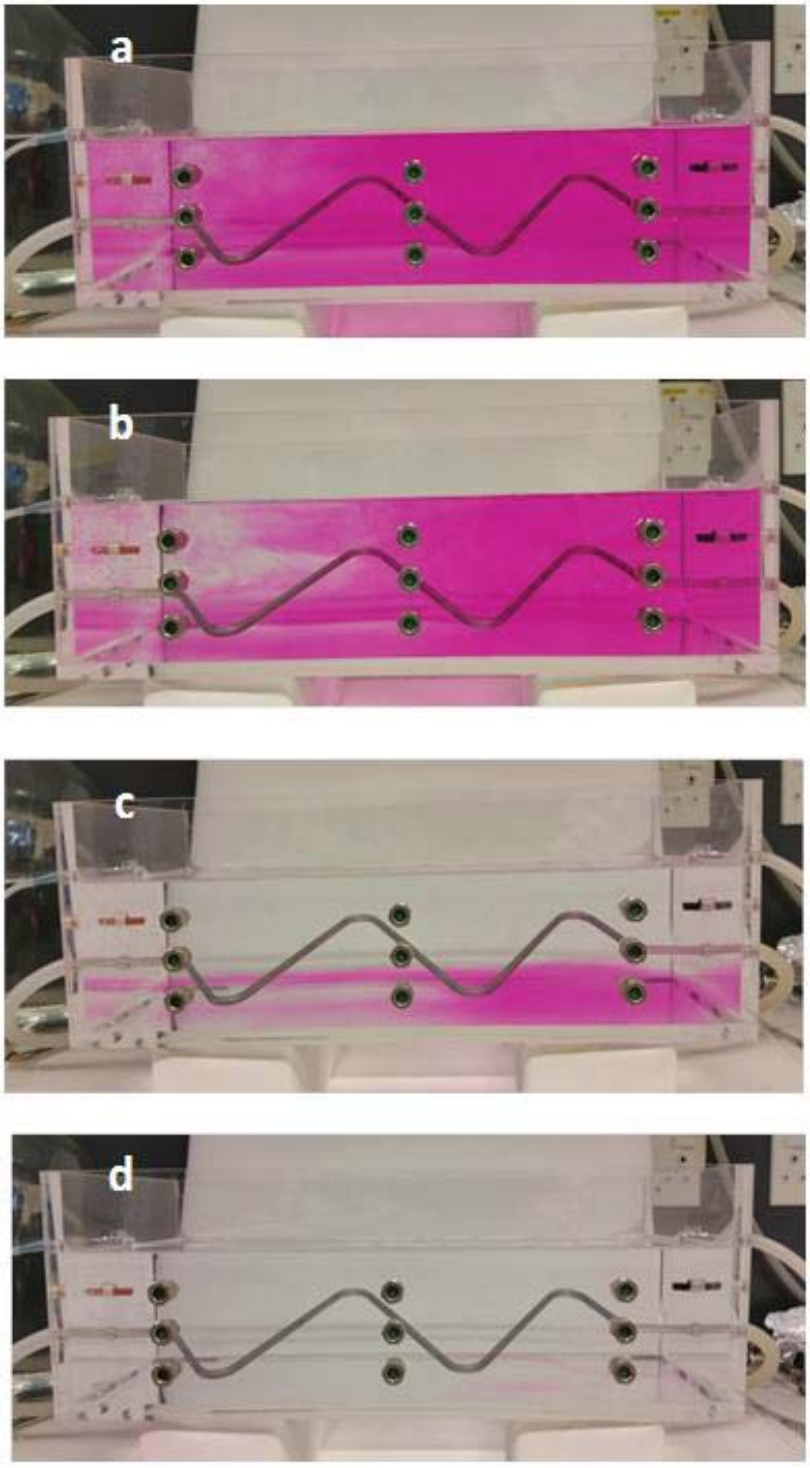

Figure 114: Images from hydrodynamic tracer study conducted at a 2 day hydraulic residence time at a temperature of 40˚C. Photographs taken at a) 0 min, b) 120 min, c) 165 min and d) 240 min

6.3.2 Effect of hydraulic residence time on reactor performance

The previous chapter described the successful testing of the proof of concept of the hybrid LFCR and showed that simultaneous sulphate reduction and partial sulphide oxidation can be achieved in a single reactor unit that is open to the atmosphere, provided there is sufficient aqueous sulphide in the bulk liquid to maintain anoxic conditions during the period after biofilm disruption or harvesting. The next

phase of research was to assess performance as a function of hydraulic residence time to evaluate the potential for high volumetric throughput.

The pH data are presented in Figure 115 and show that the pH remained relatively stable between pH 7.5 and pH 7 for the duration of the experiment, although it did trend slightly downward as the HRT decreased. The relatively stable pH is expected due to buffering by the bicarbonate and sulphide generated and the residual acetate produced from the partial oxidation of lactate. The pH in the effluent was consistently higher due to the consumption of acidity during the partial oxidation of sulphide.

The slight downward trend is consistent with a reduction in the extent of sulphate conversion and the accumulation of acetate and propionate at the low HRTs.

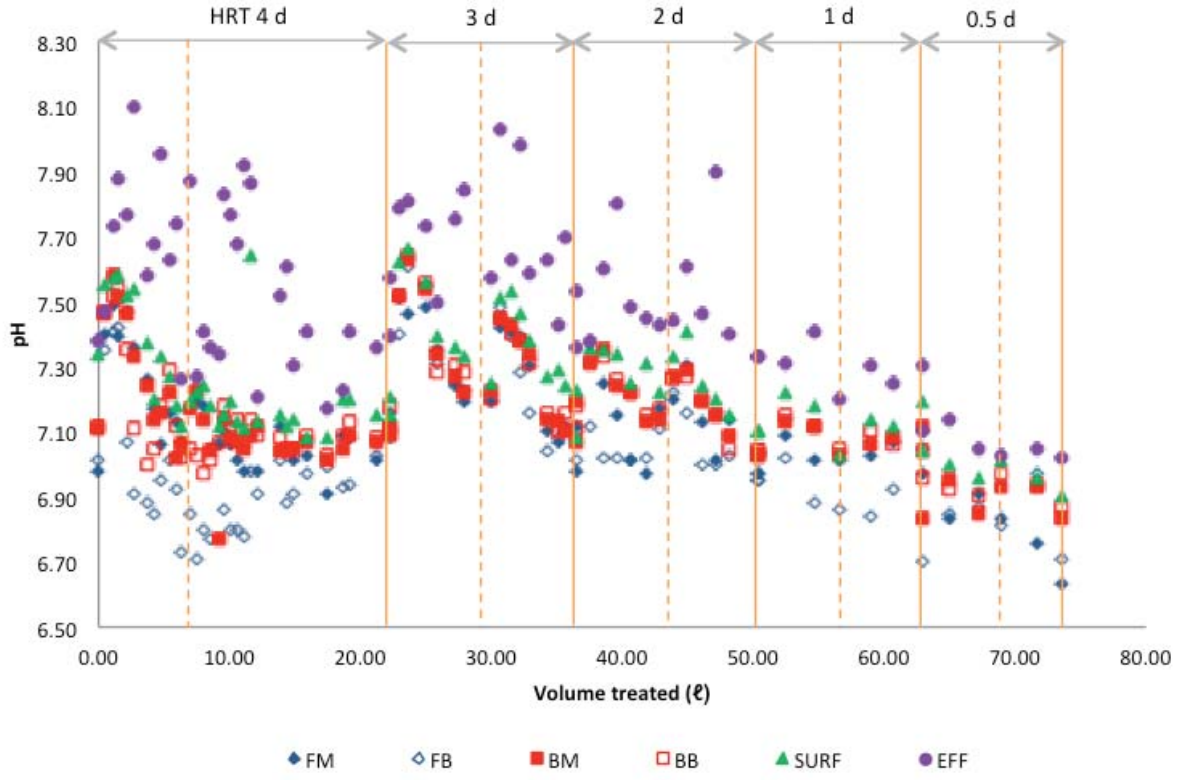

Figure 115: pH profile across the LFCR during the residence time study. The x-axis represents volume treated, rather than time to avoid the data points being squeezed together as the residence time decreased.

The aqueous sulphide data are presented in Figure 116 and show how the sulphide concentration increased to a maximum of around 250 mg/ℓ as the reactor reached optimal performance at the 4 day HRT. The sulphide concentration decreases substantially each time the FSB is disrupted or harvested, which is consistent with the conceptual model described in the previous chapter. The decrease is more significant after a harvesting event. This trend has been consistently observed and is most likely due to the fact that some remnants of the biofilm remain at the interface following disruption, but not harvesting. The presence of these fragments facilitates a more rapid regeneration of the biofilm, possibly by providing points of attachment, by maintaining a higher concentration of microbial cells at the interface or a combination of both. Similar benefits have been observed by seeding the surface with biofilm fragments after a harvesting event.

The maximum sulphide concentration decreased at the shorter HRTs, again consistent with reduction in the extent of sulphate reduction.

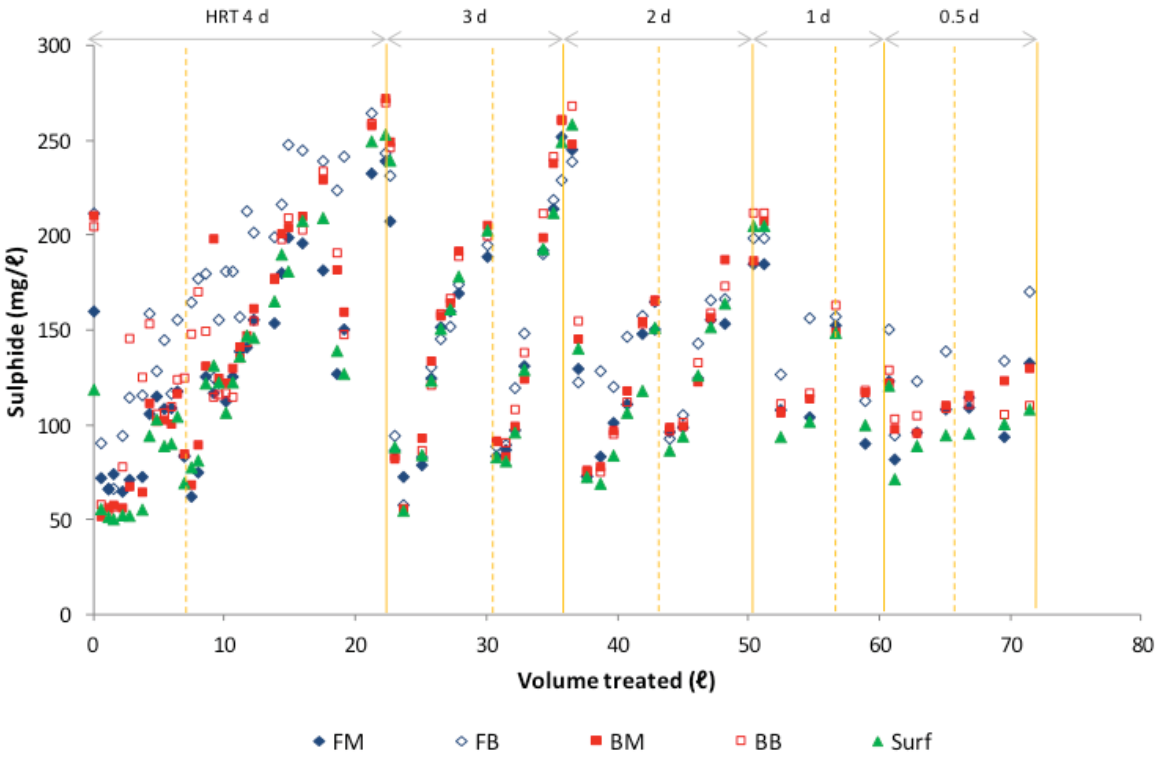

Figure 116: Aqueous sulphide concentration measured in the LFCR during the residence time study

The sulphate data (Figure 117) are consistent with the aqueous sulphide data and show near complete sulphate reduction at the 3 and 2 day HRT, with a reduction in efficiency at the shorter residence times. Nonetheless, the system is still able to achieve a steady state at a 12 hours HRT, suggesting that either there has been washout of a portion of the planktonic community or a maximum rate has been achieved.

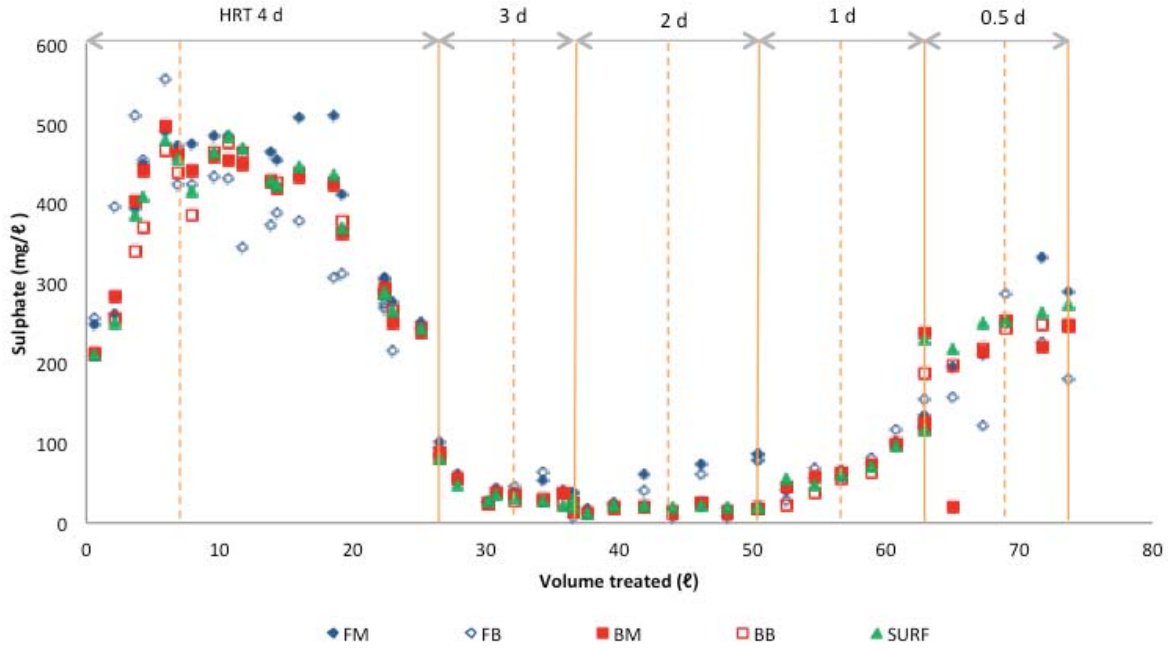

Figure 117: Residual sulphate concentration as a function of HRT

The complete dataset from the HRT study, including sulphate concentration and VFA profiles has been analysed, allowing an assessment of the impact of HRT on the dominant metabolic pathway and the effect of sulphate loading on the performance of the system. The overall system performance is summarised in Figure 118. From the data it is clear that sulphate reduction performance was not optimal at the 4 day HRT, with sulphate removal efficiencies of between 50 and 60%. During this period complete utilisation of the lactate was observed, but analysis of the reaction stoichiometry clearly showed that not all lactate was being used an electron donor for sulphate reduction. The presence of propionate in the reactor was evidence of lactate fermentation. During this period the sulphide concentration in the reactor was between 100 and 150 mg/ℓ. Previous work on lactate-based sulphate reducing systems (Oyekola *et al*., 2012) showed that the competing fermentative community was significantly inhibited at sulphide concentrations in excess of 160 mg/ℓ.

Sulphate reduction was most efficient at the three and two day HRTs, with efficiencies of over 95% consistently recorded. Collapse or harvesting of the biofilm did not have a negative effect on the sulphate reduction efficiency, despite a significant short-term reduction in sulphide concentration. This was discussed in greater detail in the previous chapter. During this period it was clear that lactate oxidation during sulphate reduction was the dominant metabolic pathway, with very little propionate being formed.

The extent of sulphate reduction decreased at the one and 0.5 day HRTs, although more than 75% of the sulphate was still being reduced at the 12 hour HRT. The fact that a steady state could be maintained clearly demonstrated the success of the biomass retention on the carbon fibres. Previous studies (Oyekola *et al.,* 2012; van Hille *et al*., 2015) showed washout of at least a portion of the sulphate reducing communities at HRTs below one day in continuous stirred tank reactors. The decrease in sulphate reduction efficiency at the 12 hour HRT coincided with significant propionate formation.

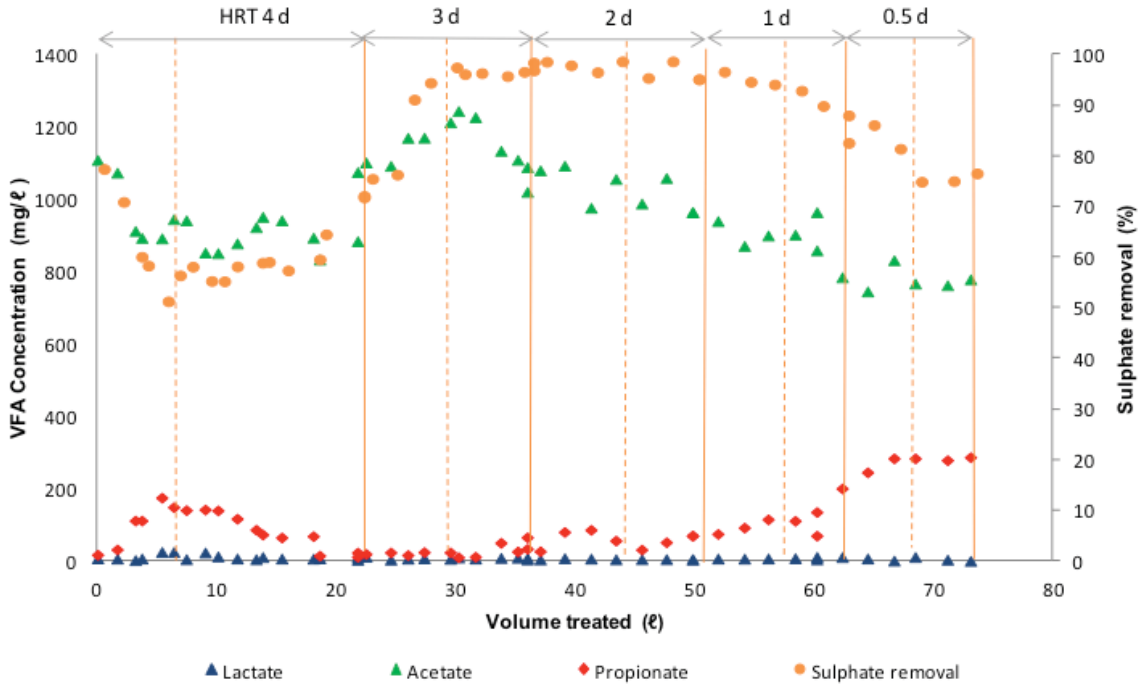

Figure 118: Summary of the data from the HRT study showing sulphate removal efficiency and VFA profiles. Dotted lines represent biofilm collapse while solid vertical lines represent complete biofilm harvesting

Despite the drop in sulphate reduction efficiency the volumetric sulphate reduction rate was highest at the 12 hour HRT, with a steady state rate of 62.5 mg/ℓ.h. The data from the current study is compared to rate date from previous studies in Figure 119. All studies were carried out using the same microbial consortium, the same feed composition and at the same temperature (30˚C). The data are similar for

HRTs down to one day (VSLR 41.7 mg/ℓ.h) but diverge significantly after that. The traditional CSTR, where there is no mechanism for biomass retention, is considered the baseline. The other reactor types considered are a similar LFCR operated as a sealed unit with no active sulphide oxidation, a CSTR coupled with a cross-flow microfiltration unit that recycled cells back to the CSTR, effectively retaining all the biomass, and the current combined sulphate reduction-sulphide oxidation channel reactor.

The hybrid (combined) channel reactor and the membrane coupled CSTR were able to achieve the highest volumetric sulphate reduction rates, primarily due to the very effective retention of biomass.

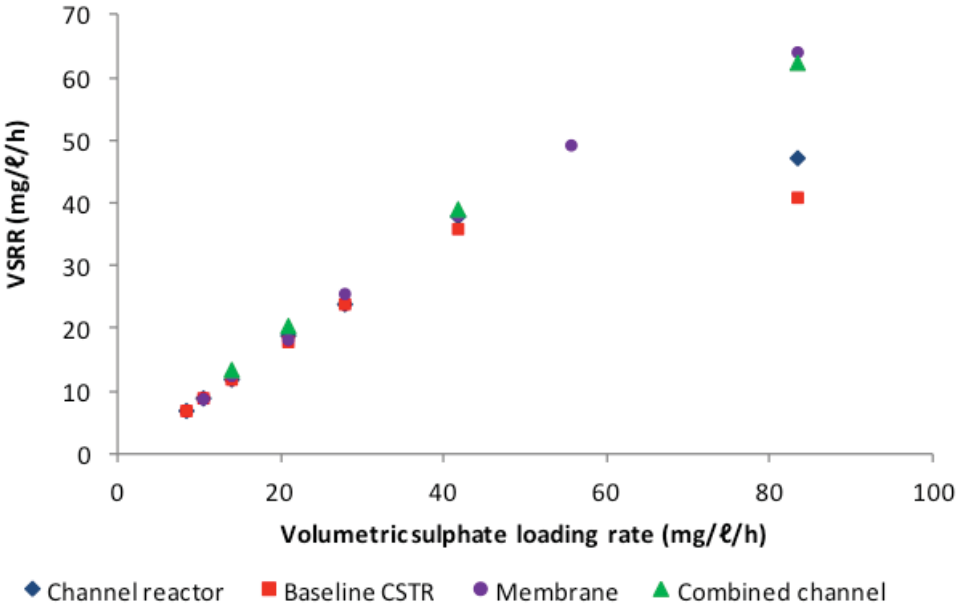

Figure 119: Volumetric sulphate reduction rates as a function of sulphate loading for the combined channel reactor, compared to data from previous studies (van Hille *et al*., 2015)

Many of the studies conducted to date, using the lactate-based feed, showed that competition between lactate fermenters and the lactate oxidising sulphate reducing species is one of the key factors impacting overall system performance, particularly under stress conditions. This was one of the key drivers for the shift from a lactate-based growth medium to an acetate-based medium, along with the fact that the acetate-based medium has been developed to more closely approximate the VFA composition of the digestate.

6.3.3 Effect of temperature on LFCR performance

Research conducted to date and presented in previous progress reports have demonstrated proof of concept of the integrated sulphate reducing – sulphide oxidising reactor and highlighted the effect of hydraulic residence time and sulphate loading on system performance. The data indicated that a 2-day HRT was optimal, achieving high volumetric sulphate reduction rates and near complete sulphide oxidation, with over 70% recovery of elemental sulphur in the floating biofilm.

Those experiments were performed at laboratory scale under controlled temperature conditions. In the field, the system would be exposed to significant seasonal variation in temperature and it is important to assess what impact that would have on the performance of both the sulphate reducing and sulphide oxidising communities in the reactor. The sections below describe the complete dataset, from 30˚C down to 10˚C.

6.3.3.1 Performance of the 2 ℓ lactate-fed reactor

The 2 ℓ lactate-fed reactor has been operated continuously for over four years and was used to demonstrate the proof of concept and perform the HRT study. During this period the carbon fibres have not been removed from the reactor, so the biomass colonisation is extensive.

Following the completion of the HRT study and the initiation of the temperature study, initially at 35˚C, the measure of elapsed time was reset to zero (13 March 2016). Operation of the reactor at 35˚C introduced a number of unanticipated challenges in terms of evaporation, biofilm composition and overall performance that will be discussed below.

After 488 days the reactor had reached relatively stable performance at a temperature of 30˚C and a 2 day HRT, so the controlled experiment to assess the effect of temperature was initiated. The experiment was run for an additional 115 days, after which the temperature was again raised to 25˚C.

The effect of temperature on pH is illustrated in Figure 120 and shows that the pH remained relatively stable between pH 6.9 and pH 7.2 for the duration of the experiment. The overall system is well buffered, with the sulphide and bicarbonate generated during the sulphate reduction reaction countered by the acidity of the residual VFAs, particularly acetate.

Some vertical stratification with respect to pH became apparent as the temperature decreased, with the pH in the bottom half of the reactor, particularly near the front, generally lower than the upper portion. The reason for this is likely to have been influenced by a number of factors that are discussed in greater detail below.

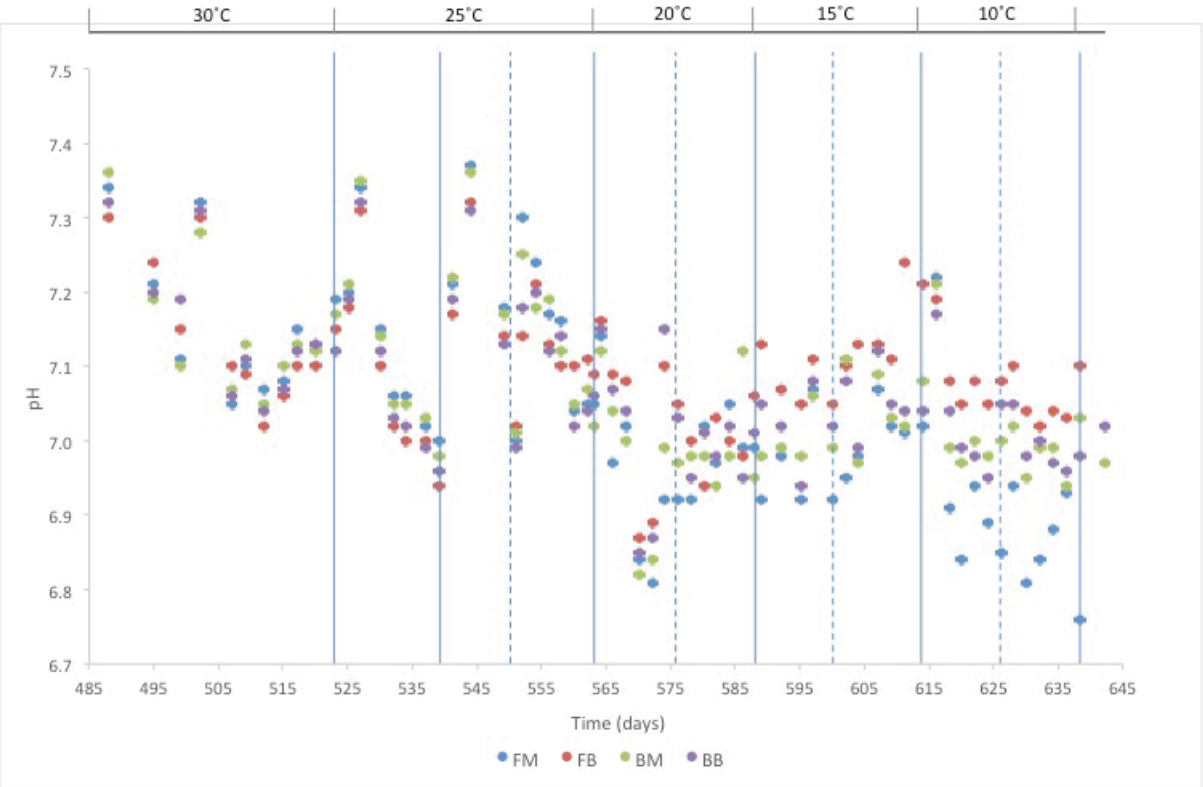

Figure 120: Graph of pH as a function of sample port and temperature. Solid vertical lines represent biofilm harvesting events, while dashed lines represent biofilm disruption, but not harvesting

The residual sulphate concentration data (Figure 121) shows a number of distinct trends as the temperature decreased. Overall, the residual sulphate increased as the temperature decreased, from an average across the reactor of between 300 and 350 mg/ℓ at 30˚C to between 700 and 800 mg/ℓ at 10˚C, which is consistent with the hypothesis that sulphate reduction rate decreases with temperature.

A more interesting trend is the distinct divergence from a relatively uniform sulphate distribution through the reactor at 30˚C to a range of as much as 400 mg/ℓ between top and bottom and front and back at 10˚C. This trend was only observed after the temperature was reduced from 30˚C to 25˚C and became more distinct as the temperature was reduced further. During the first 523 days of operation the sulphate concentration did not vary significantly as a function of position within the reactor.

The reduction in temperature had a clear impact on the distribution of planktonic cells within the reactor, with a distinct accumulation of biomass near the base, particularly in the front portion. The biomass did not settle completely, but appeared to form a colloidal suspension in the lower third of the reactor.

When the reactor was operated above ambient temperature (22 ± 1˚C), heating was achieved by pumping water through a heat exchanger near the base of the reactor. Due to the lack of turbulent mixing temperature and therefore density gradients formed within the reactor. Convective motion may have resulted in a more even distribution of planktonic cells. The effect of this would decrease as the temperature of the bulk liquid approached that of ambient.

The residual sulphate concentration in the sample withdrawn from the first port on the lower level (FB) was significantly lower than that from the rest of the reactor at 25˚C, a trend that was maintained for the duration of the experiment. This suggests that more efficient sulphate reduction was taking place in that zone, possibly due to the accumulation of biomass. Samples for DNA extraction and community structure analysis were taken from this region and once analysed will provide insight into whether the accumulated biomass consisted predominantly of sulphate reducers or other, fermentative species.

A second factor that could influence the results is possible changes in the hydrodynamics as a result of the accumulation of biomass. It is possible that this zone may have been bypassed by a significant portion of the fresh feed, creating an essentially stagnant zone where the localised HRT was substantially higher than the average HRT across the reactor.

The accumulation of biomass in the bottom third of the reactor was less pronounced toward the far end and there was less divergence between the sulphate concentration values for the BM and BB sample ports, irrespective of temperature.

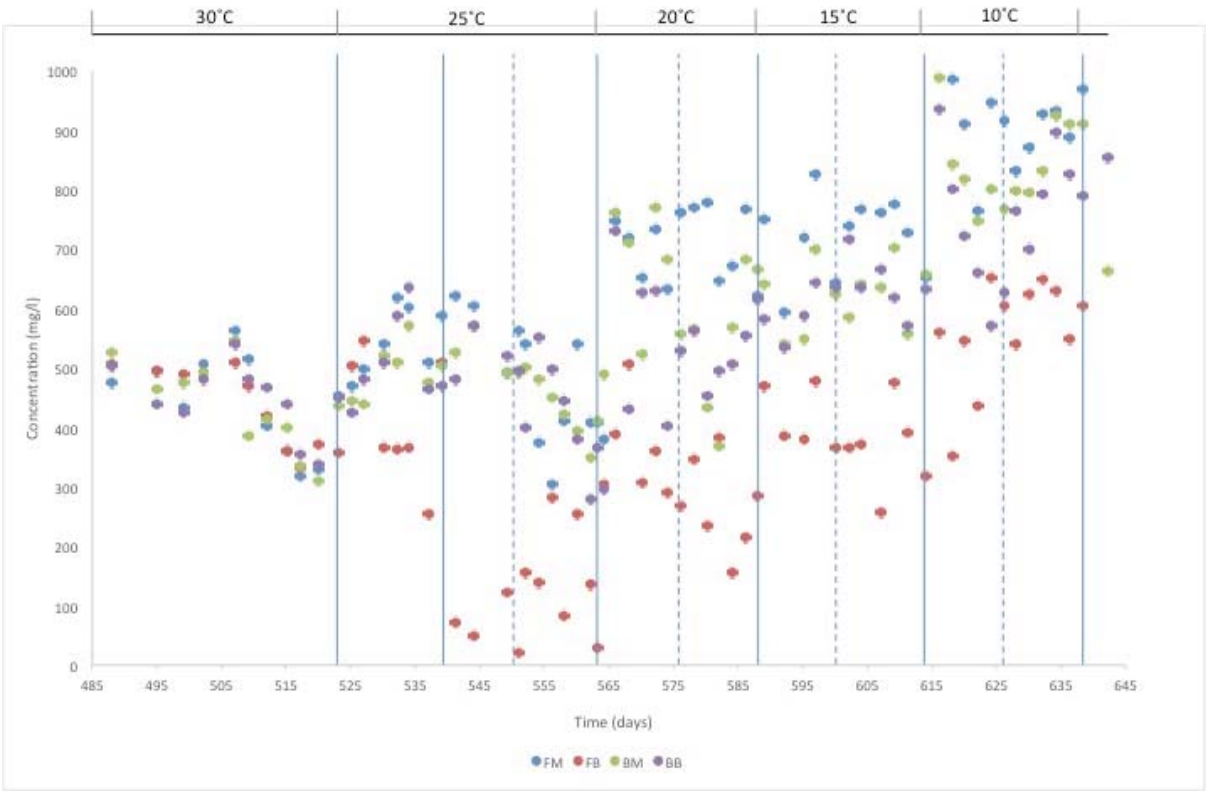

Figure 121: Graph showing residual sulphate concentration as a function of sample port and temperature. Solid vertical lines represent biofilm harvesting events, while dashed lines represent biofilm disruption, but not harvesting

The aqueous sulphide data (Figure 122) shows a similar trend to the residual sulphate data, as expected, with clear vertical stratification evident. This type of stratification was observed in the original LFCRs, which operated as sulphide oxidation reactors only. The hydrodynamic study showed that macro mixing time was less than the HRT, even at low temperature which suggests that the sulphide stratification is due to spatial differences in the rate of sulphate reduction, or the emergence of zones of significantly reduced mixing, where the real HRT is significantly longer than the mean HRT across the reactor.

This phenomenon may be a consequence of the substantial accumulation of planktonic biomass over the years of operation and may not have been as pronounced in a more recently colonised reactor. The data for the 8 ℓ reactor, presented in the next section, provides some support for this interpretation.

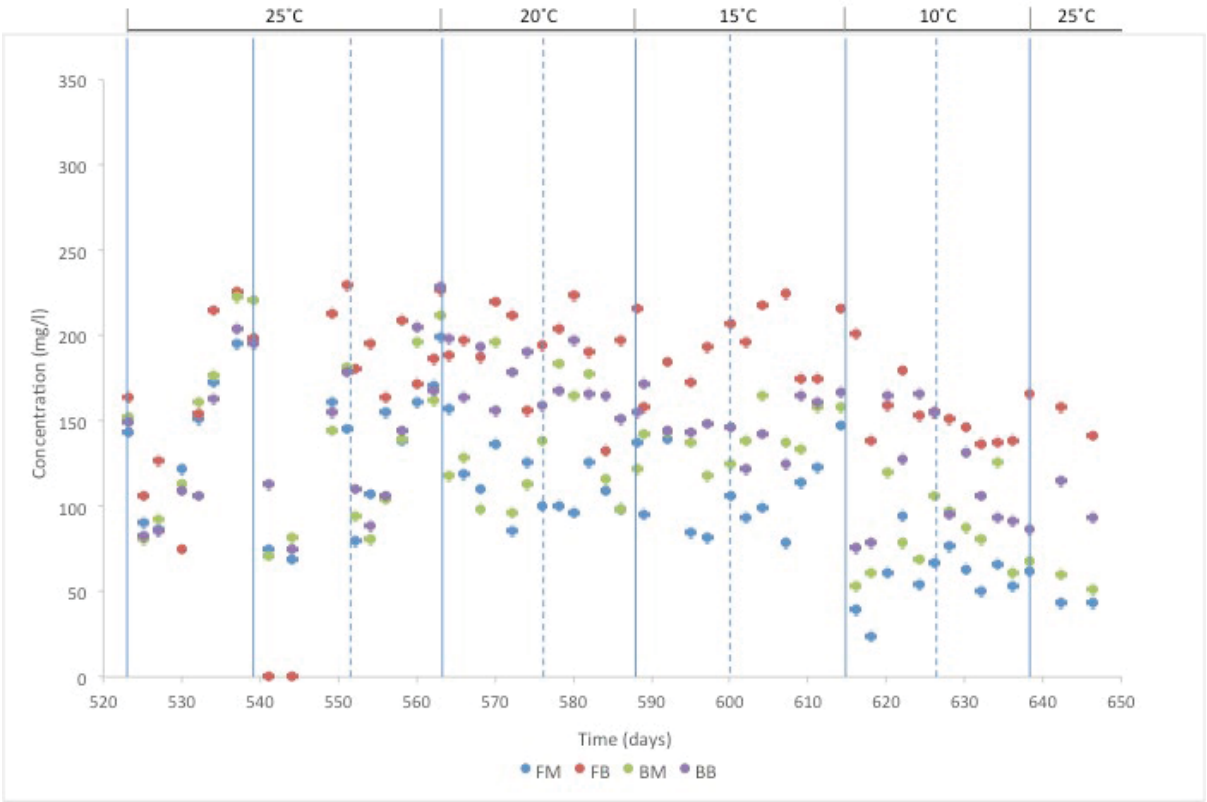

Figure 122: Graph showing the aqueous sulphide concentration as a function of sample port and temperature. Solid vertical lines represent biofilm harvesting events, while dashed lines represent biofilm disruption, but not harvesting

Overall, the reduction in temperature did result in a decrease in the volumetric sulphate reduction rate and extent of sulphate conversion, which became more pronounced below 20˚C (Figure 123). The VSRR decreased by approximately 50% between 25˚C and 10˚C. However, it is encouraging to note that sulphate reduction was not completely suppressed at 10˚C. From a process perspective, a 50% reduction in sulphate reduction rate could be overcome by reducing the flow to the reactor or adding a second reactor in series.

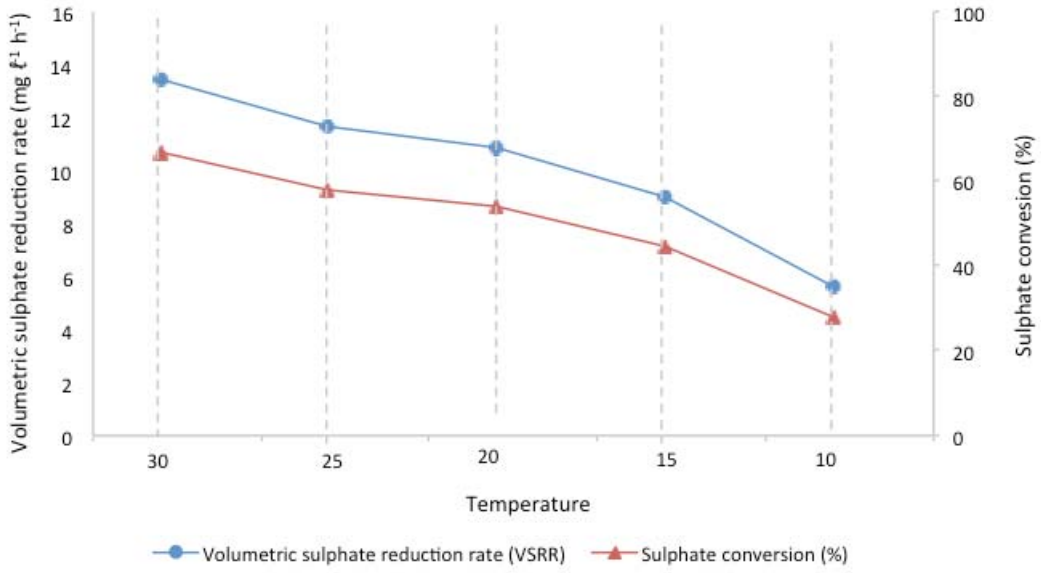

Figure 123: Comparison of mean volumetric sulphate reduction rate and sulphate conversion efficiency as a function of temperature

The VFA profile was determined for selected samples during the experiment. The data for the 10˚C phase is still being processed, but the values for 25˚C to 15˚C are presented in Figure 124.

During operation at 30˚C, where high (>80%) sulphate conversion efficiencies were observed complete consumption of the lactate in the feed was observed, with relatively little production of propionate. Propionate is a by-product of lactate fermentation by non-SRB and its presence is indicative of some competition for the lactate substrate. The SRB have a higher affinity for low concentrations of lactate (higher K_s value) and the fermentative bacteria are inhibited by high aqueous sulphide concentrations. These factors ensure that SRB dominate under optimal conditions.

At 20˚C and below residual lactate was detected in all the samples, indicating that neither the SRB nor the fermentative community was able to utilise all the substrate. This is confirmed by the reduction in the residual acetate concentration. Lactate is only partially oxidised by most SRB, with acetate as a metabolic by-product at a stoichiometric ratio of 1:1. At 25˚C and above, the consumption of 11.8 mM lactate results in the generation of the equivalent amount of acetate. The decrease in acetate concentration at low temperature is almost equivalent to the decrease in sulphate reduction, suggesting that the lower temperature is impacting the metabolic rate, rather than significantly changing the microbial community structure. Analysis of the metagenomic data will provide a clearer answer.

The data suggest that the microbial community does not contain acetate utilising SRB in significant numbers as neither the residual acetate nor the residual sulphate are consumed.

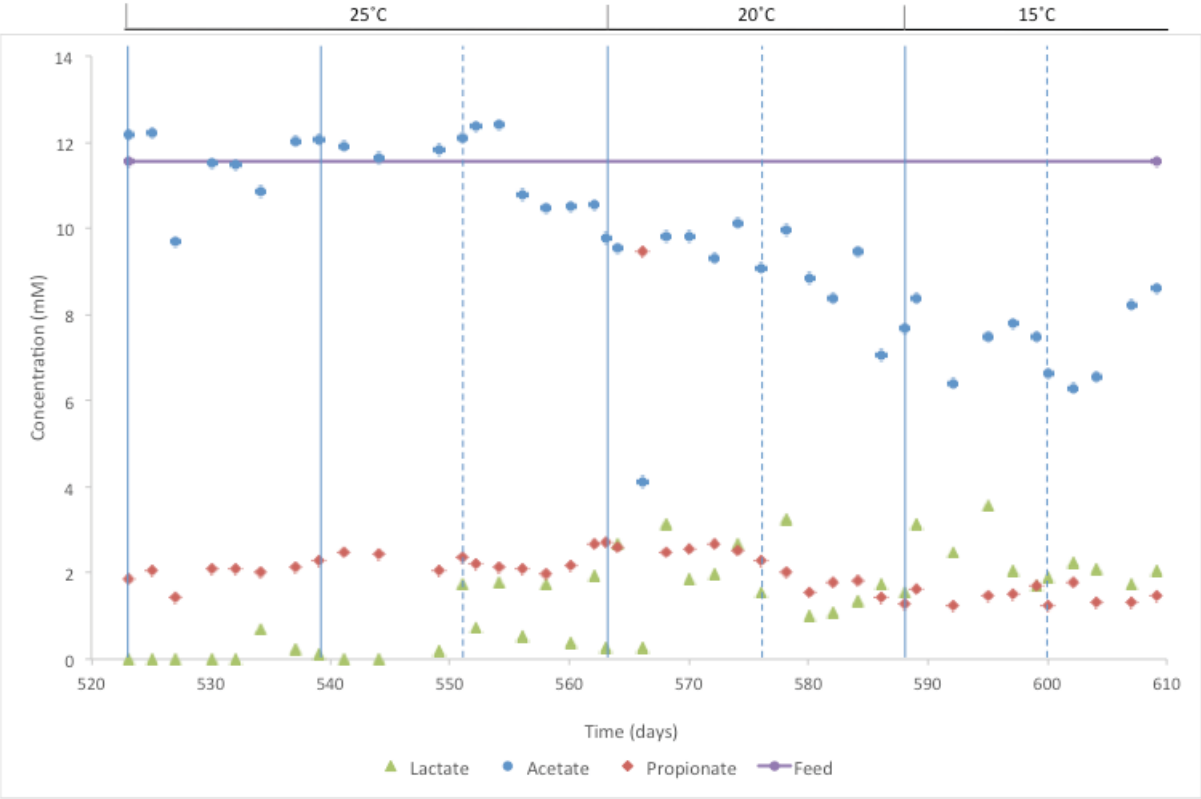

Figure 124: Volatile fatty acid profile as a function of temperature. Data represent mean values from the different sample ports. Solid vertical lines represent biofilm harvesting events, while dashed lines represent biofilm disruption, but not harvesting

6.3.3.2 Performance of the 8 ℓ lactate fed reactor

The 8 ℓ reactors were introduced into the project to determine whether the aspect ratio had a significant impact on the performance of the hybrid LFCR. Their dimensions represent a scaled-down version of the 2000 ℓ reactor units being evaluated at the pilot site.

Unlike the 2 ℓ lactate fed reactor this reactor was only set up in March 2016 so was not colonised to the same extent at the start of the temperature study. The same circulating water bath was used to control both reactors so the experiment could only start once the 2 ℓ reactor was ready.

The pH data for the 8 ℓ reactor followed at similar trend to the smaller reactor, with a marginal decrease as the temperature was lowered, but remaining above pH 6.9. In this case effluent exiting the reactor was also sampled and the pH was consistently higher than that measured in the rector. This can be attributed to the partial oxidation of some of the aqueous sulphide in the effluent stream. Elemental sulphur deposits were observed on the inside of the silicone tubing connecting the reactor to the effluent collection vessel.

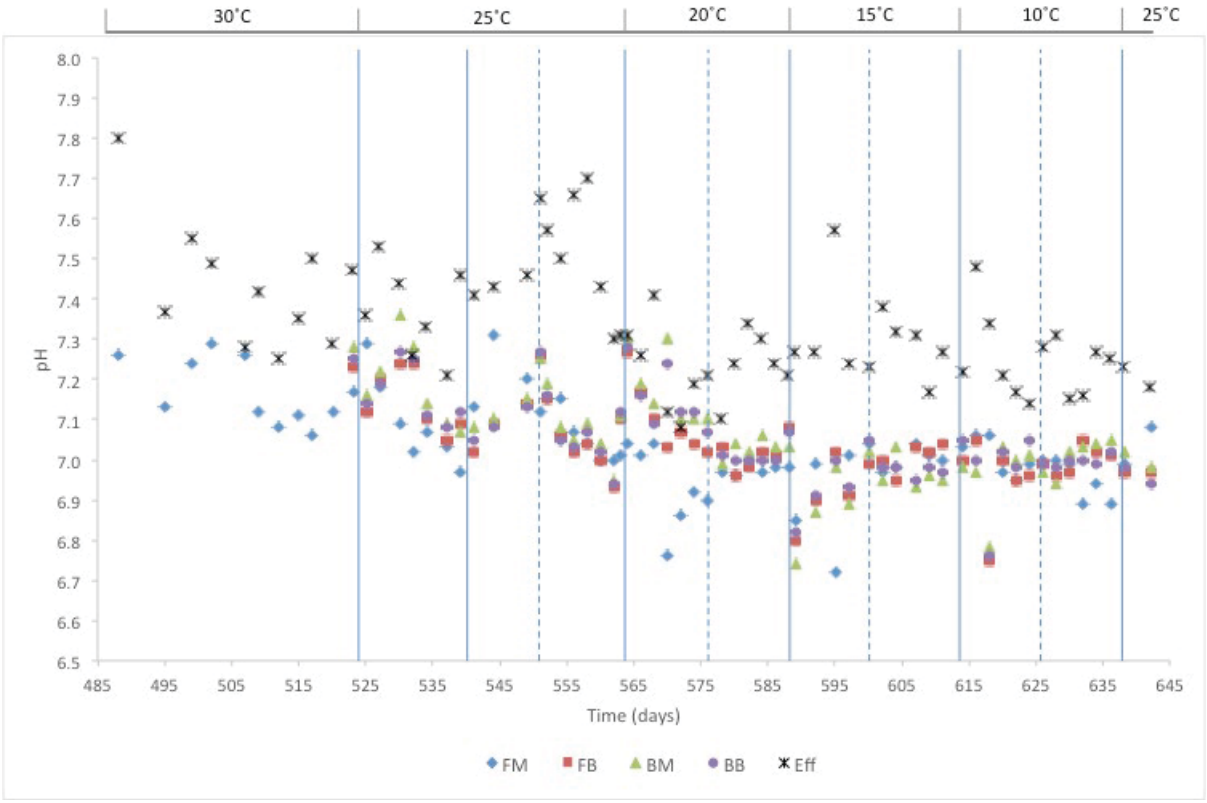

Figure 125: Graph of pH as a function of sample port and temperature for the 8 ℓ lactate fed reactor. Solid vertical lines represent biofilm harvesting events, while dashed lines represent biofilm disruption, but not harvesting

The sulphate concentration data (Figure 126) show a similar trend to that observed for the 2 ℓ reactor, with a steady increase in residual sulphate as the temperature decreases. The most noticeable difference between the two reactors is the less pronounced difference in sulphate concentration as a function of sampling position. In particular, the sulphate concentration from the lower front section of the reactor (FB) was close to the mean value across the reactor. The 8 ℓ reactor did not show the same level of accumulation of planktonic biomass in the bottom half of the reactor as the temperature decreased. This is most likely due to the fact that the reactor had not been operated for as long, prior to the start of the temperature experiment, as the 2 ℓ reactor, so the planktonic biomass concentration was lower to begin with. The difference in aspect ratio may also have played a role, with the greater width relative to the height reducing the potential for biomass accumulation near the sample port.

The sulphate concentration in the effluent was not significantly higher than that within the reactor, confirming that complete oxidation of the residual sulphide did not occur. This is consistent with the pH data, as complete oxidation to sulphuric acid would have resulted in a decrease, rather than increase in the effluent pH.

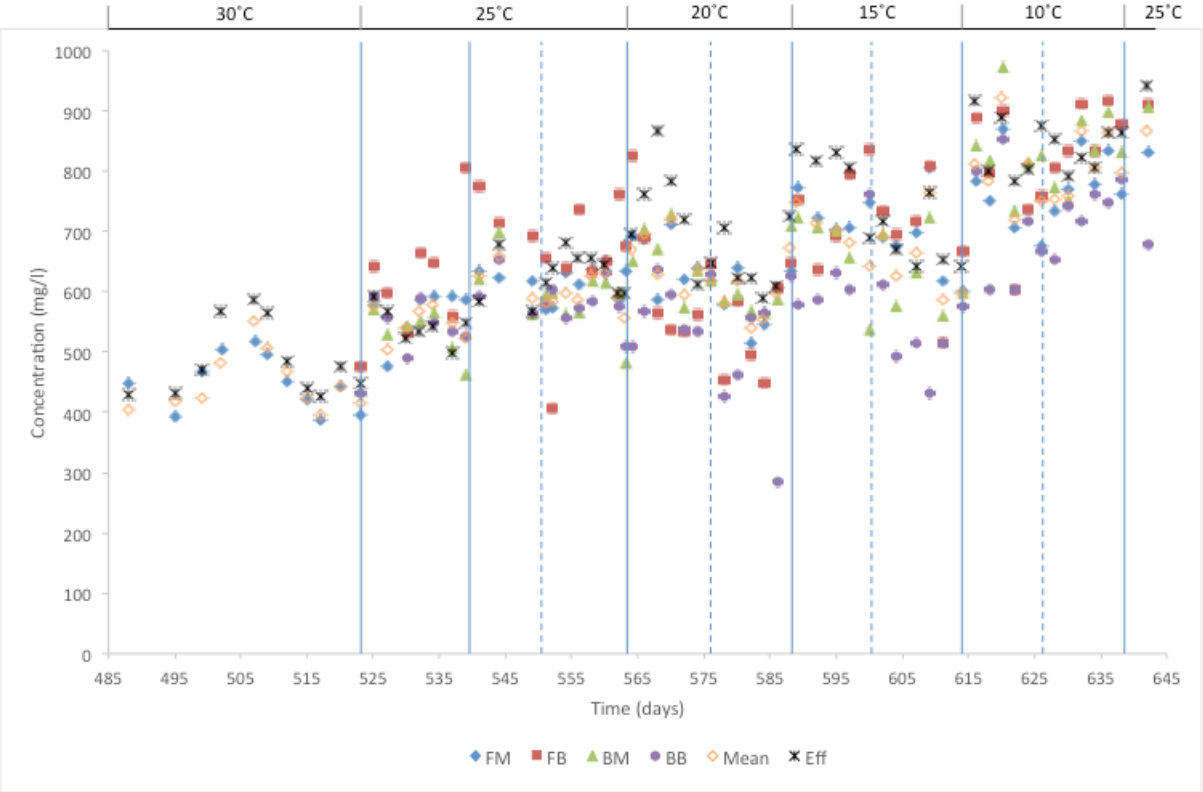

Figure 126: Graph showing residual sulphate concentration as a function of sample port and temperature for the 8 ℓ lactate fed reactor. Solid vertical lines represent biofilm harvesting events, while dashed lines represent biofilm disruption, but not harvesting

The aqueous sulphide data (Figure 127) is consistent with that of the residual sulphate, showing a general trend of decreasing as the temperature decreased. This is consistent with the reduction in sulphate reduction rate and conversion. As with the sulphate data, evidence of vertical stratification is less pronounced in the 8 ℓ reactor than in the 2 ℓ reactor and there is no significant accumulation of sulphide in the lower half of the reactor.

A comparison of the residual sulphate and aqueous sulphide data, particular in the lower temperature range (10-20˚C) show that the increase in residual sulphate concentration is more pronounced than the decrease in aqueous sulphide. This suggests that the reduction in temperature has a greater impact on sulphide oxidation than sulphate reduction. If sulphate reduction were more significantly affected the trend would be toward ever decreasing aqueous sulphide as it was oxidised at a rate faster than it was being generated.

Theoretically, sulphate reduction can occur throughout the reactor volume as the entire bulk volume is essentially anoxic, while sulphide oxidation can only occur at air-liquid interface, so is essentially a function of surface area, rather than volume. It is possible that at lower temperature the relative difference between volume-controlled and surface area-controlled reactions becomes more important.

The aqueous sulphide concentration in the effluent is significantly lower than in the reactor. The difference represents the amount of sulphide oxidised in the biofilm.

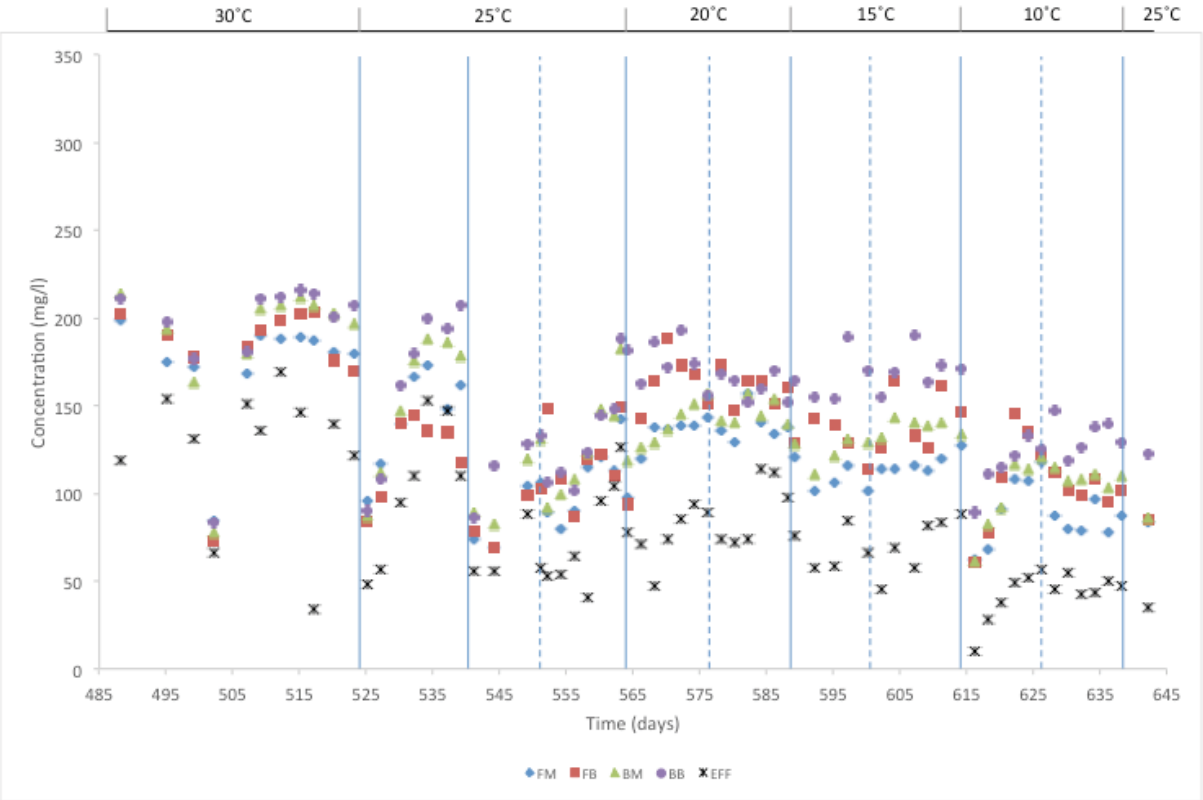

Figure 127: Graph showing aqueous sulphide concentration as a function of sample port and temperature for the 8 ℓ lactate fed reactor. Solid vertical lines represent biofilm harvesting events, while dashed lines represent biofilm disruption, but not harvesting

The effect of lower temperature on the VSRR and sulphate conversion in the 8 ℓ reactor (Figure 128) was very similar to that of the 2 ℓ reactor (Figure 123), with a reduction in VSRR of just over 50%, from approximately 13 mg/ℓ.h to around 5.7 mg/ℓ.h. This showed that while there were differences with respect to the degree of vertical stratification, the overall performance of the different reactor configurations was similar.

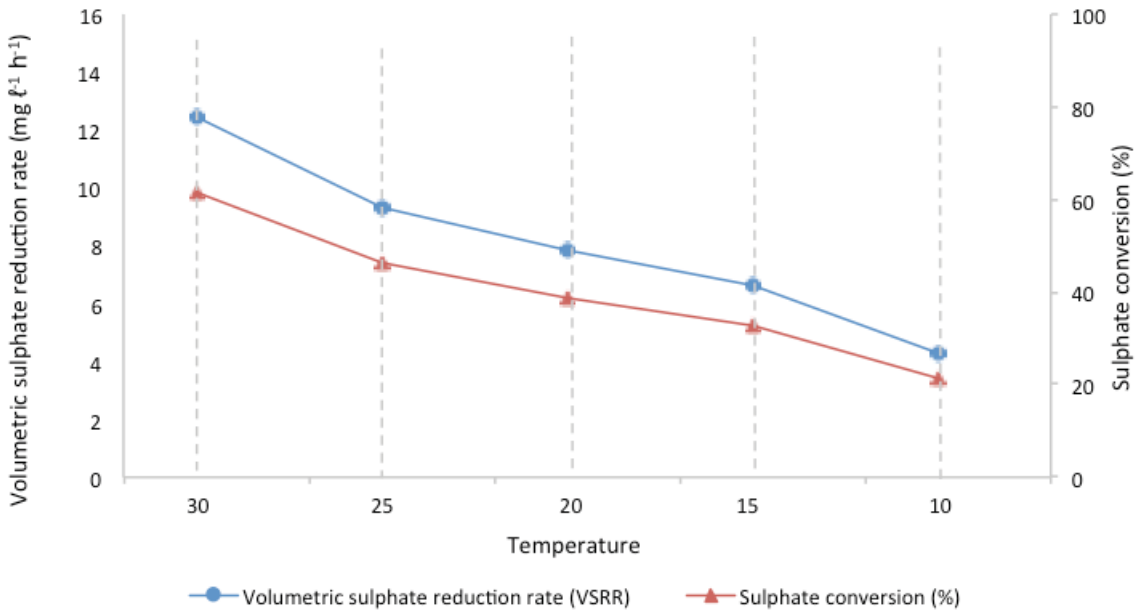

Figure 128: Comparison of mean volumetric sulphate reduction rate and sulphate conversion efficiency as a function of temperature for the 8 ℓ lactate fed reactor

6.3.3.3 Performance of the 2 ℓ acetate fed reactor

The reactors operated on the acetate-based feed have historically been more difficult to maintain and obtain stable, consistent data from and the temperature study proved no different. The microbial community appears to be more severely affected by the influx of some oxygen into the reactors following biofilm disruption and harvesting.

In addition, after stable operation at 30˚C between day 523 and 537 when the biofilm was harvested, the biofilm did not reform as quickly as normal and the performance of the reactor declined significantly in the weeks that followed. The delay in biofilm formation resulted in the complete oxidation of some of the sulphide. This lead to a significant decrease in pH (Figure 129), increase in residual sulphate (Figure 130) and dramatic decrease in aqueous sulphide from around 200 mg/ℓ to between 50 and 100 mg/ℓ (Figure 131). Between day 537 and 575 the performance of the reactor, in terms of sulphate reduction, decreased consistently, with the residual sulphate concentration increasing from around 500 mg/ℓ to almost 900 mg/ℓ. During this period the pH decreased from around pH 7.6 to pH 7.0 as a consequence of reduced sulphate reduction, which decreased alkalinity generation. In addition, less of the acetate substrate was consumed, so the higher residual acetate led to increased acidity.

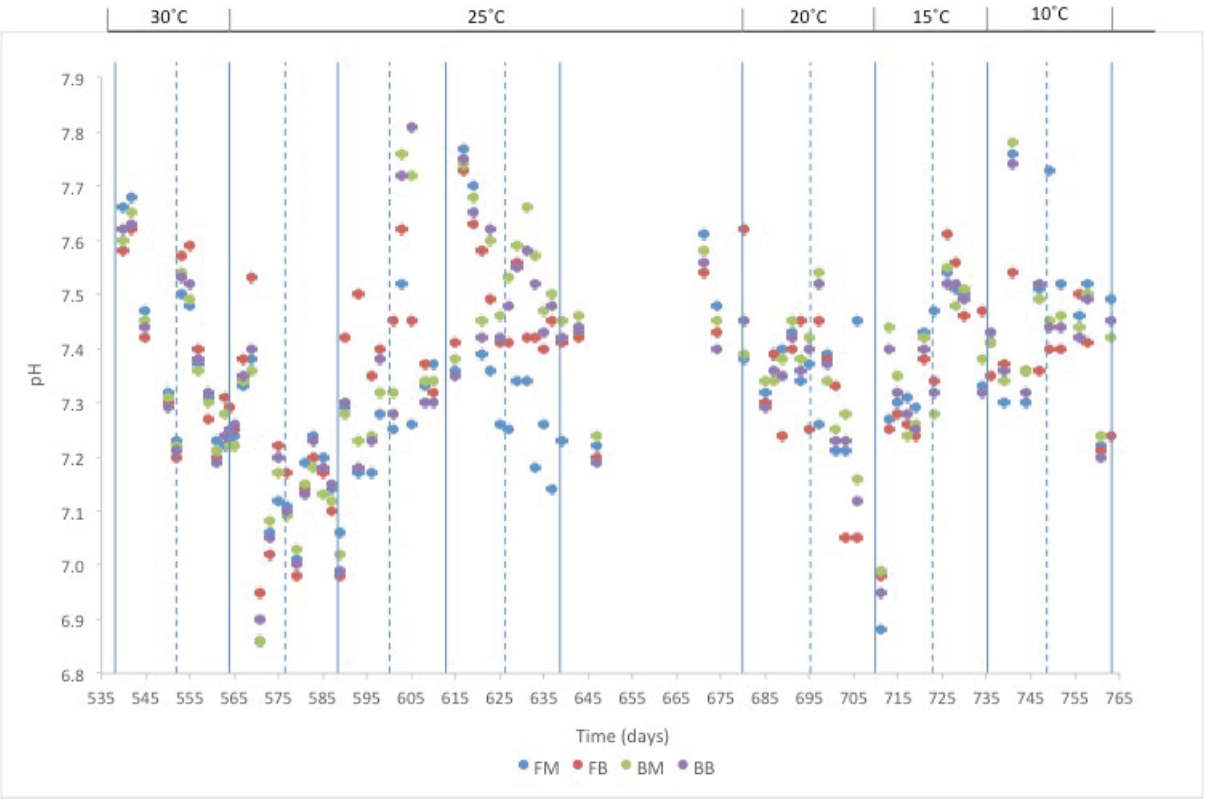

Figure 129: Graph of pH as a function of sample port and temperature for the 2 ℓ acetate fed reactor. Solid vertical lines represent biofilm harvesting events, while dashed lines represent biofilm disruption, but not harvesting

As a consequence of the instability in the system the reactor was operated at 25˚C for considerably longer than originally intended, in an effort to stabilise performance. The biofilm was disrupted and harvested periodically during this period to prevent it becoming too thick. By day 678 the reactor had stabilised, with sulphate reduction consistently in the region of 50% and the normal cycle of disruption, harvest and temperature reduction was resumed. During this period the pH stabilised between pH 7.3 and 7.4. This was higher than the lactate fed reactors by almost half a pH unit, most likely due to the lower residual acetate concentration. The partial oxidation of lactate generates an acetate molecule for each lactate consumed, so the residual acetate concentration in the lactate reactors was typically above 10 mM.

The sulphate data (Figure 130) show that the reduction in temperature had a more significant impact on the acetate fed system than the either of the lactate fed reactors, with residual sulphate concentrations close to the feed concentration measured at 10˚C. In addition, a similar phenomenon of spatial variation, as seen in the 2 ℓ lactate reactor, was observed. The residual sulphate concentration was lowest in the lower front portion of the reactor, with correspondingly higher sulphide concentrations. Again, evidence of biomass settling in this region was observed.

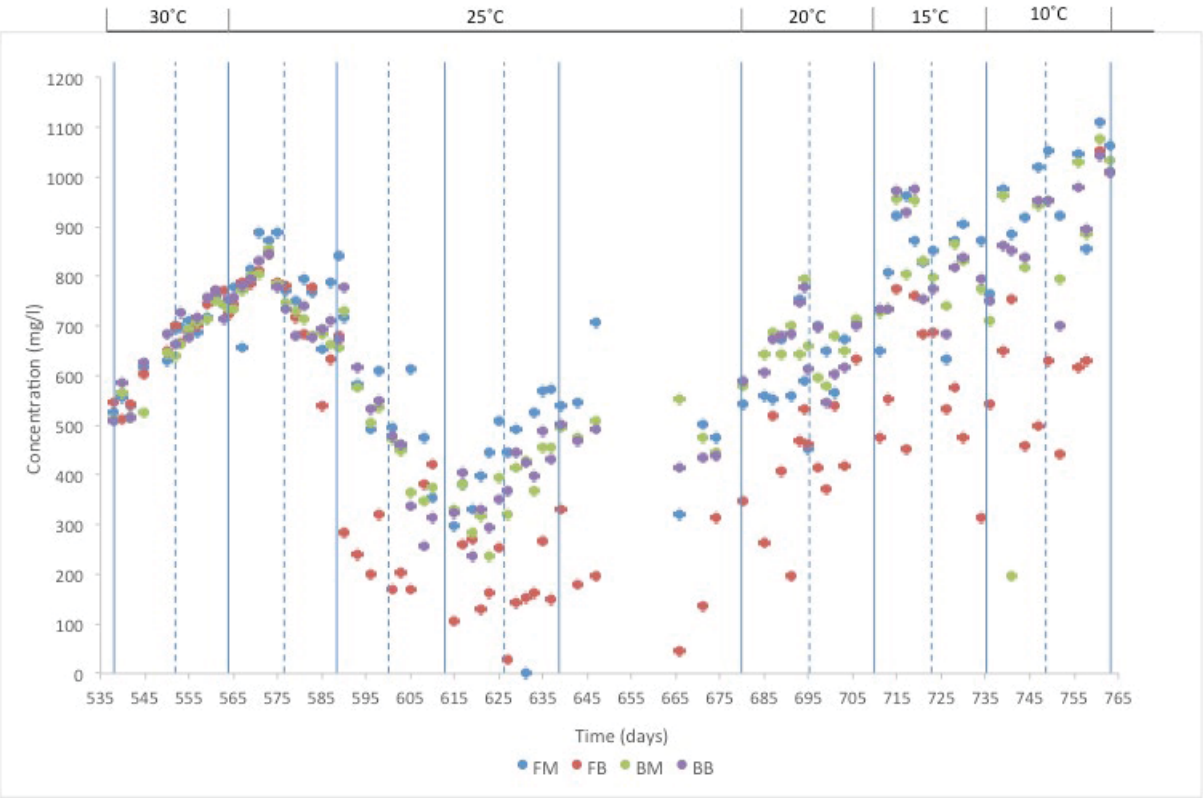

Figure 130: Graph showing residual sulphate concentration as a function of sample port and temperature for the 2 ℓ acetate fed reactor. Solid vertical lines represent biofilm harvesting events, while dashed lines represent biofilm disruption, but not harvesting

The sulphide data (Figure 131) are consistent with the sulphate reduction data, showing a consistent and steady decline in sulphide as the temperature was reduced from 20˚C to 10˚C. At the lowest temperature the sulphide concentration had fallen to below 50 mg/ℓ. This had an impact on the appearance of the biofilm, which appeared increasingly brittle and crystalline. Despite the significant decrease in available sulphide at low temperature, the overall mass of biofilm harvested did not decrease to the extent expected. A calculation, based on the sulphide available for partial oxidation at each temperature indicated that less than 25% of the biofilm mass could be accounted for by sulphur at 15˚C and less than 10% at 10˚C. Additional analysis of the harvested biofilm will be conducted to determine the major components.

A comparison of the VSRR and extent of conversion between the acetate reactor (Figure 132) and the two lactate reactors illustrates how much more severely affected the acetate utilising community was by low temperature. The VSRR at 30˚C was similar across the three reactors, at around 13 mg/ℓ.h, but at 10˚C the rate in the acetate reactor was less than half that for the corresponding lactate reactors, with less than 10% of the sulphate in the feed being reduced.

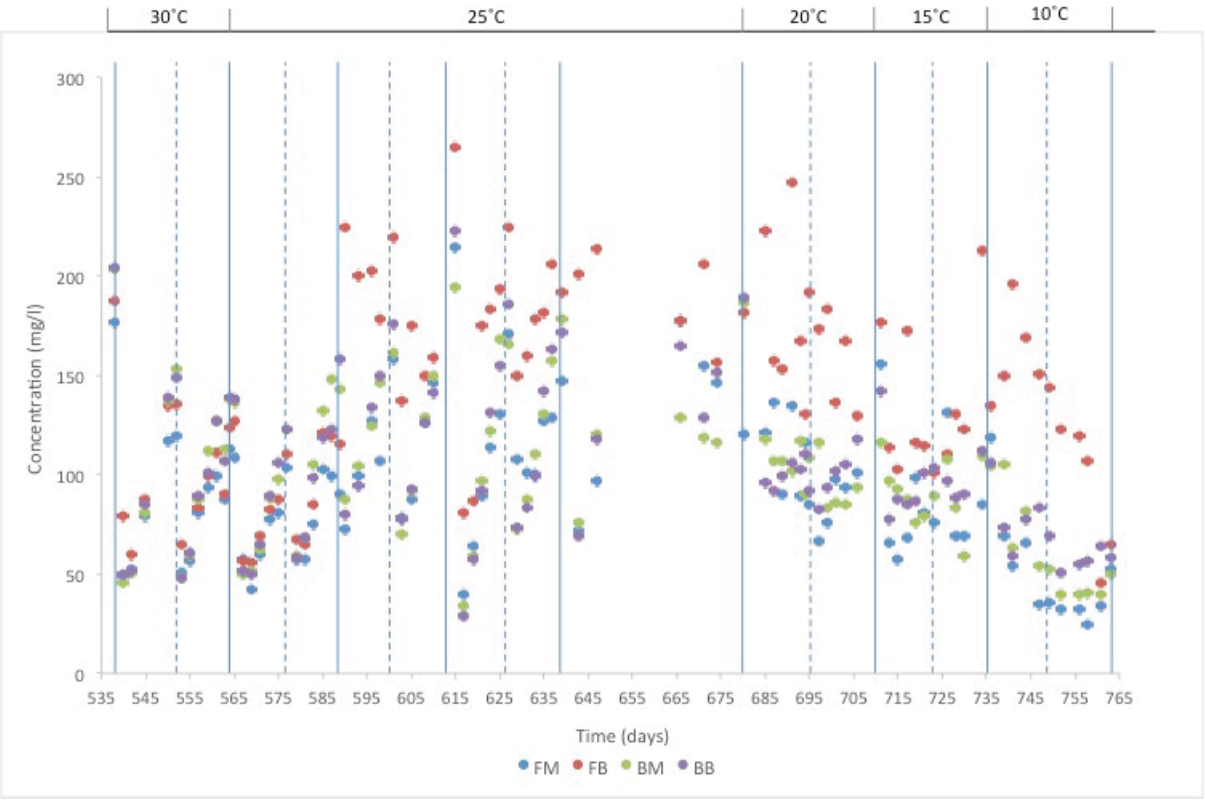

Figure 131: Graph showing aqueous sulphide concentration as a function of sample port and temperature for the 2 ℓ acetate fed reactor. Solid vertical lines represent biofilm harvesting events, while dashed lines represent biofilm disruption, but not harvesting

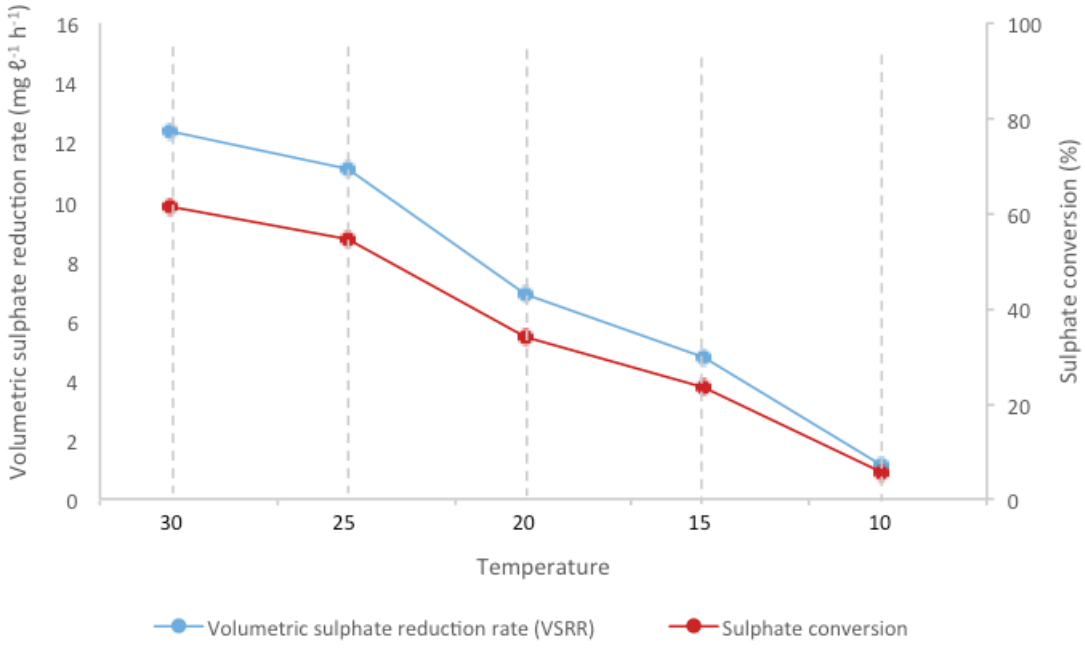

Figure 132: Comparison of mean volumetric sulphate reduction rate and sulphate conversion efficiency as a function of temperature for the 2 ℓ acetate fed reactor

6.3.4 Inoculum scale-up and pilot plant inoculation

The three 2 000 ℓ channel reactors were set adjacent to an active mine site in the Free State. Each reactor was placed on a purpose built steel stand, which provided additional structural support to prevent bulging of the walls of the Perspex reactors. The height of the stands has been staggered to facilitate gravity flow between the reactors when connected in series (Figure 133).

The first reactor was inoculated with around 380 ℓ of SRB inoculum on the 2nd of November 2015. The original intention was to use sufficient inoculum to achieve an initial sulphide concentration of around 150 mg/ℓ, to provide enough sulphide to form a complete biofilm across the surface of the reactor. However, due to a limited volume of inoculum being available the initial sulphide concentration was only 67 mg/ℓ.

After 24 hours a thin sulphur film had formed on the surface on the reactor (Figure 134), with the aqueous sulphide concentration being reduced to below 10 mg/ℓ at all points sampled. These data confirmed the presence of an active sulphide oxidising community.

The reactor was sampled again on the 10th of November and the aqueous sulphide concentrations remained low. The sulphate concentration had decreased from approximately 2 000 mg/ℓ to just over 1 700 mg/ℓ. While this showed some sulphate reduction activity, the rate (1.56 mg/ℓ.h) was significantly lower than equivalent rates achieved in the laboratory reactors.

The reactor was inoculated for a second time in May 2016, once a greater volume of inoculum had been generated. The initial sulphide concentration following inoculation was over 180 mg/ℓ, which was sufficient for the development of a complete biofilm over the surface of the reactor. After 72 hours a complete biofilm was visible and it was clear that a substantial amount of sulphate had already been deposited in the biofilm (Figure 134).

The evidence from the early stages of the pilot scale evaluation showed that the reactor could be scaled up to a 2000 ℓ volume and provided there is sufficient aqueous sulphide formation of the floating sulphur biofilm will occur at the same rate as observed in the laboratory scale reactors.

The pilot scale system has since been relocated to a second site in Mpumalanga and the evaluation of the system in continuous mode is the subject of a new WRC-funded project.

Figure 133: Photograph of the three pilot scale reactors at the pilot site. The 210 ℓ inoculum development drums are visible in the bottom right corner

Figure 134: Photograph of the pilot scale reactor 72 hours after inoculation showing complete biofilm development.

6.4 CONCLUSIONS

Following on from the successful demonstration of the proof of concept in the previous chapter, an extensive series of experiments was performed to evaluate the effect of reactor geometry, hydraulic retention time, temperature and primary electron donor. The following conclusions can be drawn from these experiments:

- The change in reactor geometry did not significantly affect the hydrodynamics within the reactor. The mixing pattern was consistent with the smaller reactor and difference in macromixing times across the two reactors was generally below 10% for all HTRs tested.

- Temperature did have a more significant impact on both the macromixing time and the mixing pattern, with extended mixing times at 10˚C and 40˚C. Despite this, the macromixing times were still less than 10% of the HRT, so the conceptual model remains valid.
- The residence time study provided very encouraging data. Almost complete sulphate reduction was observed at the 3 day and 2 day HRTs, with around 70% sulphate reduction achieved at a 12 hour HRT. The residual sulphate concentration remained relatively stable over six residence times at the 12 hour HRT, indicating that stable performance could be sustained.
- The aqueous sulphide concentration did decrease with decreasing HRT, from a maximum of around 250 mg/ℓ at a 3 day HRT to around 100 mg/ℓ at the 12 hour HRT. It was interesting to note that despite the lower aqueous sulphide concentration at the low HRTs, the magnitude of the decrease in sulphide concentration following biofilm disruption decreased substantially.
- Sulphate reduction performance in the hybrid LFCR was equivalent to other reactor configurations tested previously up to a 1 day HRT, but was substantially better than the CSTR and sealed LFCR at a 12 hour HRT, achieving a maximum rate of 62.5 mg/ℓ.h, almost equivalent the combined CSTR-membrane recycle reactor, despite being a passive system. This illustrates the benefits of biomass retention.
- The data support the hypothesis that a reduction in temperature will have a negative effect on the rate of sulphate reduction and sulphide oxidation.
- Temperature had a more significant effect on the acetate fed system, with an almost 90% reduction in the sulphate reduction rate and conversion efficiency as a consequence of decreasing the temperature from 30˚C to 10˚C.
- The acetate fed reactor was generally less stable and predictable than the lactate fed reactors, indicating that acetate utilising species are more susceptible to a range of environmental factors.
- The lactate fed reactors showed greater resilience, with the decrease in sulphate reduction rate closer to 50% over the temperature range tested.
- At 15˚C and below incomplete utilisation of lactate was observed, indicating that the lactate fermenting species are also significantly inhibited at low temperature.
- Despite the presence of residual acetate and sulphate in the lactate fed systems there was no evidence to suggest supplementary sulphate reduction by acetate utilising species, suggesting they are effectively excluded from lactate fed systems.
- For the lactate fed reactors, the overall performance across the temperature range was similar for the 2 ℓ and 8 ℓ reactors, suggesting that aspect ratio did not significantly affect performance.
- An increase in aqueous sulphide in the effluent at low temperature suggests that the sulphide oxidisers are more significantly affected by low temperature, or that the disparity between volume (sulphate reduction occurs in the bulk volume) and surface area (partial sulphide oxidation occurs in the floating biofilm) assumes greater relevance at lower temperature.
- While the lactate fed reactors performed better than the acetate fed reactor, lactate is not a viable electron donor for larger scale application, both due to cost and the fact that it is only partially oxidised, resulting in an effluent stream that still has a high COD.
- Data from the pilot site showed that the microbial consortium could achieve near complete sulphate reduction using acetate as the electron donor in large batch reactors (210 ℓ drums), although the rates were low. The floating sulphur biofilm formation in the pilot scale reactor was consistent with laboratory scale data, both in terms of FSB structure and formation rate, suggesting that the reactor can be scaled up successfully.

CHAPTER 7: MICROBIAL FUEL CELL

7.1 BACKGROUND

7.1.1 Microbial Fuel Cells

A microbial fuel cell (MFC) is an electrochemical device that makes use of the catalytic action of microorganisms to convert chemical energy to electrical energy (Kim *et al.*, 2002; Jang *et al*., 2004; Liu and Logan, 2004; Du *et al.*, 2007; Jiang and Li, 2009). The microorganisms oxidise biodegradable organic substrates and recover the electrons to the anode of the MFC, instead of a soluble electron acceptor. The electrons then travel through an external circuit and are consumed in a reduction reaction at the cathode electrode. Therefore, in the closing of the circuit, electricity is produced (Wang *et al*., 2012; Jiang and Li, 2009).

Previously, MFCs have typically had two chambers: the anode which houses the bacteria and the cathode, generally aqueous, into which air is bubbled so that oxygen can be reduced. The two compartments are separated by a proton exchange membrane (PEM) (Liu and Logan, 2004; Jang *et al*., 2004; Du *et al*., 2007; Sukkasem *et al*., 2011). The PEM allows the protons to diffuse through the PEM to be used in the oxidation reaction at the cathode, which completes the electrical circuit. It also helps to physically block the transfer of the oxygen into anode chamber (Liu *et al*., 2005).

The set-up of a typical two-chamber fuel cell is shown in Figure 135 below.

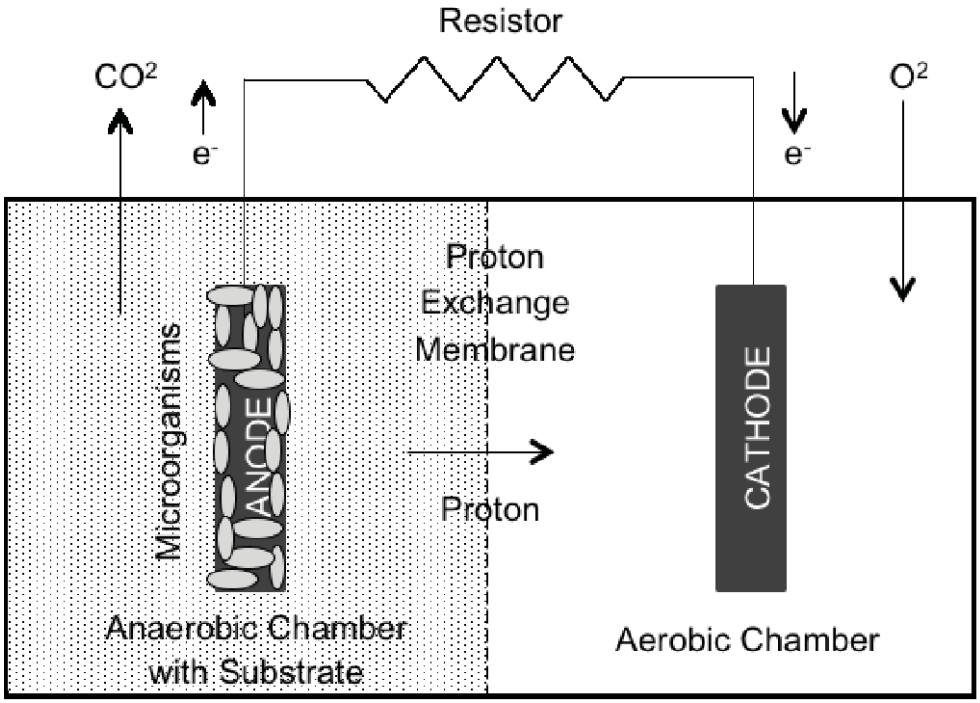

Figure 135: Schematic diagram of a typical two-chamber MFC

The anodic chamber of the MFC must be kept anaerobic in order to keep the microorganisms separated from oxygen and any other terminal electron acceptor, other than the anode, in order to achieve electrical current generation (Du *et al.*, 2007).

7.1.2 Application in Wastewater Treatment

It is evident from literature that several different configurations of MFCs, capable of producing electricity while oxidising substrate, are possible. It is also clear that several different microorganisms and substrates can be used.

MFCs have shown potential for use in wastewater treatment and several integrated MFC-wastewater treatment systems have already been attempted. These include the addition of an MFC into a simple aeration tank (Chen *et al.*, 2010), an MFC incorporated into a membrane bioreactor (MFC-MBR) (Wang *et al*., 2012; Su *et al.*, 2013) and an MFC added to a sequencing batch reactor (MFC-SBR) (Wang *et al*., 2014). There was a clear opportunity to evaluate the integration of MFCs with the wastewater treatment reactors used in this research.

An integrated MFC-wastewater treatment reactor could minimise pre-treatment steps and potentially result in improved wastewater treatment, with simultaneous power production. Integrated systems have been previously attempted and were shown to have many benefits to wastewater treatment, other than power production, such as improved sludge removal (Su *et al.*, 2013) and COD removal (Wang *et al.*, 2012). In the large scale processing of wastewater, the energy costs are significant and the concurrent production of electricity could potentially offset these. At this stage, it could not realistically produce enough electricity to surpass them.

A system of particular interest is the community of sulphate reducing bacteria (SRBs) and sulphide oxidising bacteria (SOBs) digesting ARD waste in a linear flow channel reactor (LFCR). MFC systems that utilise a mechanism in which SRBs reduce sulphate to sulphide which, in turn, is oxidised to sulphur, polysulphides or back to sulphate at the anode have been demonstrated (Rabaey *et al.*, 2006; Zhao *et al*., 2008). This was largely dependent on the potential of the anode.

The LFCR contains carbon fibres, which are suspended in the bulk liquid in order to support a microbial. These could function as an anode, as carbon fibres are conductive and are the site where significant bacterial action is taking place. This has been demonstrated in the plant bio photovoltaic fuel cell. With the considered addition of a cathode electrode, the LFCR has the potential to be modified to produce electricity, as well as function as a wastewater treatment reactor.

7.1.3 Research Approach

This research aimed to construct an integrated LFCR-MFC system and assess its performance in terms of wastewater treatment and electricity generation.

In order to have a baseline to which the electricity production of the system could be compared, it was necessary to construct a model MFC, which had previously been shown to produce electricity. The chosen base-line MFC design was consistent with a design from literature on which significant research has been conducted (Liu and Logan, 2004; Liu *et al.*, 2005; Cheng *et al.*, 2006; Cheng and Logan, 2007; Logan *et al.*, 2007; Xing *et al.*, 2008). In order to validate the assembly of the constructed MFC, the performance of a pure microbial culture (*Shewanella oneidensis* MR-1) in the constructed MFC was tested and compared to published data (Couperthwaite, 2016)

The work detailed in this document describes the use of a mixed culture of SRB and SOB for treating synthetic ARD in a single-chambered MFC in order to test the ability of the community to produce electricity, in addition to reducing sulphate in the ARD.

7.2 MATERIALS AND METHODS

The methodology for the construction and operation of the MFC were essentially identical to those of Wu *et al*. (2013). Using the same basic methodology, the performance of the SOB and SRB cultures in the MFC were assessed. Thereafter, a LFCR-MFC was set up and evaluated.

7.2.1 Cultivation of SRB and SOB consortium

A stock culture comprising of a consortium of SOBs and SRBs was grown at 30°C in a Schott bottle with constant low speed stirring in modified Postgate medium consisting of (per litre) 0.5 g KH_2PO_4, 1.0 g NH_4Cl, 2.0 g $MgSO_4.7H_2O$, 0.33 g Na_2SO_4, 1.0 g yeast extract, 0.3 g sodium citrate, 1.6 mℓ 60% sodium lactate (10 mM). For the single chambered MFCs, a 100 mℓ aliquot of modified Postgate medium was prepared at a 1.25x concentration and 25 mℓ of the stock culture added, resulting in media with the same concentration per litre as given above. The resultant cell concentration was found to be $1.18x10^9$ cells/mℓ, by direct cell counting under a light microscope. This was then used for the set-up of the four single-chambered MFCs.

For the LFCR-MFC, the same stock culture of SRBs and SOBs was used; however the culture was added directly to the reactor without dilution. This was done in an attempt to colonise the carbon microfiber anode rapidly and to provide a high concentration of sulphide necessary for the formation of the floating sulphur biofilm.

For the first 19 days after inoculation, the reactor was sampled and thereafter immediately seeded with 50 mℓ of effluent from an existing 2.125 ℓ LFCR operating at a 4 day residence time at 30°C and fed with the same modified Postgate medium shown above. This was done in an attempt to compensate for wash out of the SRB and SOB and improve colonisation of the anode by adding an active SRB culture.

7.2.2 Single-chambered MFC operation

Four identical MFCs were constructed out of Perspex to have a chamber diameter of 3 cm and length of 4 cm, resulting in a working volume of 28 mℓ (Figure 136). Stainless steel discs were used as current collectors on the anode side and stainless steel rings were used on the cathode side to allow for diffusion of air. Two Perspex ends (Figure 136), were used to hold the electrodes and current collectors in place when the assembly was bolted together. The cathode end had a hole 3 cm in diameter to allow for diffusion of air.

Carbon felt (10% wet proofed) was used for both the anode and cathode (7 cm^2). The air-cathode was coated with 2 mg/cm^2 of Pt (40 wt.% Pt/C) (unless otherwise stated) and a Nafion (5%) binder on the liquid facing side.

The cells were operated individually in parallel with a 100 kΩ resistor (unless otherwise stated) over which the cell voltage was measured (mV) at one minute intervals using a data logger (National Instruments) and recorded to a personal computer. A schematic of this setup is seen in Figure 137.

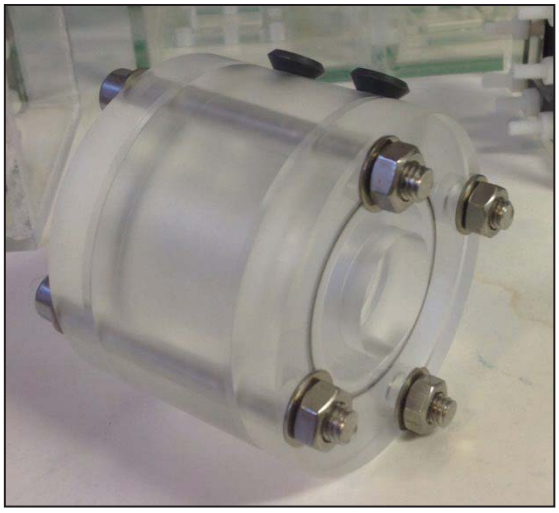

Figure 136: Photo of the constructed single chamber microbial fuel cell used in Shewanella and SRB/SOB MFC studies

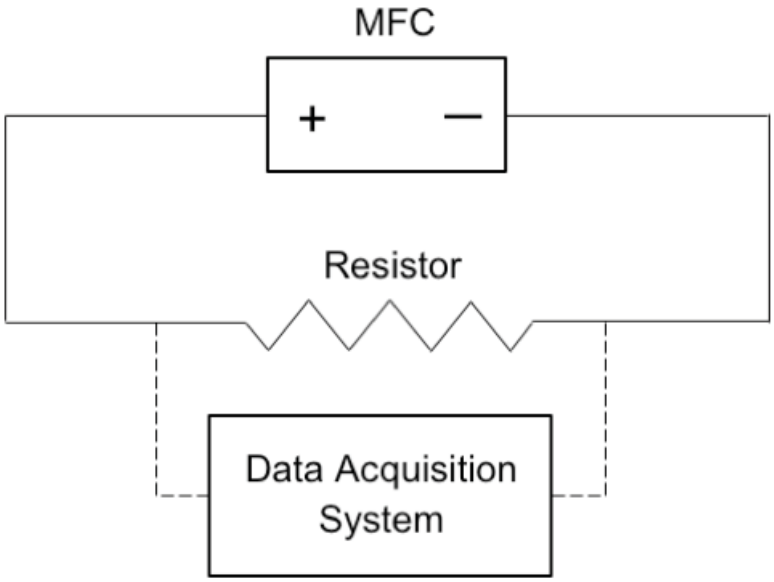

Figure 137: Schematic of electrical circuit setup for the microbial fuel cell

MFCs were sterilised with 200 vol H_2O_2 overnight before inoculation and temperature was maintained at 30°C by means of an incubator. As a result of the poor attachment of the SRB community, the MFC was fed by replacing 10 mℓ of spent media with fresh, concentrated medium every 2 days. Concentrated medium was identical to the modified Postgate medium given above, but the lactate and sulphate concentrations were increased to 15 mM. Therefore, replacing 10 mℓ of medium resulted in a fresh lactate and sulphate concentration of approximately 5.5 mM throughout the cell.

7.2.3 LFCR-MFC Operation

The LFCR-MFC was a rectangular Perspex reactor, which was open to the air at the top. The reactor was 110 mm long and 100 mm wide. An inflow and outflow valve was positioned at either end of the reactor 85 mm from the base. This allowed for a working volume of 935 mℓ.

Sampling ports were located on each end of the reactor below the inlet and outlet ports and 50 mm from the base, as well as on the side panels, 14 mm and 85 mm from the base and 18.5 mm from each end respectively. The experimental set-up of the reactor is depicted in Figure 138.

A cathode electrode, 50 mm in diameter was located on each side of the reactor with its centre 50 mm from the base. The electrodes were prepared using the same method as for the single-chambered MFCs, given above. An anode electrode was constructed by manually attaching carbon microfibers to the stainless steel rod with stainless steel wire. The brush was 100 mm long and had a diameter of 80 mm (Figure 139). As it was impossible to determine to what extent the carbon microfibers would splay and therefore the surface area of microfibers, the ratio of mass of microfibers to cathode area was kept constant at 0.1 g/cm^2 of cathode.

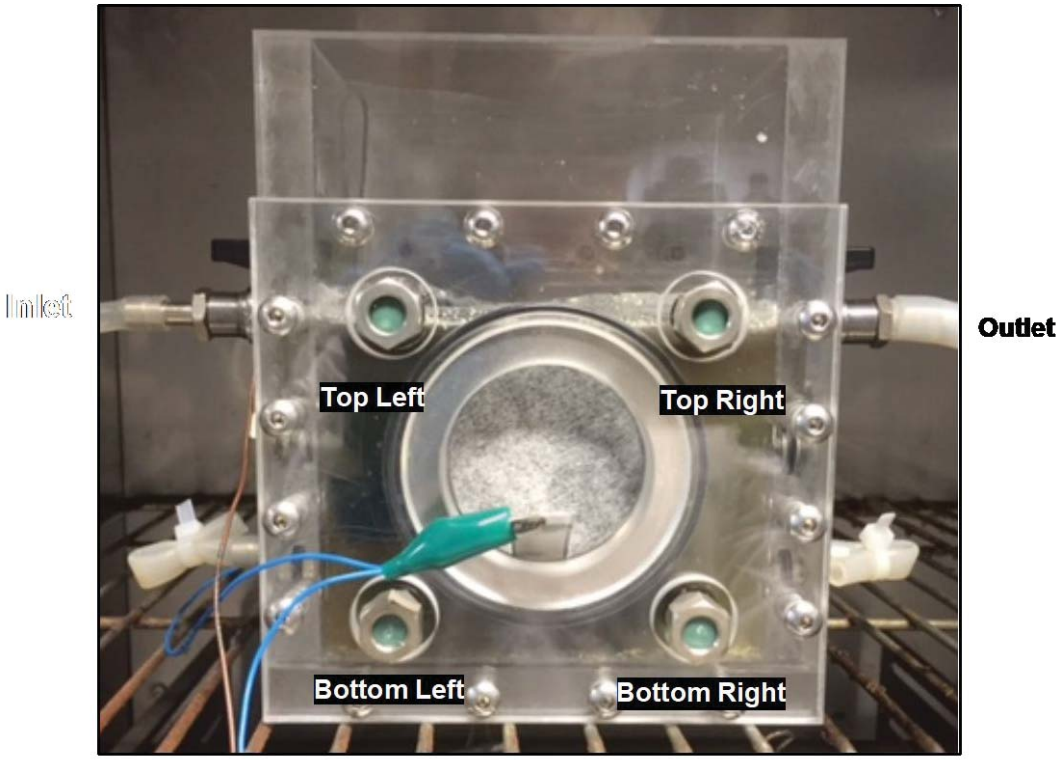

Figure 138: Photograph of LFCR-MFC set-up

The LFCR-MFC was sterilised with 200 vol H_2O_2 overnight before inoculation. The reactor was operated at a four day residence time which corresponded to a flow rate of medium of 0.162 mℓ/min. The reactor was fed modified Postgate Medium with 10 mM lactate concentration, as specified above. The temperature was maintained at ambient laboratory temperature (approximately 25°C).

The reactor was sampled as follows: 2 mℓ of sample was drawn using a syringe and needle from the sampling ports on either end of the reactor and the two lower sampling points on the side of the reactor on a daily basis. A further 6 mℓ of sample was drawn from the top of the reactor at the outlet.

Figure 139: Photograph carbon microfiber brush anode

7.2.4 Electrical Analysis

The data logger logged a potential difference value every minute for the duration of the experiment. The graphs of potential difference as a function of time were plotted using the average potential difference across 30 minute intervals, i.e. for each time point plotted, the potential difference for that point is an average of the 30 logged potential differences preceding it.

7.2.5 Chemical Analysis

For the purpose of sampling the single-chambered MFCs, triplicate 2 mℓ samples were taken. A sulphide assay (section 2.4.4) was done on each of the triplicate samples before the remainder was used for VFA measurement by HPLC (section 2.4.8), sulphate measurement by IC (section 2.4.6) and COD (section 2.4.7) assays, the latter to provide an indirect measure of available organic carbon. The remaining volume was used to measure the redox potential relative to the Ag/AgCl reference electrode and the pH of the sample (section 2.4.3).

In the case of the LFCR-MFC system, a sulphide assay was conducted on each 2 mℓ sample, taken daily from each sampling port and effluent. The remaining sample was used for both VFA analysis and sulphate measurement. The residual volume from the effluent sample was used to measure the redox potential and pH and to conduct a COD assay.

After reading the redox potential and pH and conducting a sulphide assay on the samples, 40 µℓ of $ZnCl_2$ solution (100 g/ℓ) was added to precipitate out the hydrogen sulphide. Samples were centrifuged at 14500 x *g* for 10 minutes and filtered through a 0.22 µℓ cellulose filter. These samples were then frozen until such time as HPLC, IC and COD assays could be conducted.

Samples were then analysed for COD content, to be used for determining Coulombic efficiency (CE). The CE gives an indication of fraction of the lactate digested in the MFC that was converted into electricity. The total current produced in a single feeding cycle was determined by integration of the potential versus time graph for that cycle. The change in COD concentration for that feeding cycle was then determined and the Coulombic efficiency could be determined by equation 20 below, where M is the molecular weight of oxygen (32 g/mol), I is the current (A), t is the operation time (s), F is Faraday's

constant, b is the number of electrons exchanged per mole of oxygen (4 mole-/mol) and V is the volume of the single chamber (m^3).

$$CE = \frac{M \int_0^t I dt}{FbV\Delta COD} \qquad \text{Equation 20}$$

7.3 RESULTS

7.3.1 Performance of Single-Chambered MFCs

Three single chambered MFCs were operated with a mixed SRB/SOB consortium growing on lactate and sulphate with intermittent media replenishment. A general trend in the maximum potential difference was noted for all three single-chambered MFCs. The maximum potential for each feeding cycle increased with time over the first few days after inoculation until a maximum was reached (Figure 140, Figure 141 and Figure 142). In the case of both MFC 1 and MFC 2, the maximum potential was maintained for a few feeding cycles before decreasing. In the case of MFC 1 the decrease was slow, whereas for MFC 2 the potential drops dramatically on day 27, without recovery.

MFC 3 achieved a reasonably stable maximum cell potential within 6 days (Figure 142). As a result of its reproducibility the cell was placed in parallel with a smaller resistor (10 kΩ) between days 14 and 18. As a result of the very low potential difference achieved during this time and the decrease in maximum cell potential achieved, the resistor was changed back to 100 kΩ for the remainder of the experiment.

A polarisation curve was plotted for MFC 3 and is given in Figure 143. A maximum power density of 2.86 mW/m^2 of cathode area was achieved. The maximum power density of an MFC is achieved when the resistance in the external circuit is equal to that of the internal resistance of the fuel cell. An estimation of the internal resistance of the cell can therefore be made by using slope of the linear region of the polarisation curve and from the maximum power density (Logan, 2008). The calculation of the slope of the linear region of the curve of potential difference versus current (Figure 143) revealed that the internal resistance of the MFC was approximately 20 600 Ω.

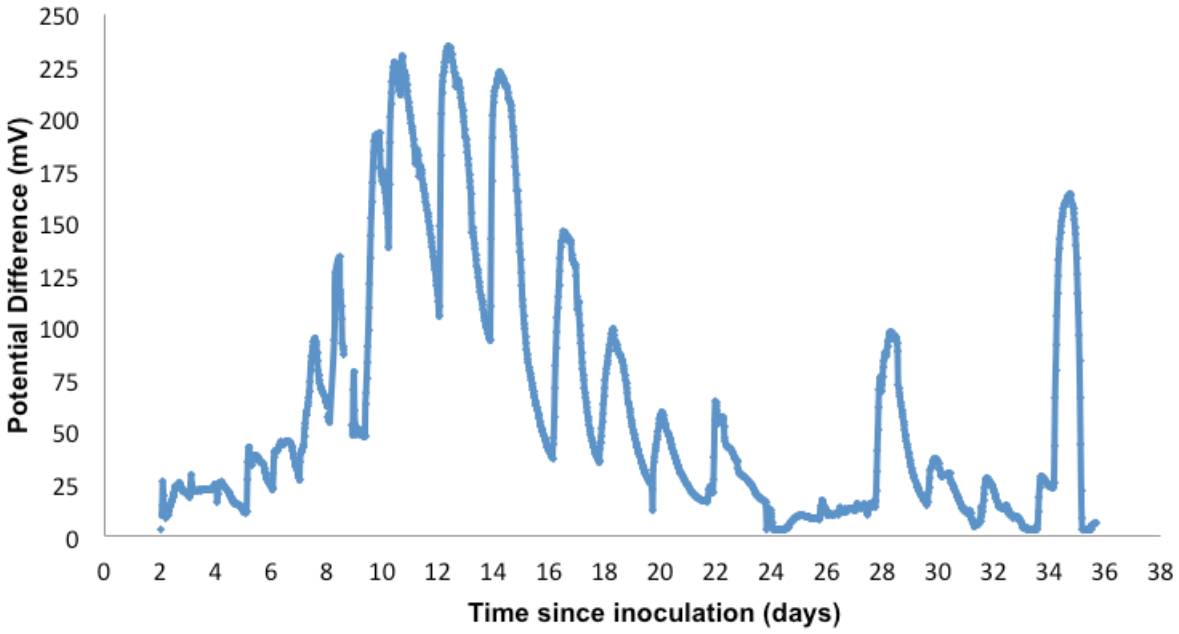

Figure 140: Cell potential versus time for MFC 1 fed 10 mM lactate in parallel with a 100 kΩ resistor and 0.2 mg/cm^2 of Pt on the cathode

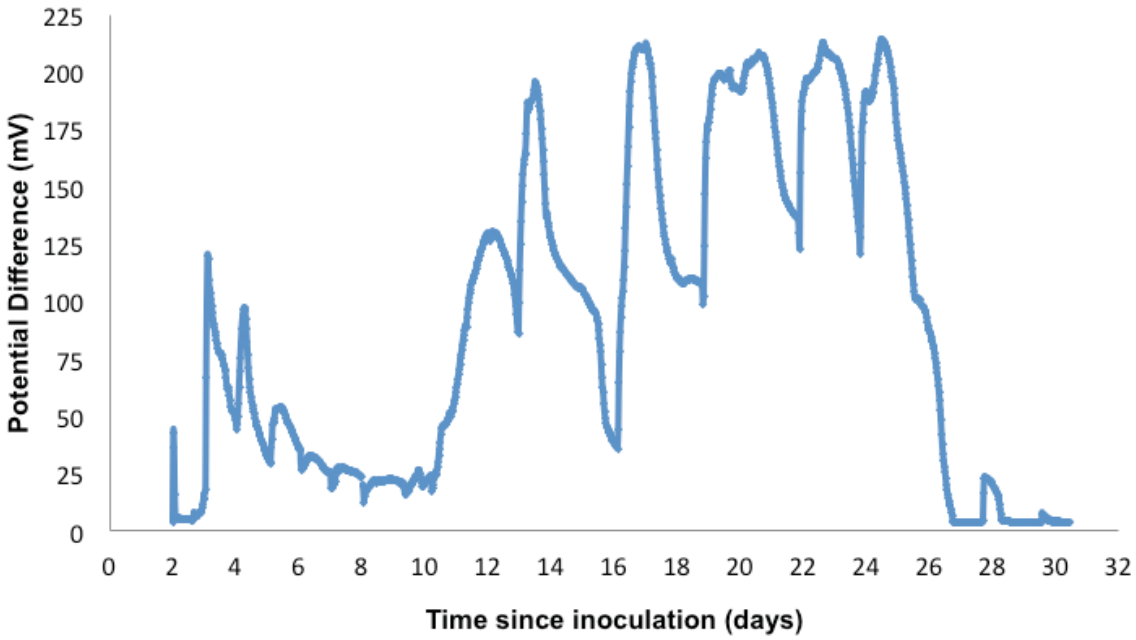

Figure 141: Cell potential versus time for MFC 2 fed 10 mM lactate in parallel with a 100 kΩ resistor and 0.2 mg/cm^2 of Pt on the cathode

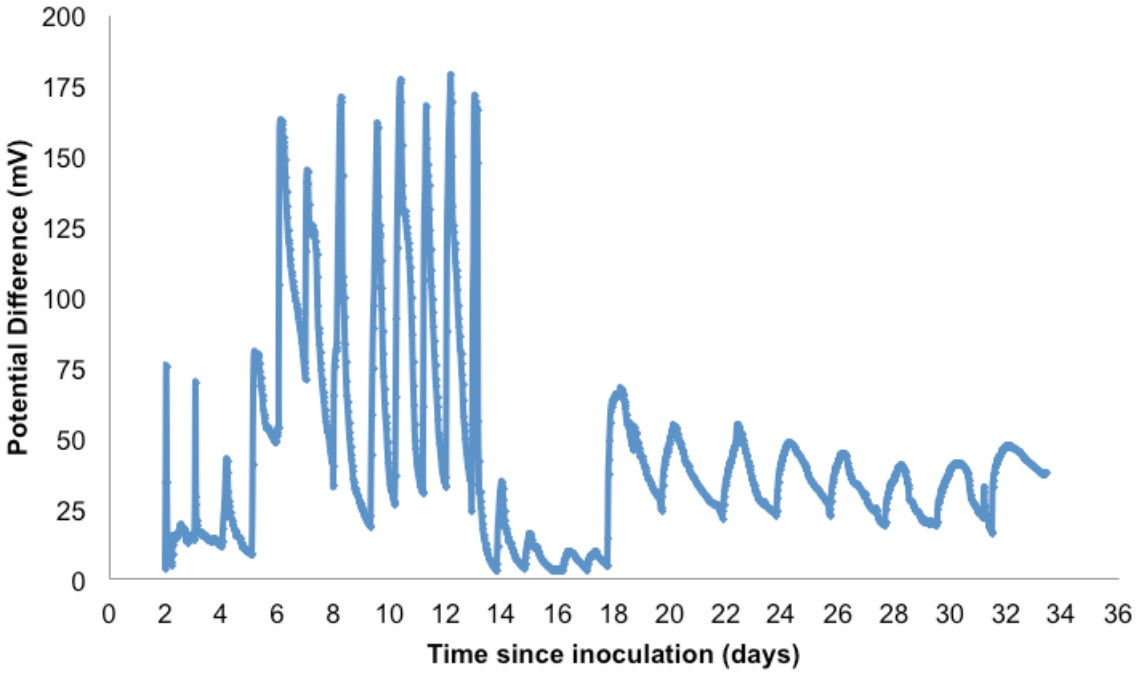

Figure 142: Cell potential versus time for MFC 3 fed 10 mM lactate in parallel with a 100 kΩ resistor and 0.2 mg/cm^2 of Pt on the cathode

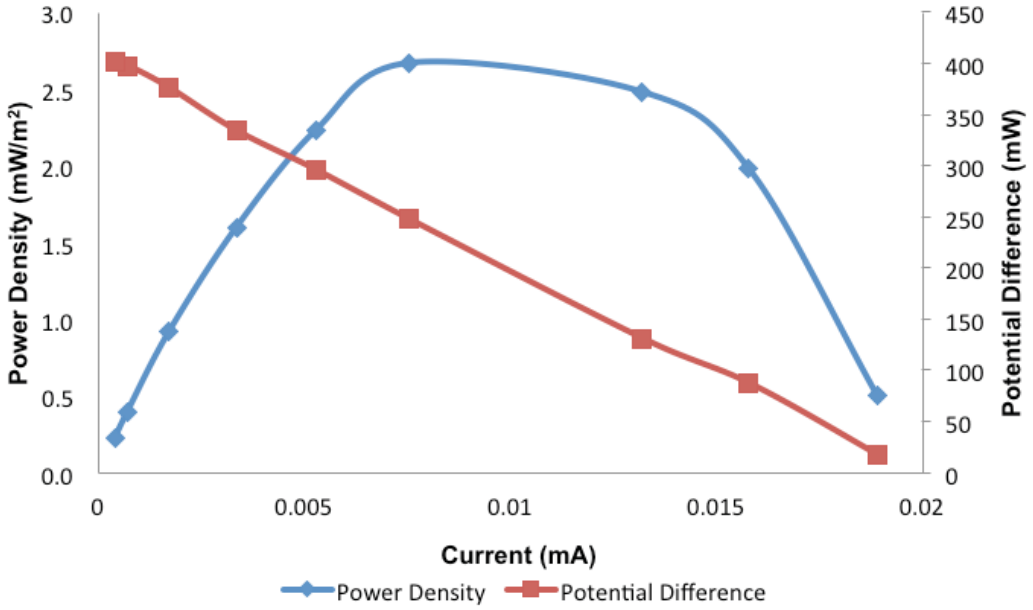

Figure 143: Power density and potential difference versus current for MFC 3

The single-chambered MFCs were fed with concentrated medium (15 mM), which resulted in a sulphate concentration of approximately 550 mg/ℓ in the MFCs when 10 mℓ of liquid contents were replaced with fresh medium.

For the duration of the experiment, the sulphate concentration within the MFC decreased (Figure 144). The rate at which the concentration decreased was similar for MFCs 1, 2 and 3. If no sulphate was reduced in the system, the sulphate concentration would become 15 mM within 8 feeding cycles, as can been seen in Figure 144. It is therefore evident that sulphate was reduced by SRBs in the system. It was also noted that the sulphate concentration was reduced to below the value of the feed (15 mM) at approximately day 11-12 for MFCs 1 and 3, but only at around day 19 for MFC 2.

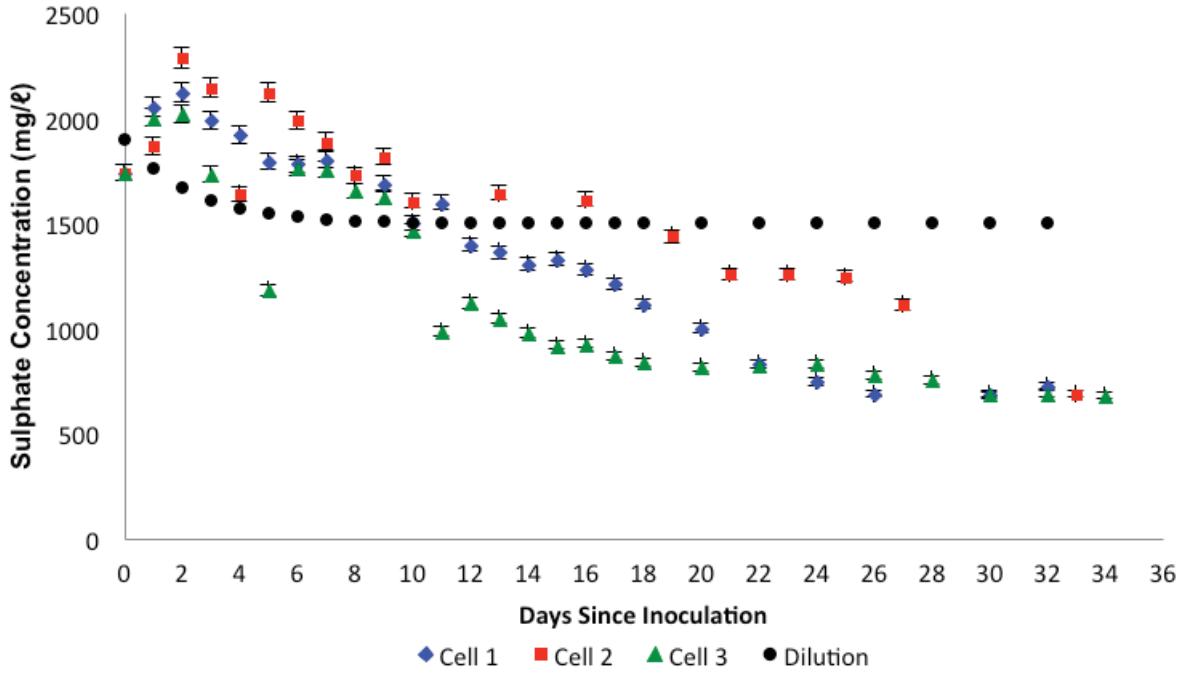

Figure 144: Sulphate concentration versus time for 3 MFCs fed concentrated modified Postgate medium

Although sulphide assays were conducted on every sample taken from each of the MFCs, the sulphide concentration was often found to be too low to be detected by the assay. Only MFC 3 had notable sulphide concentrations. The sulphide concentration as a function of time is plotted in Figure 145. It is noted that sulphide is only found in the MFC at day 10 after inoculation. The concentration then remains below 30 mg/ℓ until day 29, before increasing dramatically in the last few days of the experiment to reach a maximum of 111 mg/ℓ.

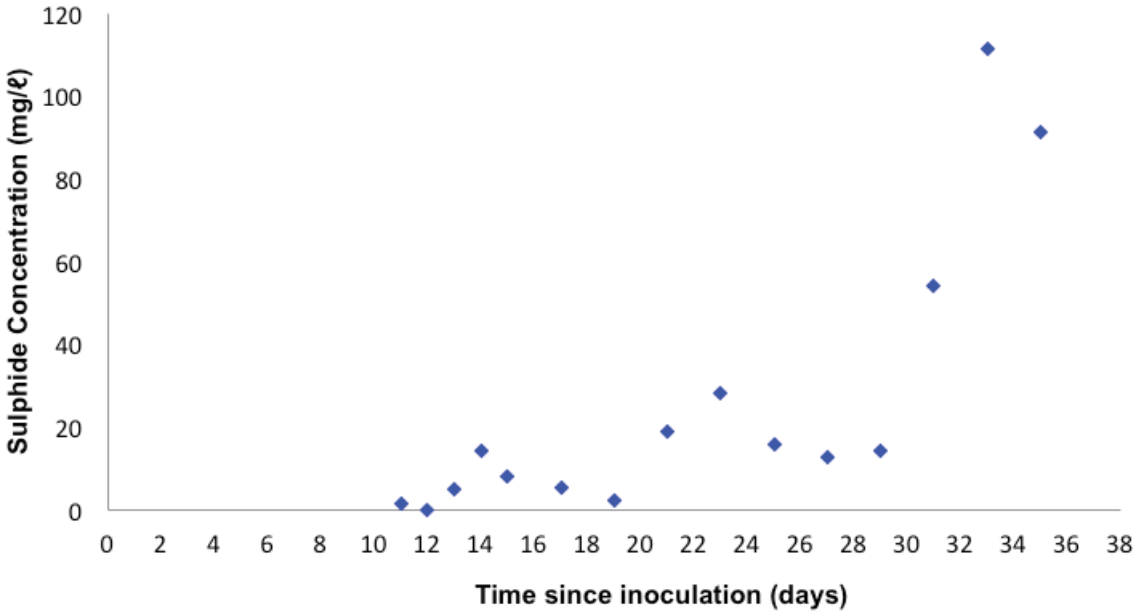

Figure 145: Sulphate concentration versus time for MFC 3 fed concentrated modified Postgate medium

Initially the COD in all three MFCs decreased rapidly before gradually increasing for the remainder of the experiment (Figure 146). The rate of increase was similar for all three MFCs. The minimum concentration of COD occurred from day 4 to 16 for MFCs 1, 2 and 3. During this time the COD remained below 500 mg/ℓ.

Although lactate, acetate, propionate, butyrate, iso-butyrate, valerate and iso-valerate were detected by HPLC in many of the samples taken from the MFCs, only the concentration of lactate, acetate and propionate are shown. Concentrations of the remaining volatile fatty acids were typically much lower than that of acetate and propionate and remained fairly constant throughout the duration of the experiment. They were also not present in earlier samples.

As can been seen from the profile of VFA concentration as a function of time (Figure 147, Figure 148 and Figure 149), the lactate concentration decreased rapidly for all three MFCs, to almost 0 mg/ℓ within the first 5 days and remained low for the remainder of the experiment. Acetate was initially present as a result of it being present in the inoculum, but also decreased to very low concentrations within 2 or 3 days after inoculation.

Between day 12 to 14, the concentration of acetate and propionate began to increase for all three MFCs. This increase in VFA concentration corresponded to the increase in COD seen in Figure 146. MFCs 2 and 3 (Figure 148 and Figure 149) had similar concentrations of acetate and propionate and both increased for the remainder of the experiment.

MFC 1 (Figure 147) showed a dramatic increase in propionate from day 16 to 24, reaching a maximum at around 1 100 mg/ℓ before decreasing again to below 150 mg/ℓ by day 30. It then remained low for the remainder of the experiment.

As can be seen from potential difference versus time graph for MFC 1 (Figure 140), the maximum cell potential reached with each feeding cycle begins to decrease from day 12 and reaches a minimum on day 14. This corresponded directly to the increase in propionate in the system during this time as shown by Figure 147. The maximum cell potential reached by MFC 1 increased after day 24, which corresponded to the lower concentration of propionate. Propionate is a product of lactate fermentation, rather than oxidation by SRB.

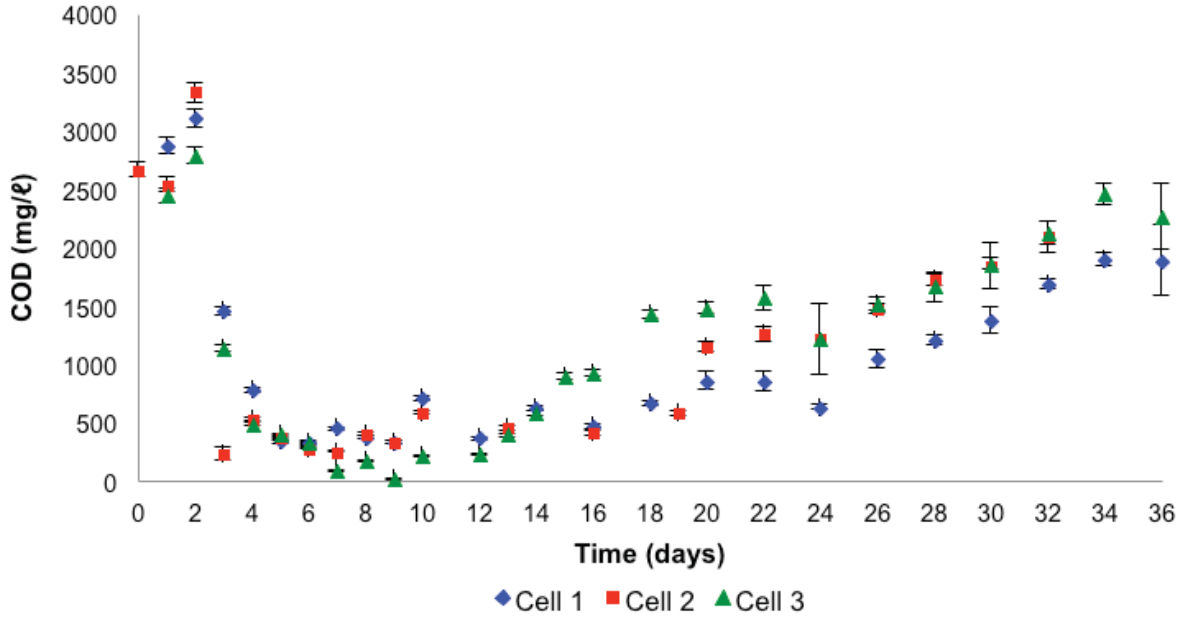

Figure 146: COD concentration versus time for 3 MFCs fed concentrated modified Postgate medium

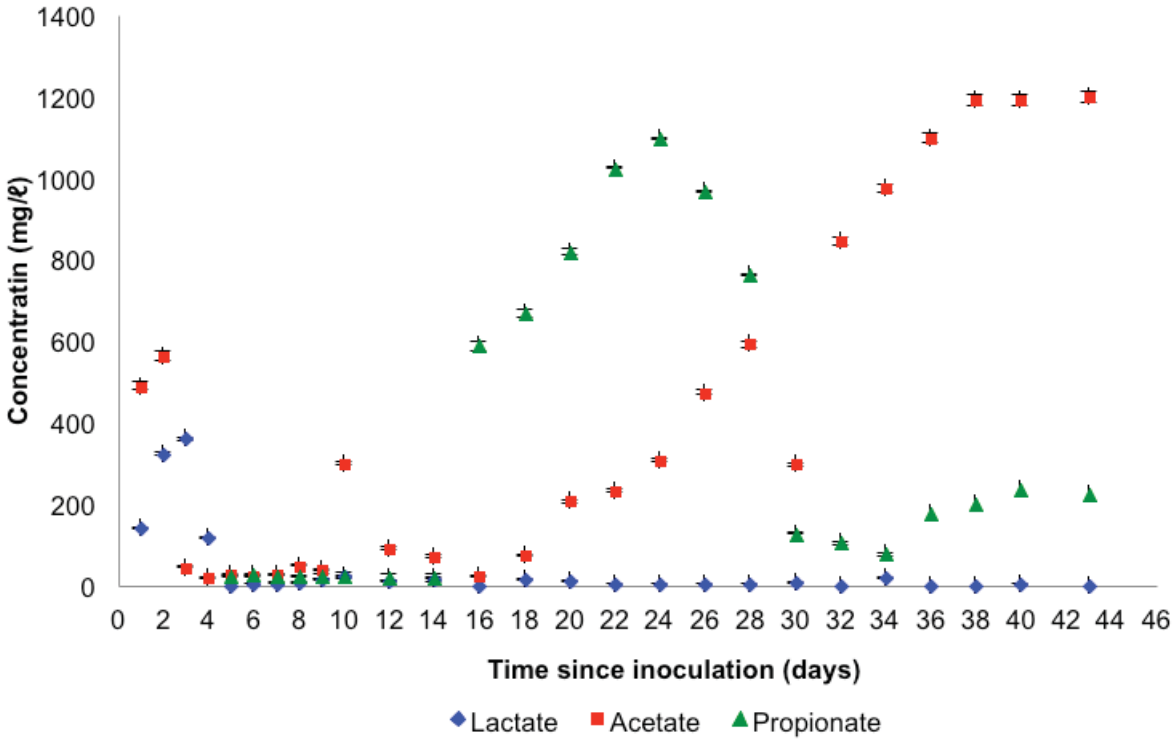

Figure 147: Concentration of volatile fatty acids versus time for MFC 1 fed concentrated Modified Postgate Medium

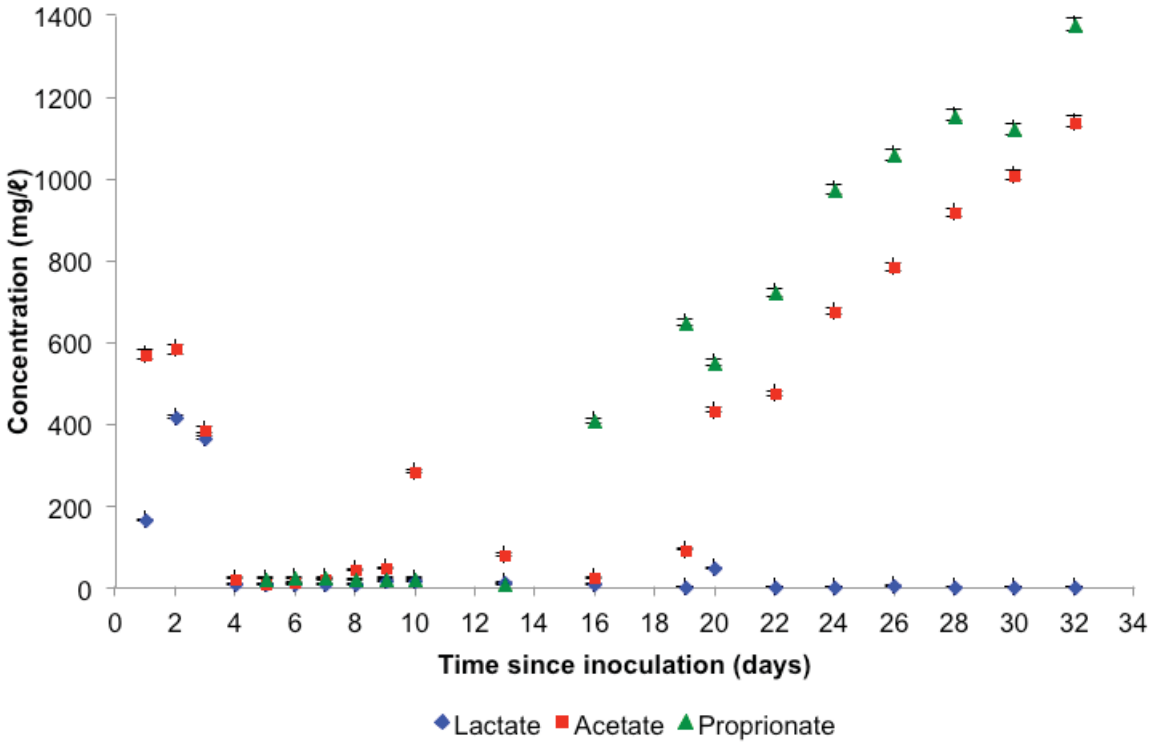

Figure 148: Concentration of volatile fatty acids versus time for MFC 2 fed concentrated modified Postgate medium

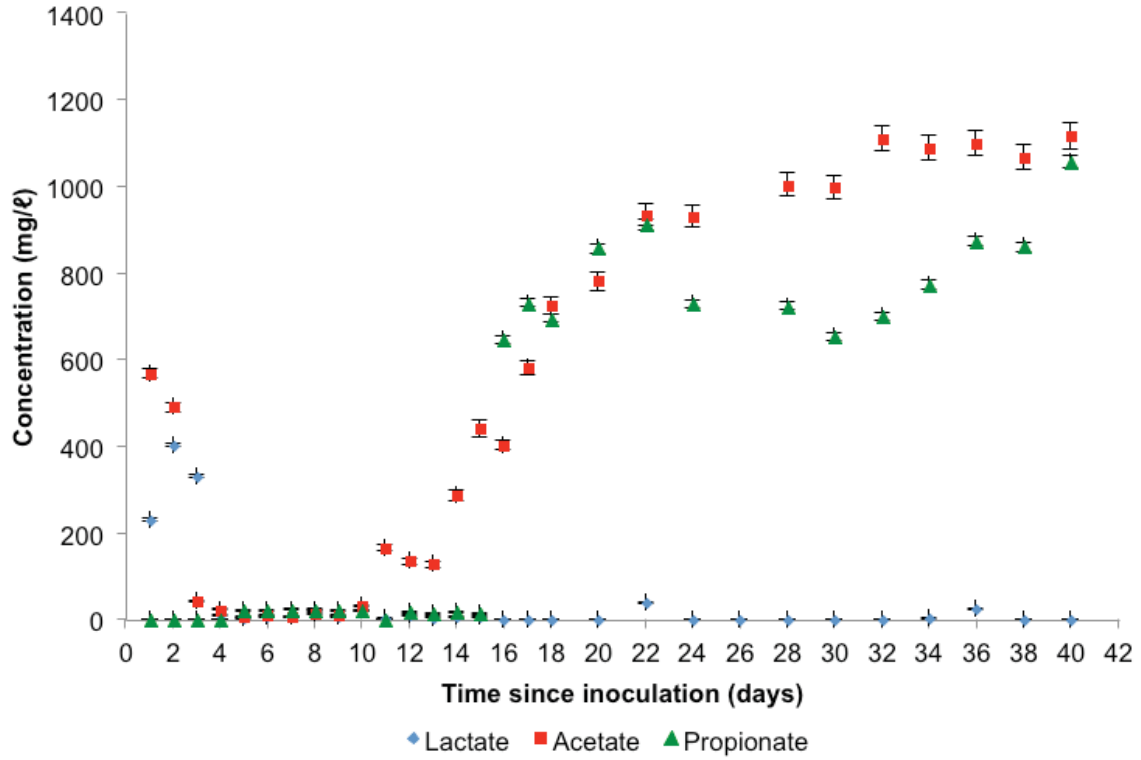

Figure 149: Concentration of volatile fatty acids versus time for MFC 3 fed concentrated modified Postgate medium

7.3.2 Performance of LFCR-MFC

After inoculation, the potential difference over the LFCR-MFC increased dramatically before reaching a maximum on the 4th day at almost 450 mV. Thereafter, it decreased gradually before remaining fairly

stable around 200 mV from day 19 onwards (Figure 150). This corresponded to the seeding of the reactor, which was stopped after day 19.

On day 34 of the experiment, once the potential difference had stabilised around 200mV and was consistent from day to day, a polarisation curve was plotted for the reactor. A maximum power density of 2.56 mW/m^2 of cathode area (9.10 mW/m^3) was achieved using a 1 kΩ. The gradient of the potential difference versus time curve for the LFCR-MFC (Figure 151) revealed that the internal resistance of the MFC was approximately 980 Ω.

The sulphide concentration measured in solution provides evidence of sulphate reduction within the system. After day 19 of the experiment, from which point the reactor was no longer seeded with effluent, trends in sulphide concentrations began to emerge (Figure 152). The concentration of sulphide in the lower level of the reactor was consistently higher than that of the levels above it. The bottom left corner of the reactor was found most frequently to have the highest concentration of sulphide, followed by the bottom right hand corner. The top left corner also had a higher concentration than the top right corner. Medium was fed on the left hand side of the reactor. The concentration of sulphide in the effluent is consistently low (approximately 20-30 mg/ℓ) compared to the sulphide concentration in the reactor (50-150 mg/ℓ). In the last 10 days of the experiment the sulphide concentration was reasonably reproducible between 50-100 mg/ℓ. This pattern was consistent with operation of the standard LFCR.

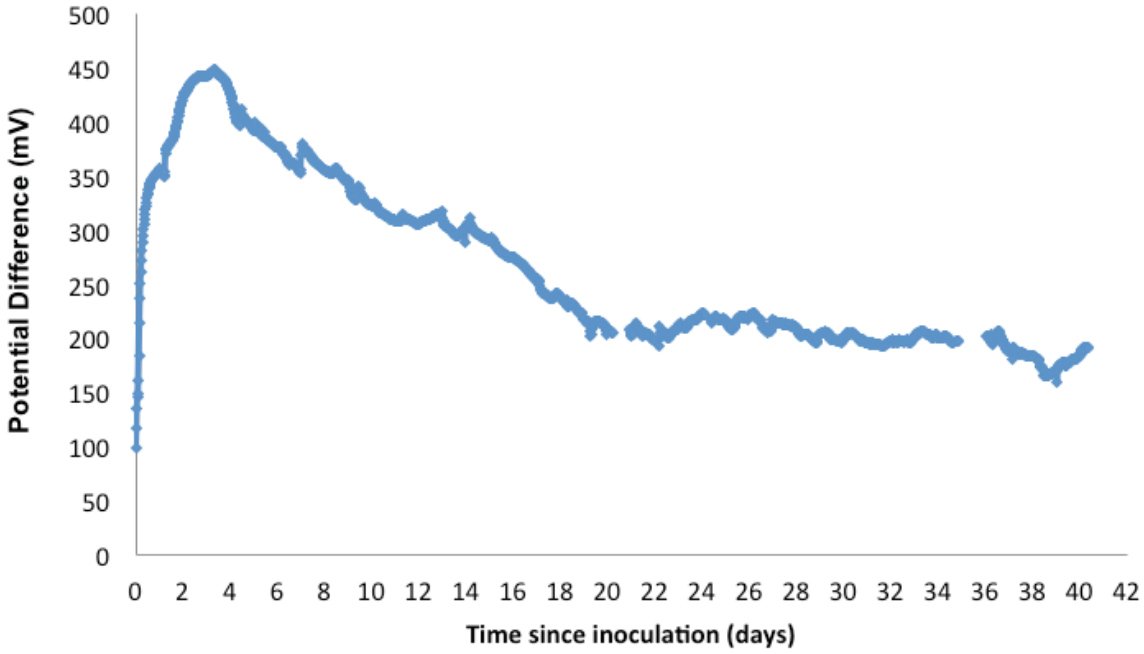

Figure 150: Potential difference versus time for the LFCR-MFC in parallel with a 10kΩ resistor and fed 10mM lactate

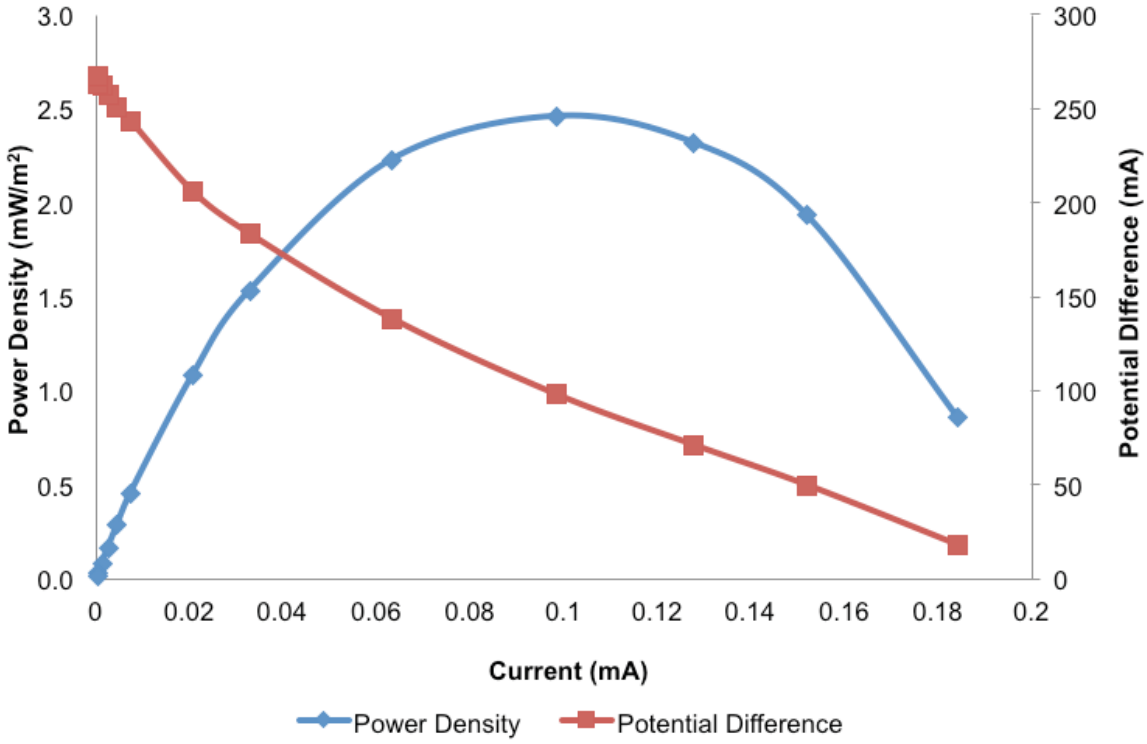

Figure 151: Power density and potential difference versus current for the LFCR-MFC fed 10mM lactate

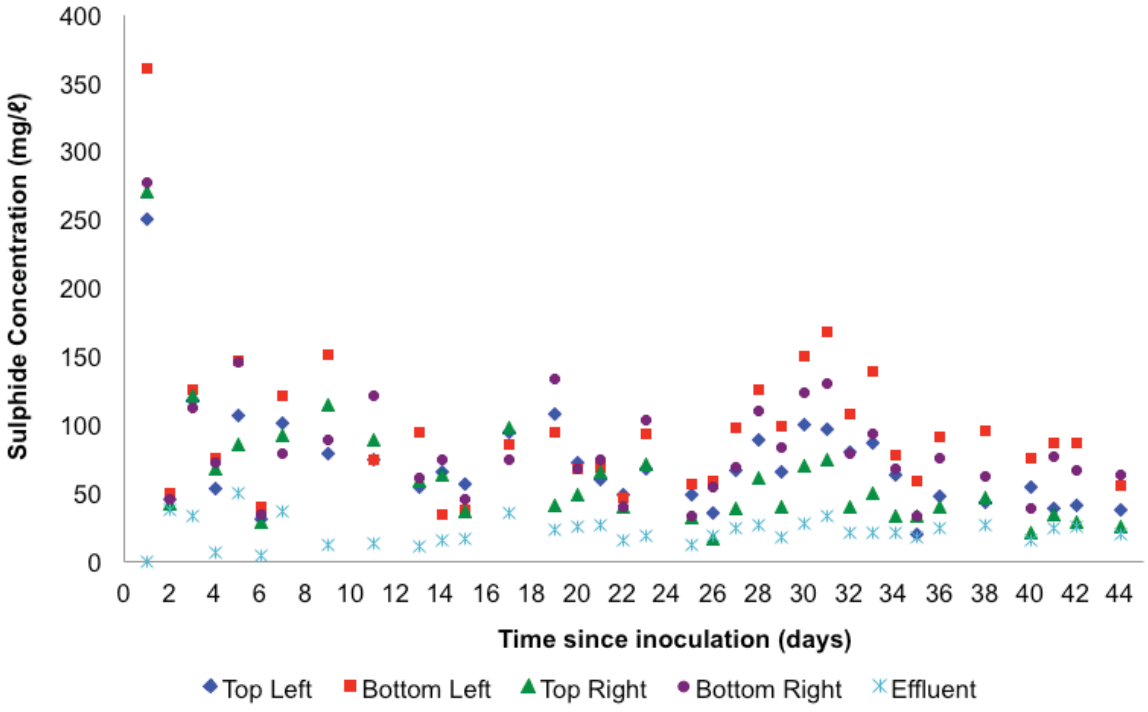

Figure 152: Sulphide concentration versus time for the LFCR-MFC in parallel with a 10kΩ resistor and fed 10mM lactate

Although the same VFAs were detected in the samples taken from the LFCR-MFC as in the single-chambered MFCs, only the concentration of lactate, acetate and propionate are shown. Concentrations

of the remaining volatile fatty acids were typically lower than 50 mg/ℓ and remained fairly constant throughout the duration of the experiment. They were also not present in earlier samples.

The concentration of lactate throughout the reactor decreased to approximately 0 mg/ℓ within the first 5 days of operation. It was noted that in many effluent samples there was some lactate present whereas it has been depleted throughout the rest of the reactor (Figure 153). This suggests some short-circuiting of the feed stream. The presence of lactate in the effluent does appear to become less frequent and in lower concentrations (below 50 mg/ℓ) after 20 days of operation.

Acetate concentration was observed to differ significantly between the different sampling ports in the reactor (Figure 154). The concentration was observed to be consistently higher for the bottom two sampling ports than for the top two ports. The concentration difference between ports on the same level was also smaller than that of ports on different levels.

The overall propionate concentration of the reactor appeared to decrease with time (Figure 155). This trend was strongest for samples taken from the bottom left port of the reactor.

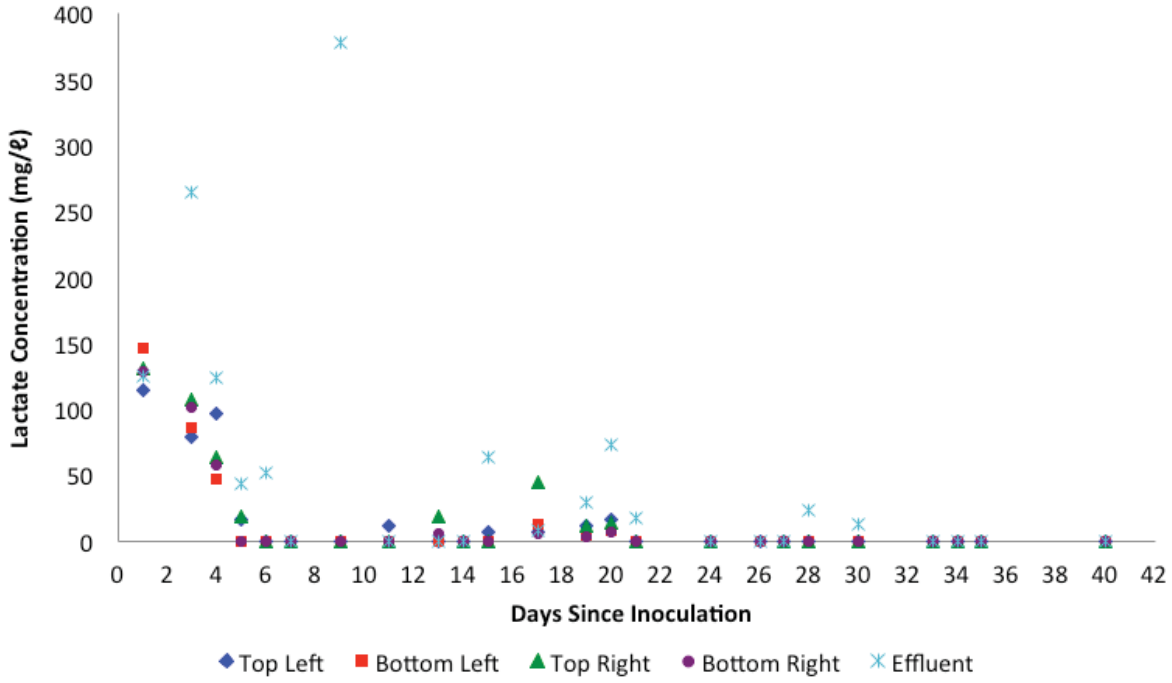

Figure 153: Lactate concentration versus time for the LFCR-MFC in parallel with a 10kΩ resistor and fed 10mM lactate

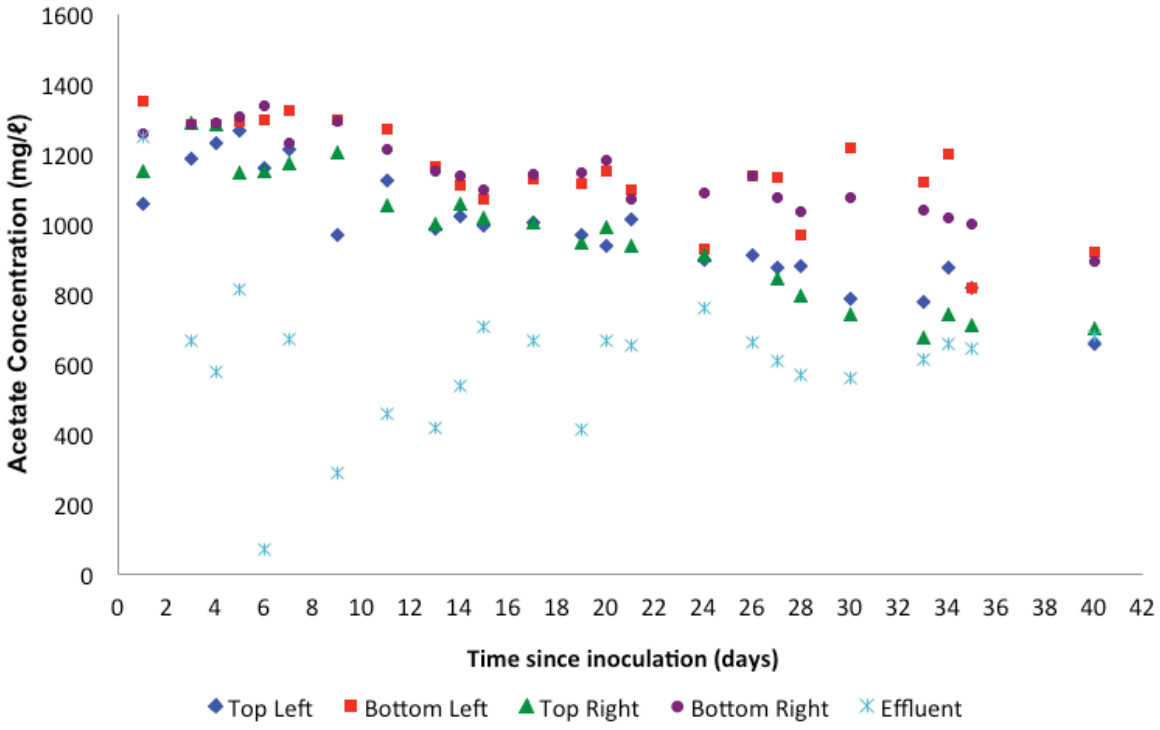

Figure 154: Acetate concentration versus time for the LFCR-MFC in parallel with a 10kΩ resistor and fed 10mM lactate

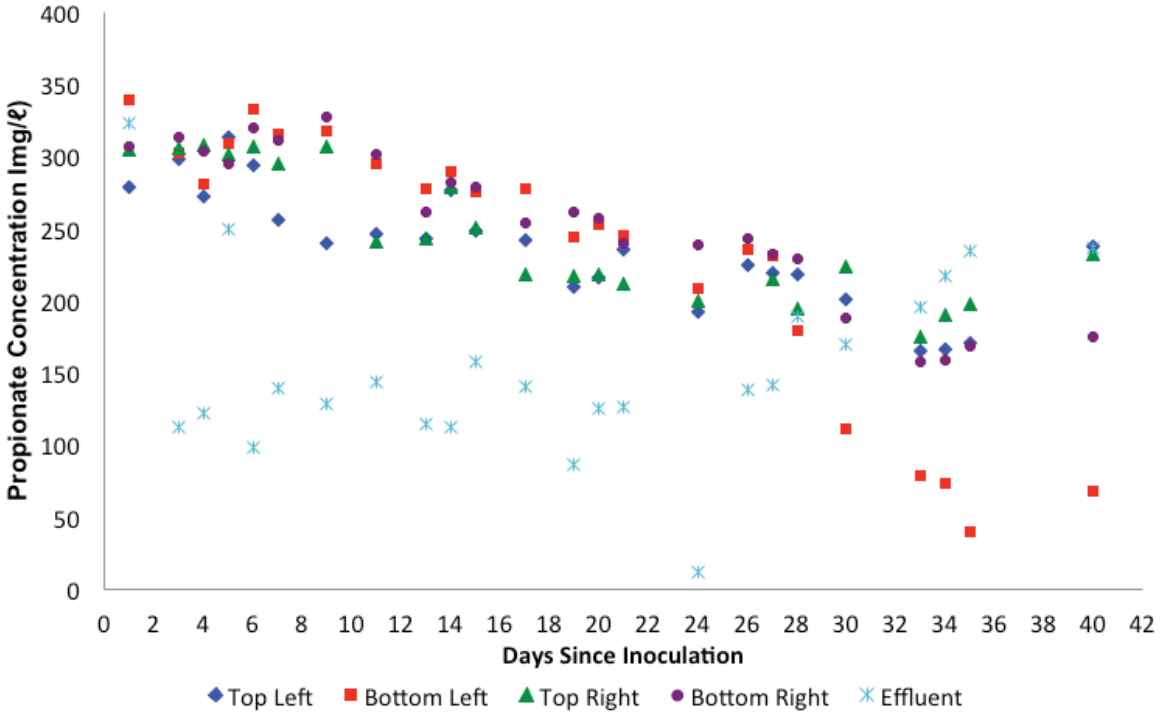

Figure 155: Propionate concentration versus time for the LFCR-MFC in parallel with a 10kΩ resistor and fed 10mM lactate

The overall pH of the system was seen to decrease steadily from around pH 8.9 to around pH 7.5 over the first 19 days after inoculation, as can be seen from Figure 156. From then on it decreased far

slower, remaining between pH 7.5 and 7. The difference in the pH of each sample drawn from the system also appeared to increase after day 19.

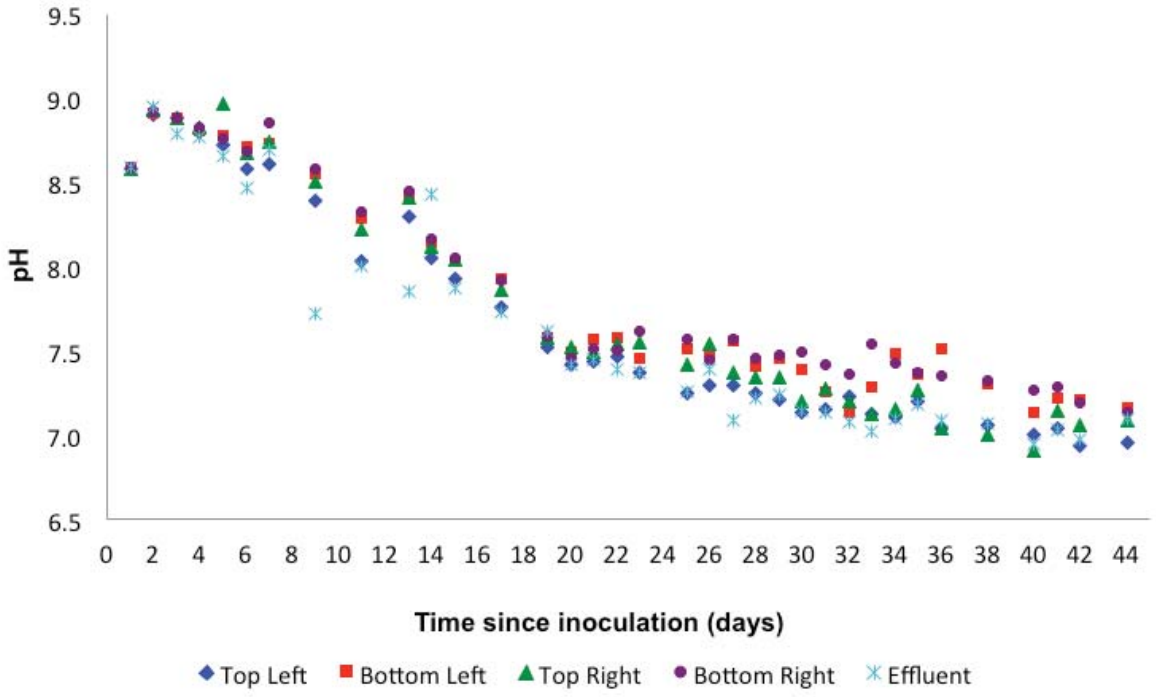

Figure 156: pH versus time for the LFCR-MFC in parallel with a 10kΩ resistor and fed 10mM lactate

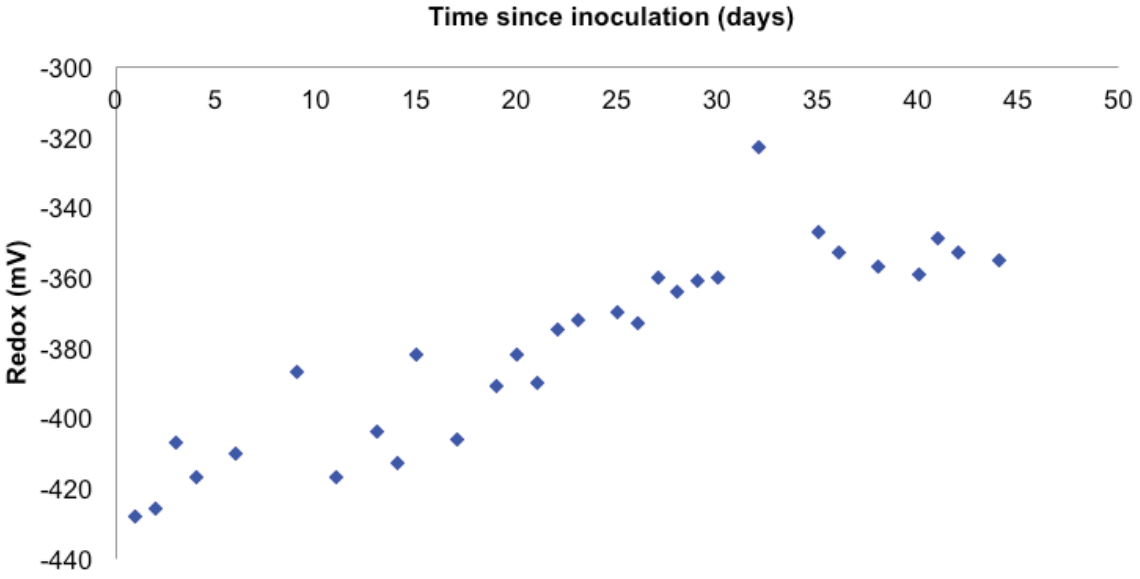

Figure 157: Redox potential (wrt Ag/AgCl reference electrode) versus time for the LFCR-MFC in parallel with a 10kΩ resistor and fed 10mM lactate

7.4 DISCUSSION

Although a slightly higher maximum power density was achieved by the single-chambered MFCs than by the LFCR-MFC, the LFCR-MFC achieved its maximum at a much lower resistance than that of the single-chambered MFCs. This indicates that the internal resistance of the flow through system is much lower than that of the smaller fed-batch MFC.

This was most likely a result of several factors. The single-chambered MFC had two carbon paper electrodes 4 cm apart. There were likely to be large mass transfer limitations within the system, as it was not mixed in any way and protons are required to diffuse the length of the reactor to partake in the reduction reaction at the cathode. In the case of the LFCR-MFC, the flow of medium through the system was likely to aid the transfer of protons to the cathode. The anode brush was also in the centre of the reactor and some of the fibres were as close as 1 cm to the cathode. The shorter distance between the two electrodes would significantly aid mass transfer and reduce internal resistance.

The current produced by the LFCR-MFC was also in the order of ten times the magnitude of the current produced by the single-chambered MFC (Figure 143 and Figure 151). The carbon fibre anode in the LFCR-MFC has a considerably larger surface, which allows for better colonisation by the SRBs, likely resulting in higher current generation.

Although the power produced by both systems was very small and at this stage could not be used in any electrical application effectively, a major advantage of the flow through LFCR-MFC system was that the power generation was fairly constant, whereas the power generation in the single-chambered MFCs cycled. The electricity produced by the continuous system has greater potential to be used directly for an electrical application, whereas the electricity produced by a cycling batch system would best be used to charge a battery and used at a later stage. As previously mentioned, the smaller fed-batch system was completely impractical for use in wastewater treatment and is unlikely to be considered for application on a larger scale.

7.4.1 Single-Chambered MFC

The slow increase in maximum potential difference achieved during the feeding cycle is believed to be due to the need for good colonisation of the MFC before electricity production can take place. The graphs of COD and VFA concentration as a function of time for the MFCs (Figure 146, Figure 147, Figure 148 and Figure 149) showed there was almost complete oxidation of substrate for the first 12-16 days of the experiment. It is likely that substrate was used for cell growth during this time. Once the electrodes had been colonised, substrate was used primarily for cell maintenance and sulphate reduction.

Over time the potential produced by the single-chambered MFC decreased. The graphs of VFA concentration versus time for all three MFCs (Figure 147, Figure 148 and Figure 149) showed there was in increase in the concentration of propionate in the MFCs, which is likely an indication of increased activity of fermentative bacteria or methanogens.

Methanogenic archaea (MA) and SRB are both prolific in wastewater treatment systems and compete actively for substrate (Lens *et al.*, 1998). Acetate utilising SRB have been shown to have higher growth rates than acetate utilising MA. The SRB also gain more energy from the consumption acetate than MA, both of which give them an advantage over the MA (Oude Elferink *et al.*, 1994; Lens *et al.*, 1998). Sulphide is toxic to many microorganisms and has been shown to inhibit their growth. However, MA have been shown to be more susceptible to sulphide inhibition than SRB, especially at lower COD/Sulphate retios (<1.6) (Lens *et al.*, 1998). It has been suggested that MA have a better capacity for attachment than SRB (Omil *et al.*, 1996).

As a result of their better attachment abilities, it is likely that MA attached to the carbon paper electrodes in the MFCs first, making it harder for SRBs to attach. The very low sulphide concentrations in the systems would also likely mean that the growth of the MA was not greatly inhibited. This, coupled with removal of 10 mℓ of liquid when the MFC was fed, could result in the gradual wash out of the SRBs from the system, thereby decreasing performance with time.

7.4.2 LFCR-MFC

A hydrodynamic study has been conducted on the 2 and 8 litre reactors on which the LFCR-MFC reactor was modelled. A slight difference in the density of the two liquids resulted in the acid sinking to the base of the reactor. A similar difference in density could be expected between sulphide and incoming sulphate waste. With an outlet port on the same level as the inlet, the vertical displacement of fluid occurred when the incoming solution reached the end of the reactor, which resulted in mixing of the bulk liquid. The study revealed that very little turbulent mixing occurred, especially at slow flow rates, and that partitioning of the solution into stagnant and flowing zones occurred.

Although a hydrodynamic study was not conducted on the LFCR-MFC, it is believed that similar stratification of layers occurred in this this reactor, especially given the slow flow rates. This phenomenon would explain the difference in sample values between ports. After seeding of the reactor was stopped on day 19, the difference in the sulphide concentration (Figure 152) and pH values (Figure 156) of the samples taken from the different sampling ports in the LFCR-MFC became more apparent and fairly regular. This is believed to be as a result of the reactor no longer being mixed by the addition of an inoculum, with mixing being driven solely by the incoming feed. The similarity in acetate concentrations in samples taken from the same level of the reactor, compared to that of samples taken on a different level (Figure 154) also provides evidence for the presence of liquid layers in the reactor.

The presence of lactate in some effluent samples suggests that there was potentially short-circuiting of incoming feed. It is likely that some of the incoming feed flows along the top of the reactor instead of sinking to the bottom and exits via the outlet before the lactate can be utilised. This was most likely as a result of the reactor being short and almost square. The decrease in lactate concentration in the effluent, after the reactor was no longer seeded and a floating sulphur biofilm was allowed to fully develop, indicates that the biofilm may reduce short-circuiting of feed.

The presence of propionate in the reactor is believed to be mostly due to the presence of fermenters and methanogens. A decrease in propionate with time is therefore likely due to the increased activity of SRBs, which results in dominance over these groups. This is opposite to the trend that was seen in the single-chambered MFCs. It is hypothesised that the microfiber anode brush allows for better attachment of the SRBs and the longer hydraulic residence time, as opposed to the removal of a third of the reactor volume which occurred in the single-chambered MFCs, resulted in less wash out of SRBs. They were therefore able to compete actively with the fermenters and methanogens.

An oxygen gradient exists within the reactor. Diffusion of oxygen occurs through the cathode electrodes on the sides of the reactor. Sulphur deposition and biofilm formation on the electrodes was assumed to have occurred by the time at which steady power production was achieved. This, coupled with the reduction reaction with oxygen, is assumed to limit oxygen transfer into the bulk liquid via the cathode electrodes. The majority of diffusion of oxygen is therefore assumed to be occurring at the air liquid interface. The largest gradient of oxygen therefore exists along the depth of the reactor.

Although the carbon microfiber brush anode is spread throughout the bulk liquid in the reactor, the majority of the fibre is concentrated in the bottom layer, especially around the bottom left end of the reactor. This, coupled with the oxygen gradient, is therefore likely to result in the bulk of the SRBs, which are anaerobic, being present in the lower level of the reactor. This assumption is supported by

the significantly lower concentrations of propionate measured in the samples taken from the bottom of reactor (Figure 155), as well as the higher concentrations of sulphide (Figure 152).

7.5 CONCLUSIONS

The study has provided confirmation of the successful operation of the MFC in the presence of SRB. This study has extended the basic demonstration of concept to further demonstrate that the LFCR can be operated as an MFC with simultaneous electricity generation, albeit at a low level, and biological sulphate reduction and sulphide oxidation, resulting in a sulphur product. In this system the carbon fibres used as the immobilisation matrix served as the anode of the MFC.

Data gathered suggest that the immobilisation of the SRB is favoured by the application of carbon fibres over the carbon mat anode. Further, the data suggest that optimum performance of the SRB – SOB-MFC requires the SRB to outcompete other groups of microbes. This can be achieved by facilitating the immobilisation of the SRB to minimise washout, resulting in an increased level of dissolved sulphide. The dominance of the SRB was confirmed by a decrease in the propionate concentration. Therefore, the relative ratio of propionate and acetate may provide an indicator variable by which to monitor and manipulate performance.

REFERENCES

ADAMS, B., GALE, I., YOUNGER, P.L., LERNER, D. and CHILTON, J. (2000) Groundwater. In: ACREMAN M (ed.) *The Hydrology of the UK. A study of change*. Routledge, London, pp 150-179.

AHRING, B., SANDBERG, M. and ANGELIDAKI, I. (1995) Volatile fatty acids as indicators of process imbalance in anaerobic digesters. Applied Microbiology and Biotechnology **43** 559-565.

AKCIL, A. and KOLDAS, S. (2006) Acid Mine Drainage (AMD): causes, treatment and case studies. Journal of Cleaner Production **14** 1139-1145.

ALI, M. and SREEKRISHNAN, T.R. (2001) Aquatic toxicity from pulp and paper mill effluents: A review. Advances in Environmental Research **5** 175-196.

ANGELIDAKI, I., ELLEGAARD, L. and AHRING, B.K. (1999) A comprehensive model of anaerobic bioconversion of complex substrates to biogas. Biotechnology and Bioengineering **63** 363-372.

ANTONOPOULOU, K.S.G. and LYBERATOS, G. (2009) Potential to produce methane from extraction by-products through anaerobic digestion, deliverable 2.3, Sustoil (unpublished).

APHA (American Public Health Association) (2005) *Standard Methods for the Examination of Water and Wastewater,* 21st Edition. American Public Health Association, Washington, D.C.

BANERJEE, S. and BISWAS, G.K. (2004) Studies on biomethanation of distillery wastes and its mathematical analysis. Chemical Engineering Journal **102** 193-201.

BASKARAN, V. and NEMATI, M. (2006) Anaerobic reduction of sulfate in immobilized cell bioreactors, using a microbial culture originated from an oil reservoir. Biochemical Engineering Journal **31** 148-159.

BLOKKER, P., SCHOUTEN, S., VAN DEN ENDE, H., DE LEEUW, J.W., HATCHER, P.G. and DAMSTE, J.S.S. (1998) Chemical structure of algaenans from the fresh water algae *Tetraedron minimum*, *Scenedesmus communis* and *Pediastrum boryanum*. Organic Geochemistry **29** 1453-1468.

BOLTES, K., LETON, P. and GARCIA-CALVO, E. (2008) Volatile fatty acid anaerobic degradation: Kinetic modelling with an inoculum under controlled conditions. Industrial and Engineering Chemistry Research **47** 5337-5345.

BOSHOFF, G., DUNCAN, J. and ROSE, P.D. (1996) An algal-bacterial integrated ponding system for the treatment of mine drainage waters. Journal of Applied Phycology **8** 442-444.

BOUALLAGUI, H., TOUHAMI, Y., BEN CHEIKH, R. and HAMDI, M. (2005) Bioreactor performance in anaerobic digestion of fruit and vegetable wastes. Process Biochemistry **40** 989-995.

BRUSER, T., LENS, P., TRUPER, H. and STEUDEL, R. (2000) The biological sulphur cycle. In: LENS P and HULSOFF POL L (eds) *Environmental Technologies to Treat Sulfur Pollution*. IWA Publishing, London, pp 47-86.

BUISMAN, C.J., GERAATS, B.G., IJSPEERT, P. and LETTINGA, G. (1990) Optimization of sulphur production in a biotechnological sulphide-removing reactor. Biotechnology and Bioengineering **35** 50-56.

BUISMAN, C.J., IJSPEERT, P., HOF, A. and JANSSEN, A.J. (1991) Kinetic parameters of a mixed culture oxidizing sulfide and sulfur with oxygen. Biotechnology and Bioengineering **38** 813-820.

BUYUKKAMACI, N. and FILIBELI, A. (2004) Volatile fatty acid formation in an anaerobic hybrid reactor. Process Biochemistry **39** 1491-1494.

CALLAGHAN, F.J., WASE, D.A.J., THAYANITHY, K. and FORSTER, C.F. (2002) Continuous co-digestion of cattle slurry with fruit and vegetable wastes and chicken manure. Biomass and Bioenergy **27** 71-77.

CARLOZZI, P., PUSHPARAJ, B., DEGL'INNOCENTI, A. and CAPPERUCCI, A. (2006) Growth characteristics of *Rhodopseudomonas palustris* cultured outdoors, in an underwater tubular photobioreactor, and investigation on photosynthetic efficiency. Applied Microbiology and Bioethanology **73** 789-795.

CHA, J., CHOI, S., YU, H., KIM, H. and KIM, C. (2010) Directly applicable microbial fuel cells in aeration tank for wastewater treatment. Bioelectrochemistry **78** 72-79.

CHAKRABORTY, N., SARKAR, G.M. and LAHIRI, S.C. (2002) The effect of pesticide (Tara-909) on biomethanation of sewage sludge and isolated methanogens. Biomass and Bioenergy **23** 75-80.

CHANDRA, R., VIJAY, V. and SUNNAROA, P. (2006) A study on biogas generation from non-edible oil seed cakes: potential and prospects in India. *Proceedings of the second joint International conference on sustainable energy and environment (SEE 2006)*. Bangkok, Thailand.

CHEN, K. and MORRIS, J. (1972) Kinetics of oxidation of aqueous sulfide by oxygen. Environmental Science and Technology **6** 529-537.

CHEN, P. (1987) *Factors influencing methane fermentation of micro-algae*. Ph.D. thesis, University of California, Berkeley, USA.

CHEN, P.H. and OSWALD, W.J. (1998) Thermochemical treatment for algal fermentation. Environment International **24** 889-897.

CHEN, Y., CHENG, J.J. and CREAMER, K.S. (2007) Inhibition of anaerobic digestion process: A review. Bioresource Technology **99** 4044-4064.

CHENG, S. and LOGAN, B.E. (2007) Ammonia treatment of carbon cloth anodes to enhance power generation of microbial fuel cells. Electrochemistry Communications **9** 492-496.

CHENG, S., LIU, H.. and LOGAN, B.E. (2006a) Increased performance of single-chamber microbial fuel cells using an improved cathode structure. Electrochemistry Communications **8** 489-494.

CHENG, S., LIU, H. and LOGAN, B.E. (2006b) Power Densities Using Different Cathode Catalysts (Pt and CoTMPP) and Polymer Binders (Nafion and PTFE) in Single Chamber Microbial Fuel Cells. Environmental Science and Technology **40(1)** 364-369.

CHIARLE, S., RATTO, M. and ROVATTI, M. (2000) Mercury removal from water by ion exchange resins adsorption. Water Research **34** 2971-2978.

CHISTI, Y. (2007) Biodiesel from microalgae. Biotechnology Advances **25** 294-306.

CHOI, E. and RIM, J.M. (1991) Competition and inhibition of sulfate reducers and methane producers in anaerobic treatment. Water Science and Technology **23** 1259-1264.

CIFERRI, O. (1983) Spirulina, the edible microorganism. Microbiological Reviews. **47** .551-578.

CISNEROS, M. and RITO-PALOMARES, M. (2004) A simplified strategy for the release and primary recovery of c-phycocyanin produced by *Spirulina maxima*. Chemical and Biochemical Engineering Quarterly **18** 385-390.

CLAUWAERT, P., VAN DER HA, D., BOON, N., VERBEKEN, K., VERHAEGE, M., RABAEY, K. and VERSTRAETE, W. (2007) Open Air Biocathode Enables Effective Electricity Generation with Micronial Fuel Cells. Environmental Science and Technology **41** 7564-7569.

COETSER, S.E., HEATH, R., MOLWANTWA, J.B., ROSE, P.D. and PULLES, W. (2005) Implementation of the degrading packed bed reactor technology and verification of the long-term performance of passive treatment plants at Vryheid Coronation Colliery. Research report no. 1348/1/05, Water Research Commission, Pretoria, South Africa.

COLLERAN, E. and PENDER, S. (2002) Mesophilic and thermophilic anaerobic digestion of sulphate-containing wastewaters. Water Science and Technology **45** 231-235.

CORBETT, C. (2001) *Development of the Rhodes BioSURE Process in the treatment of acid mine drainage wastewaters*. MSc Thesis, Rhodes University, Grahamstown, South Africa.

COUPERTHWAITE, J. (2016) *Integrating microbial fuel cells (MFCs) into the treatment of sulphate-rich wastewater*. MSc Thesis, University of Cape Town, Cape Town, South Africa.

CRISTIANI, P., CARVALHO, M.L., GUERRINI, E., DAGHIO, M., SANTORO, L. and LI, B. (2013) Cathodic and anodic biofilms in Single Chamber Microbial Fuel Cells. Bioelectrochemistry **92** 6-13.

DE SCHAMPHELAIRE, L. and VERSTRAETE, W. (2009) Revival of the biological sunlight-to-biogas energy conversion systems. Biotechnology and Bioengineering **103** 296-304.

DIJKMAN, H., BAYER, H.G. and BUISMAN, C.J.N. (1999) Biotechnology in the Mining and Metallurgical Industries: Cost Savings through Selective Precipitation of Metal Sulfides. *Proceedings of the Copper 99 International conference*, Phoenix, Arizona 113-126.

DOUCHA, J. and LIVANSKY, K. (2008) Influence of processing parameters on disintegration of *Chlorella* cells in various types of homogenizers. Applied Microbiology and Biotechnology **81** 431-440.

DU, Z., LI, H. and GU, T. (2007) A state of the art review on microbial fuel cells: A promising technology for wastewater treatment and bioenergy. Biotechnology Advances **25** 464-482.

DUERR, M., GAIR, S., CRUDEN, A. and MCDONALD, J. (2007) Hydrogen and electrical energy from organic waste. International Journal of Hydrogen Energy **32** 705-709.

DUNN, K. (1998) *The biotechnology of high rate algal ponding systems in the treatment of saline tannery wastewaters.* PhD Thesis, Rhodes University, Grahamstown, South Africa.

ERASMUS, C.L. (2005) MSc thesis, University of Cape Town, South Africa.

FENG, D., ALDRICH, C. and TAN, H. (2000) Treatment of acid mine water by use of heavy metal precipitation and ion exchange. Minerals Engineering **13** 623-642.

FEZZANI, B. and BEN CHEIKH, R. (2007) Thermophilic anaerobic co-digestion of olive mill wastewater with olive mill solid wastes in a tubular digester. Chemical Engineering Journal **132** 195-203.

FREGUIA, S., TSUJIMURA, S. and KANO, K. (2010) Proton transfer pathways in microbial oxygen biocathodes. Electrochimica Acta **55** 813-818.

GALLERT, C., BAUER, S. and WINTER, J. (1998) Effect of ammonia on the anaerobic degradation of protein by a mesophilic and thermophilic biowaste population. Applied Microbiology and Biotechnology **50** 495-501.

GAZEA, B., ADAM, K. and KONTOPOULOS, A. (1996) A review of passive systems for the treatment of acid mine drainage. Minerals Engineering **9** 23-42.

GHANGREKAR, M.M. and SHINDE, V.B. (2007) Performance of membrane-less microbial fuel cell treating wastewater and effect of electrode distance and area on electricity production. Bioresource Technology **98** 2879-2885.

GHOSH, S., CONRAD, J.R. and KLASS, D.L. (1975) Anaerobic acidogenesis of waste water sludge. Journal of the Water Pollution Control Federation **47** 30-45.

GOLUEKE, C.G., OSWALD, W.J. and GOTAAS, H.B. (1957) Anaerobic digestion of algae. Applied and Environmental Microbiology **5** 47-55.

GOSSETT, J.M., MCCARTY, P.L., WILSON, J.C. and EVANS, D.S. (1978) Anaerobic digestion of sludge from chemical treatment. Journal of the Water pollution Control Federation **50** 533-542.

GREBEN, H., BALOYI, J., SIGAMA, J. and VENTER, S.N. (2009) Bioremediation of sulphate rich mine effluents using grass cuttings and rumen fluid microorganisms. Journal of Geochemical Exploration **100** 163-168.

GUNASEELAN, V.N. (1997) Anaerobic digestion of biomass for methane production: A review. Biomass and Bioenergy **13** 83-114.

GÜNTHER, P. and MEY, W. (2008) Selection of mine water treatment technologies for the Emalahleni (Witbank) Water Reclamation Project. *Proceedings of the WISA Biennial Conference*, Sun City, South Africa

GÜNTHER, P. and NAIDU, T. (2008) Mine water reclamation – Towards zero disposal. *Proceedings of the WISA Biennial Conference*, Sun City, South Africa

HAAFIZ, M.K.M., EICHHORN, S.J., HASSAN, A. and JAWAID, M. (2013) Isolation and characterization of microcrystalline cellulose from oil palm biomass residue. Carbohydrate Polymers **93** 628-634.

HAMMACK, R.W., DVORAK, D.H. and EDENBORN, H.M. (1993) The use of biogenic hydrogen sulphide to selectively recover copper and zinc from severely contaminated mine drainage. In: TORMA AE, WEY JE and LAKSHMANAN VL (eds) *Biohydrometallurgical Technologies*, The Minerals, Metal & Materials Society, pp 631-639.

HANHOUN, M., MONTASTRUC, L., AZZARO-PANTEL, C., BISCANS, B., FRÈCHE, M. and PIBOULEAU, L. (2011) Temperature impact assessment on struvite solubility: A thermodynamic modelling approach. Biochemical Engineering Journal **167** 50-58.

HARRISON, S.T.L. (2011). Cell disruption. In M MOO-YOUNG and C WEBB (eds) *Comprehensive Biotechnology* 2nd Edition, Engineering Fundamentals of Biotechnology, Vol 2, Chapter 2.44, pp 619-640. [http://dx.doi.org/10.1016/B978-0-08-088504-9.00127-6]

HARRISON, S.T.L., RICHARDSON, C. and GRIFFITHS, M.J. (2013). Analysis of microalgal biorefineries for bioenergy from an environmental and economic perspective: focus on algal biodiesel. In BUX F (ed) *Biotechnological Applications of Microalgae: Biodiesel and Value-added Products*. Taylor and Francis Group, CRC Press.

HARRISON, S.T.L., VAN HILLE, R.P., MOKONE, T., MOTLELENG, L., SMART, M., LEGRAND, C. and MARAIS, T. (2014) *Addressing the challenges facing biological sulphate reduction as a strategy for AMD treatment*: *Analysis of the reactor stage: raw materials products and process kinetics.* WRC project K5/2110 *in press*.

HE, Z. and ANGENENT, L.T. (2006) Review: Application of Bacterial Biocathodes in Microbial Fuel Cells. Electroanalysis **18** 2009-2015.

HEDIN, R.S., NAIRN, R.W. and KLEINMANN, P.L.P. (1994) *Passive Treatment of Coal Mine Drainage*. US Bureau of Mines Information Circular 9389, US Department of the Interior, Bureau of Mines, Pittsburgh, PA., pp 1-35.

HEIDELBERG, J.F., PAULSEN, I.T., NELSON, K.E., GAIDOS, E.J., NELSON, W.C., READ, T.D., EISEN, J.A. and SESHADRI, R. (2002) Genome sequence of dissimilatory metal ion-reducing bacterium *Shewanella oneidensis*. Nature Biotechnology **20** 1118-1122.

HEIMANN, A.C., FRIIS, A.K. and JAKOBSEN, R. (2005) Effects of sulfate on anaerobic chloroethene degradation by an enriched culture under transient and steady-state hydrogen supply. Water Research **39** 3579-3586.

HELDER, M., STRIK, D.P.B.T.B., HAMELERS, H.V.M., KUIJKEN, R.C.P. and BUISMAN, C.J.N. (2012) New plant-growth medium for increased power output of the Plant-Microbial Fuel Cell. Bioresource Technology **104** 417-423.

HICKEY, R.F. and SWITZENBAUM, M.S. (1991) Thermodynamics of volatile fatty acid accumulation in anaerobic digesters subject to increases in hydraulic and organic loading. Journal of the Water Pollution Control Federation **63** 141-144

HILTON, B.L. and OLESZKIEWICZ, J.A. (1988) Sulphide-induced inhibition of anaerobic digestion. Journal of Environmental Engineering **114** 1377-1391.

HIMMEL, M. and OVEREND, B.J. (1994) *Enzymatic Conversion of Biomass for Fuels Production*. American Chemical Society, New York, pp. 292-324.

HOBSON, P.N. (1991) The treatment of agricultural wastes. In: WHEATLEY, A. (Ed.), *Anaerobic Digestion: A Waste Treatment Technology*. Elsevier Applied Science, London.

HOVE, M., VAN HILLE, R.P. and LEWIS, A.E. (2009) The effect of different types of seeds on the oxidation and precipitation of iron. Hydrometallurgy **97** 180-184.

ILLMAN, A.M., SCRAGG, A.H. and SHALES, S.W. (2000) Increase in *Chlorella* strains calorific values when grown in low nitrogen medium. Enzyme and Microbial Technology **27** 631-635.

INGELSBY, A. (2011) *Anaerobic digestion of algal biomass for bioenergy production – a feasibility study*. MSc thesis, Department of Chemical Engineering, University of Cape Town.

INTERNATIONAL ENERGY AGENCY (2004) Renewable energy: market and policy trends in IEA countries. OCED/IEA Paris, France.

JANG, J.K., PHAM, T.H., CHANG, I.S., KANG, K.H., MOON, H., CHO, K.S. and KIM, B.H. (2004) Construction and operation of a novel mediator- and membrane-less microbial fuel cell. Process Biochemistry **39** 1007-1012.

JANSSEN, A.J.H., SLEYSTER, R., VAN DER KAA, C., JOCHEMSEN, J., BONTSEMA, J. and LETTINGA, G. (1995) Biological sulphide oxidation in a fed-batch reactor. Biotechnology and Bioengineering **47** 327-333.

JARRELL, K.F., SPROTT, G.D. and MATHESON, A.D. (1984) Intracellular potassium concentration and relative acidity of the ribosomal proteins of methanogenic bacteria. Canadian Journal of Microbiology, **30** 663-668.

JIANG, J.K. and LI, B. (2009) Granular activated carbon single-chamber microbial fuel cell (GAC-SCMFCs): A design suitable for large-scale wastewater treatment processes. Biochemical Engineering Journal **47** 31-37.

JIMÉNEZ, A.M., BORJA, R. and MARTÍN, A. (2004) A comparative kinetic evaluation of the anaerobic digestion of untreated molasses and molasses previously fermented with *Penicillium decumbens* in batch reactors. Biochemical Engineering Journal **18** 121-132.

JOHNSON, D.B. and HALLBERG, K.B. (2003). The microbiology of acidic mine waters. Research in Microbiology **154** 466-473.

JOHNSON, D.B. and HALLBERG, K.B. (2005) Acid mine drainage remediation options: a review. The Science of the Total Environment **338** 3-14.

KAMYSHNY JR, A., GOIFMAN, A., GUN, J., RIZKOV, D. and LEV, O. (2004) Equilibrium distribution of polysulfide ions in aqueous solutions at 25°C: A new approach for the study of polysulfides' equilibria. Environmental Science and Technology **38** 6633-6644.

KAYHANIAN, M. (1994) Performance of a high-solids anaerobic digestion process under various ammonia concentrations. Journal of Chemical Technology and Biotechnology **59** 349-352.

KAYHANIAN, M. (1999) Ammonia inhibition in high-solids biogasification: an overview and practical solutions. Environmental Technology **20** 355-365.

KEENAN, P.J., ISA, J. and SWITZENBAUM, M.S. (1993) Inorganic solids development in a pilot-scale anaerobic reactor treating municipal solid waste landfill leachate. Water and Environmental Research, **65** 181-188.

KIM, B., KIM, H., HYUN, M. and PARK, D. (1999) Direct Electrode Reaction of Fe(III)-Reducing Bacterium, *Shewanella purefaciens*. Journal of Microbial and Biotechnology **9(2)** 127-131.

KIM, H.J., PARK, H.S., CHANG, I.S., KIM, M. and KIM, B.H. (2002) A mediator-less microbial fuel cell using a metal reducing bacterium, *Shewanella putrefaciens*. Enzyme and Microbial Technology **30**145-152.

KIM, I.S., KIM, D.H. and HYUN, S-H. (2000) Effect of particle size and sodium ion concentration on anaerobic thermophilic food waste digestion. Water Science and Technology **41** 67-73.

KOMADEL, P. and STUCKI, J.W. (1988) Quantitative assay of minerals for $Fe^{2+}$and Fe^{3+} using 1,10-phenanthroline; III, A rapid photochemical method. Clays and Clay Minerals **36** 379-381.

KOZENKO, R. and HENSON, R.H. (1996) The study of *Spirulina*; effects on the aids virus, cancer and the immune systems. Healthy and Natural **3(5)** 66-67.

LAANBROEK, H.J., GEERLIGS, H.J., PEIJENBURG, A.A.C.M. and SIESLING, J. (1983) Competition for L-lactate between *Desulfovibrio*, *Veillonella*, and *Acetobacterium* species isolated from anaerobic intertidal sediments. Microbial Ecology **9** 341-354.

LANGLEY, N., HARRISON, S.T.L. and VAN HILLE, R.P. (2012) A critical evaluation of CO_2 supplementation to algal systems by direct injection. Biochemical Engineering Journal **68** 70-75.

LETTINGA, G., VAN VELSEN, A.F.M., HOBMA, S.W., DE ZEEUW, W.J. and KLAPWIJK, B. (1980) Use of the upflow sludge blanket (USB) reactor. Biotechnology and Bioengineering **22** 699-734.

LEVIN, D.B., ZHU, H., BELAND, M., CICEK, N. and HOLBEIN, B.E. (2007) Potential for hydrogen and methane production from biomass residues in Canada. Bioresource Technology **98** 654-660.

LIN, C.Y. (1992) Effect of heavy metals on volatile fatty acid degradation in anaerobic digestion. Water Research **26** 177-183.

LIN, C.Y. (1993) Effect of heavy metals on acidogenesis in anaerobic digestion. Water Research **27** 147-152.

LIU, H., CHENG, S. and LOGAN, B.E. (2005) Production of Electricity from Acetate or Butyrate Using a Single-Chamber Microbial Fuel Cell. Environmental Science and Technology **39(2)** 658-662.

LIU, H. and LOGAN, B.E. (2004) Electricity Generation Using an Air-Cathode Single Chamber Microbial Fuel Cell in the Presence and Absence of a Proton Exchange Membrane. Environmental Science and Technology **38** 4040-4046.

LOEWENTHAL, R.E., MORGAN, B.E. and LAHAV, O. (2001) Iron and heavy metals in acid mine drainage waters – equilibrium and treatment considerations. Water Sewage & Effluent **21** 15-23.

LOGAN, B., CHENG, S., WATSON, V. and ESTADT, G. (2007) Graphite Fiber Brush Anodes for Increased Power Production in Air-Cathode Microbial Fuel Cells. Environmental Science and Technology **41** 3341-3346.

LOGAN, B.E. (2008) *Microbial Fuel Cells.* John Wiley & Sons, Inc, New Jersey, USA.

LOGAN, B.E. and REGAN, J.M. (2006) Electricity-producing bacterial communities in microbial fuel cells. Trends in Microbiology **14(12)** 512-518.

LORAX INTERNATIONAL (2003) Treatment of Sulphate Mine Effluents. Technical report, International Network for Acid Prevention (INAP).

LOVLEY, D.R., PHILLIPS, E.J. and LONGERGAN, D.J. (1989) Hydrogen and Formate Oxidation Coupled to Dissimilatory reduction of Iron or Manganese by Alteromonas putrefaciens. Applied and Environmental Microbiology **5** 700-706.

LYBERATOS, G. and SKIADAS, I. (1999) Modelling of anaerobic digestion-a review. Global Nest. The International Journal **1** 63-76.

MATSUMOTO, S., OHTAKI, A. and HORI, K. (2012) Carbon fiber as an excellent support material for wastewater treatment biofilms. Environmental Science and Technology **46** 10175-10181.

MCCARTNEY, D.M. and OLESZKIEWICZ, J.A. (1991) Sulfide inhibition of anaerobic digestion of lactate and acetate. Water Research **25** 203-209.

MCCARTNEY, D.M. and OLESZKIEWICZ, J.A. (1993) Competition between methanogens and sulphate reducers: Effect of COD: sulphate ratio and acclimatization. Water and Environmental Research **65** 655-664.

MCKENDRY, P. (2002) Energy production from biomass (part 3): gasification technologies. Bioresource Technology **83** 55-63.

MOKONE, T.P., VAN HILLE, R.P. and LEWIS, A.E. (2010). Effect of solution chemistry on particle characteristics during metal sulphide precipitation. Journal of Colloid and Interface Sciences **351** 10-18.

MOLETTA, R., VERRIER, D. and ALBAGNAC, G. (1986) Dynamic modelling of anaerobic digestion. Water Research **20** 427-434.

MOLWANTWA, J.B. and ROSE, P.D. (2013) Development of a Linear Flow Channel Reactor for sulphur removal in acid mine wastewater treatment operations. Water SA **39** 649-654.

MOLWANTWA, J.B., COETSER, S.E., HEATH, R., PULLES, W., BOWKER, M. and ROSE, P.D. (2010) *Monitoring, evaluation and long-term verification of the passive water treatment plant at Vryheid Coronation Colliery*. Research report no. 1623/1/10, Water Research Commission, South Africa.

MOORUTH, N. (2013) *An investigation towards passive treatment solutions for the oxidation of sulphide and subsequent removal of sulphur from acid mine water*. PhD thesis, University of Cape Town.

MOOSA, S. (2001) *A kinetic study on anaerobic sulphate reduction – Effect of sulphate and temperature*. PhD thesis, University of Cape Town, South Africa.

MOOSA, S., NEMATI, M. and HARRISON, S.T.L. (2002) A kinetic study on anaerobic reduction of sulphate, Part I: Effect of sulphate concentration. Chemical Engineering Science **57** 2773-2780.

MOOSA, S., NEMATI, M. and HARRISON, S.T.L. (2005). A kinetic study on anaerobic reduction of sulphate. Part II: Incorporation of temperature effects in the kinetic model. Chemical Engineering Science **60** 3517-3524.

MOUNEIMNE, A.H., CARRÈRE, H., BERNET, N. and DELGENÈS, J.P. (2003) Effect of saponification on the anaerobic digestion of solid fatty residues. Bioresource Technology **90** 89-94.

MULOPO, J. (2016) Pilot scale assessment of the continuous biological sulphate removal from coal acid mine effluent using grass cuttings as carbon and energy sources. Journal of Water Process Engineering **11** 104-109.

NAGPAL, S., CHUICHULCHERM, S., PEEVA, L. and LIVINGSTON, A. (2000) Microbial sulfate reduction in a liquid-solid fluidized bed reactor. Biotechnology and Bioengineering **70** 370-380.

NAICKER, K., CUKROWSKA, E. and MCCARTHY, T. (2003) Acid mine drainage arising from gold mining activity in Johannesburg, South Africa and environs. Environmental Pollution **122** 29-40.

NATHOO, J., JIVANI, R. and LEWIS, A.E. (2009) Freezing Your Brines Off: Eutectic Freeze Crystallization for Brine Treatment. *Proceedings of the International Mine Water Conference 2009*. International Mine Water Association, 424-430.

NEVES, L., RIBERO, R., OLIVEIRA, R. and ALVES, M.M. (2006) Enhancement of methane production from barley waste. Biomass and Bioenergy **30** 599-603.

NISHIO, N. and NAKASHIMADA, Y. (2007) Recent development of anaerobic digestion processes for energy recovery from wastes. Journal of Bioscience and Bioengineering **103** 105-112.

O'FLAHERTY, V. and COLLERAN, E. (1999) Effect of sulphate addition on volatile fatty acid and ethanol degradation in an anaerobic hybrid reactor: II: microbial interactions and toxic effects. Bioresource Technology **68** 109-120.

OLESZKIEWICZ, J.A., MARSTALLER, T. and MCCARTNEY, D.M. (1989) Effects of pH on sulfide toxicity to anaerobic processes. Environmental Technology Letters **10** 815-822.

OMIL, F., OUDE ELFERINK, S.J.W.H., LENS, P., HULSHOFF POL, L.W. and LETTINGA, G. (1997) Effect of the inoculation with *Desulforhabdus amnigenus* and pH or O_2 on the competition between sulphate reducing and methanogenic bacteria in an acetate fed UASB reactor. Bioresource Technology **60** 113-122.

OWENS, J.M. and CHYNOWETH, D.P. (1993) Biochemical methane potential of municipal solid waste (MSW) components. Water Science and Technology **27** 1-14.

OYEKOLA, O.O. (2008) *An investigation into the relationship between process kinetics and microbial community dynamics in a lactate-fed sulphidogenic CSTR as a function of residence time and sulphate loading*. Ph.D. thesis, University of Cape Town.

OYEKOLA, O.O., HARRISON, S.T.L. and VAN HILLE, R.P. (2012) Effect of culture conditions on the competitive interaction between lactate oxidizers and fermenters in a biological sulphate reduction system. Bioresource Technology **104** 616-621.

OYEKOLA, O.O., VAN HILLE, R.P. and HARRISON, S.T.L. (2009) Study of anaerobic lactate metabolism under biosulfidogenic conditions. Water Research **43:** 3345-3354.

OYEKOLA, O.O., VAN HILLE, R.P. and HARRISON, S.T.L. (2010) Kinetic analysis of biological sulphate reduction using lactate as carbon source and electron donor: Effect of sulphate concentration. Chemical Engineering Science **65** 4771-4781.

PARK, D. and ZEIKUS, J. (2002) Impact of electrode composition on electricity generation in a single-compartment fuel cell using *Shewanella putrefaciens*. Applied Microbiology and Biotechnology **59** 58-61.

PARKIN, G.F., SPEECE, R.E., YANG, C.H.J. and KOCHER, W.M. (1983) Response of methane fermentation to industrial toxicants. Journal of the Water Pollution Control Federation **55** 44-53.

PETRASEK, A.C. and KUGELMAN, I.J. (1983) Metals removal and partitioning in conventional wastewater treatment plants. Journal of the Water Pollution Control Federation **55** 1183-1190.

PINCHUK, G.E., GEYDEBREKHT, O.V., HILL, E.A., REED, J.L., KONOPKA, A.E., BELIAEV, A.S. and FREDRICKSON, J.K. (2011) Puyruvate and Lactate Metabolism by Shewanella oneidensis MR-1 under Fermentation, Oxygen Limitation, and Fumerate Respiration Conditions. Applied and Environmental Microbiology **77** 8234-8240.

PIRBADIAN, S., BARCHINGER, S.E., LUENG, K.M., BYUN, H.S., JANGIR, Y., BOUHENNI, R.A., REDD, S.B., ROMINE, M.F., SAFFARINI, D.A., SHI, L., GORBY, Y.A., GOLDBECK, J.H. and EL-NAGGAR, Y. (2014) *Shewanella oneidensis* MR-1 nanowires are outer membrane and periplasmic extentions of the extracellular electron transport components. PNAS **111** 12883-12888.

PULLES, W. and HEATH, R. (2009) The evolution of passive mine water treatment technology for sulphate removal. *Proceedings of the International Mine Water Conference 2009,* Pretoria, South Africa*.* International Mine Water Association 2-15.

PULLES, W., ROSE, P., COETSER, L. and HEATH, R. (2003) Development of integrated passive water treatment systems for the treatment of mine wastes. *Proceedings of 6th ICARD conference*, 12-18 July Cairns, Australia

RABAEY, K., CLAUWAERT, P., AELTERMAN, P. and VERSTRAETE, W. (2005) Tubular microbial Fuel Cells for Efficient Electricity Generation. Environmental Science & Technology **39** 8077-8082.

RABAEY, K., VAN DE SOMPEL, K., MAIGNIEN, L., BOON, N., AELTERMAN, P., CLAUWAERT, P., DE SCHAMPHELAIRE, L., PHAM, H.T., VERMEULEN, J., VERHAEGE, M., LENS, P. and VERSTRAETE, W. (2006) Microbial Fel Cells for Sulfide Removal. Environmental Science and Technology **40** 5218-5224.

RINGO, E., STENBERG, E. and STROM, A.R. (1984) Amino Acid and Lactate Catabolism in Trimethylamine Oxide Respiration of Alteromonas putrefaciens NCMB 1735. Applied and Environmental Microbiology **47** 1084-1089.

ROMAN., H (2004) *The degradation of lignocellulose in a biologically-generated sulphidic environment*. PhD thesis, Rhodes University.

ROSE, P. (2013) Long-term sustainability in the management of acid mine drainage wastewaters – development of the Rhodes BioSURE Process. Water SA **39** 583-592.

ROSE, P.D. (1992) *A biotechnological approach to the removal of organics from saline effluents*. Research report no. K5/410, Water Research Commission, Pretoria, South Africa.

ROSE, P.D., DUNCAN, J.R., VAN HILLE, R.P. and BOSHOFF, G.A. (1999) *Use of ponds to treat sulphate solutions and ASPAM process*. Patents: RSA 99/4585; USA 6,315,904.

ROSE, P.D., MAART, B.A., DUNN, K.M., ROWSWELL, R.A. and BRITZ, P. (1996) High rate oxidation ponding for the treatment of tannery effluents. Water Science and Technology **33(7)** 219-227.

SADDOUD, A., HASSAÏRI, I. and SAYADI, S. (2007) Anaerobic membrane reactor with phase separation for the treatment of cheese whey. Bioresource Technology **98** 2102-2108.

SAMSON, R. and LEDUY, A. (1983) Improved performance of anaerobic digestion of *Spirulina maxima* algal biomass by addition of carbon-rich wastes. Biotechnology Letters **5** 677-682.

SANCHEZ, E.P. and TRAVIESO, L. (1993) Anaerobic digestion of *Chlorella vulgaris* for energy production. Resources Conservation and Recycling **9** 127-132.

SCHOEMAN, J.J. and STEYN, A. (2001) Investigation into alternative water technologies for the treatment of underground mine water discharged by Grootvlei Propriety Mines Ltd. into the Blesbokspruit in South Africa. Desalination **133** 13-30.

SCOTT, R. (1995) *Flooding of Central and East Rand gold mines: An investigation into controls over the inflow rate, water quality and predicted impacts of flooded mines*. Research report no. 486/1/95, Water Research Commission, Pretoria, South Africa.

SEVDA, S., DOMINGUEZ-BENETTON, X., VANBROEKHOVEN, K., DE WEVER, H., SREEKRISHNAN, T.R. and PANT, D. (2013) High strength wastewater treatment accompanied by power generation using air cathode microbial fuel cell. Applied Energy **105** 194-206.

SIALVE, B., BERNET, N. and BERNARD, O. (2009) Anaerobic digestion of microalgae as a necessary step to make microalgal biodiesel sustainable. Biotechnology Advances **27** 409-416.

SIKKEMA, J., DE BONT, J.A.M. and POOLMAN, B. (1994) Interaction of cyclic hydrocarbons with biological membranes. Journal of Biological Chemistry **26** 8022-8028.

SOTO, M., MENDÉZ, R. and LEMA, J.M. (1991) Biodegradability and toxicity in the anaerobic treatment of fish canning wastewaters. Environmental Technology **12** 669-677.

SOTO, M., MENDÉZ, R. and LEMA, J.M. (1993) Sodium inhibition and sulphate reduction in the anaerobic treatment of mussel processing wastewaters. Journal of Chemical Technology and Biotechnology **58** 1-7.

SPEECE, R.E. (1993) Anaerobic biotechnology for industrial waste treatment. Water Science and Technology **17** A416-A427.

STAFFORD, D.A., HAWKES, D.L. and HORTON, R. (1990) *Methane production from waste organic matter.* CRC Press, Baca Raton, Florida.

STERRIT, R.M. and LESTER, J.M. (1980) Interaction of heavy metals with bacteria. Science of the Total Environment **14** 5-17.

SU, X., TIAN, Y., SUN, Z., LU, Y. and LI, Z. (2013) Performance of a combined system of microbial fuel cell and membrane bioreactor: Wastewater treatment, sludge reduction, energy recovery and membrane fouling. Biosensors and Bioelectronics **42** 92-98.

SUKKASEM, C., LAEHLAH, S., HNIMAN, A., O'THONG, S., BOONSAWANG, P., RARNGNARONG, A., NISOA, M. and KIRDTONGMEE, P. (2011) Upflow bio-filter circuit (UBFC): Biocatalyst microbial fuel cell (MFC) configuration and application to biodiesel wastewater treatment. Bioresource Technology **102** 10363-10370.

SUN, Y. and CHENG, J. (2002) Hydrolysis of lignocellulosic materials for ethanol production: a review. Bioresource Technology **83** 1-11.

TANG, Y.J., MEADOWS, A.L. and KEASLING, J.D. (2007a) A Kinetic Model Describing *Shewanella oneidensis* MR-1 Growth, Substrate Consumption, and Product Secretion. Biotechnology and Bioengineering **96** 125-133.

TANG, Y.J., MEADOWS, A.L., KIRBY, J. and KEASLING, J.D. (2007b) Anaerobic Central Metabolic Pathways in *Shewanella oneidensis* MR-1 Reinterpreted in the Light of Isotopic Metabolite Labeling. Journal of Bacteriology **189** 894-901.

THOMPSON, G., SWAIN, J., KAY, M. and FORSTER, C.F. (2001) The treatment of pulp and paper mill effluent: A review. Bioresource Technology **77** 275-286.

TIMMER, R., STRIK, D.P.B.T.B., HAMELERS, H.V.M. and BUISMAN, C.J.N. (2013) Electricity generation by a novel design tubular plant microbial fuel cell. Biomass and Bioenergy **51** 60-67.

TRZCINSKI, A.P. and STUCKEY, D.C. (2015) Contribution of acetic acid to the hydrolysis of lignocellulosic biomass under abiotic conditions. Bioresource Technology **185** 441-444.

UENO, Y., KAWAI, T., SATO, S., OTSUKA, S. and MORIMOTO, M. (1995) Biological production of hydrogen from cellulose by natural anaerobic microflora. Journal of Fermentation and Bioengineering, **79** 194-197.

UENO, Y., TATARA, M., FUKUI, H., MAKIUCHI, T., GOTO, M. and SODE, K. (2007) Production of hydrogen and methane from organic solid wastes by phase-separation of anaerobic process. Bioresource Technology **98** 1861-1865.

VALLERO, M.V.G., HULSHOFF POL, L.W., LETTINGA, G. and LENS, P.N.L. (2003a) Effects of NaCl on thermophilic (55°C) methanol degradation in sulfate reducing granular sludge reactors. Water Research **37** 2269-2280.

VALLERO, M.V.G., HULSHOFF POL, L.W., LETTINGA, G. and LENS, P.N.L. (2003b) Long-term adaptation of methanol-fed thermophilic (55°C) sulphate-reducing reactors to NaCl. Journal of Industrial Microbiology and Biotechnology **30** 375-382.

VALLERO, M.V.G., LETTINGA, G. and LENS, P.N.L. (2005) High rate sulfate reduction in a submerged anaerobic membrane bioreactor (SAMBaR) at high salinity. Journal of Membrane Science **253** 217-232.

VAN DEN BOSCH, P. (2008) *Biological sulfide oxidation by natron-alkaliphilic bacteria. Application in gas desulfurization*. PhD thesis, Wageningen University, Netherlands.

VAN HILLE, R.P. and MARAIS, T. (2015) *An integrated bioprocess for ARD remediation and renewable energy generation*. (Progress report 1), WRC K5/2392. Unpublished Report

VAN HILLE, R.P. and MOORUTH, N. (2011) *Investigation of sulphide oxidation kinetics and impact of reactor design during passive treatment of mine water.* Research report no. KV 268/11, Water Research Commission, Pretoria, South Africa.

VAN HILLE, R.P. and MOORUTH, N. (2013) Investigation of carbon flux and sulphide oxidation kinetics during passive biotreatment of mine water. Research report no. 2139/1/13, Water Research Commission, Pretoria, South Africa.

VAN HILLE, R.P., MOORUTH, N., MACK, C-L., RAJA, S. and HEATH, R.A. (2012) *Towards passive treatment solutions for the oxidation of sulphide and subsequent sulphur removal from acid mine water.* Research report no. 1834/1/12, Water Research Commission, Pretoria, South Africa.

VAN LANGERAK, E.P.A., GONZALES-GIL, G., VAN ELST, A., VAN LIER, J.B., HAMERLERS, H.V.M. and LETTINGA, G. (1998) Effects of high calcium concentrations on the development of methanogenic sludge in upflow anaerobic sludge blanket (UASB) reactors. Water Research **34** 1255-1263.

VENKATARAMAN, L. (1997) Review of *Spirulina platensis* (*Arthrospira*): Physiology, cell biology and biotechnology. Journal of Applied Phycology **9** 295-296.

VERVERIS, C., GEORGHIOU, K., DANIELIDIS, D., HATZINIKOLAOU, D., SANTAS, P., SANTAS, R. and CORLETI, V. (2007). Cellulose, hemicelluloses, lignin and ash content of some organic materials and their suitability for use as paper pulp supplements. Bioresource Technology **98** 296-301.

VIJAYARAGHAVAN, K., AHMED, D. and BIN IBRAHIM, M.K. (2006) Biohydrogen generation from jackfruit peel using anaerobic contact filter. International Journal of Hydrogen Energy **31** 569-579.

VOGELS, G.D., KEJTJENS, J.T. and VAN DER DRIFT, C. (1988) Biochemistry of methane production. In: ZEHNDER, A.J.B. (Ed.), *Biology of Anaerobic Microorganisms.* John Wiley and Sons, New York.

VON CANSTEIN, H., OGAWA, J., SHIMIZU, S. and LLOYD, J.R. (2008) Secretion of flavins by *Shewanella* species and their role in extracellular electron transfer. Applied Environmental Microbiology **74** 615-623.

WANG, Y., LIU, X., LI, W., LI, F., WANG, Y., SHENG, G., ZENG, R.J. and YU, H. (2012) A microbial fuel cell-membrane bioreactor integrated system for cost effective wastewater treatment. Applied Energy **98** 230-235.

WANG, Y., ZHANG, H., LI, W., LIU, X., SHENG, G. and YU, H. (2014) Improving electricity generation and substrate removal of a MFC-SBR system through optimization of COD loading distribution. Biochemical Engineering Journal **85**15-20.

WHITE, R.A., FREEMAN, C. and KANG, H. (2011) Plant-derived phenolic compounds impair the remediation of acid mine drainage using treatment wetlands. Ecological Engineering **37** 172-175.

WIEDER, R.K. and LANG, G.E. (1992) Modification of acid mine drainage in a freshwater wetland. In: MACDONALD BR (ed.) *Proceedings of the Symposium of Wetlands of the Unglaciated Appalachian Region* 43-53.

WRIGHT, A-D.G. and KLIEVE, A.V. (2011) Does the complexity of the rumen microbial ecology preclude methane mitigation? Animal Feed Science and Technology **166-167** 248-253.

WU, D., CHENG, Y.Y., LI, B.B., LI, W.W., LI, D.B. and YU, H.Q. (2013a) Electron acceptor dependence of electron shuttle secretion and extracellular electron transfer by *Shewanella oneidensis* MR-1. Bioresource Technology **136** 711-7.14.

WU, D., CHENG, Y.Y., LI, B.B., LI, W.W., LI, D.B. and YU, H.Q. (2013b) Ferric iron enhances electricity generation by *Shewanella oneidensis* MR-1 in MFCs. Bioresource Technology **135** 630-634.

WYMAN, C.E., DALE, B.E., ELANDER, R.T., HOLTZAPPLE, M., LADISCH, M.R. and LEE, Y. (2005) Coordinated development of leading biomass pretreatment technologies. Bioresource Technology **96** 1959-1966.

XING, D., XUO, Y., CHENG, S., REGAN, J.M. and LOGAN, B.E. (2008) Electricity Generation by *Rhodospeudomonas palustris* DX-1. Environmental Science and Technology **42** 4146-4151.

YEN, H-W. and BRUNE, D.E. (2007) Anaerobic co-digestion of algal sludge and waste paper to produce methane. Bioresource Technology **98** 130-134.

YOU, S., ZHAO, Q., ZHANG, J., JIANG, J., WAN, C., DU, M. and ZHAO, S. (2007) A graphite-granular membrane-less tubular air-cathode microbial fuel cell for power generation under continuously operational conditions. Journal of Power Sources **179** 172-177.

YOUNG, J.C. and MCCARTY, P.L. (1969) The anaerobic filter for waste treatment. Journal of the Water Pollution Control Federation **41:** 160-170.

YOUNGER, P.L. (1995) Hydrogeochemistry of mine waters flowing from abandoned coal workings in county Durham. Quarterly Journal of Engineering Geology **28** S101-S113.

YOUNGER P.L. (1997) The longevity of minewater pollution: a basis for decision making. The Science of the Total Environment **194/195** 457-466.

YOUNGER, P.L. (2000) Predicting temporal changes in total iron concentrations in groundwaters flowing from abandoned deep mines: a first approximation. Journal of Contaminant Hydrology **44** 47-69.

ZAGURY, G.J., NECULITA, C.M. and BUSSIÈRE, B. (2007) Passive treatment of acid mine drainage in bioreactors using sulfate-reducing bacteria: critical review and research needs. Journal of Environmental Quality **36** 1-16.

ZAYED, G. and WINTER, J. (2000) Inhibition of methane production from whey by heavy metals – protective effect of sulfide. Applied Microbiology and Biotechnology **53** 726-731.

ZEHNDER, A.J.B. (1988) *Biology of Anaerobic Microorganisms*. John Wiley and Sons, New York.

ZHANG, G., WANG, K., ZHAO, Q. and LEE, D. (2012) Effect of cathode types on long-term performance and anode bacterial communities in microbial fuel cells. Bioresource Technology **118** 249-256.

ZHAO, F., RAHUNEN, N., VARCOE, J.R., CHANDRA, A., AVIGNONE-ROSSA, C., THUMSER, A.E. and SLADE, R.C. (2008) Activated Carbon Cloth as Anode for Sulfate Removal in a Microbial Fuel Cell. Environmental Science and Technology **42** 4971-4976.

ZHOU, M., MCALLISTER, T.A. and GUAN, L.L. (2011) Molecular identification of rumen methanogens: Technologies, advances and prospects. Animal Feed Science and Technology **166-167** 76-86.

ZHU, F., WANG, W., ZHANG, X. and TAO, G. (2011) Electricity generation in a membrane-less microbial fuel cell with down-flow feeding onto the cathode. Bioresource Technology **102** 7324-7328.

ZIEMER, C.J., SHARP, R., STERN, M.D., COTTA, M.A., WHITEHEAD, T.R. and STAHL, D.A. (2000) Comparison of microbial populations in model and natural rumens using 16S-ribosomal RNA-targeted probes. Environmental Microbiology **2** 632-643.

ZUPANCIC, G.D., STRAZISCAR, M. and ROS, M. (2007) Treatment of brewery slurry in thermophilic anaerobic sequencing batch reactor. Bioresource Technology **98** 2714-2722.